Design, synthesis and characterization of new ligands and activators for the oligomerization of ethylene by iron complexes

Adrien Boudier

▶ **To cite this version:**

Adrien Boudier. Design, synthesis and characterization of new ligands and activators for the oligomerization of ethylene by iron complexes. Other. Université de Strasbourg, 2012. English. NNT : 2012STRAF029 . tel-00868786

HAL Id: tel-00868786

https://theses.hal.science/tel-00868786v1

Submitted on 2 Oct 2013

HAL is a multi-disciplinary open access archive for the deposit and dissemination of scientific research documents, whether they are published or not. The documents may come from teaching and research institutions in France or abroad, or from public or private research centers.

L'archive ouverte pluridisciplinaire **HAL**, est destinée au dépôt et à la diffusion de documents scientifiques de niveau recherche, publiés ou non, émanant des établissements d'enseignement et de recherche français ou étrangers, des laboratoires publics ou privés.

UNIVERSITÉ DE STRASBOURG

ÉCOLE DOCTORALE DES SCIENCES CHIMIQUES

UMR 7177 CNRS

THESE DE DOCTORAT

présentée par

Adrien BOUDIER

soutenue le : **24 septembre 2012**

pour obtenir le grade de :

Docteur de l'université de Strasbourg

Discipline / Spécialité : Chimie de Coordination et Catalyse

Design, synthèse et caractérisation de nouveaux ligands et activateurs pour l'oligomérisation de l'éthylène par les complexes de fer.

THÈSE dirigée par :

M. BRAUNSTEIN Pierre	Directeur de recherche CNRS, université de Strasbourg

RAPPORTEURS :

M. CRAMAIL Henri	Professeur, université de Bordeaux
M. TAILLEFER Marc	Directeur de recherche CNRS, université de Montpellier

---

MEMBRES DU JURY :

M. Richard WELTER,	Professeur à l'Université de Strasbourg,	Président du jury
M. Henri CRAMAIL,	Professeur à l'Université de Bordeaux,	Rapporteur
M. Marc TAILLEFER,	Directeur de recherche CNRS, Université de Montpellier,	Rapporteur
M. Kees ELSEVIER,	Professeur à l'Université d'Amsterdam,	Examinateur
M. Pierre-Alain BREUIL,	Ingénieur de recherche IFP Energies nouvelles,	Promoteur IFPEN
M. Pierre BRAUNSTEIN,	Directeur de recherche CNRS, Université de Strasbourg,	Directeur de thèse

A ma famille…

Remerciements

Je tiens tout d'abord à remercier M. Denis GUILLAUME et Mme Hélène OLIVIER-BOURBIGOU pour m'avoir permis d'effectuer cette thèse au sein du département Catalyse Moléculaire de la division Catalyse et Séparation d'IFP Energies nouvelles ainsi que MM. Henri CRAMAIL, Kees ELSEVIER, Marc TAILLEFER Richard WELTER pour avoir accepté de participer à mon jury de thèse.

Je remercie ensuite Pierre-Alain BREUIL pour m'avoir encadré pendant ces deux dernières années de thèse, pour ses conseils, son soutien et son énergie. Je souhaitais également remercier Lionel MAGNA pour ses conseils et son expérience en catalyse et pour m'avoir encadré pendant ma première année de thèse et par la suite co-encadré. Je tiens à remercier Pierre BRAUNSTEIN pour m'avoir suivi tout au long de cette thèse et pour ses précieux conseils.

Je tiens à remercier Séverine FORGET pour m'avoir formé aux différentes techniques du laboratoire, pour son soutien, sa gentillesse, son humour, sa bonne humeur et sa contribution à la réussite de ma thèse !!

Je remercie également tous les ingénieurs et techniciens de ce département avec qui j'ai eu de moments de plaisir et d'amitié. Un grand merci à tous !!!!!!!

Je remercie Mikaël pour ses conseils et pour avoir été mon tuteur de stage de deuxième année d'école d'ingénieur, pour sa connaissance en matière de restos et de vins (la vie, la vraie quoi !!!! La France va te manquer), Sandrine (Mme BERRARD) pour tous ces bons moments partagés, Sébastien (l'éternel post-it bleu…) pour ses connaissances techniques, sa gentillesse et son disque dur intégré dans la tête (d'autres appellent ça la mémoire mais moi je suis sûr que tu triches, ce n'est pas possible de se souvenir de tout comme ça…).

Merci à Didier pour ses anecdotes chimiques et ses chocolats, à Christophe pour ses conseils en matière d'enneigement. Merci à Olivia pour sa gentillesse, son dévouement pour les autres et son café. Merci à Manu pour sa gentillesse, son dévouement pour les autres (ça c'est quand il veut le pépère [quand il ne rentre pas d'un week-end voile]), son humour et ses moments de sport partagés.

Merci à Cedrik pour m'avoir supporté pendant un an et demi dans le bureau, pour son aide, pour les week-ends au ski (avec qui tu vas y aller maintenant hein ??) et pour les discussions autour d'une bonne bière (Guinness de préférence, tirée en 3 fois s'il vous plaît), pour m'avoir appris qu'il ne fallait jamais, oh grand jamais, couper les spaghettis (et j'en passe…).

Merci à Stéphane pour son aide en matière d'unité, sa bonne humeur son optimisme (avec Carrefour je positive). Enfin, merci à David pour sa connaissance en matière de RMN et son soutien pour les unités multiréacteurs.

Merci à Sandrine, Sylvie, Valérie et Nathalie du secrétariat d'IFPEN ainsi qu'à Soumia HNINI du LCC Strasbourg pour leur précieuse aide au niveau administratif.

Mes prochains remerciements vont à tous les thésards que j'ai connus pendant ces trois ans. Merci donc à Fabien (Fafou !!) pour tout (au moins c'est clair !!), Vinciane (t'es sûr), Alex (pour ta culture cinématographique et ton humour….un peu décalé !!), Alban (va falloir faire quelque chose avec tes cheveux, svp ?), Fabien L., Guillaume, Jérémy, Jonathan, Cécilia, Claudine, Mathias, Bertrand, Thibault, Ema.

Merci également à Didier MORVAN (pour son humour), Ludo (papi), Jérémie Ponthus pour m'avoir formé et aidé sur les analyses masses, Adeline (bon courage pour le Boston), Julie (vive CATASEPA), MOB, Duarte, Sophie, Christophe B. (DSI en force…).

Enfin mes remerciements vont tout naturellement à ma famille et mes amis qui, par leur soutien, ont énormément contribué à ce projet. A tous, merci !!!

TABLE DES MATIERES :

Abréviations

BIP	bis(imino)pyridine
calcd	calculated
°C	degrés Celsius
DEAC	chlorure de diéthylaluminium
DRX	diffraction des rayons X
equiv	équivalents
Et_2O	ether diéthylique
eV	électronvolt
EXAFS	extended X-ray absorption fine structure
FT-IR	Analyse par spectroscopie infrarouge à transformée de Fourier
	w : weak
	m : medium
	s : strong
g	gram
h	hour
HRMS	high resolution mass spectrescopy
Hz	hertz
LAO	linear alpha olefin
MAO	methylaluminoxane
mL	millilitres
MMAO	modified methylaluminoxane
NMR	nuclear magnetic resonance
	J : constante de couplage
	s : singulet
	d : doublet
	t : triplet
	q : quadruplet
ppm	part per million
SHOP	shell higher olefin process
TEA	triethylaluminum
THF	tetrahydrofuran
TIBA	triisobutylaluminum
TMA	trimethyaluminum
XANES	X-ray Absorption Near Edge Structure

INTRODUCTION GÉNÉRALE

Les oléfines de première génération telles que l'éthylène, le propylène ou le butène sont produites en grandes quantités lors des différentes étapes du raffinage du pétrole telles que le craquage catalytique (Fluid Catalytic Craking) et le craquage à la vapeur. Les procédés Fischer-Tropsch, particulièrement ceux catalysés par des systèmes à base de fer, fournissent également des coupes légères (C_2-C_9) qui contiennent des quantités importantes d'oléfines alpha linéaires encore appelées α-oléfines. Ces α-oléfines sont aujourd'hui produites à 90% par oligomérisation de l'éthylène.[1] Les applications mettant en œuvre ces composés sont nombreuses, ils interviennent dans la production de diverses qualités de polyéthylène (essentiellement oléfines alpha C_4, C_6 et C_8), la synthèse de plastifiants (oléfines alpha C_6 à C_{10}), de lubrifiants (oléfines C_8-C_{14}) et de détergents (oléfines C_{12} à C_{16}). Ces oléfines peuvent être utilisées en tant qu'additifs pour carburant si une distribution adéquate est obtenue.

Il existe deux grands types de procédés d'oligomérisation de l'éthylène : les procédés non sélectifs (dits « full range ») et les procédés sélectifs (dits « on purpose »). Seuls les premiers permettent d'atteindre des α-oléfines supérieures à C_8 via l'utilisation de métaux tels que l'aluminium (procédé Chevron-Phillips) ou le nickel (procédé SHOP)[2] alors que les seconds permettent de produire sélectivement les α-oléfines courtes comme le butène-1 par la mise en œuvre du titane (procédé Alphabutol™[3]) ou l'hexène-1 en utilisant le chrome (procédés Alphahexol™[4] et Phillips).[5]

Le fonctionnement d'un catalyseur d'oligomérisation selon l'un ou l'autre de ces mécanismes dépend d'un nombre important de paramètres. Un choix adéquat du métal ainsi que de son ligand associé permet d'obtenir la sélectivité et l'activité désirées. Contrairement aux complexes des métaux du groupe 10, peu de catalyseurs des groupes 8 et 9 ayant des activités importantes en oligomérisation/polymérisation ont été développés durant cette

[1] Vogt D. Applied homogeneous catalysis with organometallic compounds; WILEY-VCH ed.; Weinheim, **2002**.
[2] van Leeuwen P.W.N.M. Alkene oligomerization. In Homogeneous catalysis, understanding the art, Kluwer Academic Publishers ed.; Dordrecht, **2004**; 175.
[3] Commereuc, D.; Chauvin, Y.; Gaillard, J.; Léonard, J.; Andrews, J. *Hydrocarb. Processes, Int. Ed.* **1984**, 6311, 118.
[4] Olivier-Bourbigou H., Forestiere A., Saussine L., Magna L., Favre F. and Hugues F. *Oil Gas Eur. Mag.* **2010**, 36, *2*, 97.
[5] Reagan, W. K.; Pettijohn, T. M.; Freeman, J. W. Phillips Petroleum Co. US5523507A, **Jun 4**, **1996**.

période. Il faudra attendre les travaux de Gibson[6] et Brookhart[7] en 1998 pour voir apparaître les premiers systèmes à base de fer actifs en oligomérisation/polymérisation de l'éthylène. Dans ces systèmes, la nature du ligand azoté (bis(imino)pyridine) associé au fer et son mode de coordination au métal (tridente), ainsi que le mode d'activation (aluminoxane) jouent un rôle primordial sur les performances catalytiques, particulièrement sur le contrôle de la sélectivité (oligomérisation *vs* polymérisation, ramification du produit).[8]

Cette découverte a engendré un engouement dans le développement de nouveaux précurseurs de fer permettant, une fois activés, d'oligomériser l'éthylène. La majorité des systèmes catalytiques développés en oligomérisation sont à base de ligands aromatiques tridentes azotés neutres et de précurseurs de fer au degré d'oxydation +II. Ces complexes, activés par des cocatalyseurs de type méthylaluminoxane (MAO), ont montré de fortes activités et une grande sélectivité pour les α-oléfines linéaires. Lors de ces études, il est apparu qu'un changement dans la structure du ligand, engendrait des changements radicaux de réactivité. Ceci peut être illustré par les travaux effectués sur les ligands bis(imino)pyridines.[9] Ces travaux ont montré que l'introduction d'un groupement méthyle en position 6 du cycle aromatique permettait d'orienter la réaction de l'oligomérisation vers la polymérisation de l'éthylène (Schéma 1).

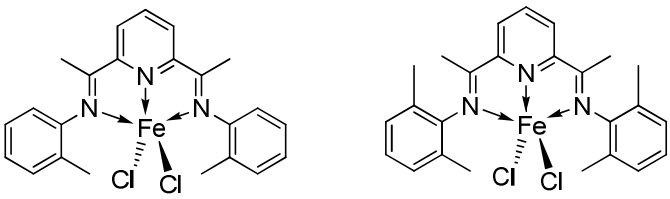

Schéma 1. Système d'oligomérisation (gauche) et de polymérisation (droite) de l'éthylène à base de fer.

Certains ligands bidentes neutres ont été développés mais les systèmes se sont révélés faiblement actifs en catalyse. Par ailleurs très peu d'études font mention de l'utilisation de ligands anioniques tridentes ou bidentes. Les complexes de fer associés à ces ligands décrits dans la littérature, se sont jusque-là avérés inactifs en oligomérisation de l'éthylène.

[6]- Britovsek, G. J. P.; Gibson, V. C.; Kimberley, B. S.; Maddox, P. J.; McTavish, S. J.; Solan G. A.; White, A. J. P.; Williams, D. J. *Chem. Commun.* **1998***,* 849.
[7]- Small, B. L.; Brookhart, M. *J. Am. Chem. Soc.* **1998**, *120*, 7143.
[8]- Small, B. L.; Brookhart, M. *Macromol.* **1999**, *32*, 2120.
[9] Gibson,V.C.; Redshaw,C.; Solan,G.A. *Chem. Rev.* **2007**, *107*, 1745.

En plus d'être une ressource très disponible, le fer présente de nombreux avantages par rapport à l'ensemble des métaux de transition utilisés en oligomérisation de l'éthylène. Il est faiblement isomérisant et conduit à des alpha-oléfines de grande pureté. Les complexes s'avèrent très actifs et peu toxiques (par rapport au chrome par exemple). Des résultats préliminaires obtenus à l'IFP Energies Nouvelles ont démontré que des performances très intéressantes en oligomérisation de l'éthylène pouvaient être obtenues grâce à la mise en œuvre d'une nouvelle famille de ligands N,N,N monoanionique, associés à du fer à l'état d'oxydation +III.[10]

Cette thèse a donc pour objectif d'approfondir l'étude des systèmes de fer(III) à base de ligands monoanioniques azotés tridentes pour développer de nouveaux systèmes catalytiques. Deux voies d'accès à ces systèmes seront abordées : la réaction entre un ligand monoanionique et un précurseur de fer(III) et l'oxydation de précurseurs de fer(II). L'accent sera également porté sur le développement de nouvelles familles de ligands tridentes N,N,L (L = N, O, S, P) et la recherche de nouveaux activateurs (le MAO et le MMAO restant les seuls cocatalyseurs efficaces dans le domaine de l'oligomérisation de l'éthylène). Cette thèse est structurée autour de 5 chapitres dont le contenu est détaillé ci-dessous :

Le chapitre 1 décrit l'ensemble des complexes de fer utilisés en oligomérisation de l'éthylène. Après une introduction sur les précurseurs de fer(II) bis(imino)pyridines, un recensement de l'ensemble des ligands tridentes neutres autres que les bis(imino)pyridines est rapporté. Une deuxième partie traite des ligands bidentes et une troisième aborde l'utilisation de ligands monoanioniques tridentes et bidentes.

[10] Rangheard, C. Oligomérisation de l'éthylène par les catalyseurs de fer. PhD thesis. Université Claude Bernard Lyon 1 (**2008**).

Dans le chapitre 2, nous présentons les résultats obtenus sur les systèmes de fer(III) synthétisés par réaction entre un ligand monoanionique tridente et un précurseur de fer(III). Il décrit de manière détaillée la caractérisation complète du complexe de fer(III) 1,2-dihydro-1,10-phénantroline (Schéma 2) et son comportement catalytique en oligomérisation de l'éthylène.

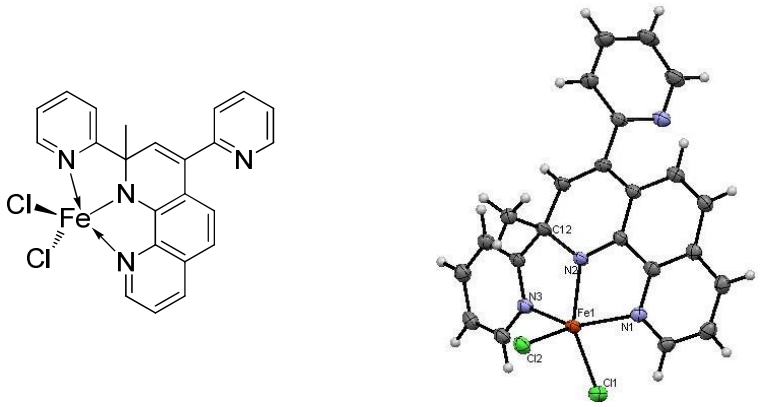

Schéma 2. Complexe de fer(III) 1,2-dihydro-1,10-phénantroline (gauche) et la structure DRX associée (droite).

Le chapitre 3 présente l'oxydation des précurseurs de fer(II) comme une voie d'accès innovante à des complexes de fer(III) binucléaires. Une analyse structurale de ces complexes est rendue possible par analyse DRX et infrarouge. Les différences de performances catalytiques en oligomérisation de l'éthylène (activité, distribution en oligomères et sélectivité en α-oléfines) entre l'espèce binucléaire de fer(III) 1,2-dihydro-1,10-phénantroline (Schéma 3) et son homologue mononucléaire (développé dans le chapitre II) seront soulignées. Les raisons de ces différences sont discutées au travers d'une proposition de mécanisme.

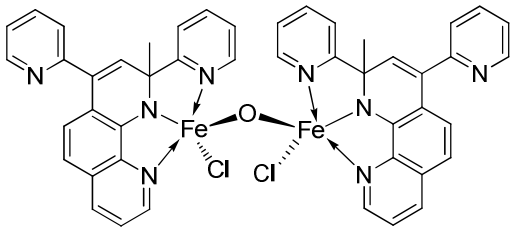

Schéma 3. Complexe binucléaire de fer(III).

Dans le chapitre 4, nous décrivons de manière détaillée la synthèse de nouveaux cocatalyseurs d'aluminium pour l'activation des précurseurs de fer. Ces nouvelles espèces ont été synthétisées par réaction entre un composé organique (phénol, diol, aminophénol) et le triméthylaluminium. L'influence de la structure du ligand (encombrement stérique, nombre de

fonction hydroxy...) sur la nature du complexe d'aluminium obtenu est décrite. Les performances de ces activateurs en oligomérisation de l'éthylène sont également discutées.

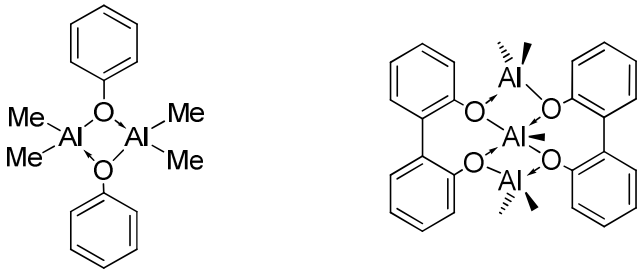

Schéma 4. Catalyseurs binucléaires (gauche) et trinucléaires (droite) d'aluminium.

Le chapitre 5 rapporte les résultats obtenus sur les ligands imino-imidazoles possédant un bras hémilabile. Le mode de coordination de ces ligands vis-à-vis du nickel a été étudié au travers d'une étude DRX (Schéma 5). L'influence de la structure du ligand sur la géométrie des complexes et ses conséquences en catalyse seront discutées.

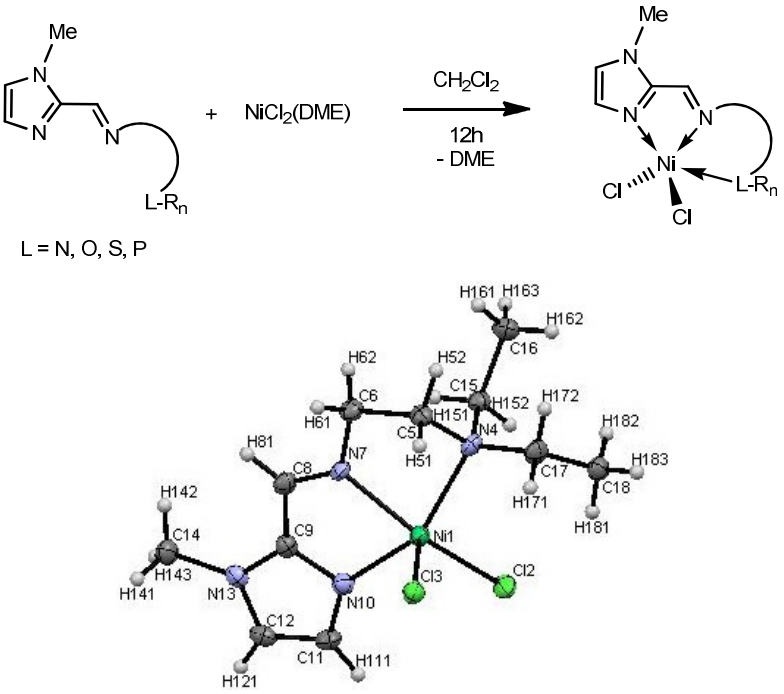

Schéma 5. Synthèse des précurseurs de nickel (haut) et exemple de structure DRX (bas).

Note : Chaque chapitre possède sa propre numérotation des molécules.

CHAPTER I

Ligands involved in the Ethylene Oligomerization by Iron Complexes: State of the Art

Abstract: Iron complexes bearing tridentate N,N,L (L = N, O, S, P) ligands represent a growing number of ethylene transformation catalysts in development. The ease of synthesis of the ligands and complexes and the large number of commercial reagents, which allow structural diversity, make these systems of great interest for both academicians and industrials. These iron precatalysts are particularly interesting because of the variations in the catalytic behavior observed by tuning ligands. Since the discovery that bis(imino)pyridine ligands can impart iron metal with high activities for ethylene oligomerization and polymerization, a great deal has focused on catalytic modification and design. In this review, we highlight ligands developed for the iron-catalyzed oligomerization of ethylene excepted bis(imino)pyridine ligands which have been widely reviewed.

Résumé : Depuis la travaux de Gibson et Brookhart démontrant l'aptitude des complexes de fer(II) bis(imino)pyridines à oligomériser l'éthylène, un grand nombre de ligands tridentes N,N,L (L = O, S, P, N) ont été développés aussi bien par les universitaires que les industriels. Ceci a été rendu possible par une synthèse des ligands simple associée à un large panel de réactifs disponibles. Les nombreuses études dans le domaine ont pu mettre en évidence que les variations structurales du ligand, et donc du complexe, impactaient les performances catalytiques. Dans ce chapitre, nous détaillons l'ensemble des ligands utilisés dans la synthèse de complexes de fer pour l'oligomérisation de l'éthylène. Les ligands bis(imino)pyridines ayant déjà fait l'objet de nombreuses revues sur le sujet ne seront développés.

Introduction

Soon after the initial discoveries of Ziegler-Natta that catalysts based on early transition metal polymerized ethylene in high temperature and pressure conditions,[1,2] efforts were performed to synthesize and develop new homogeneous catalysts enabling the transformation of ethylene. Natta and Breslow independently reported that titanium complex $TiCl_2(Cp)_2$, once activated by $AlEt_3$ or $AlEt_2Cl$, could polymerize ethylene (Figure 1).[3,4] Keim group developed P,O nickel complex which proved to be an excellent one component model catalyst for the oligomerization of ethylene as practiced in Shell's Higher Olefin Process (SHOP).[5] In the 1990s, the cyclopentadienyl-amide titanium and zirconium dichlorides complexes (constrained geometry catalysts, CGC) have been reported to polymerize ethylene with impressive results.[6,7] In 1995, Brookhart and co-workers developed a new class of nickel and palladium complexes chelated by α-diimine ligands.[8] According to the authors, nickel and palladium diimine olefin polymerization were very active late transition metal systems capable of converting α-olefins to high polymers and were the first systems in which olefin alkyl complexes have been demonstrated to be the catalyst resting state. Three years later, Brookhart and Gibson groups independently discovered that the tridentate 2,6-bis(imino)pyridine (BIP) ligand yield to highly active catalytic precatalysts once coordinated to iron center and activated by MAO (methylaluminoxane).[9-11] Since then, a large amount of work has been devoted to the modifications of this ligand and to the understanding of the chemistry of its metal derivatives. Bianchini and Gibson independently reviewed theses results.[12-14] These iron complexes represent a remarkable new generation of ethylene oligomerization catalysts that have extended the understanding of the role of electronic and steric properties of the ligands in controlling transition metal-catalyzed olefins polymerization and oligomerization.

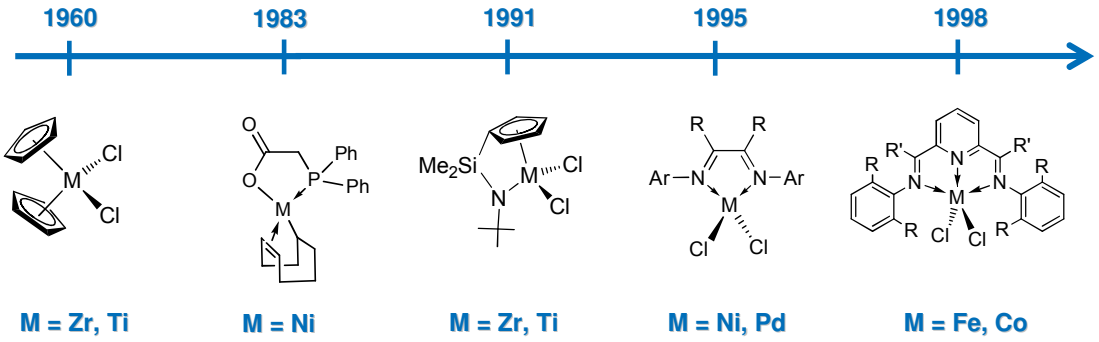

Figure 1. Chronological development of the homogeneous olefin oligomerization and polymerization catalysts.

Most of the BIP ligands are synthesized by the Schiff-base condensation of 2 equivalents of the aniline with 2,6-diacetylpyridine derivatives. The reaction can be performed either in toluene, methanol or dichloromethane at room or higher temperature. For aldimine ligands (R'= Me), a catalytic amount of acid and harsher reaction conditions were involved. The iron and cobalt complexes are obtained by addition of the ligand to the appropriated hydrated or anhydrous metal salt. Crystals of 2,6-bis[1-(2,6-diisopropylphenylimino)ethyl]pyridineiron(II) chloride suitable for X-ray diffraction analysis are grown from a layered CH_2Cl_2/pentane solution (1:1). The complex had molecular *C*s symmetry about a plane containing the iron, the two chlorides and the pyridyl nitrogen atom. The geometry of the iron center can be best described as pseudo-square-pyramidal.[11]

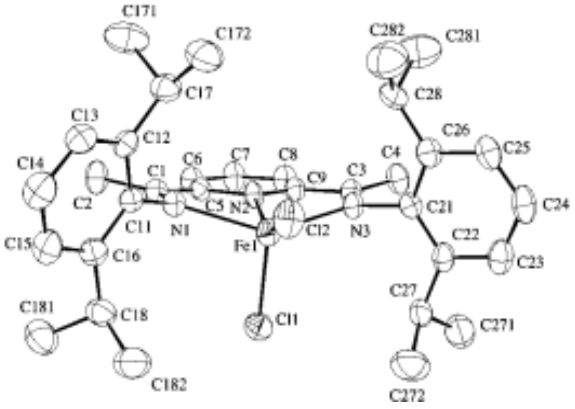

Figure 2. X-ray crystal structure of iron bis(imino)pyridine.

The nature of the catalytic reaction, i.e., oligomerization or polymerization, is determined by the bulkiness of the *o*-substituents of the aryl ring. Indeed, oligomers are obtained from mono *o*-substituted catalysts (**A** for example), except for very bulky substituents (*o*-benzyl, *o*-trifluoromethyl) on the *o*-position or *o*-Me group with *p*-bulky substituents. Di-*o*-substituted complexes yield to polymerization reactions (**B**, **C**, **D** and **E** for example), except for 2,6-difluoro and 2-fluoro-6-methyl ligands.[13] Methylaluminoxane (MAO) and modified methylaluminoxane (MMAO) remain the most efficient cocatalysts for ethylene oligomerization and polymerization by iron precursors. In an oligomerization point of view, theses compounds are the only one yielding to highly active systems. Much diversity was observed for efficient activators in the polymerization of ethylene by iron complexes. For instance, a number of alkylaluminum compounds ($AlMe_3$, $AlEt_3$, Al^iBu_3, Al^nHex_3, Al^nOct_3), inefficient toward ethylene oligomerization, succeeded in activating iron precursors for ethylene polymerization.[15]

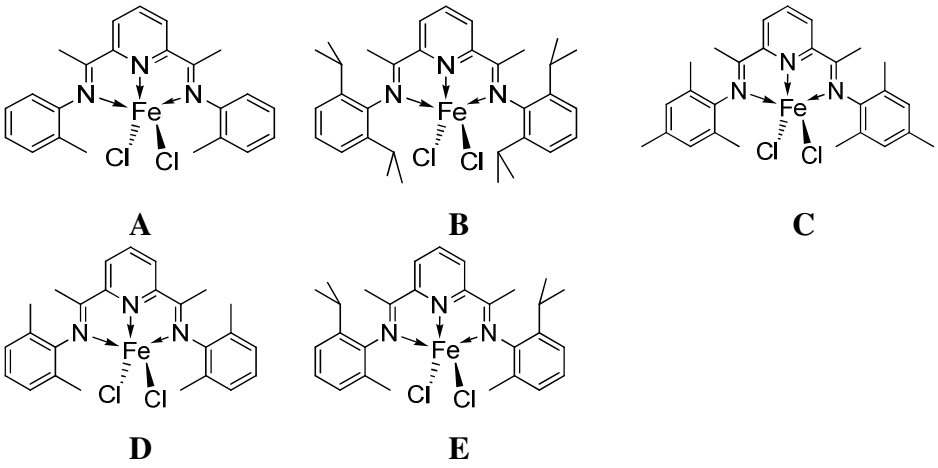

Scheme 1. Iron(II) precatalysts for ethylene transformation.

Under optimized conditions (1000 equiv of MMAO, 30 bar and 90 °C), iron precatalyst **A** oligomerizes ethylene with high activity (7×10^7 g/mol•h•atm) yielding to a full range (C_4-C_{24}) distribution of oligomers with an excellent selectivity in α-olefins (>99%).[9] The oligomer distribution is Schulz-Flory type (K = 0.70). The Schulz-Flory coefficient K (eq. 1) represents the probability of chain transfer,[16] a high K value means that a catalyst produces high molecular weight oligomers. This precursor **A** exhibited the highest activity among all iron precatalysts reported in literature.

$$K = \frac{k_{prop}}{(k_{prop} + k_{ch\,transfer})} = \frac{molC_{n+2}}{molC_n} \qquad \textbf{eq. 1}$$

In this review, we present the recent development of iron systems chelated by neutral and anionic tridentate and bidentate ligands for the oligomerization of ethylene. The aim of this part is to make a state of the art of the ligands developed in this field. Bis(imino)pyridine compounds are excluded because of the many reviews already published on this family of ligands.

I. Neutral tridentate ligands

1. Derivations of the bis(imino)pyridine ligands

a. Modifications of the central ring

One of the alternative variants of the bis(imino)pyridine ligands was to replace the pyridine central ring by other N-heterocycles.[17-21] The aim of investigating theses entities was to study the impact of differences of basicity brought by central ring on the catalysis. Iron precursors chelated by **1** and **2** displayed low activities in ethylene polymerization (10^5 g/mol•h•atm for **1** and 10^4 g/mol•h•atm for **2**) compared to iron(II) bis(imino)pyridine analogues (10^7 g/mol•h•atm).[10,11,19] Ligands **3** and **4** failed to ligate iron.[18]

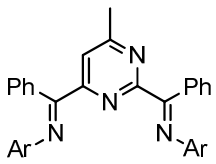

Ar = 2,6-$Me_2C_6H_3$, 2,4,6-$Me_3C_6H_2$
2,6-(^{i}Pr)$_2C_6H_3$ or 2-MeC_6H_4

1

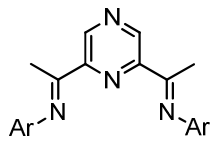

Ar = 2,6-$Me_2C_6H_3$, 2,6-(^{i}Pr)$_2C_6H_3$
or 1-naphthyl

2

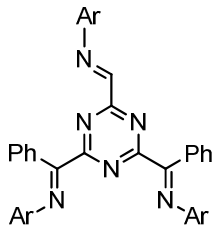

Ar = 2,4,6-$Me_3C_6H_2$

3

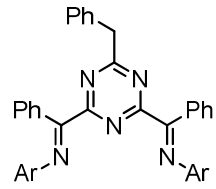

Ar = 2,4,6-$Me_3C_6H_2$

4

Scheme 2. Various bis(imino)N-heterocycles ligands.

b. Modifications of the imino groups

Diversity was brought by the modification of the imino group while keeping six membered pyridine central ring. Ligands **5** and **6** led to poorly active systems for ethylene oligomerization (<10^5 g/mol•h•atm). Butene was majority obtained in very low quantity (<0.1 g).[22] Iron complexes containing bis(oxazoline)pyridine ligand **7** polymerized ethylene using

MAO as cocatalyst.[23] Iron precursors associated with ligand **8** were active in ethylene oligomerization producing 1-butene and 1-hexene (5.7×10^5 g/mol•h•atm).[24] Tested for homopolymerization of isoprene, ligands **9** and **10** chelated respectively on $FeCl_2$ and $FeCl_3$ were inactive. Activity was noticed for homopolymerization of 1,3-butadiene by iron precatalyst associated with **9** (R = H) and **10** (R = H and ^{t}Bu) upon activation with MMAO.[25] Under 1 bar of ethylene, iron precursors in association with ligand **11** polymerize ethylene using MAO as cocatalyst.[26] Compared to their parent bis(imino)pyridine system, iron complexes bearing **12** and **13** exhibited lower activities in ethylene polymerization.[27]

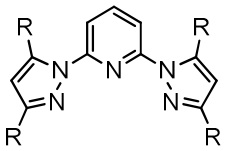

R = Me or Ph

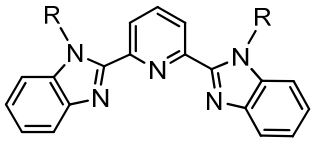

R = H or Me

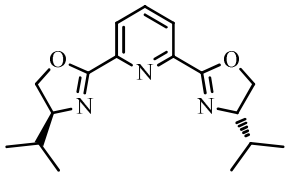

5

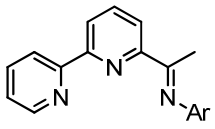

Ar = 2,6-(^{i}Pr)$_2$C$_6$H$_3$

6

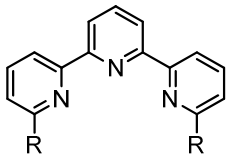

R = H, 3,5-Me$_2$(C$_6$H$_3$) or 2,4,6-Me$_3$(C$_6$H$_2$)

7

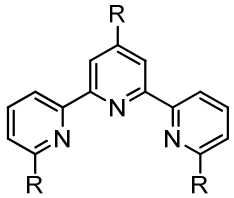

R = H or ^{t}Bu

8

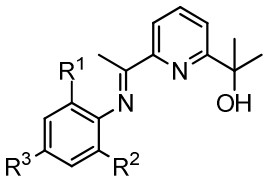

R^1 = Me or ^{i}Pr
R^2 = Me or ^{i}Pr
R^3 = H or Me

9

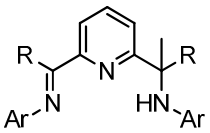

R = H or Me
Ar = 2,6-(^{i}Pr)$_2$C$_6$H$_3$ or 2,4,6-Me$_3$C$_6$H$_2$

10

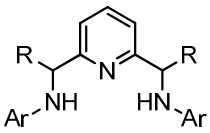

Ar = 2,6-(^{i}Pr)$_2$C$_6$H$_3$ or 2,4,6-Me$_3$C$_6$H$_2$

11 **12** **13**

Scheme 3. Variants structure of ligands.

2. Five-membered L-heterocycle ligands

Tenza and co-workers tested a large range of tridentate ligands with five-membered central rings.[22] Under ethylene atmosphere, the iron complexes ligated by **14** and **15** oligomerized ethylene with moderate activities (1.2×10^5 g/mol•h•atm). Butenes and hexenes were obtained with low selectivity for α-olefin and a majority of butenes (> 80%). The inversion of N and S atoms on the heterocycle led to a decrease in activity (1.2×10^5 g/mol•h•atm for **14** and 0.3×10^5 g/mol•h•atm for **15**). Upon activation with a mixture TEA/TA ($AlEt_3$/$[Ph_3C][Al(O^tBu^F)_4]$), iron precursors oligomerized ethylene with an order of magnitude lower than upon activation with MAO. According to the authors, this is the first example of active iron catalysts chelated by ligands with five-membered N-heterocycle central ring. Furan **16** and thiophene **17** ring did not succeed in ligating iron. Other studies involving theses ligands led to the same observation.[18,28-30] The rather poor donor properties of the oxygen and sulfur atom could be the reason of this failure. The same trend is observed with ligand **18**.[22] The authors explain this result by the presence of the methyl group on the nitrogen atom. Britovsek and co-workers worked on the development of iron complexes chelated by furan **19**[18] ligands. Unforunately, no coordination was observed.

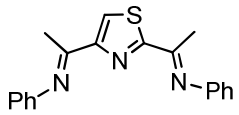

14

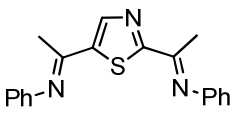

15

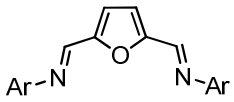

16

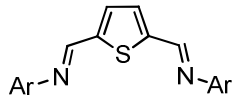

17

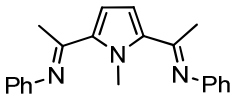

18

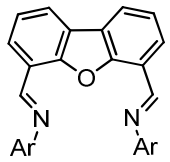

19

Scheme 4. Five-membered bis(imino)L-heterocycle.

3. Bis(carbene)pyridine ligands

McGuiness and co-workers developed iron bis(carbene)pyridine complexes and tested them in ethylene oligomerization and polymerization.[31] Ligand **20** was obtained by deprotonation of the corresponding imidazolium bromides using $KN(SiMe_3)_2$. Treatment of iron dibromide with the carbene **20** in tetrahydrofuran gave the bis(ligand) $[FeBr_2(\mathbf{20})_2]^{2+}[FeBr_4]^{2-}$. The reaction with **21**, bearing the bulkier 2,6-^{i}Pr$_2$ substituent, generated the monoligand iron complex $[FeBr_2(\mathbf{21})]$.[32-34] Treated by MAO, iron precursors were totally inactive in ethylene transformation. Chelated on iron or cobalt, ligands **22** led to inactive catalysts for the ethylene transformation, while on titanium or chromium, high activities were obtained for the ethylene polymerization. Ligand **22** was chelated on titanium and chromium centers yielding to highly active catalysts for the oligomerization and polymerization of ethylene. Such bis(carbene) ligands were less suited to iron and cobalt olefin polymerization catalysts than to earlier transition-metal counterparts.

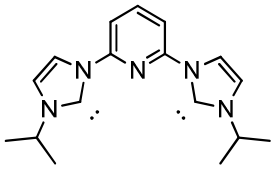

20

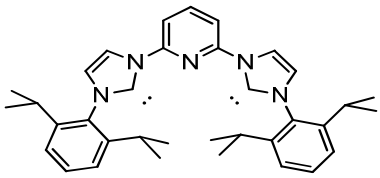

21

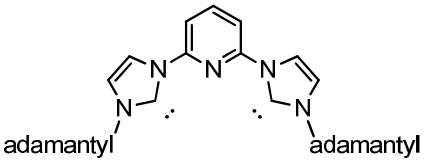

22

Scheme 5. Bis(carbene)pyridine ligands.

4. Benzimidazole fonctionnalized ligands

Following the discovery of bis(imino)pyridyl iron complexes,[9-11,35] a range of tridentate ligands based on pyridyl central moiety functionalized with benzimidazolyl, benzoxazolyl or benzothiazolyl groups were studied by Sun and co-workers (Scheme 6).[36-41] Under optimized conditions, iron precatalysts associated with ligands **23** and activated by the appropriated cocatalyst oligomerized ethylene with a range of activity of 10^4-10^5 g/mol•h•atm.[40] Oligomers were obtained with high selectivity for α-olefins (>99%) and followed a Schulz-Flory distribution in a range of 0.46 to 0.62. The best activity was obtained for R^1 = ^{i}Pr (4.7×10^5

g/mol•h•atm). Replacing the ^{i}Pr group by a small one (Me or Et) led to a decrease in activity (~2×10^5 g/mol•h•atm).

Under reduced pressure (10 atm), iron precatalysts chelated by ligands **24**-**25** have been tested in combination with MMAO and MAO.[38,39] α-olefins were obtained with high selectivity (>99%). Complexes obtained from ligands **25** were by far more active than those obtained from ligands **24**. In the first case, the best activity was obtained when $R^1 = {}^{i}$Pr and $R^2 = R^3 = H$ (4.1×10^5 g/mol•h•atm) while for ligand **24** $R^1 = R^2 = Me$ was the best candidate (0.9×10^5 g/mol•h•atm). Therefore, the correlation of the alkyl substituents (on the aryl and on the benzimidazolyl ring) and the activity is not clearly correlated to the structure of the ligand and is specific to each precatalyst. Considering ligands **23-25**, it was observed that iron catalysts substituted by halogen as *o*-subsituents on the aryl ring exhibited the lowest activity (10^4 g/mol•h•atm).[38-40] The introduction of substituent on the phenyl ring of the benzimidazolyl moiety was investigated, iron precursors obtained from ligand **25** exhibited lower activities than their homologues for ethylene oligomerization (synthesized from ligand **25** with $R^3 = H$). For $R^3 = Me$, the highest activity was obtained for $R^1 = R^2 = Me$ (1.0×10^5 g/mol•h•atm). Whereas for $R^3 = Cl$, $R^1 = Me$ and $R^2 = H$ led to the best candidate (0.9×10^5 g/mol•h•atm). Iron(III) complexes bearing 2-(benzimidazol)-6-(1-arymiminoethyl)pyridines **23** remained less active ($R^1 = Me$, 2.2×10^4 g/mol•h•atm) than iron(II) analogues ($R^1 = Me$, 9.2×10^4 g/mol•h•atm).[36] In both cases, activities remained quite low.

Sun and co-workers studied benzothioazolyl and benzoxazolylpyridyl ligands **26** and **27** considering the electronic properties.[37,41] All precursors behaved as good precatalysts for ethylene oligomerization (10^5-10^6 g/mol•h•atm) and showed moderate activity towards ethylene polymerization (<10^4 g/mol•h•atm). Oligomers were obtained with good selectivity (>97%). Considering benzothiazolyl ligands **26**, the highest activity was obtained for $R^1 = R^2 = Me$ (11.0×10^5 g/mol•h•atm; α>97%) whereas **27** formed the most active iron system for ethylene oligomerization when $R^1 = Et$ and $R^2 = H$ (10.2×10^5 g/mol•h•atm). There was no significant variation on catalytic activities for complexes chelated by ligands **26** and **27**. For instance, with $R^1 = Me$ and $R^2 = H$, complex with **26** showed an activity of 11.0×10^5 g/mol•h•atm while the association of **27** and iron showed an activity of 8.4×10^5 g/mol•h•atm. These complexes exhibited better activities than ligands **23**,[40] **24**[39] and **25**.[38]

MMAO, MAO and chloroalkylaluminums were tested. Whereas $AlEt_2Cl$ succeed in activating iron precatalysts chelated by ligands **23** and **25**, $Fe/AlEt_2Cl$ systems to afford short chain oligomers with very low activity ($<10^4$ g/mol•h•atm). Ligand **27** yielded to inactive systems when $AlEt_2Cl$ or $AlEt_3$ were used as cocatalyst for Al/Fe ratio of 200. The most effective cocatalysts are MAO and MMAO. Increasing the Al/Fe ratio from 500 to 1000 implied a gain in activity ($R^1 = {}^i$Pr and R^2 = H for ligand **25**; from 0.6×10^5 g/mol•h•atm to 2.6×10^5 g/mol•h•atm). Beyond this value the activity dramatically decreased (Al/Fe=1500; 1.2×10^5 g/mol•h•atm). It was also determined that the higher the temperature, the lower is the activity observed ($R^1 = {}^i$Pr and R^2 = H for ligand **25**; from 2.6×10^5 g/mol•h•atm at 20 °C to 0.1×10^5 g/mol•h•atm at 60 °C). Indeed, at high temperature the concentration of ethylene in solution was lower than at room temperature. The selectivity of α-olefins decreased with the increase in temperature. An increase in ethylene pressure (from 1 to 10 atm) resulted in a higher activity ($R^1 = {}^i$Pr and R^2 = H for ligand **25**; from 0.9×10^5 g/mol•h•atm at 1 atm to 2.6×10^5 g/mol•h•atm at 10 atm) due to the increase in concentration of ethylene in solution. Higher pressure also induced high selectivity for α-olefins.

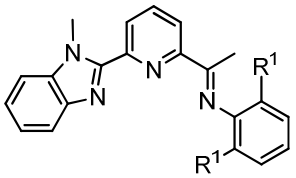

R^1= H or Alk
R^2= H or Me

23

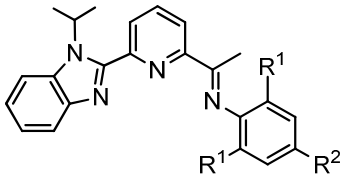

R^1= H or Alk
R^2= H or Me

24

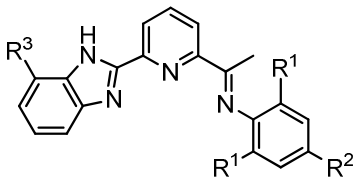

R^1= H or Alk
R^2= H or Me
R^3= H, Me or Cl

25

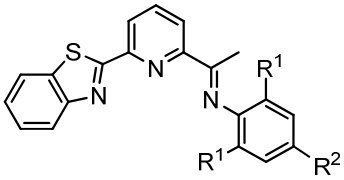

R^1= H or Alk
R^2= H or Me

26

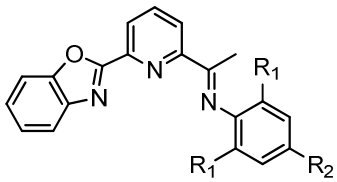

R_1= H or Alk
R_2= H or Me

27

Scheme 6. Benzimidazolyl, benzoxazolyl and benzothiazolyl derivatives.

5. Phenanthrolinyl ligands

Considering the great potential of iron tridentate complexes for ethylene oligomerization, Sun and co-workers designed ligands based on imino-phenanthroline group.[42-45] The iron(II) complexes ligated by 2-imino-1,10-phenanthrolines **28** reported by Sun upon activation with MAO promote oligomerization and polymerization of ethylene (Schulz-Flory distribution in the range of 0.30 to 0.62).[44-46] Under optimized conditions (catalyst: 2 μmol; toluene (100 mL); Al/Fe: 1000; 40 °C; 1 h), the highest activity was obtained for $R^1 = R^2 = R^3 = Cl$ and $R^4 = Me$ (4.5×10^6 g/mol•h•atm). Selectivity of α-olefins was quite low (>87%) and low molecular-weight waxes was formed (6.4×10^5 g/mol•h•atm). The highest free-waxes oligomerization activity was obtained when $R^1 = Br$, $R^2 = Me$, $R^3 = H$ and $R^4 = Me$ (2.9×10^6 g/mol•h•atm). Olefins were formed with a selectivity of 92%. For methylketimine complexes ($R^4 = Me$), the larger the bulkiness of the aryl group, the higher the oligomerization activity. Replacement of a single *o*-methyl group on the imino-aryl ring by a brome gives better activity in oligomerization. Aldimine ligands chelated on iron were as active as methylketimine analogues. However, phenylketimine ($R^4 = Ph$) ligands formed the lowest active iron systems for ethylene oligomerization (0.6×10^6 g/mol•h•atm). Very low activities were observed with $AlEt_2Cl$ or $AlEtCl_2$ as cocatalysts. $AlEt_3$ succeeded in activating iron precursors with low activity (~10^4 g/mol•h•atm). MMAO and MAO led to the best active species for ethylene oligomerization (~10^6 g/mol•h•atm). Increasing both the temperature and the ethylene pressure first led to both an initial gain in activity and in α value and in second led to a decrease. The influence of steric properties of the C-imino groups has been investigated by the use of 2-ethyl-ketimino-1,10-phenanthroline ligands **29**.[42] Compared with their analogues,[44,45] precursors exhibited better thermal stability and similar activities for oligomerization (2.1×10^6 g/mol•h•atm for $R^1 = Me$ and $R^2 = H$) and polymerization (0.2×10^6 g/mol•h•atm) over a period of 30 minutes. In comparison with the alkyl analogues, halogen substituents (R^1 =F or Cl) led to quite good activities (0.8×10^6 g/mol•h•atm) and no low molecular-weight waxes were observed. Incorporating phenyl substituent on the phenanthrolinyl ligand **30** has been reported to give, in combination with MMAO and under 10 atm of ethylene, moderate activities (2.7×10^5 g/mol•h•atm).[47] 1-butene was majoritary obtained with very high selectivity (>99%). Symmetric 2,9-bis(imino)-1,10-phenanthrolinyl ligands **31** containing various substituents on the aryl ring form with $FeCl_2$ inactive catalysts toward ethylene oligomerization and polymerization.[43] 2-oxazoline/benzoxazole-1,10-

phenanthrolinyl and 2-(benzimidazol-2-yl)-1,10-phenanthrolyl ligands **32**-**34** have been involved in the design of iron precursors and used in ethylene oligomerization.[48,49] Iron precatalysts associated with ligands **34** oligomerized ethylene with a hit of activity of 1.2×10^5 g/mol•h•atm ($R^1 = R^2 = H$) over a period of 20 minutes.[49] Short oligomers were obtained, up to 95% of butenes with a selectivity in 1-butene >92%. Alkylation of the amine group of the benzimidazolyl ring of ligand **34** induced a decrease in activity. Among the alkyl substituents no structural-activity relationship was set up. Precursors synthesized from ligands **32** and **33** were slightly less active (<10^5 g/mol•h•atm) with lower selectivity in 1-butene (<60-80%).

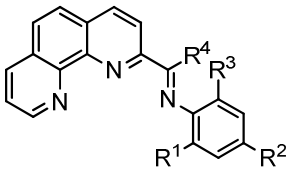

R^1= Me, Et, ^{i}Pr, Cl or Br
R^2= H, Me, Br, Cl or F
R^3= H, Et, F, Cl, Me
R^4= H, Me or Ph

28

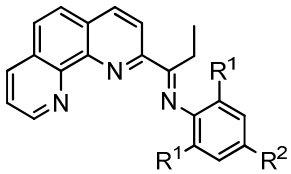

R^1= Me, Et, ^{i}Pr, Cl or F
R^2= H or Me

29

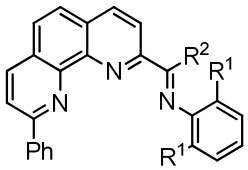

R^1= Me, Et or ^{i}Pr
R^2= Me or Ph

30

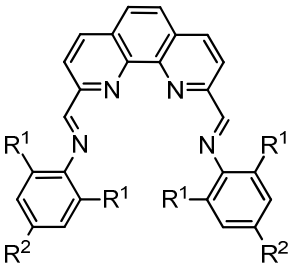

R^1= Me or ^{i}Pr
R^2= Hor Me

31

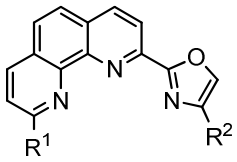

R^1= H or Ph
R^2= Hor Me

32

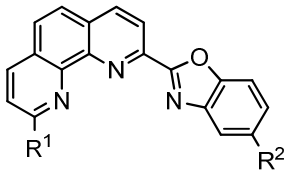

R^1= H or Ph
R^2= H, Me or ^{t}Bu

33

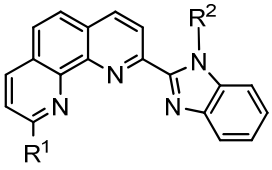

R^1= H or Me
R^2= H, Me, Et, ^{i}Pr or Bn

34

Scheme 7. Phenanthroline ligands.

6. Quinoline and quinoxazoline ligands

One-pot synthesis was employed for iron complexes chelated by ligand **35**.[50] Upon treatment with MMAO, these precursors showed low activities toward ethylene oligomerization (<10^5 g/mol•h•atm). Butenes were majority obtained (>90%) with a hit of selectivity for 1-butene of 98% (R^1 = Cy and R^2 = Me). Increasing the R^1 substituent (from Me to ^{i}Pr or Cy), while keeping R^2 = Me, led to a gain of activity (6.0×10^4 g/mol•h•atm for R^1 = Me, 9.2×10^4 g/mol•h•atm for R^1 = ^{i}Pr and 9.4×10^4 g/mol•h•atm for R^1 = Cy) The same trend was observed for the R^2 substituent (from H to Me while keeping R^1 = H, Me, ^{i}Pr or Cy).

Ferrous chlorides bearing 2,8-bis(pyridylimino)quinoline **36** exhibited unique activity toward ethylene polymerization.[51] Only ligands having methyl groups at *o*-positions led to corresponding precursors. Activated by a substantial excess of MAO (up to 2500), iron precatalysts polymerized ethylene for temperature up to 80 °C. No or very low activities were observed in a range of 40-60 °C. At 100 °C and for Al/Fe = 3000, the activity was four times higher and higher molecular weight was observed for polyethylene. Introduction of a methyl group at *p*-position induced a slight decrease in activity (2.5×10^5 g/mol•h•atm *vs* 2.1×10^5 g/mol•h•atm). Sun and co-workers used 2-quinoxalinyl-6-iminopyridines **37** [52] to synthesize active iron systems in oligomerization and polymerization of ethylene.[53] Under 1 atmosphere of ethylene, activities were above 10^5-10^6 g/mol•h•atm with a hit at 12.0×10^5 g/mol•h•atm for R^1 = R^2 = Me. Screening of all substituents among R^1 and R^2 did not succeed in establishing a relationship between activity and structure of complexes. Short olefins mainly butenes were obtained (C_4-C_{10}). For R^1 = R^2 = Me, Increasing the pressure implies a decrease in oligomerization activity (2.2×10^5 g/mol•h•atm) a little activity toward polymerization of ethylene (0.8×10^5 g/mol•h•atm).

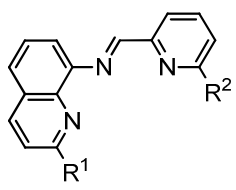

R^1= H, Me, ^{i}Pr or Cy
R^2= H or Me

35

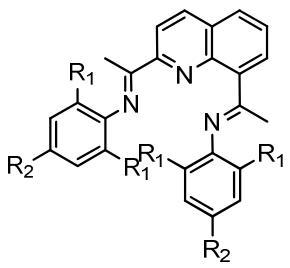

R^1= Me
R^2= H or Me

36

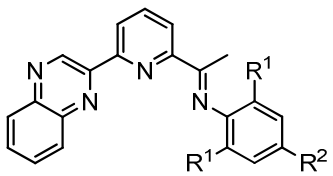

R^1= Me, Et, ^{i}Pr, F, Cl or Br
R^2= H or Me

37

Scheme 8. Quinoline and quinoxaline derivatives.

7. Pendant donor α-diimine ligands

Ligands containing α-diimine moiety have been widely used for the synthesis of complexes engaged in transformation of olefins.[8,54,55] Small developed new precatalysts chelated by α-diimine ligands with pendant S,P,N and O donors.[56-58] These studies exhibited the potential of iron precursors bound by other atom than nitrogen to oligomerize ethylene and so brought diversity among the large library of existing precatalysts. Method used to synthesize ligands allowed the authors to get access to a variety of complexes (Scheme 9).

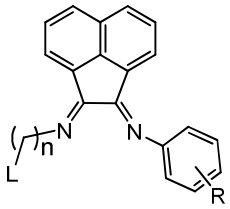

L = SR, PR_2, NR_2, OR, *o*-pyridine, morpholine
n = 2 or 3
R = 2,6-Me, 2,6-^{i}Pr, 2,6-^{t}Bu

Scheme 9. α-diimine N,N,L ligands.

Independently of the nature of the L atom, increasing the length of the bond of the pendant donor implies a decrease in activity. A bond of two spacers was found to be the optimum length. So n = 2 for all complexes described afterwards (excepted for L = *o*-pyridine for which n = 1). Tested in cyclohexane and activated by MMAO, iron precursors chelated by sulfur atom were slightly more active than those bound by phosphorous and both were by far more active than iron precatalysts bearing α-diimine ligands with nitrogen pendant donor. The only precatalyst chelated by N,N,O entity was inactive. For L = S-4-(^{t}Bu)Ph and R^1 = 2,4,6-Me_3, iron complex oligomerized ethylene with a hit of activity of 1.3×10^6 g/mol•h•atm whereas for L = PPh_2, R^1 = 2,6-$^i Pr_2$ was the best candidate with an activity of 1.0×10^6 g/mol•h•atm. 0.7×10^6 g/mol•h•atm was the highest activity considering nitrogen atom (L = *o*-pyridine and R^1 = 2,6-Me_2). Generally, α-olefins were obtained with high selectivity (>99%) and no polymer was formed. Reducing the steric environment of the dialkyl-amino donor (L = NR_2) led to a decrease in catalysis whereas changing the group on the *o*-position on the N-aryl ring did not have a real impact on the performance of the precatalysts (5.2×10^5 g/mol•h•atm for R^1 = 2,6-Me_2 and 6.8×10^5 g/mol•h•atm for R^1 = 2,6-$^i Pr_2$).

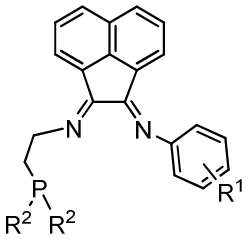

R^1= 2-^{i}Pr-6-Me, 2,6-^{i}Pr$_2$, 2,4,6-Me$_3$, 2,4-Me$_2$
R^2= Ph, 3,5-Me$_2$-Ph, 2-Me-Ph, CyH

38

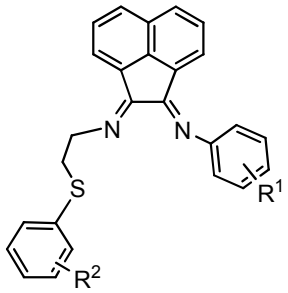

R^1= 2,6-^{i}Pr$_2$, 2,4,6-Me$_3$, 2,6-Me$_2$, 2,6-Me$_2$-4-^{t}Bu, 2,6-Me$_2$-4-Br
R^2= 4-Cl, 4-^{t}Bu, 3,5-Me$_2$, 4-OMe, 2,6-Me$_2$, 3,5-Me2

39

Scheme 10. N,N,P and N,N,S ligands.

O- and *m*-substituents on the P and S pendant donor reduced the capacity of precatalysts to transform ethylene. Considering the phosphorous atom, replacing the phenyl rings by cyclohexyl ones led to a decrease in activity (6.9×10^5 g/mol•h•atm for R^2= Ph and 2.1×10^5 g/mol•h•atm for R^2= CyH). The influence of electronics variations was set out with N, N, S ligands. For R^1= 2,6-Me$_2$, complex with *p*-^{t}Bu substituent on the thioether ring was more active than its analogues functionalized on the *p*-position by chloro and methoxy groups (8.1×10^5 g/mol•h•atm for R^2= 4-^{t}Bu; 3.1×10^5 g/mol•h•atm R^2= 4-Cl and 5.8×10^5 g/mol•h•atm for R^2= 4-OMe). Tested under the same conditions, mono *o*-Me substituted iron(II) bis(imino)pyridine exhibited an activity of 1.5×10^6 g/mol•h•atm revealing the great potential of α-diimine ligands with pendant S and P donor.

8. "Orphan" tridentate ligands

Like in the cases of bis(imino)furan **16** and bis(imino)thiophene **17**, ligands **40** and **41** did not succeed in ligating iron.[18] Polymerization of ethylene was observed when ligand **42** was used.[59] Tridentate ligands **43** and **44** led to inactive iron precursors towards ethylene oligomerization either with $AlEt_3$ or MAO as cocatalysts.[60] Reaction of ligands **45** with $FeCl_2$ in *n*-BuOH at elevated temperature gave mononuclear complex for Ar = 2,6-$Me_2C_6H_3$ while the binuclear complex was obtained for Ar = 2,4,6-$Me_3C_6H_2$. In both cases, neutral N,NH,NH ligands were coordinated to the metal center. Upon activation with MAO in high ratio (Al/Fe = 400), iron precursors oligomerized ethylene with quietly low activities (~10^3 g/mol•h•atm).[61,62] Cobalt analogues exhibited higher activities (~10^4 g/mol•h•atm).

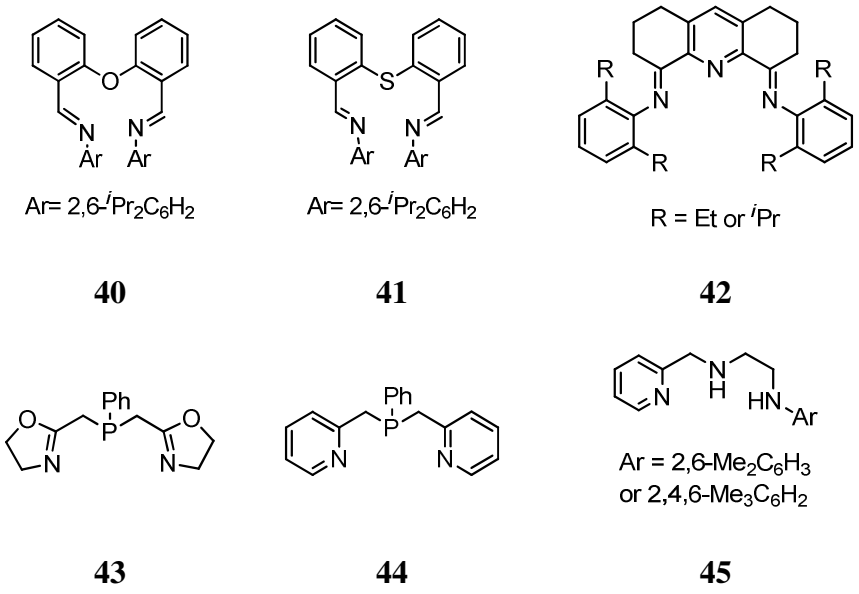

Scheme 11. Various tridentate ligands.

II. Bidentate ligands

Lower interest was brought to develop bidentate iron precatalysts for the oligomerization and/or polymerization of ethylene. The main reason could be that these systems yield to lower activities in comparison with tridentate analogs. However, regarding to the literature, iron complexes bearing bidentate ligands were good activators in atom transfer radical polymerization.[63]

Wang *et al.* synthesized iron, cobalt and nickel complexes bearing N, N ligands **46** for the ethylene oligomerization (Scheme 12). When MAO was used as cocatalyst, iron complexes exhibited low activity toward ethylene oligomerization while moderate activities were obtained with 1500 equiv of MMAO (5.50×10^5g/mol•h•atm). With higher ratio, the activity slightly decreased (5.18×10^5g/mol•h•atm for Al/Fe = 2000).[64] Sun and co-workers prepared a series of 2-(Ethylcarboxylato)-6-iminopyridyl complexes from ligands **47**.[65] Ferrous complexes were characterized by FT-IR spectroscopy. The slight wavenumber shift of 10-20 cm^{-1} in the C=O stretching vibrations suggested the presence of a weak interaction between the iron and the carbonyl oxygen of the ester group. However, all complexes were chelated by bidentate ligands excepted for R = Et. In this case, crystals exhibited a Fe-O bond of 2.3769 Å. Upon activation of MAO (Al/Fe = 1000) in dichloromethane, all ferrous complexes exhibited moderate activities in ethylene oligomerization and polymerization (~10^4 g/mol•h•atm). Olefins were obtained in good to high linear α-selectivities (93% for R = Br to

99% for R = Me). Bowkamp *et al.* coordinated dimine ligand $(Ph_2CN)_2C_2H_4$ **48** on iron(II) center.[66] Treatment of ferrous chloride complexes with MAO in toluene under pressure of ethylene (5 bar) did not yield to ethylene uptake. While α-diimine iron(II) complexes bearing ligands **49** developed by Chirik in 2004 polymerized ethylene with low activities.[67] The activity of the four coordinated iron precatalysts was significantly diminished in comparison to the Brookhart-Gibson five coordinated iron(II) dichloride complexes. The origin of this effect is most likely electronic rather than steric in origin.[68] Ligands **50** and **51** also yield to poorly active systems in the same conditions as for ligand **49**.

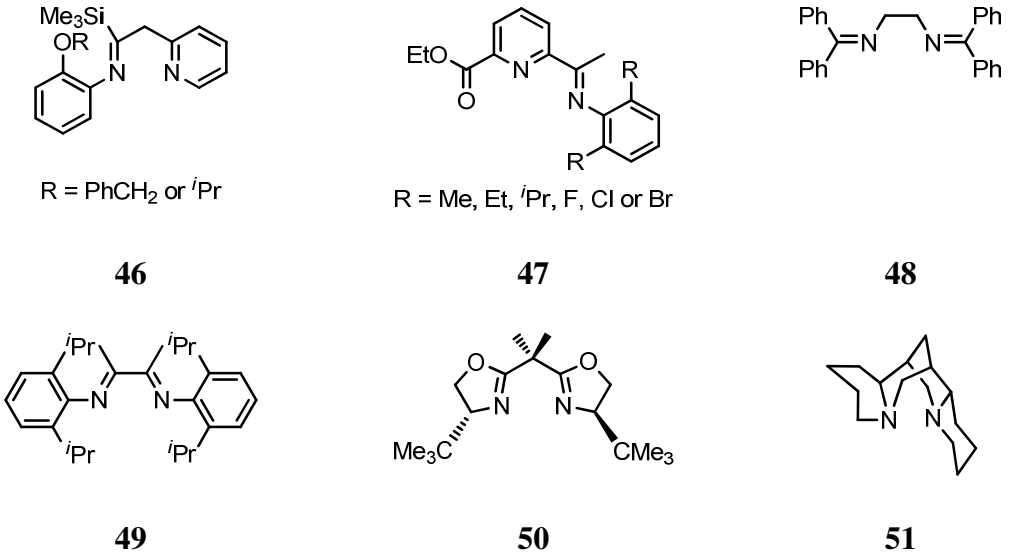

46 **47** **48**

49 **50** **51**

Scheme 12. Bidentate ligands.

Stephan and co-workers reported on the use of pyridine- and imidazole-phosphinimine ligands **52**, **53** and **54** in the synthesis of bidentate iron(II) complexes.[68] Tested in oligomerization process, complexes exhibited very low activities ($<10^3$ g/mol•h•atm). The same behavior was observed for ligands **55** developed by Kempe *et al.*[69] New bidentate bis(imino)cyclodisphophazane ligands **56** led to inactive system when associated with iron center. However, they yield to active systems once coordinated to nickel and cobalt center.[70] Sun and coworkers developed a range of bidentate ligand based on quinoxaline **57**[71] and quinolines ligands (**58** and **59**).[72,73] The iron complex containing 2-(2-pyridyl)quinoxaline ligands gave only marginal activity. According to the authors, this result may be attributed to the improper electronic environment provided by coordinated iron centers. Upon activation with MMAO, systems involving ligands **58** exhibited activities toward ethylene dimerization while bidentate iron(II) dichloride complexes bearing susbstituted 8-(benzimidazol-2-

yl)quinolines were active toward ethylene polymerization. However, activities remained low in both cases (~10^4 g/mol•h•atm). Sun *et al.* synthesized a series of 2-(benzimidazolyl)pyridine derivatives (**60**, **61** and **62**), starting from *o*-phenylenediamine and 2,6-dimethylpyridine.[40] Treatment of theses ligands with iron or cobalt dichloride gave the desired N,N bidentate complexes. Upon activation with MAO, MMAO or DEAC, these iron and cobalt complexes gave low ethylene oligomerization activities (~ 10^4 g/mol•h•atm).

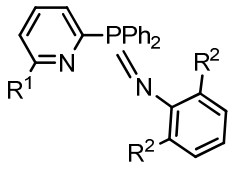

R^1= H, Me, Bn, $SiMe_3$ or Ph
R^2= Me or ^{i}Pr

52

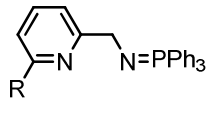

R = H, Me or Ph

53

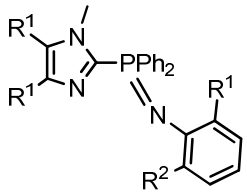

R^1= H, Ph, C_4H_4 or ^{t}Bu
R^2= Me or ^{i}Pr

54

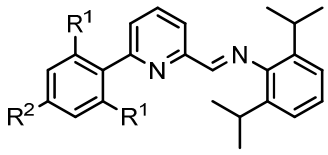

R^1= Me or Ph
R^2= H or ^{i}Pr

55

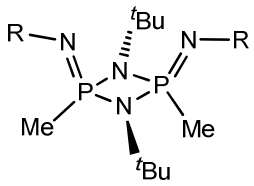

R = $SiMe_3$, 2,6-^{i}PrC_6H_3 or 1-adamantyl

56

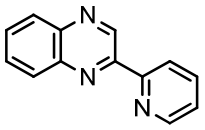

57

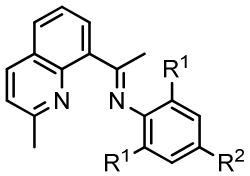

R^1= Me, Et or ^{i}Pr
R^2= H or Me

58

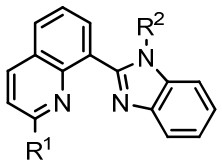

R^1= Me, Et, Pr or Ph
R^2= H, Me, Et or ^{i}Pr

59

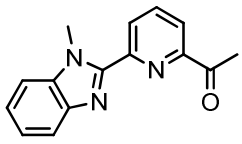

60

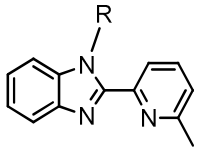

R = H or Me

61

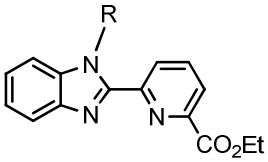

R = H or Me

62

Scheme 13. Bidentate ligands.

III. Anionic ligands

Very few examples of anionic ligands used in the design of new efficient iron precatalysts for the transformation of ethylene were reported.

The 2,5-bis(imino)pyrrole **63** were synthesized by condensation of pyrrole-2,5-dicarboxaldehyde with 2,6-di-iso-propylaniline in methanol.[21] Previously depronated by *n*-BuLi in Et_2O, the lithium salt of **63** was then chelated on iron center. Two equiv of depronated ligand were chelated on iron center yielding to [Fe(**63**)$_2$]. It is apparent that **63** acted exclusively as a monoanionic bidentate ligand but not as a tridentate one. Upon activation with MAO, no ethylene uptake was observed with neutral bisligand complex [Fe(**63**)$_2$]. Britovsek and co-workers developed iron complexes in association with bis(imino)carbozole ligands **64**.[17,18] Deprotonation of these ligands can be achieved in THF solution using either *n*-BuLi at room temperature or NaH at 65 °C. Only mesityl ligands were isolated as lithium salts and characterized by NMR spectroscopy. The others deprotonated ligands were used *in situ*. For R= Me and ^{t}Bu and R'= 2,4,6-$Me_3C_6H_2$, Ph and ^{i}Pr, iron(III) complexes were obtained by reaction of the lithium salt ligand with $FeCl_3$. Only one iron(II) complex was synthesized from deprotonated ligand (R=Me and R'= Ph). All iron complexes led to form inactive precursors for ethylene transformation upon activation with MAO. According to the authors, the absence of any activity was most likely a consequence of steric crowding around the metal center. Matsui and Mastunaga independently reported the use of ligands **64** in combination with iron(II)[74] or iron(III)[75] precursors for the polymerization of ethylene.

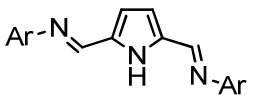

Ar = 2,6-^{i}PrC$_6$H$_3$

63

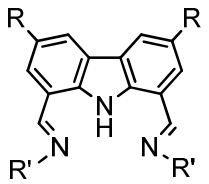

R'= 2,4,6-$Me_3C_6H_2$, Ph or ^{i}Pr
R = ^{t}Bu or Me

64

Scheme 14. Tridentate N,N(H),N ligands.

Conclusion

Since the discovery of the bis(imino)pyridine systems, a wide range of complexes have been developed for the ethylene oligomerization by iron complexes. Most of the systems are composed of iron(II) complexes chelated by neutral N,N,N tridentate ligands. The framework of the ligands was composed of benzimidazole, phenanthroline, pyridine, quinoline or quinoxaline rings. Diversity was brought by the use of tridentate N,N,L (L = N,S,P and O) ligands. The highest activity was observed for L = S and P. In general, iron complexes oligomerize ethylene with activities in the range of 10^4 g/mol•h•atm - 10^6 g/mol•h•atm and high selectivities. In spite of many efforts, none of the ligands mentioned in this chapter yield to systems enable to transform ethylene with similar or higher activities than for bis(imino)pyridine iron complexes (10^7 g/mol•h•atm). The catalytic behavior and the product distribution could be tuned by the modifications of the ligands on the different positions of the ligands backbone although in some cases the correlation is not so obvious. Some examples of neutral bidentate ligands were reported but activities remained lower in comparison with tridentate analogs. No activity was observed for the anionic bidentate and tridentate systems described.

Bibliography studies on the binuclear iron complexes used in ethylene oligomerization and on activators for the oligomerization of ethylene by iron complex will be reported in chapter III and chapter IV, respectively.

Bibliography

1. Natta, G. *Angew. Chem.* **1956**, *68*, 393.
2. Ziegler, K.; Holzkamp, E.; Martin, H.; Breil, H. *Angew. Chem.* **1955**, *67*, 541.
3. Natta, G.; Pino, P.; Mazzanti, G.; Giannini, U. *J. Am. Chem. Soc.* **1957**, *79*, 2975.
4. Breslow, D. S.; Newburg, N. R. *J. Am. Chem. Soc.* **1957**, *79*, 5072.
5. Peuckert, M.; Keim, W. *Organometallics* **1983**, *2*, 594.
6. Kaminsky, W. *Macromol. Chem. Phys.* **1996**, *197*, 3907.
7. Brintzinger, H. H.; Fischer, D.; Mülhaupt, R.; Rieger, B.; Waymouth, R. M. *Angew. Chem. Int. Ed. Engl.* **1995**, *34*, 1143.
8. Johnson, L. K.; Killian, C. M.; Brookhart, M. *J. Am. Chem. Soc.* **1995**, *117*, 6414.
9. Small, B. L.; Brookhart, M. *J. Am. Chem. Soc.* **1998**, *120*, 7143.
10. Britovsek, G. J. P.; Gibson, V. C.; Kimberley, B. S.; Maddox, P. J.; McTavish, S. J.; Solan, G. A.; White, A. J. P.; Williams, D. J. *Chem. Commun.* **1998**, 849.
11. Small, B. L.; Brookhart, M.; Bennett, A. M. A. *J. Am. Chem. Soc.* **1998**, *120*, 4049.
12. Bianchini, C.; Giambastiani, G.; Luconi, L.; Meli, A. *Coord. Chem. Rev.* **2010**, *254*, 431.
13. Bianchini, C.; Giambastiani, G.; Rios, I. G.; Mantovani, G.; Meli, A.; Segarra, A. M. *Coord. Chem. Rev.* **2006**, *250*, 1391.
14. Gibson, V. C.; Redshaw, C.; Solan, G. A. *Chem. Rev.* **2007**, *107*, 1745.
15. Radhakrishnan, K.; Cramail, H.; Deffieux, A.; Francois, P.; Momtaz, A. *Macromol. Rapid Commun.* **2003**, *24*, 251.
16. Flory, P. J. *J. Am. Chem. Soc.* **1940**, *62*, 1561.
17. Gibson, V. C.; Spitzmesser, S. K.; White, A. J. P.; Williams, D. J. *Dalton Trans.* **2003**, 2718.
18. Britovsek, G. J. P.; Gibson, V. C.; Hoarau, O. D.; Spitzmesser, S. K.; White, A. J. P.; Williams, D. J. *Inorg. Chem.* **2003**, *42*, 3454.
19. Beaufort, L.; Benvenuti, F.; Noels, A. F. *J. Mol. Catal. A: Chem* **2006**, *260*, 210.
20. Beaufort, L.; Benvenuti, F.; Noels, A. F. *J. Mol. Catal. A: Chem* **2006**, *260*, 215.
21. Dawson, D. M.; Walker, D. A.; Thornton-Pett, M.; Bochmann, M. *J. Chem. Soc. , Dalton Trans.* **2000**, 459.

22. Tenza, K.; Hanton, M. J.; Slawin, A. M. Z. *Organometallics* **2009**, *28*, 4852.

23. Nomura, K.; Sidokmai, W.; Imanishi, Y. *Bull. Chem. Soc. Jpn.* **2000**, *73*, 599.

24. Britovsek, G. J. P.; Baugh, S. P. D.; Hoarau, O.; Gibson, V. C.; Wass, D. F.; White, A. J. P.; Williams, D. J. *Inorg. Chim. Acta* **2003**, *345*, 279.

25. Nakayama, Y.; Baba, Y.; Yasuda, H.; Kawakita, K.; Ueyama, N. *Macromolecules* **2003**, *36*, 7953.

26. Gibson, V. C.; Redshaw, C.; Solan, G. A.; White, A. J. P.; Williams, D. J. *Organometallics* **2007**, *26*, 5119.

27. Britovsek, G.; Gibson, V.; Mastroianni, S.; Oakes, D.; Redshaw, C.; Solan, G.; White, A.; Williams, D. *Eur. J. Inorg. Chem.* **2001**, *2001*, 431.

28. Van Stein, G. C.; Van Koten, G.; Blank, F.; Taylor, L. C.; Vrieze, K.; Spek, A. L.; Duisenberg, A. J. M.; Schreurs, A. M. M.; Kojić-Prodić, B.; Brevard, C. *Inorg. Chim. Acta* **1985**, *98*, 107.

29. Yates, P. C.; Drew, M. G. B.; Trochagrimshaw, J.; Mckillop, K. P.; Nelson, S. M.; Ndifon, P. T.; Mcauliffe, C. A.; Nelson, J. *J. Chem. Soc. Dalton* **1991**, 1973.

30. Bailey, N. A.; Eddy, M. M.; Fenton, D. E.; Moss, S.; Mukhopadhyay, A.; Jones, G. *Journal of the Chemical Society-Dalton Transactions* **1984**, 2281.

31. McGuinness, D. S.; Gibson, V. C.; Steed, J. W. *Organometallics* **2004**, *23*, 6288.

32. Danopoulos, A. A.; Tsoureas, N.; Wright, J. A.; Light, M. E. *Organometallics* **2004**, *23*, 166.

33. Andersen, R. A.; Faegri, K.; Green, J. C.; Haaland, A.; Lappert, M. F.; Leung, W. P.; Rypdal, K. *Inorg. Chem.* **1988**, *27*, 1782.

34. Danopoulos, A. A.; Tulloch, A. A. D.; Winston, S.; Eastham, G.; Hursthouse, M. B. *Dalton Trans.* **2003**, 1009.

35. Britovsek, G. J. P.; Mastroianni, S.; Solan, G. A.; Baugh, S. P. D.; Redshaw, C.; Gibson, V. C.; White, A. J. P.; Williams, D. J.; Elsegood, M. R. J. *Chem. Eur. J.* **2000**, *6*, 2221.

36. Hao, P.; Chen, Y. J.; Xiao, T. P. F.; Sun, W. H. *J. Organomet. Chem.* **2010**, *695*, 90.

37. Gao, R.; Li, Y.; Wang, F. S.; Sun, W. H.; Bochmann, M. *Eur. J. Inorg. Chem.* **2009**, 4149.

38. Xiao, L. W.; Gao, R.; Zhang, M.; Li, Y.; Cao, X. P.; Sun, W. H. *Organometallics* **2009**, *28*, 2225.

39. Chen, Y. J.; Hao, P.; Zuo, W. W.; Gao, K.; Sun, W. H. *J. Organomet. Chem.* **2008**, *693*, 1829.

40. Sun, W. H.; Hao, P.; Zhang, S.; Shi, Q. S.; Zuo, W. W.; Tang, X. B.; Lu, X. M. *Organometallics* **2007**, *26*, 2720.

41. Song, S. J.; Gao, R.; Zhang, M.; Li, Y.; Wang, F. S.; Sun, W. H. *Inorg. Chim. Acta* **2011**, *376*, 373.

42. Zhang, M.; Zhang, W. J.; Xiao, T.; Xiang, J. F.; Hao, X.; Sun, W. H. *J. Mol. Catal. A: Chem.* **2010**, *320*, 92.

43. Wang, L. O.; Sun, W. H.; Han, L. Q.; Yang, H. J.; Hu, Y. L.; Jin, X. G. *J. Organomet. Chem.* **2002**, *658*, 62.

44. Jie, S. Y.; Zhang, S.; Sun, W. H.; Kuang, X. F.; Liu, T. F.; Guo, J. P. *J. Mol. Catal. A: Chem.* **2007**, *269*, 85.

45. Sun, W. H.; He, S. Y.; Zhang, S.; Zhang, W.; Song, Y. X.; Ma, H. W. *Organometallics* **2006**, *25*, 666.

46. Sun, W. H.; Zhang, S.; Zuo, W. W. *C. R. Chimie* **2008**, *11*, 307.

47. Jie, S.; Zhang, S.; Sun, W. H. *Eur. J. Inorg. Chem.* **2007**, 5584.

48. Zhang, M.; Gao, R.; Hao, X.; Sun, W. H. *J. Organomet. Chem.* **2008**, *693*, 3867.

49. Zhang, M.; Hao, P.; Zuo, W. W.; Jie, S. Y.; Sun, W. H. *J. Organomet. Chem.* **2008**, *693*, 483.

50. Wang, K.; Wedeking, K.; Zuo, W.; Zhang, D.; Sun, W. H. *J. Organomet. Chem.* **2008**, *693*, 1073.

51. Zhang, S.; Sun, W. H.; Xiao, T. P.; Hao, X. *Organometallics* **2010**, *29*, 1168.

52. Adewuyi, S.; Li, G.; Zhang, S.; Wang, W.; Hao, P.; Sun, W. H.; Tang, N.; Yi, J. *J. Organomet. Chem.* **2007**, *692*, 3532.

53. Sun, W. H.; Hao, P.; Li, G.; Zhang, S.; Wang, W. Q.; Yi, J. J.; Asma, M.; Tang, N. *J. Organomet. Chem.* **2007**, *692*, 4506.

54. Svejda, S. A.; Brookhart, M. *Organometallics* **1999**, *18*, 65.

55. Svejda, S. A.; Brookhart, M. *Organometallics* **1998**, *18*, 65.

56. Small, B. L.; Rios, R.; Fernandez, E. R.; Carney, M. J. *Organometallics* **2007**, *26*, 1744.

57. Schmiege, B. M.; Carney, M. J.; Small, B. L.; Gerlach, D. L.; Halfen, J. A. *Dalton Trans.* **2007**, 2547.

58. Small, B. L.; Rios, R.; Fernandez, E. R.; Gerlach, D. L.; Halfen, J. A.; Carney, M. J. *Organometallics* **2010**, *29*, 6723.

59. Appukuttan, V. K.; Liu, Y.; Son, B. C.; Ha, C. S.; Suh, H.; Kim, I. *Organometallics* **2011**, *30*, 2285.

60. Kermagoret, A.; Tomicki, F.; Braunstein, P. *Dalton Trans.* **2008**, 2945.

61. Davies, C. J.; Fawcett, J.; Shutt, R.; Solan, G. A. *Dalton Trans.* **2005**, 2630.

62. Cowdell, R.; Davies, C. J.; Hilton, S. J.; Marechal, J. D.; Solan, G. A.; Thomas, O.; Fawcett, J. *Dalton Trans.* **2004**, 3231.

63. Shaver, M. P.; Allan, L. E. N.; Rzepa, H. S.; Gibson, V. C. *Ang. Chem. Int. Edit.* **2006**, *45*, 1241.

64. Wang, L.; Zhang, C.; Wang, Z. X. *Eur. J. Inorg. Chem.* **2007**, 2477.

65. Sun, W. H.; Tang, X. B.; Gao, T. L.; Wu, B.; Zhang, W. J.; Ma, H. W. *Organometallics* **2004**, *23*, 5037.

66. Volbeda, J.; Meetsma, A.; Bouwkamp, M. W. *Organometallics* **2009**, *28*, 209.

67. Bart, S. C.; Hawrelak, E. J.; Schmisseur, A. K.; Lobkovsky, E.; Chirik, P. J. *Organometallics* **2003**, *23*, 237.

68. Spencer, L. P.; Altwer, R.; Wei, P.; Gelmini, L.; Gauld, J.; Stephan, D. W. *Organometallics* **2003**, *22*, 3841.

69. Irrgang, T.; Keller, S.; Maisel, H.; Kretschmer, W.; Kempe, R. *Eur. J. Inorg. Chem.* **2007**, *2007*, 4221.

70. Axenov, K. V.; Leskela, M.; Repo, T. *J. Catal.* **2006**, *238*, 196.

71. Shao, C.; Sun, W. H.; Li, Z.; Hu, Y.; Han, L. *Catal. Commun.* **2002**, *3*, 405.

72. Song, S.; Xiao, T.; Redshaw, C.; Hao, X.; Wang, F.; Sun, W. H. *J. Organomet. Chem.* **2011**, *696*, 2594.

73. Xiao, T.; Zhang, S.; Kehr, G.; Hao, X.; Erker, G.; Sun, W. H. *Organometallics* **2011**, *30*, 3658.

74. Matsui, S.; Nitabaru, M.; Tsuru, K.; Fujita, T.; Suzuki, Y.; Takagi, Y.; Tanaka, H. Mitsui Chemicals, Inc. Japan. Catalysts for olefin polymerization and polymerization method. WO 9954364, **Jun 4**, **2002**.

75. Matsunaga, P. T. Exxon Chemical Patents Inc., USA. Tridentate ligand-containing metal catalyst complexes for olefin polymeriza-tion. WO 9957159 A1, **Apr 29**, **1999**.

CHAPTER II

Anionic *N*,*N*,*N*-Ligand for the Selective Iron(III)-Catalyzed Oligomerization of Ethylene

Abstract: This chapter deals with the synthesis of iron(III) complexes chelated by a tridentate monoanionic ligand. Only the complex chelated by a monoanionic 1,2-dihydro-1,10-phenathroline ligand was active toward catalytic ethylene transformation. This complex has been characterized by FT-IR, EXAFS and XANES spectroscopy, mass spectrometry and X-ray diffraction. When activated by MAO, this precatalyst forms a stable active species for the selective oligomerization of ethylene. Up to 63 wt% of butenes is obtained with a selectivity of 98% in 1-butene. Considering the inactivity of iron(II) and iron(III) complexes chelated by related neutral ligand and of an iron(II) precursor chelated by the same monoanionic ligand, the synergistic influence of the anionic character of the ligand and the +III oxidation state of the iron precursor for the oligomerization of ethylene is thus established.

Résumé : L'étude des complexes de fer(III) chélatés par un ligand monoanionique tridente a montré que seul le ligand 1,2-dihydro-1,10-phénantroline, sous sa forme anionique, a conduit à une espèce de fer(III) active. Ce complexe de fer a été caractérisé par spectrométrie FT-IR, EXAFS et XANES, par spectrométrie de masse et par diffraction des rayons X. Activé par le MAO, le complexe de fer(III) conduit à une espèce active stable sur 2 heures de réaction et produit majoritairement du butène (63%) avec une sélectivité en butène-1 de 98%. L'inactivité des précurseurs de fer(II) et de fer(III) chélatés par le ligand sous forme neutre ainsi que celle du précurseur de fer(II) chélaté par ce même ligand sous sa forme anionique a mis en évidence la nécessité d'avoir un ligand anionique coordinné sur du fer à l'état d'oxydation +III.

Introduction

Linear α-olefins (LAO) are of considerable importance in the chemical and petrochemical industries. They represent an expanding market with a total demand of 4.2 million tons in 2008 and an estimated average annual growth rate of 3.5% (2006-2020). The demand for LAO is growing faster in the C_4-C_{10} range than in the C_{12+} range. Light LAO (C_4-C_8) are mainly used as comonomers in the copolymerization of ethylene to produce high-density polyethylene and linear low-density polyethylene. Several processes lead from short (C_4-C_8) to full range (C_6-C_{30}) distributions in LAOs, such as the Shell Higher Olefin Process (SHOP), Gulfene process (Chevron-Phillips), Ethyl process (Ineos) or Idemitsu process[1-4] whereas other processes are highly selective for the formation of 1-butene (AlphaButol™[5,6]) or 1-hexene (AlphaHexol™[4] and Phillips processes).[7,8] Whereas iron catalysts proved to be good polymerization catalysts, the initial discoveries of Brookhart[9,10] and Gibson[11,12] triggered considerable interest for iron(II) complexes with neutral tridentate N,N,N ligands as precursors to highly active and selective catalysts for the oligomerization of ethylene.[13-21] The exact mechanism of olefin polymerization/oligomerization and whether the active species formed by treatment of the catalyst precursor with MAO is an iron(II) or an iron(III) species remain under discussion.[22-24] Only few catalytic systems have been reported so far using iron(III) precursors,[25-27] and they led to good activities and modest selectivities for light C_4-C_{12} LAO (Schulz-Flory constant ~ 0.6). Whereas mostly neutral tridentate N,N,N ligands-based systems have been published, a larger diversity of ligands is highly desirable and crucial for optimizing an iron-based oligomerization process. Only few examples have been reported on the use of anionic ligands, in combination with iron(II)[22,28] or iron(III)[29] precursors, but these afforded inactive or poorly active systems, suggesting that an electron-rich central donor group might be detrimental for catalytic activity.[22]

We report here preliminary results on a novel catalytic system based on an iron(III) complex formed by treatment of an anionic ligand with an iron(III) precursor. This remarkably stable precatalyst affords interesting selectivity in the oligomerization of ethylene to short chain linear α-olefins.

I. Synthesis and characterization of iron complexes

1. Systems involving ligand 1,2-dihydro-1,10-phenanthroline

The condensation reaction of 2-acetylpyridine with 8-aminoquinoline was performed in refluxing methanol with formic acid as catalyst. The original ligand 2-methyl-2,4-di(pyridin-2-yl)-1,2-dihydro-1,10-phenanthroline (H**1**) was obtained in low yield (30%) due to both undesired hydrolysis reaction and purification process (Scheme 1).[30] The presence of both the enolizable 2-acetylpyridine ketone and the 8-aminoquinoline enables a Mannich-type reaction to take place, followed by a cyclization under mild conditions which involves aromatic C–H activation and C–C bond formation. Full characterization of the ligand and a proposed mechanism for its formation were previously reported.[31]

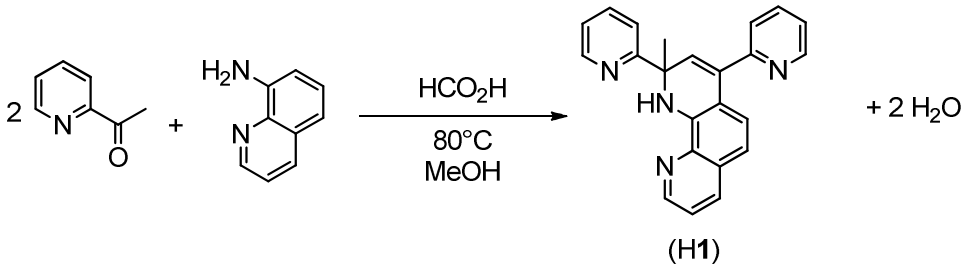

Scheme 1. Condensation reaction of acetylpyridine with 8-aminoquinoleine derivative.

Crystals suitable for an X-ray diffraction study of (H**1**) were grown from a concentrated CH_2Cl_2 solution (Figure 1). Selected bonds distances and angles are listed in the caption to Figure 1. The C12 atom is only 0.380 Å away from the plane N1-C10-N11. The slight twist of the ring containing the N11 nitrogen is consistent with the value of the N11-C12-C19 angle (107.98(15)°). The pyridine ring at C12 is almost perpendicular to the mean plane defined by the phenanthroline entity (82.69 Å) while the methyl group at the C12 atom pointed down to this plane.

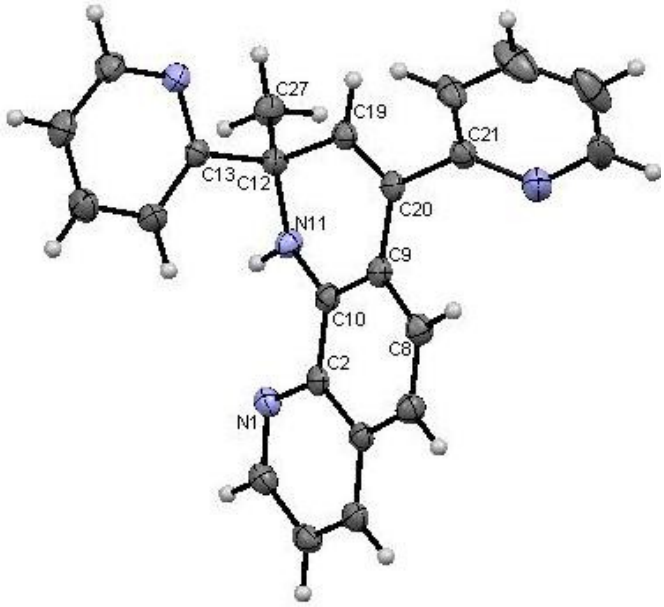

Figure 1. ORTEP view and atom numbering scheme of the structure of (H**1**). Thermal ellipsoids are represented at the 50% level. Selected bond distances (Å) and angles (°): C12-C27 = 1.530(3), C12-C13 = 1.542(3), C19-C20 = 1.341(3), C10-N11 = 1.371(2), C20-C21 = 1.496(2); N1-C2-C10 = 117.44(17), C2-C10-N11 = 119.33(17), N11-C12-C19 = 107.98(15), C13-C12-C27 = 109.43(15), C20-C9-C8 = 124.05(17)

Five metal complexes were synthesized from ligand (H**1**), coordinated as a neutral ligand in [$FeCl_2$(H**1**)], [$CoCl_2$(H**1**)] and [$FeCl_3$(H**1**)] or as an anionic ligand in iron(II) and iron(III) complexes [FeCl(**1**)] and [$FeCl_2$(**1**)], respectively (Scheme 2). Iron and cobalt precursors are possible candidates for catalytic oligomerization studies.[32-34] Their coordination properties are often similar but the catalytic performances are in general lower for cobalt compared to iron. Complexes chelated by the neutral ligand were synthesized by stirring an equimolar mixture of the ligand and the metal precursor ($FeCl_2 \cdot 4H_2O$ for [$FeCl_2$(H**1**)], $CoCl_2 \cdot 6H_2O$ for [$CoCl_2$(H**1**)] and $FeCl_3$ for [$FeCl_3$(H**1**)]) in THF overnight. The desired complexes were isolated in good yield as pink powders for the iron(II) and cobalt(II) complexes and as a purple powder for the iron(III) compound. Complexes [FeCl(**1**)] and [$FeCl_2$(**1**)] were synthesized by deprotonation of (H**1**) with *n*-BuLi, the solution being subsequently added to $FeCl_2 \cdot 1.5$THF or $FeCl_3$, respectively. The purple iron(III) complex shows good stability in the solid-state and in solution.

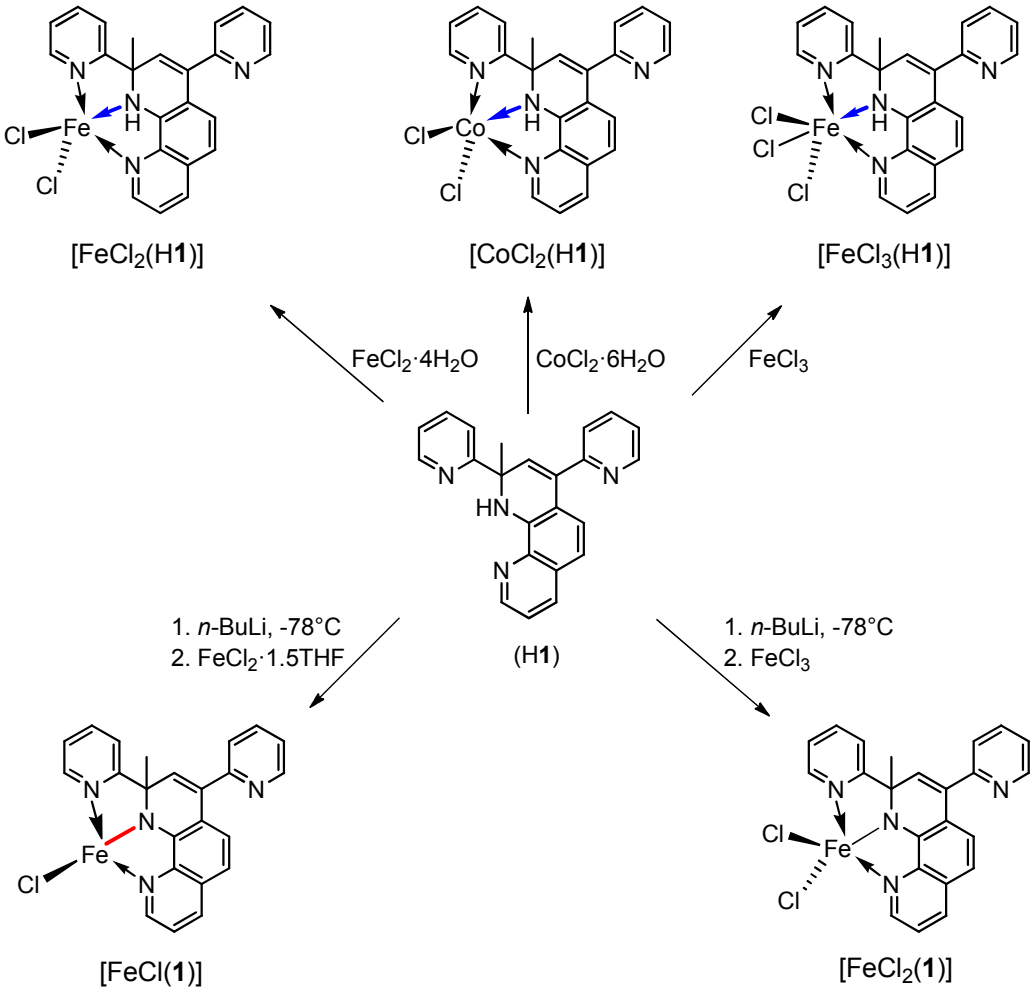

Scheme 2. 1,2-dihydro-1,10-phenanthroline iron and cobalt complexes.

All complexes were characterized by FT-IR spectroscopy. Their spectra exhibit the expected shift of the absorption band of the imino groups of the heterocycles ($\nu_{C=N}$) to lower wavenumbers, associated with a weaker intensity in comparison with the free ligand (Figure 2). These observations confirm the effective coordination of the ligand on the iron center.[20,25] The presence of the N-H bond in the FT-IR spectra of complexes [$FeCl_2$(H**1**)], [$CoCl_2$(H**1**)] and [$FeCl_3$(H**1**)] confirms the coordination of the neutral ligand to the metal. The absorption band of the N-H group is shifted in comparison with the free ligand (3373 cm^{-1} for ligand (H**1**)). This shift is more significant for the iron(III) complex [$FeCl_3$(H**1**)] (2962 cm^{-1}) than for iron(II) or cobalt(II) complexes [$FeCl_2$(H**1**)] and [$CoCl_2$(H**1**)] (3144 cm^{-1}). This is probably due to the increase of the acidic character of the iron(III) resulting from the inductive effect of the third chloride ligand. For complexes [FeCl(**1**)] and [$FeCl_2$(**1**)], the absence in the FT-IR spectra of the N-H band in the region 3300-3100 cm^{-1} confirms the anionic character of the ligand (Figure 2).

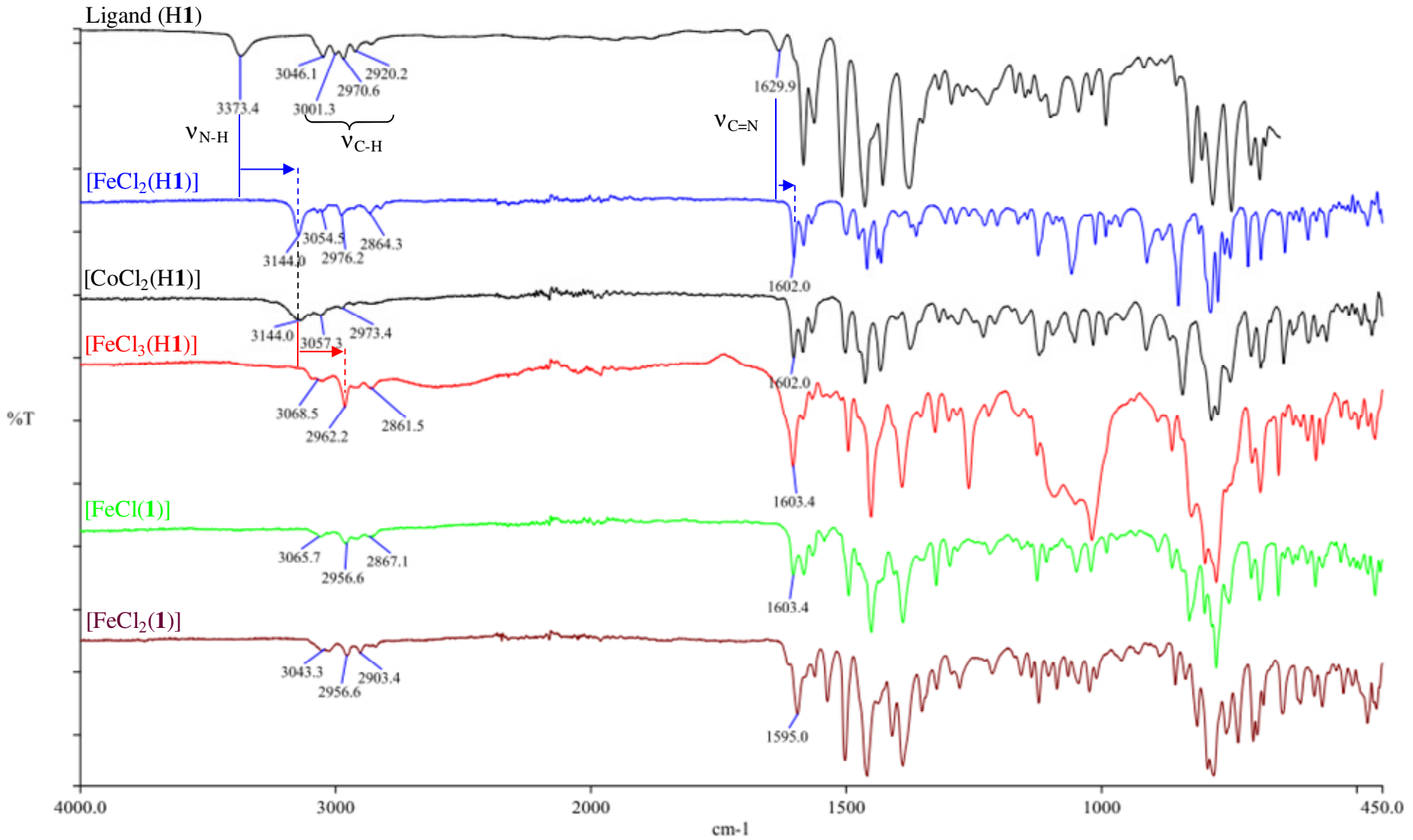

Figure 2. FT-IR spectra of ligand (H**1**) and corresponding iron and cobalt complexes.

XANES (X-ray Absorption Near Edge Structure) has been used to investigate the structure of inorganic complexes and to characterize iron active species in both mononuclear and binuclear non-heme iron enzymes.[35] The oxidation state of metal center can be deduced from the energy shift of the absorption edge or from pre-edge absorption features. Curves represent a projection of the electronic density of a sample and the oxidation state of complex is determined by their shape. We have used XANES to directly probe the oxidation state of the iron center in [$FeCl_2$(**1**)]. Measurements were performed on [$FeCl_2$(**1**)] and on two iron complexes taken as references: $FeCl_3$ and [$FeCl_2$(**BIP**)] (**BIP** = 2,6-bis-[1-(2-methylphenylimino)ethylpyridine iron(II) chloride) (Scheme 3).

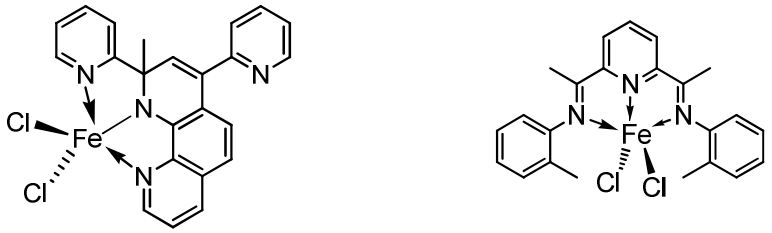

[$FeCl_2$(**1**)] [$FeCl_2$(**BIP**)]

Scheme 3. Structures of complexes [$FeCl_2$(**1**)] (left) and [$FeCl_2$(**BIP**)] (right).

XANES spectra for these three complexes are shown in Figure 3 with an expanded view of the 1s⟶3d pre-edge. The spectrum of [$FeCl_2$(**BIP**)] has a pre-edge peak at ~7112 eV with the same intensity as for [$FeCl_2$(**1**)]. The energy of the edge position (right part of the spectrum) is dependent upon the effective nuclear charge of the absorbing metal atom. This charge is governed by a combination of effects, including the formal metal oxidation state, the number and type of ligating atoms and the coordination geometry.[36,37] In our case, the ligand environment for both complexes [$FeCl_2$(**1**)] and [$FeCl_2$(**BIP**)] is similar; thus changes in the edge energy can be correlated to the iron oxidation state. The spectra for $FeCl_3$ and [$FeCl_2$(**1**)] have similar pre-edge features, each with a maximum at *ca.* 7114 eV, with a lower intensity for compound [$FeCl_2$(**1**)] in agreement with the +III oxidation state of its metal center (Figure 3).

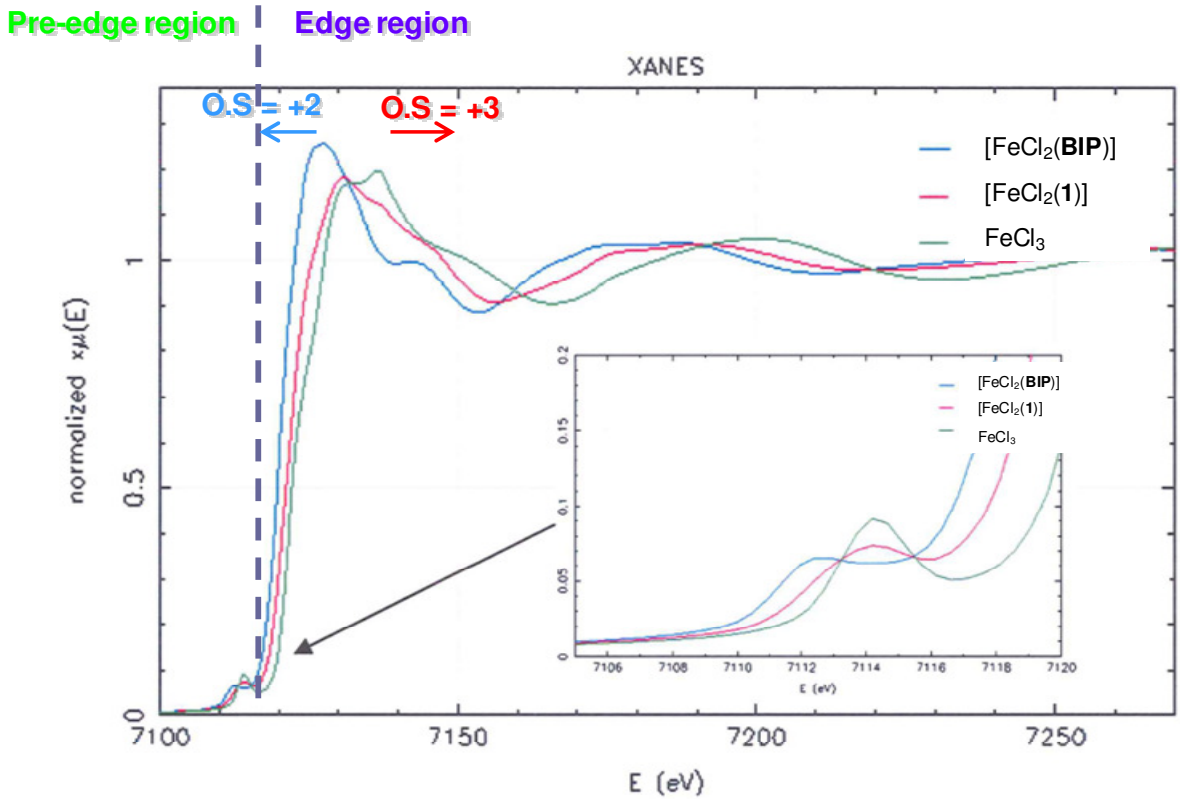

Figure 3. XANES spectra of [$FeCl_2$(**BIP**)] (blue), [$FeCl_2$(**1**)] (red) and $FeCl_3$ (green).

EXAFS (Extended X-ray absorption fine structure) spectroscopy provides information on the types of ligating atoms and very accurate first-shell iron-ligand distances. The nature of the atoms in the first coordination sphere of [$FeCl_2$(**1**)] was checked by comparison with the results obtained with [$FeCl_2$(**BIP**)]. From the similarity of the curves shapes one concludes that the two complexes have the same environment in the first coordination sphere of the metal (Figure 4). The Fe-N and Fe-Cl bond distances were determined and their values confirm the presence of a covalent Fe-N bond (Fe-N = 2.02±0.02 Å) and two dative bonds (Fe-N = 2.31±0.06 Å and 2.17±0.03 Å).

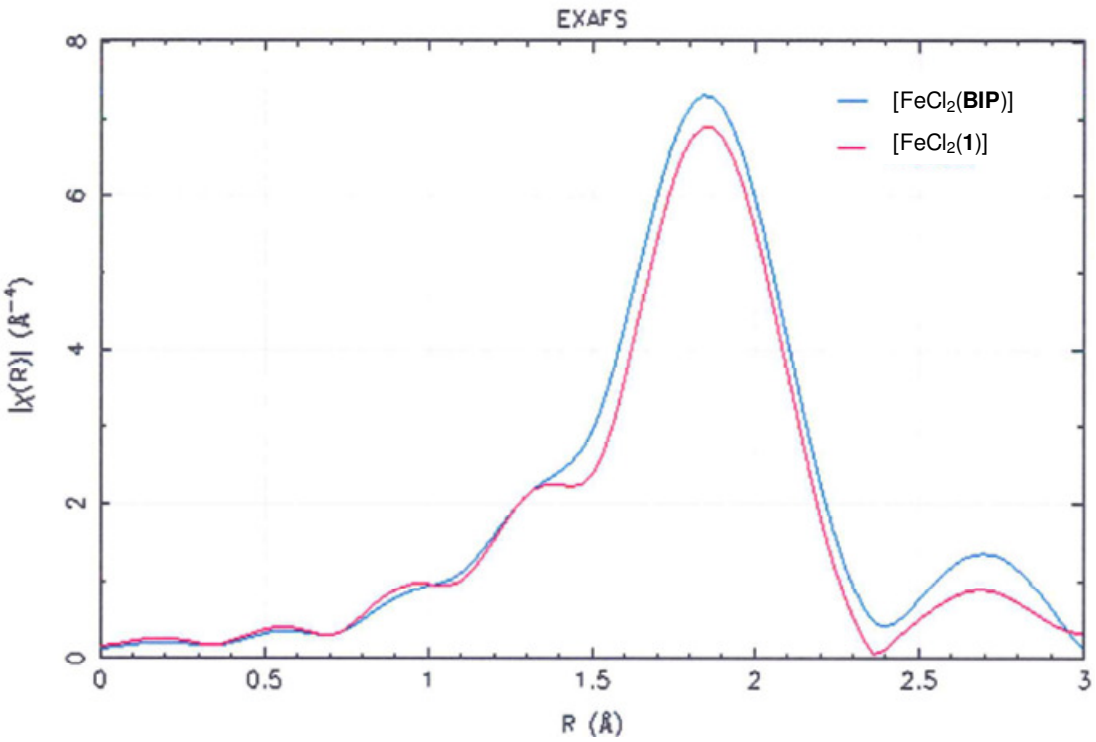

Figure 4. Fourier transform of EXAFS functions for [$FeCl_2$(**BIP**)] (blue) and [$FeCl_2$(**1**)] (red).

To better characterize the new iron complexes, high resolution mass spectrometry was performed on [$FeCl_2$(**1**)], [$FeCl_2$(H**1**)] and [$FeCl_3$(H**1**)]. The highest peaks for [$FeCl_2$(**1**)] ($M^{+\cdot}$: $C_{23}H_{17}N_4FeCl_2$), [$FeCl_2$(H**1**)] ($M^{+\cdot}$: $C_{23}H_{18}N_4FeCl_2$) and [$FeCl_3$(H**1**)] $(M\text{-}H)^+$: $C_{23}H_{17}N_4Fe_1Cl_3$) showed the expected isotopic distributions and allowed a clear identification of the complexes. Attempts to obtain satisfactory elemental analyses failed for the iron complexes although in the case of [$FeCl_2$(**1**)], the ratio Cl/Fe was in line with the expected value (see Experimental Section).

Attempts to obtain single crystals of [$FeCl_2$(H**1**)] and [$FeCl_3$(H**1**)] remained unsuccessful. However, slow diffusion of diethyl ether into a concentrated CH_2Cl_2 solution of the cobalt complex [$CoCl_2$(H**1**)] afforded single crystals suitable for X-ray diffraction (Figure 5). The metal coordination geometry is distorted trigonal bipyramidal, with the external nitrogen atoms N1 and N3 and Cl2 in the equatorial plane and the central nitrogen atom N2 and Cl1 in the apical positions. The N-H hydrogen is on the same side as the methyl group at C7 with respect to the pyridyl substituent at C9. As already observed with the free ligand (H**1**), the pyridine ring bore by the C6 carbon is almost perpendicular to the phenanthroline-type core. The presence of a N-H bond on the central nitrogen atom N2 was confirmed by FT-IR analysis ($\nu_{N\text{-}H}$ = 3144 cm^{-1}). The N2-Co1 bond length of 2.219(2) Å is typical for a dative bond.[38]

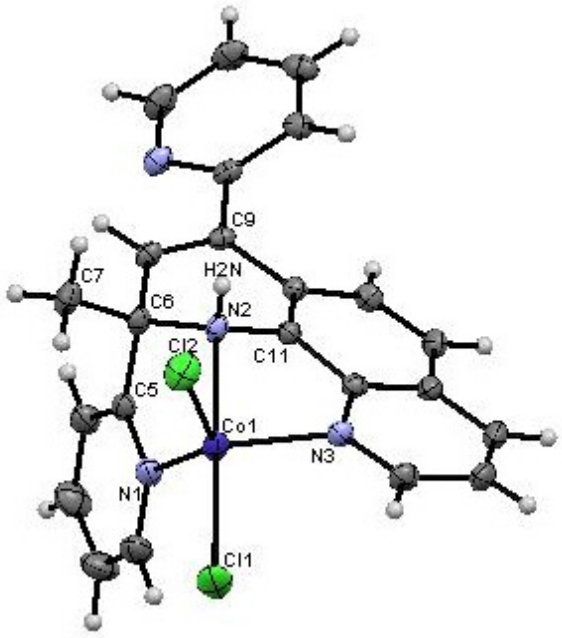

Figure 5. ORTEP and atom numbering scheme of complex [$CoCl_2$(H**1**)]. Thermal ellipsoids are represented at the 50% level. Selected bond distances (Å) and angles (°): Co1-N1 = 2.126(2), Co1-N2 = 2.219(2), Co1-N3 = 2.077(2), Co1-Cl1 = 2.301(1), Co1-Cl2 = 2.316(1), N2-H2N = 0.88(2); N1-Co1-N2 = 73.85(7), N2-Co1-N3 = 77.65(7), N1-Co1-Cl2 = 132.62(6), N3-Co1-Cl2 = 111.39(5), N2-Co1-Cl2 = 90.35(5), N3-Co1-Cl1 = 100.25(5), N2-Co1-Cl1 = 168.40(5), Cl2-Co1-Cl1 = 100.97(3).

Crystals of [$FeCl_2$(**1**)] suitable for X-ray diffraction were grown by diffusion of pentane into a chlorobenzene solution of the complex under inert atmosphere at room temperature (Figure 6). Selected bond lengths and angles are given in Figure 6. The metal is pentacoordinated, with a pseudo-square-pyramidal coordination geometry. The methyl and the free pyridyl groups are perpendicular to the plane defined by the iron atom and the three coordinated nitrogen atoms (N1, N2 and N3). The metrical parameters confirm the +III oxidation state of the metal, the short Fe-N2 bond distance of 1.950(2) Å being indicative of a covalent bond.[22,39] Compared to its orientation in [$CoCl_2$(H**1**)], the pyridine ring bore by the C12 carbon becomes coplanar to the Fe1, N1, N2 plane in [$FeCl_2$(**1**)]. The lengths of the dative bonds N1-Fe1 and N3-Fe1 are comparable to those for the cobalt(II) analog. The structural data confirm the results obtained by FT-IR spectroscopy (disappearance of the absorption band of the N-H group), XANES (oxidation state of +III) and EXAFS (iron environment and bond distances).

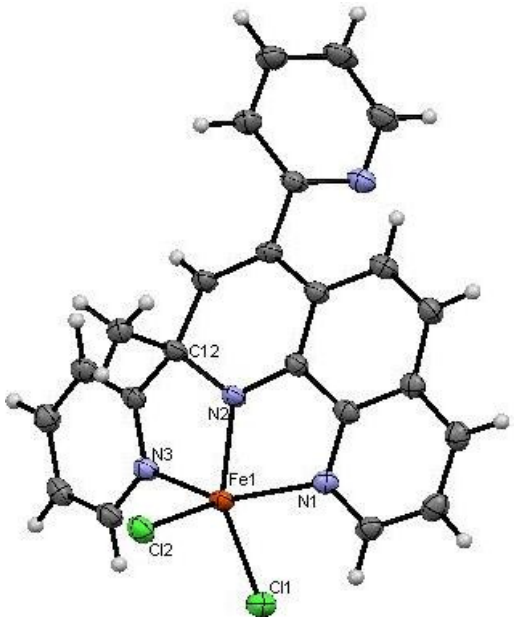

Figure 6. ORTEP and atom numbering scheme of complex [$FeCl_2$(**1**)] in [$FeCl_2$(**1**)]·C_6H_5Cl. The molecule of solvent has been omitted for clarity. Thermal ellipsoids are represented at the 50% level. Selected bond distances (Å) and angles (°): Fe1-N1 = 2.167(3), Fe1-N2 = 1.950(2), Fe1-N3 = 2.158(3), Fe1-N3 = 2.158(3), Fe1-Cl1 = 2.259(9), Fe1-Cl2 = 2.239(8); N1-Fe1-N2 = 77.42(10), N3-Fe1-N2 = 75.70(10), N1-Fe1-Cl2 = 104.75(7), N3-Fe1-Cl2 = 99.95(7), N2-Fe1-Cl2 = 111.12(8), N3-Fe1-Cl1 = 97.25(7), N2-Fe1-Cl1 = 141.27(8), Cl2-Fe1-Cl1 = 107.60(3).

2. Extension to bis(pyridylimino)isoindoline and di-(2-picolyl)amine ligands

Similarly to [$FeCl_2$(**1**)], [$FeCl_2$(**2**)] and [$FeCl_2$(**3**)], were obtained by deprotonation of (H**2**) and commercial (H**3**), respectively, and complexation with $FeCl_3$ in THF. The tridentate ligand (H**2**) was previously synthesized according to literature procedure and used without further purification.[40] The iron complexes [$FeCl_2$(**2**)][29] and [$FeCl_2$(**3**)] were synthesized in good yield (70%), as brown and green powders, respectively (Scheme 4).

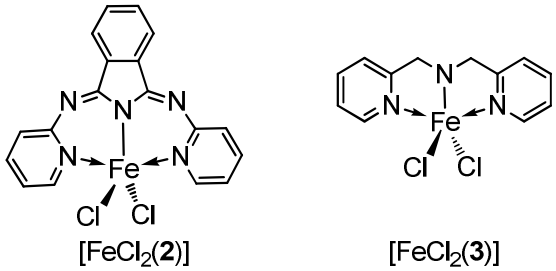

Scheme 4. Structures of iron(III) complexes.

Both complexes were characterized by FT-IR spectroscopy. For complex [$FeCl_2$(**2**)], the disappearance of the N-H band in the region of 3300-3100 cm^{-1} along with the shift of the absorption band of the imino bond ($\nu_{C=N}$) confirmed the coordination and the anionic character of the ligand.

In the case of [$FeCl_2$(**3**)], an IR absorption band at 3253 cm^{-1} casted doubt on the bonding mode of the ligand. However, the modification of the color of the solution when *n*-BuLi was added and the formation of a precipitate upon addition to the iron(III) solution provide a clear indicator of the metal complexation. Moreover, only minor modification of the absorption band of the imino group was observed. All iron(III) complexes show good stability in the solid state and in solution.

II. Reactivity of iron complexes toward ethylene

The catalytic activity of iron(II) and iron(III) complexes for the oligomerization of ethylene has been evaluated under commonly used pressure (30 bar) and optimised temperature (80 °C) in toluene. Below this temperature, no ethylene uptake was noticed.

The precatalyst [$FeCl_2$(**1**)], shows a good and stable activity in the presence of MAO at a ratio Al/Fe = 200 (Table 1, entry 1). Ethylene consumption was steady over 2 h with an activity of 2.16×10^5 g(products)·(mol(Fe)·h)$^{-1}$. Short chain oligomers (C_4-C_8) were obtained, with up to 63 wt% of butenes with a selectivity in 1-butene >97 wt% (Table 1, entry 1). Increasing the MAO concentration to reach a ratio Al/Fe = 500 led to a similar activity and a slight increase in polymer formation (14 wt%, Table 1, entry 2). With the alkylating agents trimethylaluminum (TMA) and diethylaluminum chloride (DEAC), tested at a ratio Al/Fe = 200, no consumption of ethylene was observed. Thus, MAO is crucial for activating the precatalyst. When additional TMA was used in a ratio MAO/TMA/Fe = 200/20/1, the activity slightly decreased and up to 66% of butenes were produced with a fraction of 1-butene > 98 wt%. For comparison, other Fe(II) or Fe(III) complexes bearing the 1,2-dihydro-1,10-phenanthroline ligand ([$FeCl_2$(H**1**)] and [$FeCl_3$(H**1**)]), or its deprotonated form [FeCl(**1**)], have been evaluated. But none of these complexes have shown activity toward ethylene oligomerization. These results reveal that both the anionic character of the ligand (complexes [$FeCl_2$(H**1**)] and [$FeCl_3$(H**1**)] *vs* complex [$FeCl_2$(**1**)]) and the +III oxidation state of the metal center (complexes [$FeCl_2$(H**1**)] and [FeCl(**1**)] *vs* complex [$FeCl_2$(**1**)]) are key parameters for obtaining an active catalyst.

The structure observed with [$CoCl_2$(H**1**)] reveals steric hindrance around the metal center due to one of the pyridine rings. The same geometry can be proposed for complex [$FeCl_2$(H**1**)] and so the steric bulk could prevent either the alkylation of iron center by MAO or the coordination of ethylene to the active species. One hypothesis for the nature of the active species formed by treatment of MAO with [$FeCl_2$(**1**)] is the cationic [FeMe(**1**)]$^+$[Cl-MAO]$^-$.[41,42] The first step would consist in the alkylation of the iron center by an exchange of X ligands with MAO yielding the intermediate [FeClMe(**1**)]. Subsequent chloride abstraction by MAO would lead to the active species. The fact that only one chloride is ligated to iron in [FeCl(**1**)] prevents the formation of a cationic methyl iron compound. Indeed, reaction of [FeCl(**1**)] with MAO probably yields [FeMe(**1**)] whose electrophilicity is lower because of the neutral form of the active species. This would decrease and even prevent the reactivity of the iron intermediate toward ethylene. Iron(II)-like complexes chelated by anionic 1,8-bis(imino)carbazolide ligands were inactive toward ethylene transformation.[22] Regarding the complex [$FeCl_3$(H**1**)], its inactivity is more difficult to rationalize.

Table 1. Catalytic ethylene oligomerization with iron precatalyst [$FeCl_2$(**1**)].[a]

Entry	Catalyst	Cocatalyst (eq.)	Activity[b]	Oligomer distribution[c,d]			PE
				C_4 (1-C_4)[e]	C_6 (1-C_6)[e]	$C_{\geq 8}$	
1	[$FeCl_2$(**1**)]	MAO (200)	2.16	63 (97)	18 (89)	7	12
2	[$FeCl_2$(**1**)]	MAO (500)	2.13	61 (95)	19 (87)	6	14
3	[$FeCl_2$(**1**)]	MAO/TMA (200/20)	1.34	66 (98)	16 (93)	7	12
4	[$FeCl_2$(**2**)]	MAO (500)	0[f]	-	-	-	-
5	[$FeCl_2$(**3**)]	MAO (500)	0[f]	-	-	-	-

[a] Fe (20 μmol), toluene (50 mL), ethylene pressure 30 bar, 80 °C, reaction time 2 h. [b] $\times 10^5$ g(products)·mol^{-1}(Fe)·h^{-1} estimated over the steady period of ethylene consumption. [c] Determined by GC. [d] wt% among all the products formed. [e] wt% in the C_n fraction. [f] no ethylene uptake.

Under the same conditions, no activity was obtained with complexes [$FeCl_2$(**2**)] and [$FeCl_2$(**3**)] (Table 1, entries 4 and 5). Considering the bis(pyridylimino)isoindoline iron(III) complex, increasing the length of the tether between the central and the donor function (from 5 membered ring for [$FeCl_2$(**1**)] to 6 membered ring for [$FeCl_2$(**2**)]) is detrimental to catalyst performance (Scheme 5). Small *et al.* reported on similar results with iron(II) bearing donor modified α-diimine with pendant functionnalization.[17] Active iron centers for the transformation of olefins are usually chelated by ligands bearing 2 atoms between two heteroatoms linked to the metal.[15,43,44] Moreover, the addition of a carbon atom in the backbone of the bis(pyridylimino)isoindoline ligand allows access of the imine donors to the front side of the complex, closing down the space available to either alkylate the iron center or

coordinate an olefin. The inactivity observed with complex [$FeCl_2$(**3**)] could be either due to the weak donor character of the ligand (H**3**) or to the unsuccessful chelation of the ligand in its anionic form, which would decrease considerably the reactivity of the iron center.

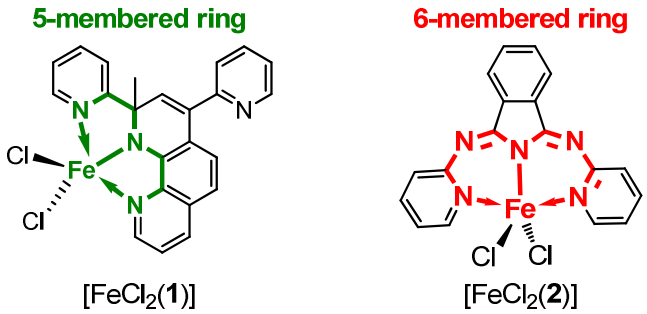

Scheme 5. Length of the tether between the central and donor function.

Conclusion

In summary, we have presented a series of iron(III) complexes chelated by tridentate anionic and neutral *N*,*N*,*N* ligands. While the ferric complexes chelated by anionic bis(pyridylimino)isoindoline and di-(2-picolyl)amine ligand showed no activity with MAO as activator in oligomerization of ethylene, the fully characterized complex ligated by the anionic 1,2-dihydro-1,10-phenanthroline ligand is the first catalytic system with an iron(III) precursor bearing an anionic nitrogen donor ligand for the selective oligomerization of ethylene to short chain oligomers (C_4-C_6). The catalyst exhibits high activity (up to 2.16×10^5 $g\cdot mol^{-1}(Fe)\cdot h^{-1}$) for ethylene oligomerization and high stability with time, using a reasonable amount of MAO (Al/Fe = 200). Up to 66 wt% of butenes were obtained with a selectivity >98 wt% in 1-butene. The synergistic influence of the anionic character of the ligand and the +III oxidation state of the iron precursor on the catalytic activity are thus established. Steric hindrance and electronic factors were suggested to explain the inactivity of other iron(III) catalysts.

Acknowledgement

We thank IFP Energies nouvelles for their support and Dr. J. Ponthus for the HRMS measurements. The LCC also thanks the CNRS and the Ministère de la Recherche for support. We are grateful to Dr. M. Corral Valero and Dr. V. Moizan-Basle for the EXAFS and XANES spectroscopy measurements. We also thank Erwann Jeanneau (Université Claude Bernard – Lyon 1) and Dr. Roberto Pattacini (Strasbourg) for the X-ray crystal structures.

Experimental section

General consideration

All operations were carried out using standard Schlenk techniques under inert atmosphere. FT-IR spectra were recorded in the region 4000-450 cm^{-1} on a Perkin-Elmer Spectrum one FT-IR spectrometer (ATR mode, ZnSe diamond). Mass spectra were collected with an Agilent 6890 N apparatus with Agilent 5975B inert XL EI/CI MSD mass spectrometer. Deuterated solvent (CD_2Cl_2) was purchased from Sigma-Aldrich or Eurisotop. The solvents were freeze-pumped and stored over 4 Å molecular sieves under argon. All chemical shifts are reported in ppm *vs* $SiMe_4$ and were determined with reference to residual solvent peaks.[45] Chemical shifts values (δ) are given in ppm. Gas chromatographic analysis were performed on an Agilent 6850 series II or Varian CP-3800 equipped with autosamplers and fitted with PONA columns (50 m, 0.2 mm diameter, 0.5 μm film thickness). Diffraction data were collected on a Nonius Kappa CCD diffractometer with graphite monochromated Mo-Kα radiation (λ = 0.71073 Å). Data were collected using Ψ scans; the structure was solved by direct methods using the SIR97 software and the refinement was by full-matrix least squares on F^2. No absorption correction was used. Chlorobenzene was dried and freshly distilled prior to use. X-ray absorption spectra (XANES and EXAFS) were recorded at the Deutsches Elektronen-Synchrotron (DESY) in Hamburg. Toluene, THF, pentane and dichloromethane were dried by a solvent purification system (SPS-M-Braun). Starting materials were purchased from Aldrich and used without further purification. Ligand (H**1**) was obtained by a published procedure.[31] Ligand (H**2**) was previously synthesized[40] and used without further purification. Ligand (H**3**) was commercially available from Sigma-Aldrich and used without further purification.

Synthesis and Characterization of ligand and iron complexes

- **Synthesis of 2,4-di(pyridin-2-yl)-2-methyl-1,2-dihydro-1,10-phenanthroline** (H**1**)

2-Acetylpyridine (9.3 g, 76.2 mmol) and 8-aminoquinoline (5.5 g, 38.1 mmol) were dissolved in anhydrous methanol (120 mL). Formic acid (1.8 mL, 45.7 mmol) was added to the solution. The reaction mixture was refluxed for 72 h. The solvent was evaporated under reduced pressure and the excess ketone was removed under vacuum at 60 °C. The crude product was purified by flash chromatography on alumina and then on silica (solvent: CH_2Cl_2/AcOEt 80/20). The desired ligand (H**1**) was obtained as a yellow solid (3.2 g, 30% yield).

^{1}H NMR (300 MHz, CD_2Cl_2, 298 K): δ 1.90 (s, 3H), 6.17 (d, 1H, $^4J_{HH}$ = 2.3 Hz), 6.95 (d, 1H, $^3J_{HH}$ = 8.6 Hz), 7.00 (s, 1H), 7.11 (ddd, 1H, $^3J_{HH}$ = 7.3 Hz), 7.29 (ddd, 1H, $^3J_{HH}$ = 7.6 Hz), 7.32 (d, 1H, $^3J_{HH}$ = 8.5 Hz), 7.35 (dd, 1H, $^3J_{HH}$ = 8.2 Hz), 7.49 (dt, 1H, $^3J_{HH}$ = 7.9 Hz), 7.59 (dt, 1H, $^3J_{HH}$ = 7.94 Hz), 7.62 (td, 1H, $^3J_{HH}$ = 7.5 Hz), 7.76 (td, 1H, $^3J_{HH}$ = 7.6 Hz), 8.02 (dd, 1H, $^3J_{HH}$ = 8.3 Hz), 8.60 (dq, 1H, $^3J_{HH}$ = 4.8 Hz), 8.69 (dq, 1H, $^3J_{HH}$ = 4.9 Hz), 8.75 (dd, 1H, $^3J_{HH}$ = 4.2 Hz).

^{13}C{^{1}H} NMR (75 MHz, CD_2Cl_2, 298 K): δ 31.1, 59.1, 113.8, 115.5, 120.3, 121.8, 121.9, 122.7, 123.9, 125.1, 128.9, 130.0, 136.1, 136.5, 136.8, 136.9, 137.7, 140.6, 148.0, 149.61, 149.64, 158.2, 166.6.

FT-IR (cm^{-1}): 3372, 3048, 2964, 2923, 1732, 1632, 1583, 1563, 1508, 1463, 1428, 1377, 1294, 1225, 1100, 1045, 991, 823, 804, 782, 745, 690.

- **Synthesis of (2-methyl-2,4-di(pyridin-2-yl)-1,10-phenanthrolin-1(2H)-yl)iron(III) dichloride** [$FeCl_2$(**1**)]

n-BuLi (0.61 mL, 1.1 mmol, 1.78 N in hexane) was added to a solution of (H**1**) (0.378 g, 1.1 mmol) in 15 mL of anhydrous THF at -78 °C. The solution became red and was stirred at -78 °C for 1 h. The solution was then added dropwise to $FeCl_3$ (0.175 g, 1.1 mmol) in 10 mL of anhydrous THF at 0 °C. The reaction mixture became purple. After the reaction mixture was stirred for 1 h at 0 °C and then overnight at room temperature, the volume of solvent was reduced to 5 mL. Pentane (20 mL) was added to precipitate the complex which was filtered, washed with pentane (3×20 mL) and isolated as a purple solid (0.490 g, 95% yield).

FT-IR (cm^{-1}): 3059, 2957, 2870, 1603, 1585, 1495, 1450, 1388, 1323, 1297, 1107, 1126, 1047, 1020, 827, 779, 775, 750, 690, 653, 581, 464.

Elemental analysis for $C_{23}H_{17}Cl_2FeN_4 \cdot C_6H_5Cl$, calcd: C, 59.16; H, 3.77; Cl, 18.07; Fe, 9.49; N, 9.52%. Found: C, 52.00; H, 3.75; Cl, 19.20; Fe, 10.30; N, 9.85%. Despite several attempts, no better analyses could be obtained. However, the ratio Cl/Fe of 2 is in line with the expected compound crystallized with one equivalent of chlorobenzene.

Mass spectrometry: molecular ions ($M^{+\cdot}$: $C_{23}H_{17}N_4Fe_1Cl_2$) were observed for 7 isotopes of the complex isotopic pattern: 473.02216 (err. 0.14 ppm), 475.01744 (err. 0.04 ppm), 476.02072 (err.-0.12 ppm), 477.01447 (err. 0.00 ppm), 478.01790 (err. 0.15 ppm), 479.01157 (err. 0.10 ppm), 480.01490 (err. 0.04 ppm).

Some dark violet crystals were obtained by slow diffusion of pentane into a chlorobenzene solution of the reaction mixture.

EXAFS: Bond lengths determined by EXAFS spectroscopy (Å): Fe-N = 2.31±0.06, Fe-N = 2.02±0.02, Fe-N = 2.17±0.03, Fe-Cl = 2.24±0.01, Fe-N = 2.32±0.02

- **Synthesis of (2-methyl-2,4-di(pyridin-2-yl)-1,10-phenanthrolin-1(2H)-yl)iron(II) dichloride** [$FeCl_2$(H**1**)]

The ligand (H**1**) (0.80 g, 2.3 mmol) and $FeCl_2 \cdot 4H_2O$ (0.54 g, 2.3 mmol) were dissolved in 40 mL of THF. The reaction mixture was stirred at room temperature overnight. The complex precipitated. The solid was filtered and washed with Et_2O (3×20 mL). The complex was obtained as a pink powder (0.810 g, 74% yield).

FT-IR (cm^{-1}): 3144, 3071, 2975, 2864, 1602, 1583, 1499, 1459, 1431, 1363, 1306, 1285, 1229, 1204, 1163, 1124, 1058, 1012, 991, 911, 849, 786, 772, 758, 748, 713, 688, 640, 595, 559, 479.

Elemental analysis for $C_{23}H_{18}Cl_2FeN_4$, calcd: C, 57.89; H, 3.80; N, 11.74%. Found: C, 58.65; H, 4.28; N, 11.12%.

Mass Spectrometry: Molecular ions ($M^{+\cdot}$: $C_{23}H_{18}N_4Fe_1Cl_2$) were observed for 8 isotopes of the complex isotopic pattern: 474.03009 (err. 0.36 ppm), 475.03345 (err. 0.32 ppm), 476.02529 (err.-0.04 ppm), 477.02863 (err. 0.40 ppm), 478.02232 (err. -0.04 ppm), 479.02567 (err. 0.44 ppm), 480.01937 (err. -0.15 ppm), 481.02254 (err. 0.02 ppm).

- **Synthesis of (2-methyl-2,4-di(pyridin-2-yl)-1,10-phenanthrolin-1(2H)-yl)cobalt(II) dichloride** [$CoCl_2$(H**1**)]

[$CoCl_2$(H**1**)] was synthesized by the method used for [$FeCl_2$(H**1**)] but starting from $CoCl_2 \cdot 6H_2O$ as precursor. The product was obtained as a pink solid (0.169 g, 95% yield).

FT-IR (cm^{-1}): 3145, 3069, 2980, 2654, 1602, 1584, 1567, 1501, 1432, 1374, 1231, 1156, 1122, 1052, 990, 841, 784, 747, 688, 643, 625, 595, 559, 491, 470.

- **Synthesis of (2-methyl-2,4-di(pyridin-2-yl)-1,10-phenanthrolin-1(2H)-yl)iron(III) trichloride** [$FeCl_3$(H**1**)]

[$FeCl_3$(H**1**)] was synthesized by the method used for [$FeCl_2$(H**1**)] but starting from $FeCl_3$ as precursor. The complex was obtained as a purple solid (0.270 g, 95% yield).

FT-IR (cm^{-1}): 3057, 2963, 2917, 2859, 1603, 1584, 1469, 1451, 1390, 1325, 1260, 1162, 1092, 1018, 1020, 862, 822, 775, 689, 653, 581, 464.

Elemental analysis for $C_{23}H_{18}Cl_3FeN_4$, calcd: C, 53.89; H, 3.54; N, 10.93%. Found: C, 51.87; H, 4.01; N, 9.87%.

Mass Spectrometry: the ions $(M\text{-H})^+$: $C_{23}H_{17}N_4Fe1Cl_3$) were observed for 4 isotopes of the complex isotopic pattern: 474.03009 (err. 0.36 ppm), 475.03345 (err. 0.32 ppm), 476.02529 (err.-0.04 ppm), 477.02863 (err. 0.40 ppm), 478.02232 (err. -0.04 ppm), 479.02567 (err. 0.44 ppm), 480.01937 (err. -0.15 ppm), 481.02254 (err. 0.02 ppm).

- **Synthesis of (2-methyl-2,4-di(pyridin-2-yl)-1,10-phenanthrolin-1(2H)-yl)iron(II) chloride** [FeCl(**1**)]

n-BuLi (0.55 mL, 0.9 mmol, 1.6 $mol \cdot L^{-1}$ in hexanes) were added to a solution of ligand (H**1**) (0.31 g, 0.9 mmol) in 6 mL of anhydrous THF at -78 °C. The solution became red and was stirred at room temperature for 1 h. The solution was added dropwise to a solution of $FeCl_2 \cdot 1.5THF$ (0.21 g, 0.9 mmol) in 10 mL of anhydrous THF. The solution was stirred at room temperature for 16 h and the solvent evaporated under vacuum. The product was extracted with CH_2Cl_2 (5×10 mL) and the solution concentrated to 10 mL. Pentane (20 mL) was added to precipitate the complex which was filtered and washed with Et_2O (2×10 mL) and obtained as a red solid (0.260 g, 67% yield).

FT-IR (cm^{-1}): 3043, 2957, 2903, 2842, 1595, 1561, 1537, 1459, 1410, 1389, 1361, 1278, 1123, 1087, 1045, 1024, 856, 812, 780, 756, 732, 703, 645, 583, 567, 526, 479, 461.

Elemental analysis for $C_{23}H_{17}ClFeN_4$, calcd: C, 62.68; H, 3.89; Cl, 8.04; Fe, 12.67; N, 12.71%. Found: C 61.18, H 4.94, N 11.13%.

- **Synthesis of complex** [$FeCl_2$(**2**)]

n-BuLi (0.25 mL, 0.65 mmol, 2.5 mol.L^{-1} in hexane, 1 eq.) was added to a solution of the ligand (H**2**) (0.196 g, 0.65 mmol, 1 eq.) in 10 mL of anhydrous THF at -78 °C. The solution became red and was stirred at -78 °C for 1 h. A solution of $FeCl_3$ (0.105 g, 0.65 mmol, 1 eq.) in 10 mL of anhydrous THF at 0 °C was added dropwise to the solution of deprotonated ligand. The reaction mixture became brown and was stirred overnight at room temperature. The solvent was evaporated and the product was extracted with dried toluene (3×20 mL). Anhydrous pentane (20 mL) was added to precipitate the complex which was filtered, washed with pentane (3×20 mL) and obtained as a brown solid (0.190 g, 70% yield).

FT-IR (cm^{-1}): 2955, 2869, 1610, 1560, 1512, 1467, 1427, 1363, 1134, 1082, 1040, 762, 731, 690, 541.

- **Synthesis of complex** [$FeCl_2$(**3**)]

[$FeCl_2$(**3**)] was synthesized by the method used for [$FeCl_2$(**2**)]. The complex was obtained as a green solid (0.160 g, 70% yield).

FT-IR (cm^{-1}): 3253, 3068, 2878, 1602, 1478, 1437, 1414, 1257, 1204, 1154, 1052, 1016, 765, 642, 519, 464.

Crystallographic data and structure refinement details

	(H**1**)	$[CoCl_2(H\mathbf{1})]\cdot CH_2Cl_2$	$2[FeCl_2(\mathbf{1})]\cdot C_6H_4Cl$
Formula	$C_{23}H_{18}N_4$	$C_{23}H_{18}Cl_2CoN_4\cdot CH_2Cl_2$	$2(C_{23}H_{17}Cl_2FeN_4)\cdot C_6H_4Cl$
Cryst. system	Monoclinic	Monoclinic	Triclinic
Space group	$P2_1/c$	$P2_1/c$	P_1
a (Å)	11.265(2)	9.7422(5)	8.2054(6)
b (Å)	9.461(1)	10.1743(5)	11.2363(9)
c (Å)	16.750(2)	24.2493(12)	12.647(1)
Cell volume (Å^3)	1746.8	2381.5(2)	1141.96(16)
Density	1.332	1.576	1.547
Z	4	4	1
F(000)	736	1148	543
T (K)	150	173	110
θmin-θmax (°)	4.0 – 66.8	2.1 – 30.1	3.6 – 29.7
H	-13/13	-13/13	-11/11
K	-11/10	-13/14	-15/15
L	-19/18	-29/34	-17/17
μ (mm^{-1})	0.64	1.19	0.98
Measd. reflexions	12963	20429	21921
Indep. reflexions	3071	6962	5729
R_{int}	0.041	0.049	0.054
$R[F^2 > 2\sigma(F^2)]$	0.049	0.045	0.046
$wR(F^2)[F^2 > 2\sigma(F^2)]$	0.129	0.098	0.126
S	0.96	1.02	0.97
$\Delta\rho_{min}$, $\Delta\rho_{max}$ (e.Å^{-3})	-0.39, 0.39	-0.63, 0.61	-0.66, 0.92

Iron-catalysed oligomerization of ethylene

All catalytic reactions were carried out in a magnetically stirred 250 mL stainless steel autoclave. The toluene and the cocatalyst were first introduced under ethylene atmosphere. The iron precursor was then added. The reactor was sealed and fed with ethylene up to half the desired pressure (15 bars in our case). The reactor was heated at 80 °C and then 30 bars of ethylene pressure were applied. During catalysis, the pressure was maintained through a continuous feed of ethylene from a bottle placed on a balance used to monitor the ethylene uptake. At the end of the test, stirring was stopped and the reactor was cooled down to 25 °C. The gaseous effluents were collected in a 15 L polyethylene bottle filled with water. The reactor was then cooled to -5 °C and liquid effluents were collected from the bottom of the reactor. The liquid effluents were weighed. The catalyst and the cocatalyst were quenched by addition of EtOH. Liquid effluents were collected by trap to trap distillation (140 °C, $6 \cdot 10^{-2}$ mbar) to separate waxes and PE from oligomers ($<C_{14}$). Aliquots of gaseous and liquid effluents were then analyzed by GC.

Bibliography

1. Vogt D. *Applied homogeneous catalysis with organometallic compounds;* WILEY-VCH ed.; Weinheim, **2002**.

2. Van Leeuwen P.W.N.M. Alkene oligomerization. In *Homogeneous catalysis, Understanding the art*, Kluwer Academic Publishers ed.; Van Leeuwen P.W.N.M., Ed.; Dordrecht, **2004**; pp 175-190.

3. Speiser, F.; Braunstein, P.; Saussine, W. *Acc. Chem. Res.* **2005**, *38* (10), 784.

4. Olivier-Bourbigou, H.; Forestière, A.; Saussine, L.; Magna, L.; Favre, F.; Hugues, F. *Oil Gas Eur. Mag.,* **2010**, p 97.

5. Aljarallah, A. M.; Anabtawi, J. A.; Siddiqui, M. A. B.; Aitani, A. M.; Alsadoun, A. W. *Catal. Today* **1992**, *14*, 1.

6. Commereuc, D.; Chauvin, Y.; Gaillard, J.; Léonard, J.; Andrews, J. *Hydrocarb. Processes, Int. Ed.* **1984**, *6311*, 118.

7. Reagan, W. K.; Freeman, J. W.; Conroy, B. K.; Pettijohn, T. M.; Benham, E. A. Process for the preparation of a catalyst for olefin polymerization. EP0608447A1, **Jan 26**, **1993**.

8. Reagan, W. K.; Pettijohn, T. M.; Freeman, J. W. Process of trimerizing and oligomerizing olefins using chromium compounds. US US5523507A, **Jun 4**, **1996**.

9. Small, B. L.; Brookhart, M. *J. Am. Chem. Soc.* **1998**, *120*, 7143.

10. Small, B. L.; Brookhart, M.; Bennett, A. M. A. *J. Am. Chem. Soc.* **1998**, *120*, 4049.

11. Britovsek, G. J. P.; Gibson, V. C.; Kimberley, B. S.; Maddox, P. J.; McTavish, S. J.; Solan, G. A.; White, A. J. P.; Williams, D. J. *Chem. Commun.* **1998**, 849.

12. Britovsek, G. J. P.; Mastroianni, S.; Solan, G. A.; Baugh, S. P. D.; Redshaw, C.; Gibson, V. C.; White, A. J. P.; Williams, D. J.; Elsegood, M. R. J. *Chem. Eur. J.* **2000**, *6*, 2221.

13. Bianchini, C.; Giambastiani, G.; Rios, I. G.; Mantovani, G.; Meli, A.; Segarra, A. M. *Coord. Chem. Rev.* **2006**, *250*, 1391.

14. Bianchini, C.; Giambastiani, G.; Luconi, L.; Meli, A. *Coord. Chem. Rev.* **2010**, *254*, 431.

15. Gibson, V. C.; Redshaw, C.; Solan, G. A. *Chem. Rev.* **2007**, *107*, 1745.

16. Schmiege, B. M.; Carney, M. J.; Small, B. L.; Gerlach, D. L.; Halfen, J. A. *Dalton Trans.* **2007**, 2547.

17. Small, B. L.; Rios, R.; Fernandez, E. R.; Carney, M. J. *Organometallics* **2007**, *26*, 1744.

18. Small, B. L.; Rios, R.; Fernandez, E. R.; Gerlach, D. L.; Halfen, J. A.; Carney, M. J. *Organometallics* **2010**, *29*, 6723.

19. Sun, W. H.; Hao, P.; Zhang, S.; Shi, Q. S.; Zuo, W. W.; Tang, X. B.; Lu, X. M. *Organometallics* **2007**, *26*, 2720.

20. Sun, W. H.; Hao, P.; Li, G.; Zhang, S.; Wang, W. Q.; Yi, J. J.; Asma, M.; Tang, N. *J. Organomet. Chem.* **2007**, *692*, 4506.

21. Wang, K.; Wedeking, K.; Zuo, W.; Zhang, D.; Sun, W. H. *J. Organomet. Chem.* **2008**, *693*, 1073.

22. Gibson, V. C.; Spitzmesser, S. K.; White, A. J. P.; Williams, D. J. *Dalton Trans.* **2003**, 2718.

23. Raucoules, R.; de Bruin, T.; Raybaud, P.; Adamo, C. *Organometallics* **2008**, *27*, 3368.

24. Tondreau, A. M.; Milsmann, C.; Patrick, A. D.; Hoyt, H. M.; Lobkovsky, E.; Wieghardt, K.; Chirik, P. J. *J. Am. Chem. Soc.* **2010**, *132*, 15046.

25. Hao, P.; Chen, Y. J.; Xiao, T. P. F.; Sun, W. H. *J. Organomet. Chem.* **2010**, *695*, 90.

26. Ionkin, A. S.; Marshall, W. J.; Adelman, D. J.; Shoe, A. L.; Spence, R. E.; Xie, T. Y. *J. Polym. Sci. Pol. Chem.* **2006**, *44*, 2615.

27. Ionkin, A. S.; Marshall, W. J.; Adelman, D. J.; Fones, B. B.; Fish, B. M.; Schiffhauer, M. F. *Organometallics* **2006**, *25*, 2978.

28. Matsui, S.; Nitabaru, M.; Tsuru, K.; Fujita, T.; Suzuki, Y.; Takagi, Y.; Tanaka, H. Catalysts for olefin polymerization and polymerization method. WO 9954364 A1, **Jun 4**, **2002**.

29. Matsunaga, P. T. Tridentate ligand-containing metal catalyst complexes for olefin polymerization. WO 9957159 A1, **Apr 29**, **1999**.

30. Rangheard, C. Oligomérisation de l'éthylène par les catalyseurs de fer. PhD thesis. Université Claude Bernard Lyon 1, **2008**.

31. Rangheard, C.; Proriol, D.; Olivier-Bourbigou, H.; Braunstein, P. *Dalton Trans.* **2009**, 770.

32. Xiao, L. W.; Gao, R.; Zhang, M.; Li, Y.; Cao, X. P.; Sun, W. H. *Organometallics* **2009**, *28*, 2225.

33. Zhang, M.; Hao, P.; Zuo, W. W.; Jie, S. Y.; Sun, W. H. *J. Organomet. Chem.* **2008**, *693*, 483.

34. Song, S.; Xiao, T.; Redshaw, C.; Hao, X.; Wang, F.; Sun, W. H. *J. Organomet. Chem.* **2011**, *696*, 2594.

35. Westre, T. E.; Loeb, K. E.; Zaleski, J. M.; Hedman, B.; Hodgson, K. O.; Solomon, E. I. *J. Am. Chem. Soc.* **1995**, *117*, 1309.

36. Roe, A. L.; Schneider, D. J.; Mayer, R. J.; Pyrz, J. W.; Widom, J.; Que, L. *J. Am. Chem. Soc.* **1984**, *106*, 1676.

37. Kau, L. S.; Spira-Solomon, D. J.; Penner-Hahn, J. E.; Hodgson, K. O.; Solomon, E. I. *J. Am. Chem. Soc.* **1987**, *109*, 6433.

38. Sun, W. H.; He, S. Y.; Zhang, S.; Zhang, W.; Song, Y. X.; Ma, H. W. *Organometallics* **2006**, *25*, 666.

39. Balogh-Hergovich, E.; Speier, G.; Reglier, M.; Giorgi, M.; Kuzmann, E.; Vertes, A. *Eur. J. Inorg. Chem.* **2003**, 1735.

40. Siegl, W. O. *J. Org. Chem.* **1977,** *42*, 1872.

41. Babik, S. T.; Fink, G. *J. Mol. Catal. A: Chem.* **2002,** *188*, 245-253.

42. Britovsek, G. J. P.; Gibson, V. C.; Spitzmesser, S. K.; Tellmann, K. P.; White, A. J. P.; Williams, D. J. *J. Chem. Soc. , Dalton Trans.* **2002**, 1159.²

43. Chen, Y. J.; Hao, P.; Zuo, W. W.; Gao, K.; Sun, W. H. *J. Organomet. Chem.* **2008**, *693*, 1829.

44. Jie, S. Y.; Zhang, S.; Sun, W. H.; Kuang, X. F.; Liu, T. F.; Guo, J. P. *J. Mol. Catal. A: Chem.* **2007**, *269*, 85.

45. Fulmer, G. R.; Miller, A. J. M.; Sherden, N. H.; Gottlieb, H. E.; Nudelman, A.; Stoltz, B. M.; Bercaw, J. E.; Goldberg, K. I. *Organometallics* **2010,** *29*, 2176.

CHAPTER III

Assembling Iron Ions through Oxygen: a New Route to Binuclear Iron(III) Complexes. Application to Ethylene Oligomerization.

Abstract: This chapter reports on a new procedure to prepare binuclear iron(III) complexes. The oxidation by molecular oxygen of iron(II) complexes [$FeCl_2$(H**1**)] and [$FeCl_2$(H**2**)] chelated by tridentate nitrogen ligands (H**1**) = 1,2-dihydro-1,10-phenanthroline and (H**2**) = 1,3-bis(2'-pyridylimino)isoindoline yielded the binuclear complexes [(L)FeCl(μ-O)FeCl(L)] [L = **1**, **2**]. The formation of the iron-oxygen bonds was accompanied by amine deprotonation at the central nitrogen site, which was characterized by FT-IR spectroscopy. Upon activation with MAO, the binuclear complex [(**1**)FeCl(μ-O)FeCl(**1**)] chelated by the anionic 1,2-dihydro-1,10-phenanthroline **1** was active and stable for ethylene oligomerization. Higher activity and different selectivities were obtained with this precatalyst compared to its mononuclear iron(III) analog [$FeCl_2$(**1**)]. A cooperative effect between the two metal centers is therefore suggested to occur.

Résumé : Ce chapitre décrit une nouvelle voie de synthèse de complexes de fer(III) binucléaires. L'oxydation des précurseurs de fer(II) [$FeCl_2$(H**1**)] et [$FeCl_2$(H**2**)] chélatés par les ligands azotés tridentes (H**1**) = 1,2-dihydro-1,10-phénantroline et (H**2**) = 1,3-bis(2'-pyridylimino)isoindoline a conduit à la formation d'espèces binucléaires de formule générale [(L)FeCl(μ-O)FeCl(L)] avec [L = **1**, **2**]. L'étude par spectrométrie infrarouge a mis en évidence que la formation de la liaison Fe-O-Fe s'accompagnait de la déprotonation de l'amine centrale secondaire. Activé par le MAO, le complexe binucléaire [(**1**)FeCl(μ-O)FeCl(**1**)] s'est avéré actif et stable dans les conditions d'oligomérisation de l'éthylène. En comparaison aux résultats obtenus avec son homologue mononucléaire [$FeCl_2$(**1**)], une meilleure activité et des sélectivités différentes ont été obtenues avec l'espèce binucléaire. Un effet coopératif entre les deux centres métalliques est supposé.

Introduction

The cooperative effect between two metallic centers, inspired by Nature's catalysts, enzymes, is subject of intensive research in organometallic chemistry and catalysis.[1-10] A large diversity of binuclear compounds has been generated and efficiently applied to various organic transformations, such as the rhodium-catalyzed asymmetric hydrogenation[11] or the hydroamination of olefins catalyzed by phenylene-bridged binuclear lanthanide complexes.[12] Numerous bimetallic complexes have been used in olefin polymerization (ethylene, styrene…), as recently reviewed by Delferro and Marks,[13] and a binuclear titanium constrained-geometry catalyst (CGC) exhibits higher styrene homopolymerization activity than its mononuclear analogs and produces ethylene-styrene copolymers with a styrene incorporation over 50% (Scheme 1).[14]

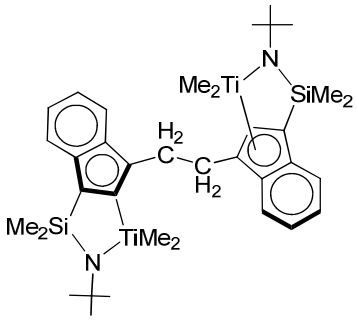

Scheme 1. $CGCTi_2$ catalyst for ethylene-styrene copolymerization.[14]

In systems involving bimetallic (Zr and Ni) complexes, a cooperative effect between the two metal centers afforded highly branched polyethylene (Scheme 2).[15] This Zr/Ni complex enables the efficient enchainment of branched oligomers formed at the Ni center to the polymer grown at the Zr center.

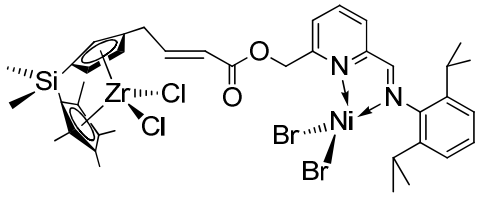

Scheme 2. Bimetallic complex developed by Kuwabara *et al.*[15]

Iron and cobalt binuclear complexes were developed for both oligomerization and polymerization of ethylene (Scheme 3).[16-20] Upon treatment with MAO, MMAO or Al^iBu_3, the iron(II) complexes showed high activity for ethylene oligomerization or polymerization. A methylene-bridged binuclear bis(imino)pyridyl iron(II) complex (Scheme 3), activated with

Al^{i}Bu$_3$, exhibits higher activity than the corresponding mononuclear iron catalysts and leads to higher molecular weight linear polyethylene. The marked differences in activity and product distribution versus the mononuclear analog were assigned to the combined electronic and steric effects of the iron centers. In the case of ethylene oligomerization (non-symmetric complexes), these catalysts afford a Schulz-Flory distribution of α-olefins with high selectivity but low activity.

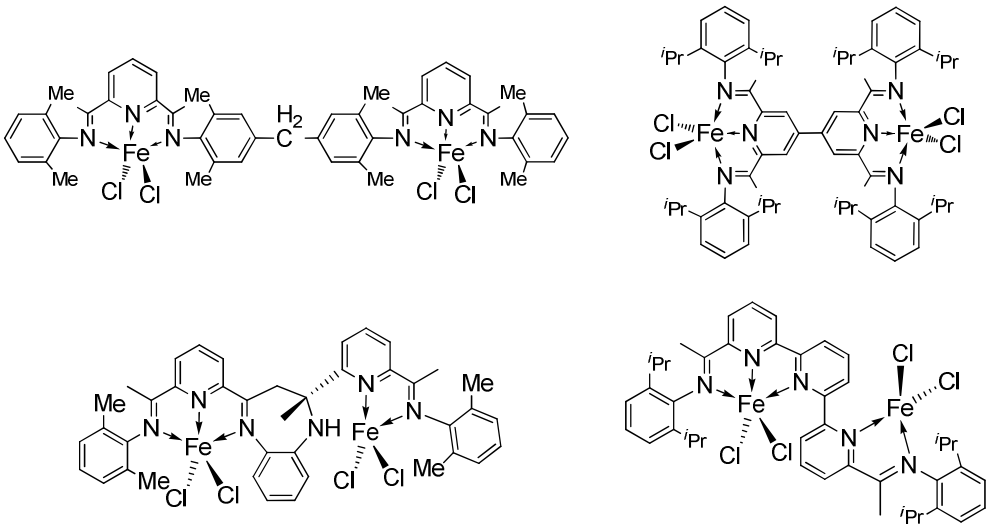

Scheme 3. Symmetric (top) and non-symmetric (bottom) binuclear complexes.

Roesky *et al.* have developed an interesting access to oxo-bridged bimetallic complexes Al-O-M (M = Zr, Ti, Hf, Sn, Ln) starting from well-defined [(L)Al(OH)(Me)] precursors.[21] These systems led to active precatalysts in ethylene polymerization upon activation with moderate amounts of MAO. For example [(L)AlMe(μ-O)ZrMeCp$_2$] (Scheme 4) exhibits catalytic activity on the order of 10^6 g(products)·(mol(catalyst)·h)$^{-1}$ at a cocatalyst to catalyst ratio of only 136.

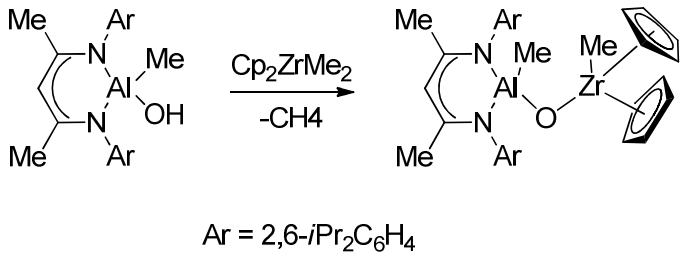

Scheme 4. Formation of the Al-O-Zr bridge.[21]

To the best of our knowledge, no example of binuclear iron complex involving an oxo-bridge has been reported to be active for the transformation of ethylene, although such structures are recurrent in enzymes such as hemerythyrin, ribonucleotide, reductase, methane monooxygenase or purple acid phosphatase.[22,23] In the course of our studies detailed in Chapter II, we observed the formation of oxo-bridged diiron complexes. We present below an original and straightforward access to binuclear iron(III) pre-catalysts for the oligomerization of ethylene by oxidation of iron(II) complexes with O_2.

I. Synthesis of the complexes

1. System involving the 1,2-dihydro-1,10-phenanthroline ligand

Bubbling oxygen through an acetonitrile solution of the pink precursor [$FeCl_2$(H**1**)] (synthesized in Chapter II) for 1 h affords a purple solid in high yield (>90%) (Scheme 5). The comparison between the FT-IR spectra of the iron(II) precursor and the oxidized product confirms the deprotonation of the secondary amine (disappearance of the absorption band at 3145 cm^{-1}) and the formation of the Fe-O-Fe linkage (absorption bands at 744 cm^{-1} and 464 cm^{-1}) (Figure 1). The new absorption band at 1391 cm^{-1} is however difficult to assign, it might involve the free pyridine group. A structure of the μ-oxo diiron(III) complex [(**1**)FeCl(μ-O)FeCl(**1**)] is proposed in Scheme 5. Protonation of the free pyridine by the HCl liberated cannot be completely ruled out.

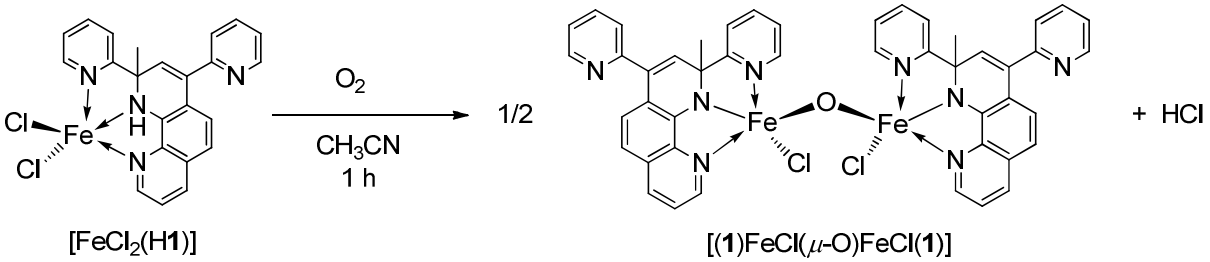

Scheme 5. Oxidation of complex [$FeCl_2$(H**1**)].

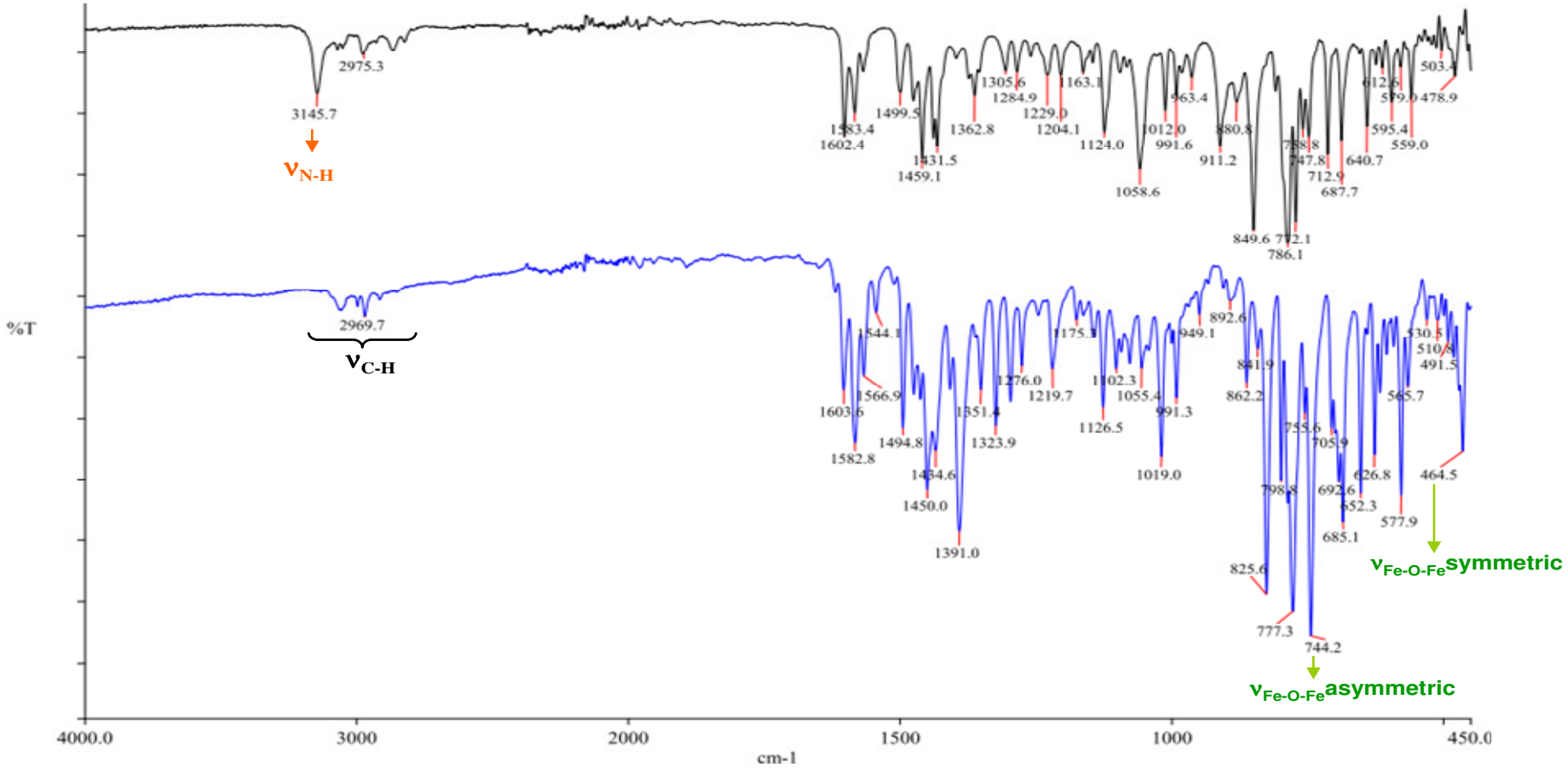

Figure 1. FT-IR spectra of the complex [$FeCl_2$(H**1**)] (black) and the corresponding oxidized complex [(**1**)FeCl(μ-O)FeCl(**1**)] (blue)

In the course of the synthesis of [$FeCl_2$(**1**)] (see Chapter II), some dark violet crystals were obtained by slow diffusion of Et_2O into a MeCN solution of the reaction mixture. An X-ray diffraction analysis revealed for [{Fe_2Cl_2(μ-O)}(**1-1**)]$_2$·2Et_2O the unexpected structure shown in Figure 2. Two oxo-bridges connect two binuclear units that result from a C-C coupling reaction between two phenanthroline moieties at the *p*-position of their central ring. Each Fe(III) center carries a terminal chloride ligand and is pentacoordinated. A symmetry axis passing through the oxygen atoms relates the two halves of the molecule. Unfortunately, the quantity of crystals obtained was too low to perform the usual analyses and the experimental conditions required to obtain this complex are not yet clearly identified.

Attempts to obtain this product ([{Fe_2Cl_2(μ-O)}(**1-1**)]$_2$) by direct addition of two equivalents of *n*-BuLi (in order to induce the C-C coupling and the deprotonation of the amine) remained unsuccessful.

With the hope to obtain the C-C coupling product **1-1**, a further attempt aiming at liberating the anionic ligand **1** from the metal was performed by addition of an aqueous solution of KOH 10 wt% to a solution of [$FeCl_2$(**1**)] in CH_3CN. This quantitatively released the reprotonated ligand (H**1**) and ^{1}H, ^{13}C NMR and mass spectroscopy analyses of the organic layer pointed out the absence of any dimeric product. The tetranuclear complex [{Fe_2Cl_2(μ-O)}(**1-1**)]$_2$ possibly formed during the crystallization process and the exact mechanism of its formation remains unclear at this point. However, this interesting tetranuclear structure provides evidence for the possible formation of Fe-O-Fe moieties with this N,N,N ligand.

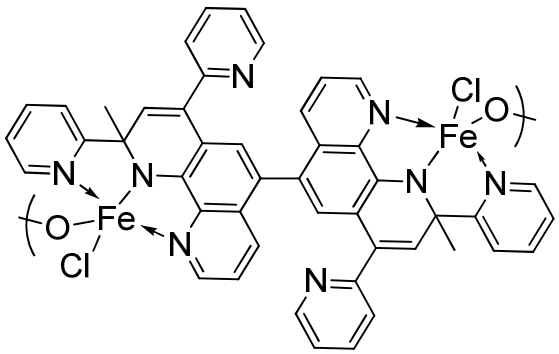

(**1-1**)(Fe(μ-O)Cl)$_2$

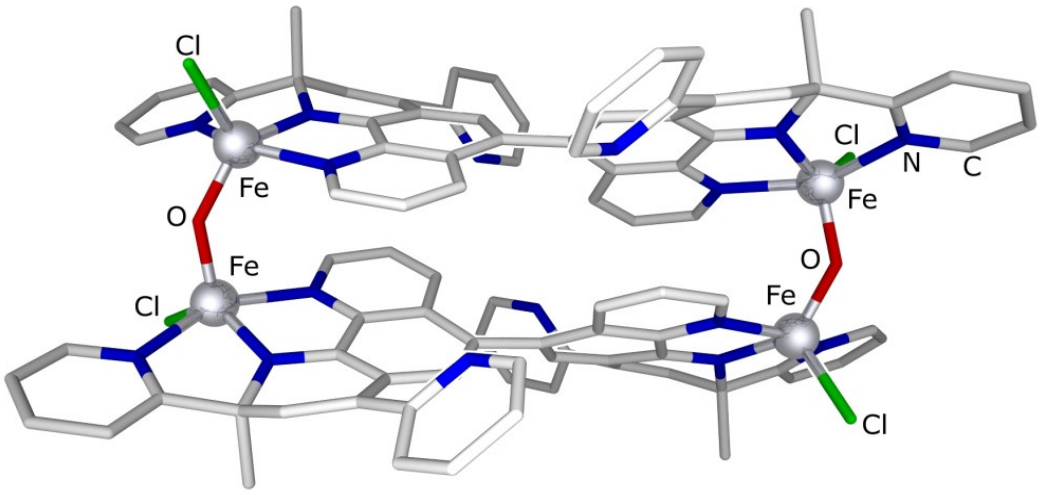

Figure 2. Structure of $[\{Fe_2Cl_2(\mu\text{-}O)\}(\mathbf{1}\text{-}\mathbf{1})]_2$ in $[\{Fe_2Cl_2(\mu\text{-}O)\}(\mathbf{1}\text{-}\mathbf{1})]_2\cdot 2Et_2O$ Molecules of solvent have been omitted for clarity. Selected bond distances (Å) and angles (°): Fe(1)-O(1) = 1.780(3), Fe(2)-O(1) = 1.787(3), Fe(1)-N(2) = 1.978(3), Fe(2)-N(5) = 1.968(3), Fe(1)-N(1) = 2.178(3), Fe(2)-N(4) = 2.187(4), Fe(1)-N(3) = 2.180(3), Fe(2)-N(6) = 2.194(3), Fe(1)-Cl(1) = 2.2496(14), Fe(2)-Cl(2) = 2.2489(14); Fe(1)-O(1)-Fe(2) = 139.27(16).

2. Extension to the 1,3-bis(2'-pyridylimino)isoindoline ligand

The iron(II) complex $[FeCl_2(H\mathbf{2})]$ was synthesized by stirring an equimolar mixture of the ligand (H**2**) and the metal precursor ($FeCl_2\cdot 4H_2O$) in dry THF. The complex was isolated as a green powder.

Upon bubbling dry oxygen through the solution overnight, the ferrous complex $[FeCl_2(H\mathbf{2})]$ in acetonitrile solution smoothly converts to the binuclear ferric complex $[(\mathbf{2})FeCl(\mu\text{-}O)FeCl(\mathbf{2})]$ (Scheme 6). Characterization by FT-IR spectroscopy confirmed the presence of a Fe-O-Fe linkage with the two characteristic bands at 770 cm^{-1} and 477 cm^{-1} (Figure 3).[24] Moreover, no absorption band in the ν(NH) region of the amino group was detected, thus revealing the deprotonation of the central N donor group during the oxidation reaction. Balogh-Hergovich *et al.* reported another route to obtain the complex $[(\mathbf{2})FeCl(\mu\text{-}O)FeCl(\mathbf{2})]$ by refluxing the ligand 1,3-bis(2'-pyridylimino)isoindoline (H**2**) with the iron precursor $FeCl_3\cdot 6H_2O$ for 8 h in methanol.[24] Using this approach, we also obtained the complex in high yield as a brown solid. Similarities between the FT-IR spectra of the two binuclear complexes (the oxidized one and the one synthesized from $FeCl_3\cdot 6H_2O$) confirmed

the structure of the oxidized complex [(**2**)FeCl(μ-O)FeCl(**2**)]. Note that using the Balogh-Hergovich method with ligand (H**1**) remained unsuccessful.

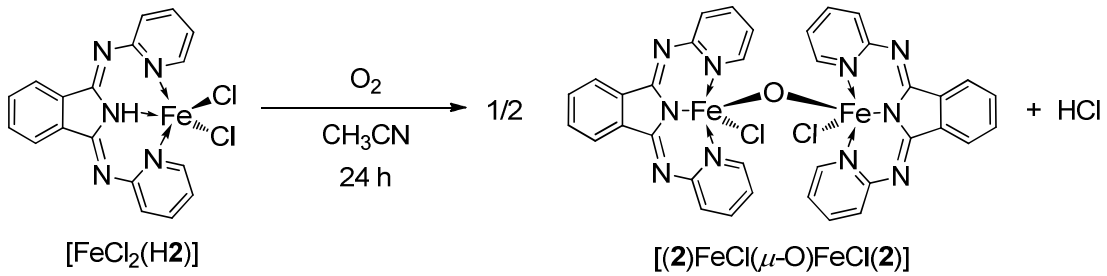

Scheme 6. Oxidation of the complex [$FeCl_2$(H**2**)].

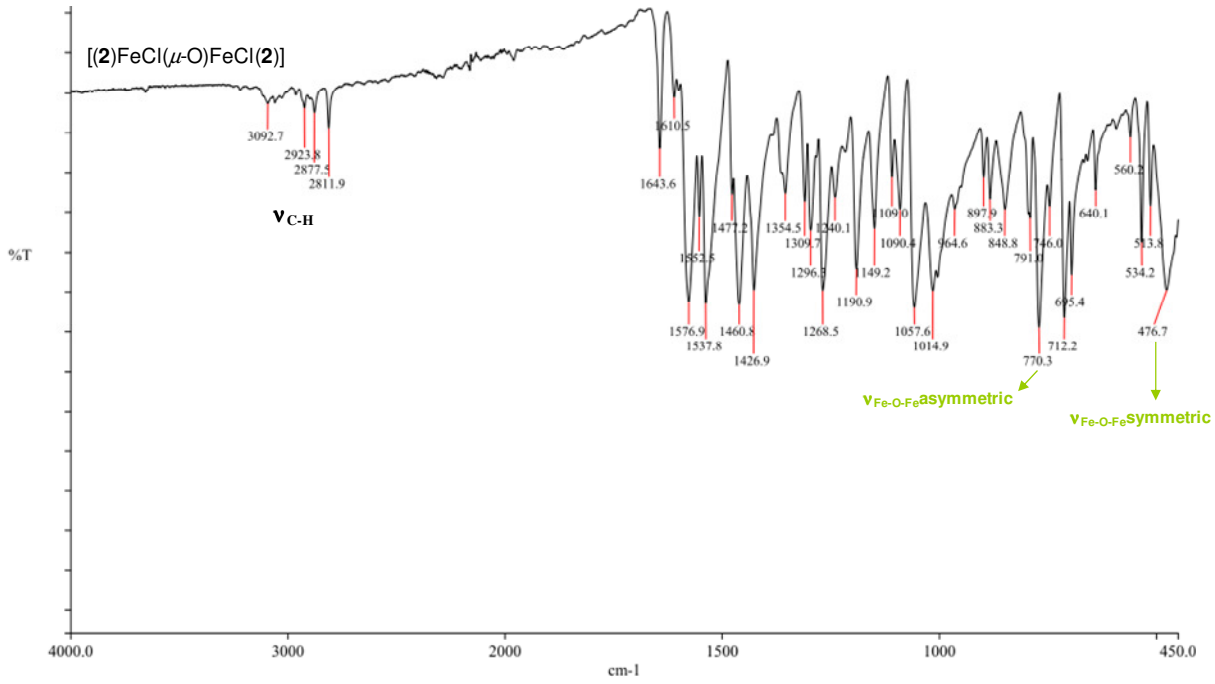

Figure 3. FT-IR spectrum of the oxidized complex [(**2**)FeCl(μ-O)FeCl(**2**)]

Single crystals suitable for X-ray diffraction of the oxidized complex [(**2**)FeCl(μ-O) FeCl(**2**)] were grown from concentrated THF solution (Figure 4). The structure is that of a μ-oxo dimer. The two iron atoms are in a distorted trigonal bipyramidal coordination geometry. The oxygen and chloride atoms and the nitrogen atom N4 of the tridentate ligand form the equatorial plane, while two further nitrogen atoms N8 and N18 of the ligand occupy apical

positions. The metal-metal distance of 3.251 Å remains shorter than in bis(cyclopentadienyl) binuclear μ-oxo titanium complex (3.633 Å)[25] or in bimetallic Zr-O-Ti system (3.754 Å).[26] The Fe-O-Fe angle (131.1(3)°) is significantly smaller than in related complexes chelated by the tetradentate, amine-containing ligand tris(2-pyridylmethyl)amine (179.9(7)°) or *N,N*-bis(2-pyridylmethyl)glycinamide (176.0(5)°).[27,28] The average Fe-N distances of 2.145 Å involving the chelating pyridines are consistent with dative bonds and the Fe-N4 bond length of 2.002(5) Å with a covalent bond.[29] Values of the bond lengths and angles are close to those reported in the literature for related systems.[24] The parallel arrangement of the isoindolinate ligands in this complex is favored by their π-π stacking interactions.

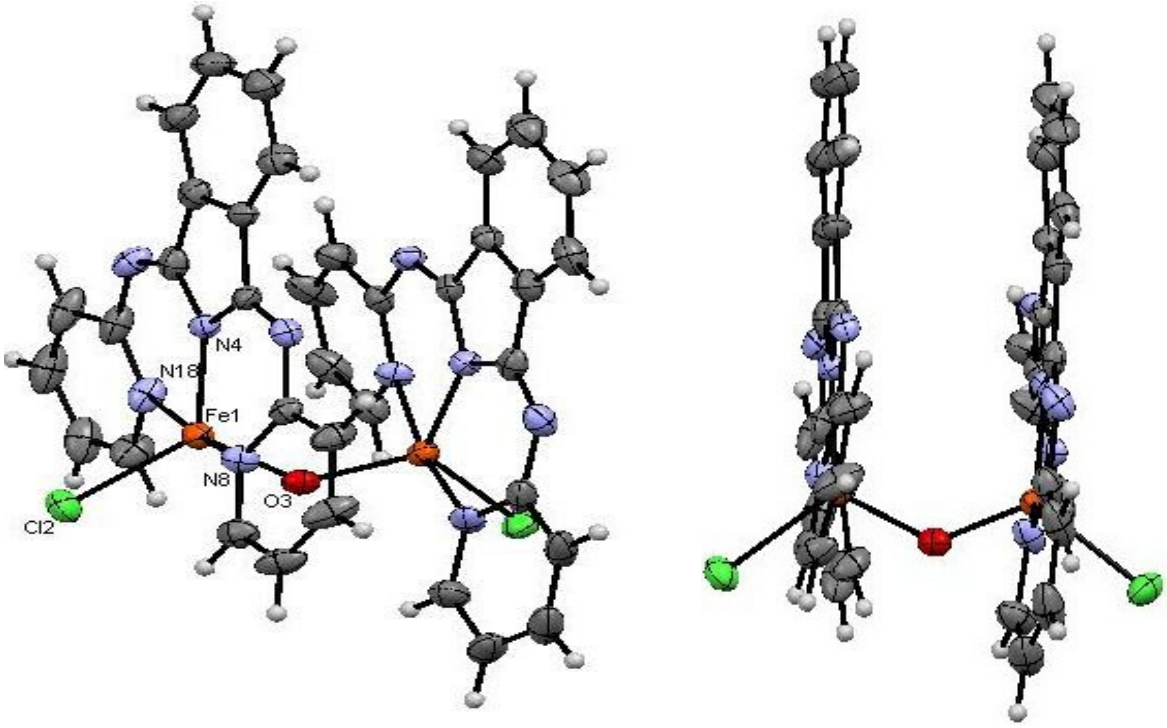

Figure 4. ORTEP views of oxidized diiron(III) complex [(**2**)FeCl(μ-O)FeCl(**2**)]. Thermal ellipsoids are represented at the 50% level. Selected bond lengths (Å) and angles (°): Fe(1)-N(4) = 2.002(5), Fe(1)-N(8) = 2.152(5), Fe(1)-N(18) = 2.139(5), Fe(1)-Cl(2) = 2.264(19), Fe(1)-O(3) = 1.786(3), Fe1-O1-Fe1' = 131.1(3), N4-Fe1-N8 = 85.8(2), N4-Fe1-N18 = 86.1(2), Cl2-Fe1-N4 = 123.5(15), O3-Fe1-N4 = 119.8(2), Cl2-Fe1-O3 = 116.6(17).

II. Reactivity of the binuclear complexes toward ethylene

1. Catalytic results

The newly prepared binuclear complexes were tested as pre-catalysts for ethylene oligomerization upon activation with MAO (methylaluminoxane) at 30 bar and the results are summarized in Table 1. Only the complex obtained from oxidation of [$FeCl_2$(H**1**)] oligomerized ethylene (Table 1, entry 1) with an activity of 13.5×10^5 g(products)·(mol(Fe)·h)$^{-1}$ at 30 °C. The complex [(**1**)FeCl(μ-O)FeCl(**1**)] exhibited good stability under the oligomerization reaction conditions as indicated by the linear ethylene uptake (Figure 5). At 30 °C, the mononuclear complex [$FeCl_2$(H**1**)] was inactive (Table 1, entry 2). For comparison (see Chapter II), the activity of the mononuclear complex [$FeCl_2$(H**1**)] was 2.16×10^5 g(products)·(mol(Fe)·h)$^{-1}$ at 80 °C (Table 1, entry 3).

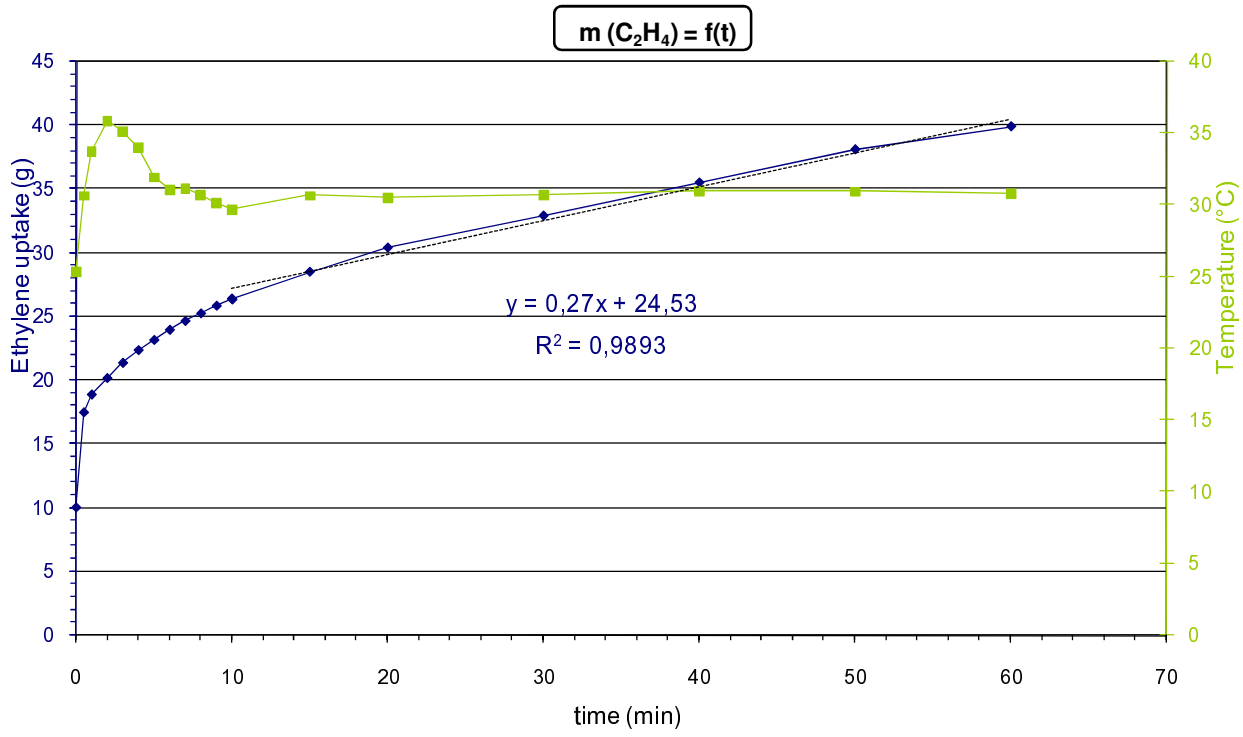

Figure 5. Monitoring of the ethylene uptake as a function of time and temperature during the oligomerization reaction.

Ethylene oligomerization by the binuclear complex [(**1**)FeCl(μ-O)FeCl(**1**)] yielded light olefins among the oligomers, with up to 31 wt% of butenes with an α-selectivity in 1-butene

of 94 wt%. In comparison with results obtained with [$FeCl_2$(**1**)], the α-selectivity decreased from 97 to 94% for 1-butene and from 90 to 71% for 1-hexene. A larger amount of waxes and polyethylene was also formed. No ethylene uptake was observed with complex [$FeCl_2$(H**1**)] (Table 1, entry 4).

The binuclear iron precursor [(**2**)FeCl(μ-O)FeCl(**2**)], obtained by oxidation of [$FeCl_2$(H**2**)], was inactive after MAO activation (Table 1, entries 5 and 6). The same explanations as proposed in Chapter II can be put forward to explain such inactivity (steric hindrance and detrimental 6-membered rings). The ferrous complex [$FeCl_2$(H**2**)] was also inactive toward ethylene (Table 1, entry 7). For comparison (see Chapter II), no ethylene uptake was detected with the ferric complex [$FeCl_2$(**2**)] (Table 1, entry 8).

Table 1. Catalytic ethylene oligomerization with mononuclear and binuclear complexes.[a]

Entry	Complex	T (°C)	Activity[c]	Oligomers distribution[d,e]			Waxes and PE
				C_4 (1-C_4)[f]	C_6 (1-C_6)[f]	$C_{\geq 8}$	
1	[(**1**)FeCl(μ-O)FeCl(**1**)]	30	13.5	31 (94)	12 (71)	8	49
2	[$FeCl_2$(**1**)]	30	0[g]	-	-	-	-
3[b]	[$FeCl_2$(**1**)]	80	2.2	63 (97)	18 (90)	7	12
4	[$FeCl_2$(H**1**)]	80	0[g]	-	-	-	-
5	[(**2**)FeCl(μ-O)FeCl(**2**)]	30	0[g]	-	-	-	-
6	[(**2**)FeCl(μ-O)FeCl(**2**)]	80	0[g]	-	-	-	-
7	[$FeCl_2$(H**2**)]	80	0[g]				
8	[$FeCl_2$(**2**)]	80	0[g]				

[a] n(Fe) = 7.8 μmol, MAO (Al/Fe = 200), ethylene pressure 30 bar, 60 min, toluene (50 mL). [b] n(Fe) = 20 μmol, 120 min. [c] $\times 10^5$ g(products)·(mol(Fe)·h)$^{-1}$ estimated over the steady period of ethylene consumption. [d] Determined by GC. [e] wt% among all the products formed. [f] wt% in the C_n fraction. [g] no ethylene uptake.

2. Toward an understanding of the Fe-O-Fe bond effect

All the experiments performed above showed the specificity of [(**1**)FeCl(μ-O)FeCl(**1**)] for ethylene oligomerization. Since experimental data on the mechanism of activation of this kind of complex with MAO are rare, it is difficult to explain this particular behavior. The significant variations in activities and product distribution (short chain oligomers and waxes/polymers) observed with the mononuclear and the binuclear complexes may suggest the involvement of different active species.

Catalytic results obtained with binuclear complex [(**1**)FeCl(μ-O)FeCl(**1**)] could be attributable to a cooperative process involving the two proximate electrophilic centers. Sun

and Schumann independently reported that binuclear nickel or iron complexes showed higher activity and produced higher molecular weight polyethylene than the mononuclear complexes.[19,30] Fan and coworkers also reported the selective activation of metallic center in a methylene-bridged bimetallic cobalt/nickel complex chelated by 2,6-bis(imino)-pyridine and α-diimine moities.[31] Once activated by MAO or TEA, these bimetallic systems exhibited higher activities than the sum of the individual activities of the corresponding nickel and cobalt complexes. Furthermore, significant differences in product distribution (quantity of waxes and polymers) and the decrease of the α-selectivity are consistent with the supposed cooperative effect. Taking these arguments into account, a hypothetical structure of a binuclear species active under our reaction conditions is proposed in Scheme 7. The increase of catalytic activity may also be attributed to the formation of a more stable cationic intermediate compared mononuclear precatalyst [$FeCl_2$(**1**)].

The higher activity could be attributed to the enhanced electrophilicity of the cationic iron in (**1**)Fe^+-O-FeMe(**1**) compared to the mononuclear cationic species FeMe(**1**)$^+$. The oxygen atom would decrease the electronic density around the cationic iron centers and thus increase their electrophilic reactivity. A mechanism for the formation of the active species is proposed in Scheme 7.

The first step of this suggested mechanism is the monoalkylation by exchange of the X ligand between the binuclear complex and the "alkylating agent" in the MAO. The unsymmetrical intermediate [(**1**)FeCl-O-FeMe(**1**)] would then react with the "electrophilic centers" present in the MAO by an acid-base reaction to form the cationic center stabilized by the counter anion [MAO-Cl]$^-$. Successive insertions of ethylene into the Fe^+-Me bond and *β*-H elimination of propylene would yield the binuclear active species. This species would be composed of two sites: the coordination site of the olefins (cationic center) and the chain growth site (neutral center).

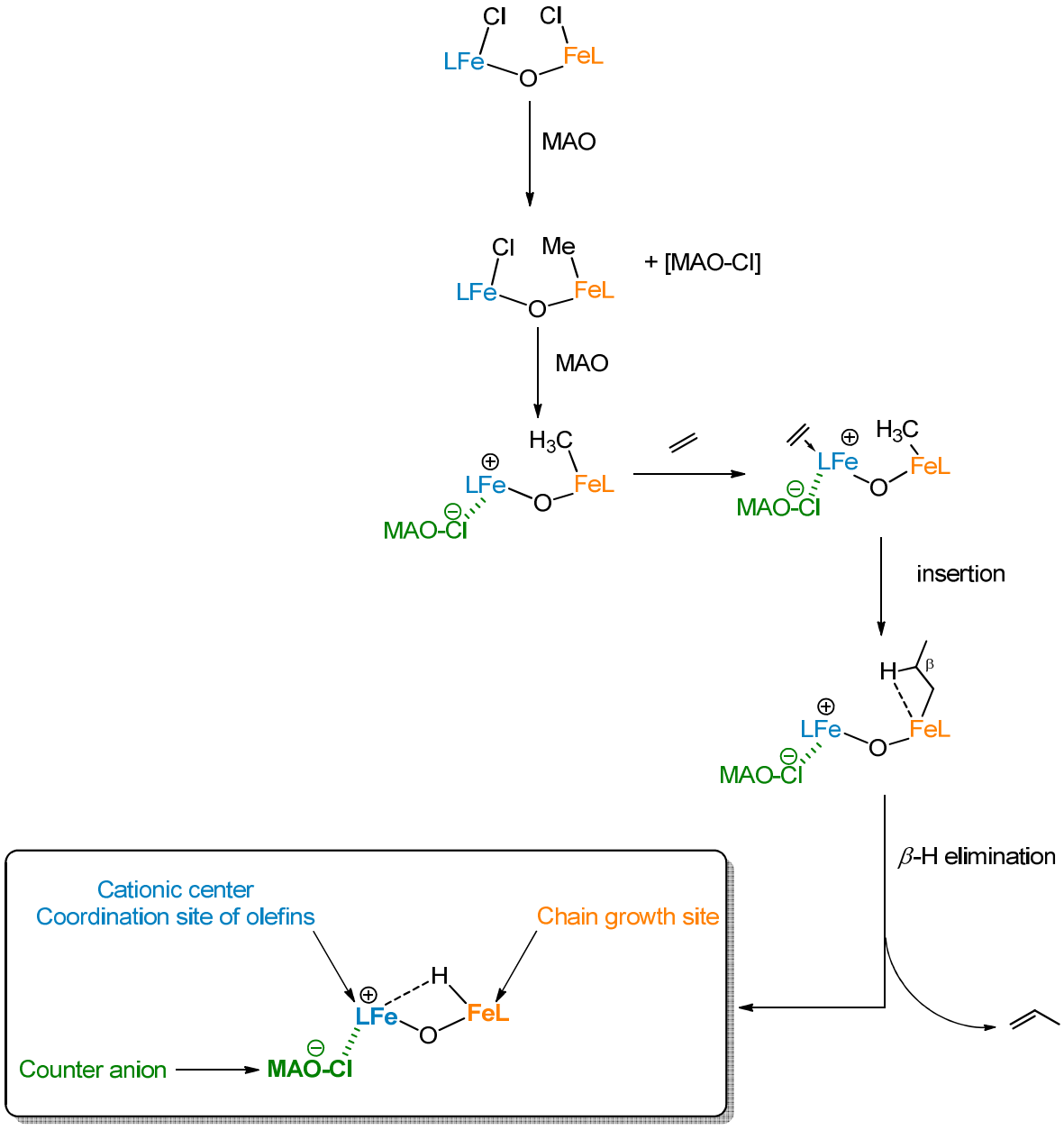

Scheme 7. Hypothetical structure of binuclear active species.

Details of the composition of C_4 and C_6 fractions are given in Table 2. A mechanism focusing on the formation of C_6 oligomers is proposed (Scheme 8). The first step of the ethylene oligomerization cycle is the dative coordination of ethylene on the cationic center (Scheme 8, orange cycle). The ethylene is then inserted into the Fe-H bond. Two molecules of ethylene are successively inserted into the Fe-Et and Fe-Bu bonds, respectively. Finally, 1-C_6 is released after a chain termination process (β-H elimination).

The larger amount of 2-ethyl-1-butene (2-Et-1-C_4) in the C_6 fraction reinforces the hypothesis of a binuclear active species. This olefin can be obtained by the 1,2-insertion of a

molecule of 1-butene into the Fe-Et bond (Scheme 8, blue cycle). However, this reaction is disfavored owing to the privileged coordination and insertion of ethylene (shorter olefin). The β-H transfer from the alkyl chain to a coordinated molecule of ethylene allows a switch in the coordination mode (Scheme 8). In this way, the 1,2-insertion of 1-butene into the Fe-Et bond becomes feasible. The 2,1-insertion of 1-butene into the Fe-Et bond leads to an internal C_6 product (Scheme 8, grey cycle).

Finally, the larger amount of polymers formed remains difficult to explain. We could suggest the presence of another non-selective active species formed during the oxidation process or during the reaction with MAO.

Table 2. Oligomers distributions focused on the C_4 and C_6 fractions.[a,b]

Complex	C_4			C_6			
	1-C_4[c]	*trans*-2-C_4[c]	*cis*-2-C_4[c]	1-C_6[c]	2-Et-1-C_6[c]	*trans*-3-C_6[c]	*cis*-3-C_6[c]
[(**1**)FeCl(μ-O)FeCl(**1**)]	94	4	2	71	17	10	2
[$FeCl_2$(**1**)]	97	2	1	90	3	4	3

[a] Determined by GC. [b] wt% among all the products formed. [c] wt% in the C_n fraction.

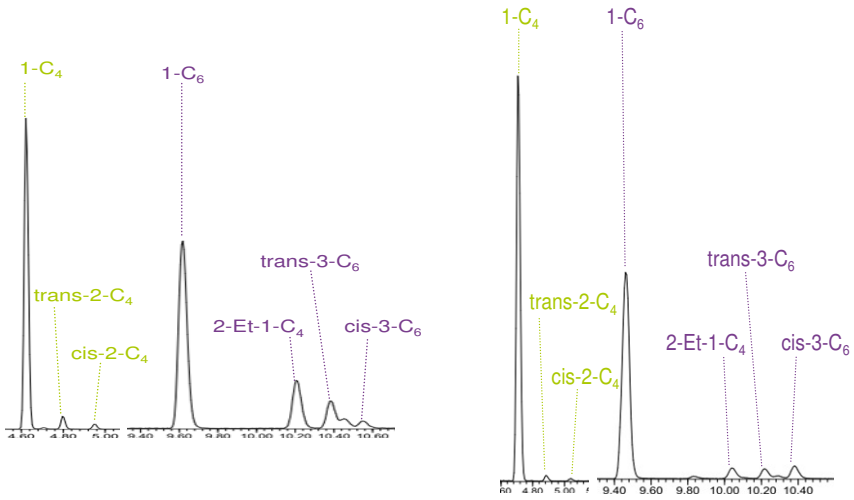

Figure 6. Focus on the C_4 and C_6 fractions for [(**1**)FeCl(μ-O)FeCl(**1**)] (left) and [$FeCl_2$(**1**)] (right).

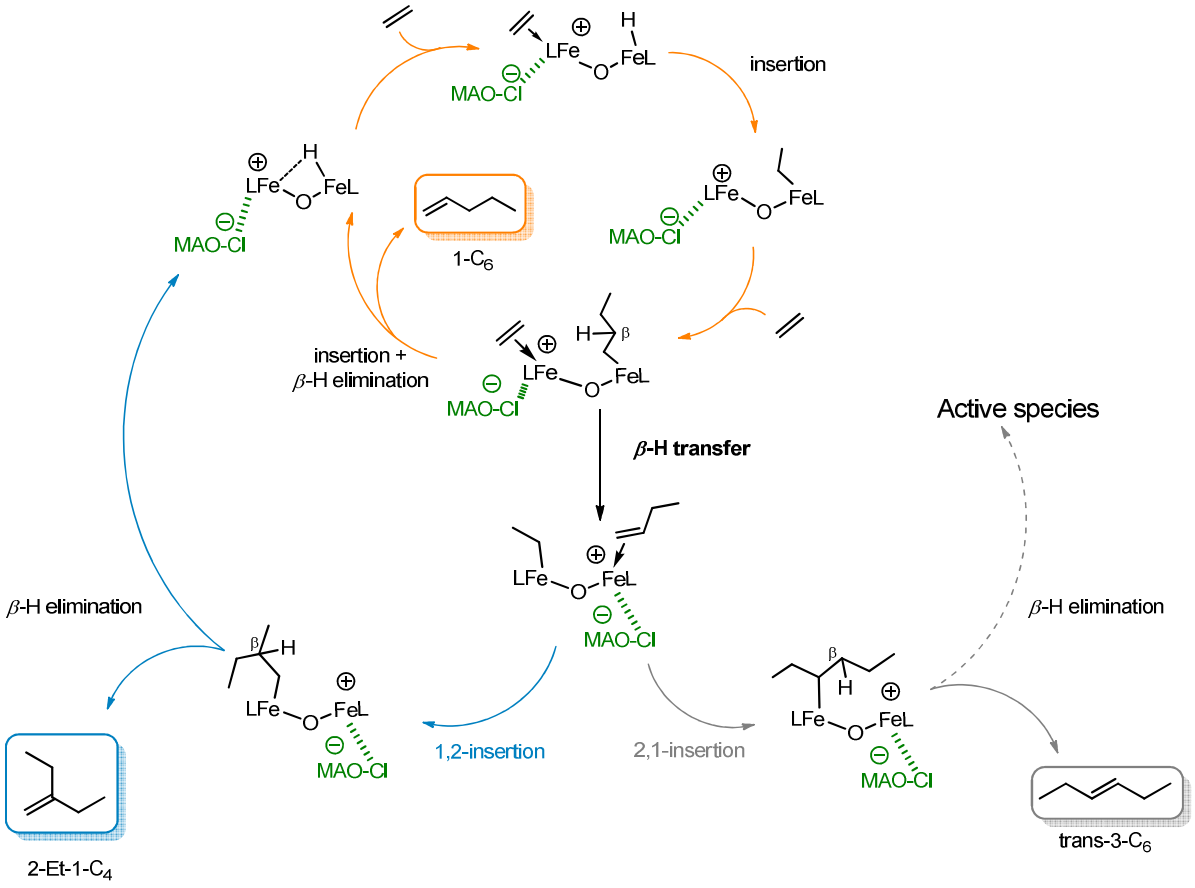

Scheme 8. Proposed catalytic cycle for the formation of C_6 oligomers.

Conclusion

We described the synthesis of μ-oxo-bridged binuclear iron(III) complexes [(L)FeCl(μ–O)FeCl(L)] by oxidation of corresponding ferrous complexes chelated by tridentate N,NH,N ligand. The oxidation reaction resulted in the formation of iron-oxygen bonds and in the deprotonation of the central amino group. An X-ray diffraction study of [(**2**)FeCl(μ–O)FeCl(**2**)] and FT-IR spectroscopy confirmed the formation of both the Fe-O-Fe moiety and the anionic character of the ligand. While the ferric complex chelated by the anionic 1,3-bis(2'-pyridylimino)isoindoline ligand showed no activity under MAO activation (steric hindrance is suggested to explain such inactivity), we highlighted the complex [(**1**)FeCl(μ–O)FeCl(**1**)] as the first catalytic system with μ-oxo-bridged binuclear iron(III) precursor bearing an anionic nitrogen donor ligand for ethylene oligomerization. Under mild conditions (concentration and temperature), this catalyst exhibits high activity (13.5×10^5 g(products)·(mol(Fe)·h)$^{-1}$). Moreover, no activity was obtained at the same temperature with the related mononuclear analogous complex [$FeCl_2$(**1**)]. The oxygen bridge and the cooperative effect between the two iron centers are suggested to explain the specific features of this pre-catalyst (higher activity, formation of more branched or internal olefins among the oligomers formed).

Acknowledgement

We thank IFP Energies nouvelles for their support and Dr. J. Ponthus for the HRMS measurements. The LCC also thanks the CNRS and the Ministère de la Recherche for support. We also thank Erwann Jeanneau (Université Claude Bernard – Lyon 1).

Experimental section

General consideration

All manipulations were carried out using standard Schlenk techniques under inert atmosphere. THF, pentane and diethyl ether were dried by a solvent purification system (SPS-M-Braun). Acetonitrile was degassed and dried over molecular sieves (4 Å). Commercial starting materials were purchased from Sigma-Aldrich and Alfa Aesar and used without further purification. Gas chromatographic analysis were performed on an Agilent 6850 series II or Varian CP-3800 instrument equipped with autosamplers and fitted with PONA columns (50 m, 0.2 mm diameter, 0.5 μm film thickness). FT-IR spectra were recorded in the region 4000-450 cm^{-1} on a Perkin-Elmer Spectrum one FT-IR spectrometer (ATR mode, ZnSe diamond). Diffraction data were collected on a Nonius KappaCCD diffractometer with graphite monochromated Mo-Kα radiation (λ = 0.71073 Å). Data were collected using Ψ scans; the structures were solved by direct methods using the SIR97 software and the refinement was by full-matrix least squares on F^2. No absorption correction was used. The tridentate ligand (H**2**) was synthesized according to literature procedures and used without further purification.[32] The synthesis of complex [$FeCl_2$(H**1**)] was described in Chapter II.

Synthesis and Characterization of the Iron Complexes

- **Synthesis of the binuclear complex** [(**1**)FeCl(*μ*–O)FeCl(**1**)]

The complex [$FeCl_2$(H**1**)] (0.110 g, 0.23 mmol) was dissolved in 20 mL of degassed CH_3CN. O_2 was bubbled through the reaction mixture for 15 min. The solution changed color from pink to purple and was stirred for 60 min. at room temperature under O_2 atmosphere. The reaction mixture was evaporated under vacuum and dissolved in degassed chlorobenzene and 15 mL of pentane were added to precipitate the complex which was filtered and washed with pentane (3×15 mL). The product was obtained as a purple solid (0.190 g, 93% yield).

FT-IR (cm^{-1}): 2968w, 1603m, 1583m, 1567m, 1544w, 1450s, 1391s, 1324m, 1297m, 1219m, 1126m, 1056m, 1019w, 862m, 826s, 777s, 744s, 685m,, 652m, 604w, 591w, 578m, 492w, 464m.

- **Synthesis of the complex** [$FeCl_2$(H**2**)]

The ligand (H**2**) (0.300 g, 3.3 mmol) and $FeCl_2 \cdot 1.5THF$ (0.235 g, 3.3 mmol) were dissolved in 40 mL of dried THF. The reaction mixture was stirred at room temperature overnight. The complex precipitates and the mixture was filtered and the precipitate was washed with Et_2O (3× 20 mL). The iron complex was obtained as a green powder (1.362 g, 96% yield).

FT-IR (cm^{-1}): 3290w, 3221w, 3137w, 3072w, 1657w, 1627m, 1612w, 1554m, 1517m, 1466m, 1430m, 1374w, 1297w, 1206m, 1103m, 1057m, 1016w, 867w, 797m, 785m, 770s, 737w, 709s, 693w, 668m, 637w, 541w, 519m.

- **Synthesis of the complex** [(**2**)FeCl(μ–O)FeCl(**2**)] **according to the literature procedure**

The ligand (H**2**) (0.559 g, 1.9 mmol) and $FeCl_3 \cdot 6H_2O$ (0.503 g, 1.9 mmol) were dissolved in 50 mL of MeOH. The reaction mixture was refluxed (80 °C) overnight. The complex precipitates and the mixture was filtered and the precipitate was washed with CH_3CN (3× 15 mL). The complex was obtained as a brown powder (0.612 g, 82% yield).

FT-IR (cm^{-1}): 2840w, 1644m, 1610w, 1577m, 1553w, 1538s, 1461s, 1427s, 1355w, 1310w, 1296m, 1267s, 1190m, 1057s, 1015s, 898w, 849w, 791m, 770s, 712m, 640w, 534m, 476m.

- **Synthesis of the binuclear complex** [(**2**)FeCl(μ–O)FeCl(**2**)] **by oxidation**

This dinuclear complex was synthesized by the same method as used for [(**1**)FeCl(μ–O)FeCl(**1**)]. The complex was obtained as a brown solid (0.148 g, **82%** yield).

FT-IR (cm^{-1}): 3092w, 2923w, 2877w, 2811w, 1643m, 1576m, 1552w, 1537s, 1472w, 1461s, 1432s, 1355w, 1309w, 1296w, 1269m, 1191s, 1149m, 1056s, 1014s, 898w, 848s, 770s, 712s, 640w, 560w, 534m, 477m.

Some brown crystals were grown from a concentrated THF solution.

Crystallographic data and structure refinement details

	[{$Fe_2Cl_2(\mu$-O)}(**1**-**1**)]$_2$·2Et_2O	[(**2**)FeCl(μ-O)FeCl(**2**)]
Formula	$C_{92}H_{64}Cl_4Fe_4N_{16}O_2$·2($C_4H_{10}O$)	$C_{38}H_{24}Cl_2Fe_2N_{10}O$
Cryst. system	Orthorhombic	Orthorhombic
Space group	*P*bcn	*P*ccn
a (Å)	19.1126(3)	12.544(5)
b (Å)	26.6732(9)	13.338(5)
c (Å)	17.5989(5)	21.453(5)
Cell volume (Å^3)	8971.8	3589(2)
Density	1.436	1.590
Z	4	8
F(000)	4000	1744
T (K)	173	293
θmin-θmax (°)	1.3 – 26.0	3.6 – 29.5
h	-20/23	-16/10
k	-32/22	-12/18
l	-19/21	-26/29
μ (mm^{-1})	0.82	1.01
Measd. reflections	49987	11670
Indep. reflections	8819	4366
R_{int}	0.108	0.078
R [$F^2 > 2\sigma(F^2)$]	0.067	0.079
$wR(F^2)$ [$F^2 > 2\sigma(F^2)$]	0.162	0.298
S	1.04	1.00
$\Delta\rho_{min}$, $\Delta\rho_{max}$ (e·Å^{-3})	-0.39, 0.50	-2.30, 1.25

Iron-catalyzed oligomerization of ethylene

All catalytic reactions were carried out in a magnetically stirred 250 mL stainless steel autoclave. The toluene and the cocatalyst were first introduced under ethylene atmosphere. The iron precursor was then added. The reactor was sealed and fed with ethylene up to the half of the desired pressure (15 bars in our case). The reactor was heated at the desired temperature (30 °C or 80 °C) and then 30 bar of ethylene pressure were applied. During catalysis, the pressure was maintained through a continuous feed of ethylene from a bottle placed on a balance used to monitor the ethylene uptake. At the end of the test, stirring was stopped and the reactor was cooled down to 25 °C. The gaseous effluents were collected in a 15 L polyethylene bottle filled with water. The reactor was then cooled to -5 °C and the liquid effluents were collected from the bottom of the reactor and weighed. The catalyst and the cocatalyst were quenched by addition of EtOH. Liquid effluents were distilled by trap to trap technique (140 °C, 6.10^{-2} mbar) to separate waxes and polymers (not soluble in hot xylenes) from oligomers ($<C_{14}$). Aliquots of gaseous and liquid effluents were then analyzed by GC. The reactor was then washed three times with xylene at 140 °C and dried in vacuum (10^{-2} Torr) at 140 °C overnight. Finally, the reactor was cooled down to room temperature and fed up with ethylene (30 bar).

Bibliography

1. Kurtz, D. M. *Chem. Rev.* **1990,** *90*, 585.

2. Sanders-Loehr, J. In *Iron Carriers and Iron Proteins*, Loehr, T. M., Ed.; VCH: New York, **1989**; p 373.

3. Broussard, M. E.; Juma, B.; Train, S. G.; Peng, W. J.; Laneman, S. A.; Scott, A.; Stanley, G. G. *Science* **1993,** *260*, 1784.

4. Matthews, R. C.; Howell, D. K.; Peng, W. J.; Spencer, G.; Treleaven, W. D.; Stanley, G. G. *Angew. Chem., Int. Ed. Engl.* **1996,** *35*, 2253.

5. Sola, E.; Torres, F.; Jimenez, M. V.; Lopez, J. A.; Ruiz, S. E.; Lahoz, F. J.; Elduque, A.; Oro, L. A. *J. Am. Chem. Soc.* **2001,** *123*, 11925.

6. Jimenez, M. V.; Sola, E.; Lahoz, F. J.; Oro, L. A. *Organometallics* **2005,** *24*, 2722.

7. Nowlan, D. T.; Singleton, D. A. *J. Am. Chem. Soc.* **2005,** *127*, 6190.

8. Pirrung, M. C.; Liu, H.; Morehead, A. T. *J. Am. Chem. Soc.* **2002,** *124*, 1014.

9. Sammis, G. M.; Danjo, H.; Jacobsen, E. N. *J. Am. Chem. Soc.* **2004,** *126*, 9928.

10. Tschan, M. J. L.; Süss-Fink, G.; Chérioux, F.; Therrien, B. *Chem. Eur. J.* **2007,** *13*, 292.

11. Patureau, F. W.; de Boer, S.; Kuil, M.; Meeuwissen, J.; Breuil, P. A.; Siegler, M. A.; Spek, A. L.; Sandee, A. J.; de Bruin, B.; Reek, J. N. H. *J. Am. Chem. Soc.* **2009,** *131*, 6683.

12. Yuen, H. F.; Marks, T. J. *Organometallics* **2008,** *27*, 155.

13. Delferro, M.; Marks, T. J. *Chem. Rev.* **2011,** *111*, 2450.

14. Guo, N.; Li, L.; Marks, T. J. *J. Am. Chem. Soc.* **2004,** *126*, 6542.

15. Kuwabara, J.; Takeuchi, D.; Osakada, K. *Chem. Commun.* **2006,** 3815.

16. Zhang, S.; Sun, W. H.; Kuang, X. F.; Vystorop, I.; Yi, J. J. *J. Organomet. Chem.* **2007,** *692*, 5307.

17. Zhang, S.; Vystorop, I.; Tang, Z. H.; Sun, W. H. *Organometallics* **2007,** *26*, 2456.

18. Armitage, A. P.; Champouret, Y. D. M.; Grigoli, H.; Pelletier, J. D. A.; Singh, K.; Solan, G. A. *Eur. J. Inorg. Chem.* **2008,** *2008*, 4597.

19. Wang, L.; Sun, J. *Inorg. Chim. Acta* **2008,** *361*, 1843.

20. Barbaro, P.; Bianchini, C.; Giambastiani, G.; Rios, I. G.; Meli, A.; Oberhauser, W.; Segarra, A. M.; Sorace, L.; Toti, A. *Organometallics* **2007,** *26*, 4639.

21. Mandal, S. K.; Roesky, H. W. *Acc. Chem. Res.* **2010,** *43*, 248.

22. Vincent, J. B.; Olivier-Lilley, G. L.; Averill, B. A. *Chem. Rev.* **1990,** *90*, 1447.

23. Choi, S. Y.; Eaton, P. E.; Kopp, D. A.; Lippard, S. J.; Newcomb, M.; Shen, R. *J. Am. Chem. Soc.* **1999,** *121*, 12198.

24. Balogh-Hergovich, E.; Speier, G.; Reglier, M.; Giorgi, M.; Kuzmann, E.; Vertes, A. *Eur. J. Inorg. Chem.* **2003,** 1735.

25. Luo, S.; Shen, B.; Li, B.; Song, H.; Xu, S.; Wang, B. *Organometallics* **2009,** *28*, 3109.

26. Gurubasavaraj, P. M.; Roesky, H. W.; Sharma, P. M. V.; Oswald, R. B.; Dolle, V.; Herbst-Irmer, R.; Pal, A. *Organometallics* **2007,** *26*, 3346.

27. Kojima, T.; Leising, R. A.; Yan, S.; Que, L. *J. Am. Chem. Soc.* **1993,** *115*, 11328.

28. Ito, S.; Okuno, T.; Matsushima, H.; Tokii, T.; Nishida, Y. *J. Chem. Soc. , Dalton Trans.* **1996,** 4479.

29. Boudier, A.; Breuil, P. A.; Magna, L.; Rangheard, C.; Ponthus, J.; Olivier-Bourbigou, H.; Braunstein, P. *Organometallics* **2011,** *30*, 2640.

30. Luo, H. K.; Schumann, H. *J. Mol. Catal. A: Chem* **2005,** *227*, 153.

31. Sun, T.; Wang, Q.; Fan, Z. *Polymer* **2010,** *51*, 3091.

32. Siegl, W. O. *J. Org. Chem.* **1977,** *42*, 1872.

CHAPTER IV

Well-Defined Cocatalysts enabling the Activation of Iron Precursors for the Oligomerization of Ethylene

Abstract: This chapter reports the discovery of well-defined cocatalysts enabling the activation of iron(II) and iron(III) complexes for the oligomerization of ethylene. The reaction of trimethylaluminum ($AlMe_3$) with organic compounds containing hydroxyl or/and amino groups was studied. A first screening involving phenol derivatives and alcohols led to active systems (10^5 g·(mol(Fe)·h)$^{-1}$). The reaction of phenol with TMA yielded a well-defined cocatalyst with general formula $[AlMe_2(OPh)]_2$ enabling the activation of the iron complex. A second screening was carried out to extend the study to diols, 2-aminophenol and *o*-phenylenediamine. Among all the organic compounds tested *in situ* with $AlMe_3$, the aromatic diols exhibited the highest activities with an optimum obtained for 2,2'-dihydroxybiphenyl. The optimized diol/Al ratio of 2/3 yielded well characterized trinuclear aluminum complexes. Activated by 500 equivalents of well-defined aluminum cocatalysts, the iron(II) bis(imino)pyridine precursor **A** $[FeCl_2(L)]$ (L = 2,6-$(ArN{=}CMe)_2C_5H_3N$, Ar = 2-methylphenyl) oligomerized ethylene with high activities (~10^6 g·(mol(Fe)·h)$^{-1}$). Although the activities observed with the isolated cocatalysts remained lower than when cocatalysts were formed *in situ*, we succeeded in activating an iron(II) complex with an isolated, well-defined cocatalyst which represents a real breakthrough in this field.

Résumé : Ce chapitre rapporte la découverte de nouveaux cocatalyseurs permettant l'activation des précurseurs de fer(II) et de fer(III) pour l'oligomérisation de l'éthylène. Ces activateurs ont été obtenus par réaction entre le TMA (triméthylaluminium) et une molécule organique possédant une ou plusieurs fonctions hydroxyl et/ou amine. L'utilisation de composés phénoliques et d'alcools aliphatiques saturés a donné des activités de 10^5 $g\cdot(mol(Fe)\cdot h)^{-1}$. La réaction entre le phénol et le TMA a conduit à un cocatalyseur binucléaire de formule générale $[AlMe_2(OPh)]_2$ qui a permis l'activation du complexe de fer(II) bis(imino)pyridine. Ce concept a été étendu aux composés de types diols, 2-aminophénol et *o*-phénylènediamine. Parmi tous les composés testés *in situ* avec le TMA, les diols aromatiques ont conduit aux meilleurs performances catalytiques avec un optimum pour la 2,2'-dihydroxybiphényl. Un ratio diol/Al optimal de 2/3 a conduit à des complexes d'aluminium trinucléaires de structures bien définies. Activés par 500 équivalents de cocatalyseurs parfaitement définis, le complexe de fer(II) bis(imino)pyridines **A** $[FeCl_2(L)]$ (avec L = 2,6-$(ArN{=}CMe)_2C_5H_3N$ et Ar = 2-méthylphényle) oligomérise l'éthylène avec activités atteignant les 10^6 $g\cdot(mol(Fe)\cdot h)^{-1}$. Bien que ces activités soient un cran en dessous de celles obtenues lors des tests des activateurs formés *in situ*, nous sommes parvenus à activer les complexes de fer avec des activateurs isolés et parfaitement caractérisés ce qui constitue en soit une réelle avancée dans le domaine.

Introduction

Organoaluminum compounds play a key role in the activation of metal complexes for the polymerization and oligomerization of ethylene.[1-3] Upon treatment with suitable aluminum activators, bis(imino)pyridine iron and cobalt complexes either oligomerize or polymerize ethylene with high activities.[2] Although methylaluminoxanes (MAO) remains the most efficient cocatalyst for the oligomerization of ethylene by iron precursors,[4,5] its exact structure remains unclear, despite extensive investigations.[1] Such activators with general formula $[\text{-Al(Me)-O-}]_n$ (with n~3-40) are obtained by controlled hydrolysis of trimethylaluminum.[6] Several structures have been proposed on the basis of various analyses and parallel studies involving for example triisobutylaluminum (TIBA = Al^iBu_3).[7,8] The proposed structures vary from one-dimensional linear chains, two-dimensional structures, three-dimensional clusters to cyclic and cage structures. The characterization of MAO by ^{27}Al NMR spectroscopy has shown that tetracoordinated Al centers predominate in MAO solutions, although tricoordinated Al sites were also identified.[9,10] However, the structure of MAO cannot be directly elucidated because of the multiple equilibria present in its solutions, and residual trimethylaluminum in MAO solutions appears to participate in equilibria that interconvert various MAO oligomers. An inherent problem is the presence of trimethylaluminum in MAO which is itself inactive in the oligomerization of ethylene. Free TMA can be removed by evaporation but it is difficult to reduce the CH_3/Al ratio to less than 1.5.[11]

Drawbacks in the use of MAO are its very low solubility in aliphatic solvents and poor storage stability in solution. Alternatives such as modified methylaluminoxanes (MMAO) are commercialized by Akzo Nobel. This activator was synthesized by controlled hydrolysis of a mixture of trimethylaluminum and triisobutylaluminum. In comparison with MAO, 25% of the methyl groups have been replaced by isobutyl groups. The incorporation of triisobutyl moieties in the structure confers better solubility in aliphatic solvents and longer storage stability. Moreover, MMAO can be produced at lower cost due to the lower price of TIBA in comparison with TMA. Unfortunately, MAO and MMAO generally require high Al/Fe ratios (between 500 and 2000 equiv.) for catalysts activation, which remains a constraint for their industrialization.

Other cocatalysts can activate iron complexes for ethylene oligomerization but led to lower activities than MAO or MMAO. Sun *et al.* reported on the oligomerization of ethylene

by iron(III) complexes bearing 2-(benzimidazole)-6-(1-aryliminoethyl)pyridines activated by diethylaluminumchloride (DEAC = $AlEt_2Cl$) and MAO. Although DEAC succeeded in activating iron catalysts (Al/Fe = 500; $0.75\times10^4 g\cdot(mol(Fe)\cdot h)^{-1}$), the activities remained 30 times lower than when MAO was used (Al/Fe = 1000; $21.8\times10^4 g\cdot(mol(Fe)\cdot h)^{-1}$).[12] The same trend was observed with iron(II) complexes bearing 2-(benzimidazol-2-yl)-1,10-phenanthrolyl ligand. Activities observed with DEAC (Al/Fe = 1000; $7.27\times10^5 g\cdot(mol(Fe)\cdot h)^{-1}$) as cocatalyst remained 5 times lower than with MMAO (Al/Fe = 1000; $35.1\times10^5 g\cdot(mol(Fe)\cdot h)^{-1}$).[13]

Here we report the study and the development of new cocatalysts allowing the activation of iron(II) and iron(III) complexes for ethylene oligomerization. Cocatalysts were formed by reaction of phenols, alcohols, diols, aminophenol or 1,2-benzendiamine with $AlMe_3$ and are possibly used *in situ* or as isolated species.

I. Screening of various mono-hydroxyl organic compounds

1. General procedure

Alcohol and phenol derivatives were pretreated to be as dry as possible before any reaction with TMA to avoid undesired reactions. The solid organic compounds were washed twice with dry toluene and placed under vacuum for 2 h (10^{-2}Torr; 40 °C) whereas the liquid ligands were degassed by freeze pump method and dried with molecular sieves (3 Å). All the cocatalysts were synthesized using the following procedure. To a solution of one equivalent of the mono-hydroxyl ligand at -78 °C in dry toluene was added one equivalent of TMA. The solution was stirred for 30 min at -78 °C. The colorless solution was brought to room temperature and stirred for 30 min. Without further characterization, the catalytic performances of the cocatalysts formed in situ were tested. Results are summarized in Table 1.

2. Results of the preliminary screening

Before testing new organic compounds, a first series of experiments involving the following cocatalysts was carried out: TMA (trimethylaluminum), TEA (triethylaluminum), TIBA (triisolbutyulaluminum), EADC (ethylaluminumdichloride), DEAC (diethylaluminumchloride), DIBALH (diisobutylaluminumhydride), (TMA/BEt_3) = 1:1, MAO (methylaluminoxanes). Some of these activators have been reported to activate iron complexes for the ethylene polymerization (see TMA, TEA, TIBA)[3] or nickel (EADC and DEAC)[14,15] and titanium complexes (TEA)[16] for ethylene oligomerization. However, only MAO succeeded in activating the iron complex **A** (Scheme 1) (Table 1, entries 1-8).

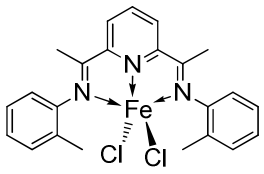

Scheme 1. Iron(II) complex **A.**

A surprisingly interesting activity of 9.3×10^5g·(mol(Fe)·h)$^{-1}$) was observed by combining phenol **1** with TMA with a distribution in oligomers comparable to that obtained with MAO (Table 1, entry 8 *vs* entry 9). Introducing substituents at the *o*- or *p*-positions of the phenol resulted in a decreased activity of the catalytic system (Table 1, entries 10 and 11) and in slightly shorter olefins (K = 0.67). Beside phenols, alcohols were tested and showed a different behavior. While cyclohexanol led to an active catalytic system (6.7×10^5g·(mol(Fe)·h)$^{-1}$), Table 1, entry 12), the *tert*-butanol associated with TMA did not allow the activation of the iron complex (Table 1, entry 13). Finally, tests involving either the organic compound **1** without TMA or the cocatalyst (**1**/$AlMe_3$) without the iron(II) complex, gave inactive systems (Table 1, entries 14 and 15), similarly to TMA when used alone as cocatalyst with the iron(II) complex (Table 1, entry 1), thus proving the necessary combination of these three components.

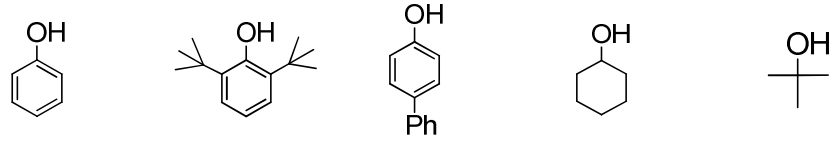

1 **2** **3** **4** **5**

Scheme 2. Phenol derivatives and alcohol ligands library.

Table 1. Results of oligomerization using different cocatalysts.[a]

Entry	Cocatalyst	Activity[b]	K
1	TMA	0[e]	-
2	TEA	0[e]	-
3	TIBA	0[e]	-
4	EADC	0[e]	-
5	DEAC	0[e]	-
6	DIBALH	0[e]	-
7	TMA/BEt_3 (1/1)	0[e]	-
8[c]	MAO	3890.3	0.69
9	**1**/$AlMe_3$ (1/1)	9.3	0.70
10	**2**/$AlMe_3$ (1/1)	3.6	0.67
11	**3**/$AlMe_3$ (1/1)	4.6	0.67
12	**4**/$AlMe_3$ (1/1)	6.7	0.69
13	**5**/$AlMe_3$ (1/1)	0[e]	-
14	**1**	0[e]	-
15[d]	**1**/$AlMe_3$	0[e]	

[a] Iron precursor (10 µmol), cocatalyst (500 equiv), toluene (25 mL), P_{C2H4} = 30 bar, T = 50 °C, 1h, selectivities >98%. [b]$\times10^5$ g·(mol(Fe)·h)$^{-1}$. [c] Iron precursor (20 µmol), MAO (200 equiv), toluene (50 mL), P_{C2H4} = 30 bar, T = 80 °C. [d] test was performed without iron complex. [e] no ethylene uptake.

3. Reaction between phenol and $AlMe_3$

Focusing on the products that may be formed by the reaction of phenol with TMA, we synthesized in good yield (80%) an aluminum complex having the structure proposed in Scheme 3. The ^1H NMR spectrum of the solid obtained in C_6D_6 (Figure 1) is consistent with the binuclear structures presented in the literature.[17] This symmetric structure exhibits a binuclear core based on two tetracoordinated aluminum atoms. The ^1H NMR signal corresponding to the methyl groups is shifted to lower values in C_7D_8 (-0.33 ppm) in comparison with signals in C_6D_6 (-0.29 ppm). Voigt *et al.* studied the interactions of $Al(C_6F_5)_3$ with benzene and toluene and in both cases the arene were coordinated in an η^1 fashion, yielding the complexes $Al(C_6F_5)_3$·toluene and $Al(C_6F_5)_3$·benzene.[18] The NMR spectra of theses complexes in C_6D_6 exhibited differences in chemical shifts of the fluorine atoms for the two complexes. For instance, the chemical shift of the *o*-fluorine of $Al(C_6F_5)_3$·toluene was found at -121.2 ppm while that of $Al(C_6F_5)_3$·benzene was at -123.1 ppm. This illustrates the influence of the arene solvents on the chemical shifts of aluminum compounds and could explain the differences observed in ^1H NMR for our binuclear complex.

This binuclear cocatalyst $[AlMe_2(OPh)]_2$ yielded the same catalytic results than the mixture **1**/$AlMe_3$.

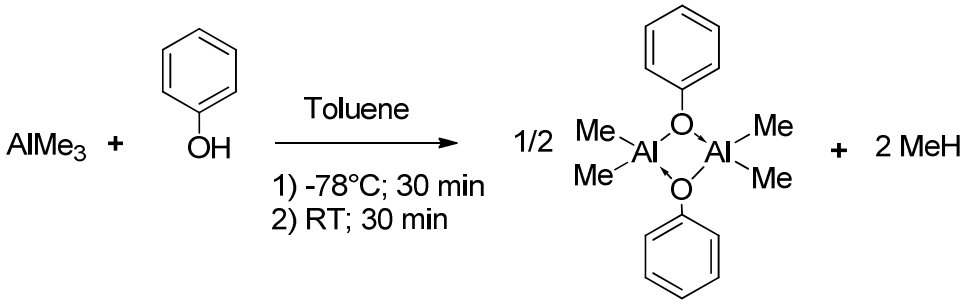

Scheme 3. Proposed reaction between **1** and $AlMe_3$ (1:1).

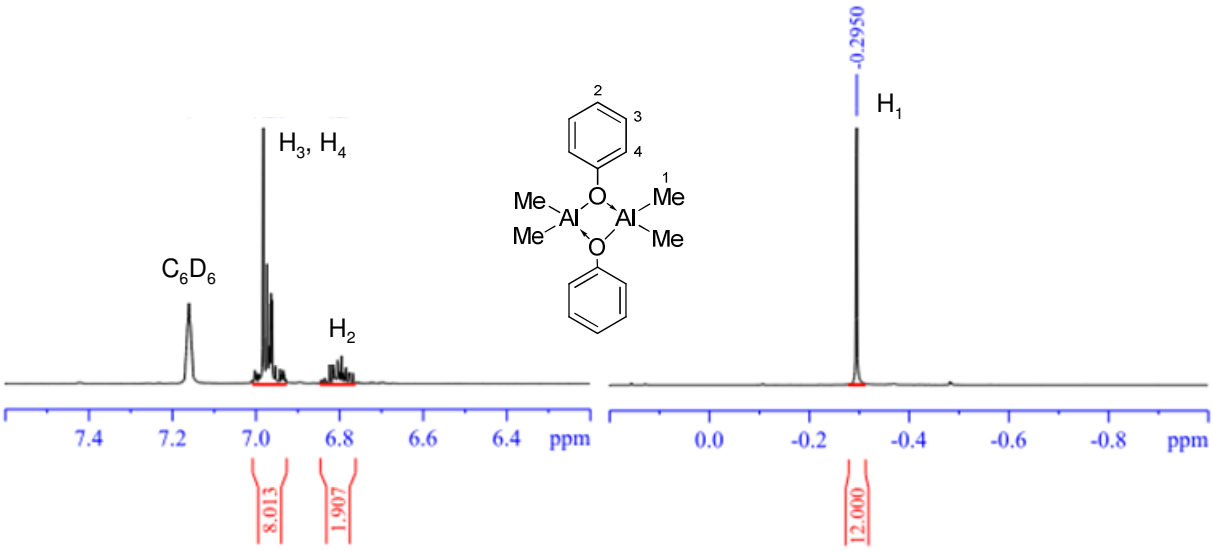

Figure 1. ^{1}H NMR spectrum of the binuclear complex $[AlMe_2(OPh)]_2$ in C_6D_6.

Controversial experimental and theoretical findings render the nature of the active species in the bis(imino)pyridine iron catalyst system still a matter of debate.[19-21] However, a structure could be proposed for intermediate species according to previous experiments and studies in the literature. Let us first consider the nature of the intermediates formed by reaction of an iron complex with a high ratio of TMA (Al/Fe = 500). Talsi *et al.* used ^{1}H NMR spectroscopy to determine the nature of theses intermediates. The activation of the iron complex chelated by 2,6-bis-[1-(2,6-dimethylphenylimino)-ethyl]pyridine with $AlMe_3$ formed bimetallic species. Because of the large excess of $AlMe_3$, all chlorides linked to iron were substituted by methyl groups.[22] Based on these results, a structure **B** was proposed for this intermediate species (Scheme 4). Although $AlMe_3$ was able to activate the iron precursor for the polymerization of ethylene, no oligomerization activity was observed in our case (Table 1, entry 1). This indicates that results obtained in polymerization on activators cannot be transposed directly to oligomerization systems.

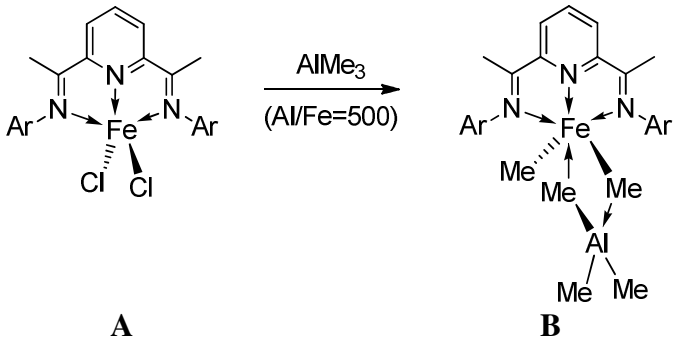

A **B**

Scheme 4. Proposed active species formed by reaction of **A** with $AlMe_3$ (Ar = 2-MeC_6H_4).

We established that the addition of phenol to $AlMe_3$ yielded an efficient binuclear cocatalyst for the oligomerization of ethylene. Results obtained with phenol derivatives indicated that increasing the steric bulk on the *o*-position of the aryl ring had a detrimental effect on the catalysis. Taking into account the structure of complex **B** and our previous results, a structure could be proposed for an intermediate species obtained by reaction of the iron complex with the binuclear complex synthesized in I.3 (green box, Scheme 5). Increasing the steric bulk of the organic compound (phenol, phenol derivatives or alcohol) would decrease the accessibility to the iron center and so the activity of the system. A mechanism leading to active species consistent with literature data and our results is proposed in Scheme 5. The first step is the exchange of chloride ligands leading to the dialkylation of the iron center. Chloride abstraction by [AlMeCl(OPh)] rather than [$AlMe_2$(OPh)] as Lewis acid would result in the formation of ion pairs. The substitution of a methyl group by a chloride atom increases the Lewis acidity of the aluminum center owing to the higher inductive effect of the chloride ligand. Finally, coordination of ethylene would release [$AlMe_2$(OPh)].

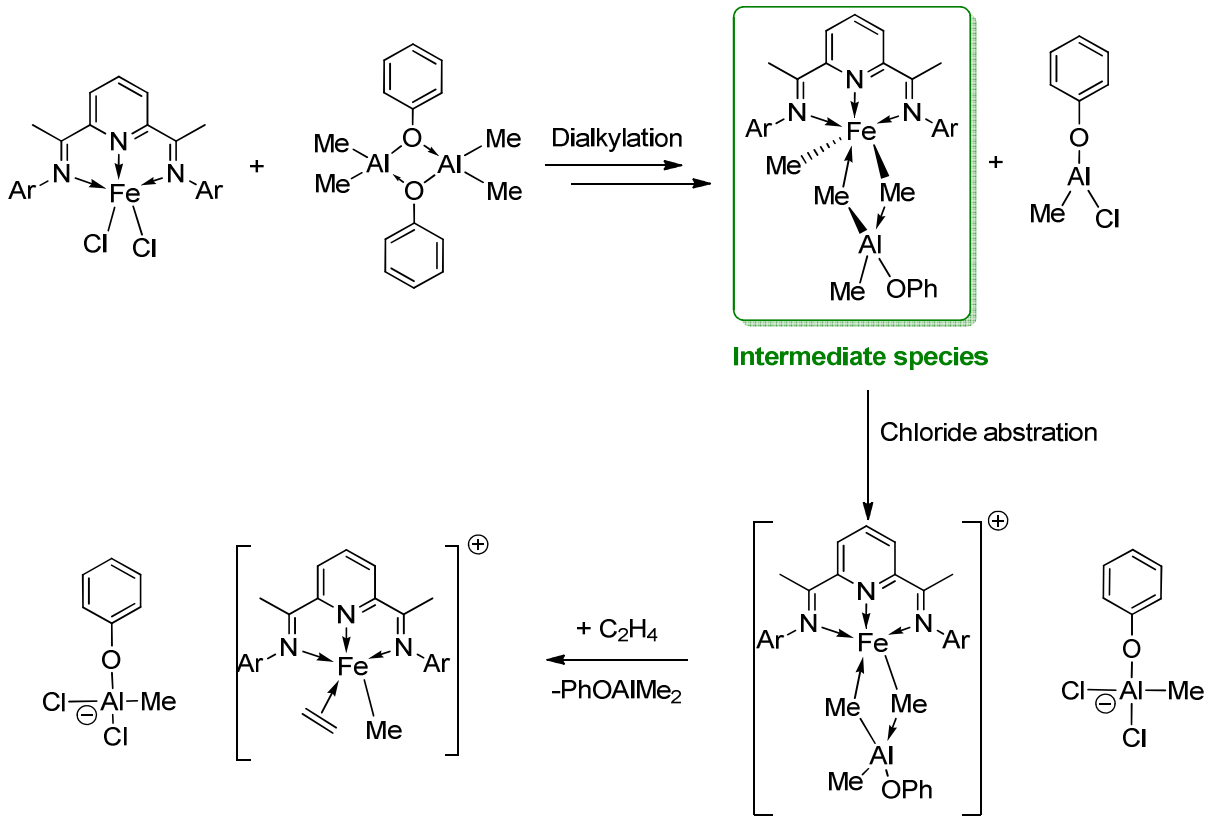

Scheme 5. Proposed mechanism involving cationic species.

II. Screening of diols, aminophenol and diaminobenzene compounds

A non-hydrolytic synthetic route was mentioned in the previous paragraph to synthesize new cocatalysts enabling the activation of the iron complex for the oligomerization of ethylene. Phenol proved to be the best candidate for this reaction. Following this study, we focused on increasing and/or modifying the number of substituents and reactive functional groups of the organic compounds in order to better mimic possible structures present in MAO. Therefore, the following study involves diols, 2-aminophenol and *o*-phenylenediamine compounds.

The different organic compounds were pretreated and tested using the same general procedure as for phenol and alcohol ligands (see I.1.). Two equivalents of TMA were engaged, keeping the ratio functional group to aluminum equal to 1. During syntheses, the solution turned cloudy with the diols **6**-**8**, **11**-**13** and a white solid precipitated with compounds **9**, **14** and **15**.

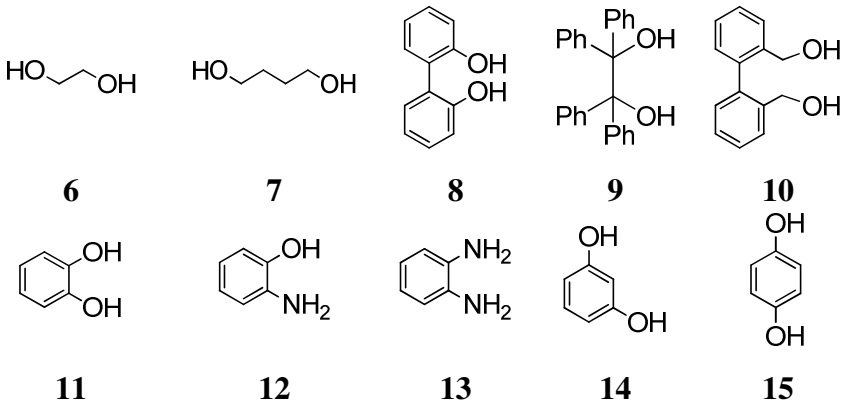

Scheme 6. Diols, 2-aminophenol and *o*-phenylenediamine compounds tested.

The catalytic results are summarized in Table 2. In all active systems, a full range C_4-C_{24} oligomers was produced with a high selectivity in α-olefins (>98%). Aromatic compounds led to better cocatalysts, although in some cases no activity was observed as for **9**, **10**, **14** and **15** (Figure 2). Increasing the length of the linker between the two oxygen atoms of the aliphatic compounds led to an increase of activity up to 12.9×10^5 g·(mol(Fe)·h)$^{-1}$ (Table 2, entry 1 *vs* entry 2). The compounds **9** and **10** gave inactive systems despite structural similarities with **8** which exhibited the highest potential in giving active cocatalyst (60×10^5g·(mol(Fe)·h)$^{-1}$, Table 2, entries 3-5). The steric bulk of ligand **9** caused by the phenyl rings may explain its inactivity. The pyrocatechol **11** gave interesting results in

oligomerization of ethylene with an activity of 22.7×10^5 g·(mol(Fe)·h)$^{-1}$ (Table 2, entry 6). The replacement of hydroxyl by aminogroups led to a slight decrease of activity (Table 2, entries 7 and 8). The distribution of oligomers with **13** was slightly shorter than with **12** (*K* = 0.67 for **13** *vs K* = 0.70 for **12**). Finally, no activity was observed with cocatalysts **14** and **15** (Table 2, entries 9 and 10). A comparison of the activities of the organic compounds tested is shown in Figure 2. Note that results previously obtained mono-hydroxyl compounds are also reported.

Table 2. Results of oligomerization with cocatalyst **6**/(2 $AlMe_3$)-**15**/(2 $AlMe_3$).[a]

Entry	Organic compound	Activity[b]	K
1	**6**	2.9	0.66
2	**7**	12.9	0.69
3[c]	**8**	60.0	0.70
4	**9**	0[d]	-
5	**10**	0[d]	-
6	**11**	22.7	0.69
7	**12**	11.0	0.70
8	**13**	10.6	0.67
9	**14**	0[d]	-
10	**15**	0[d]	-

[a] Iron precursor (10 µmol), $AlMe_3$ (500 equiv), toluene (25 mL), P_{C2H4} = 30 bar, T = 50 °C, 60 min, selectivities >98%. [b] $\times10^5$ g·(mol(Fe)·h)$^{-1}$. [c] reaction time: 25 min.[d] no ethylene uptake.

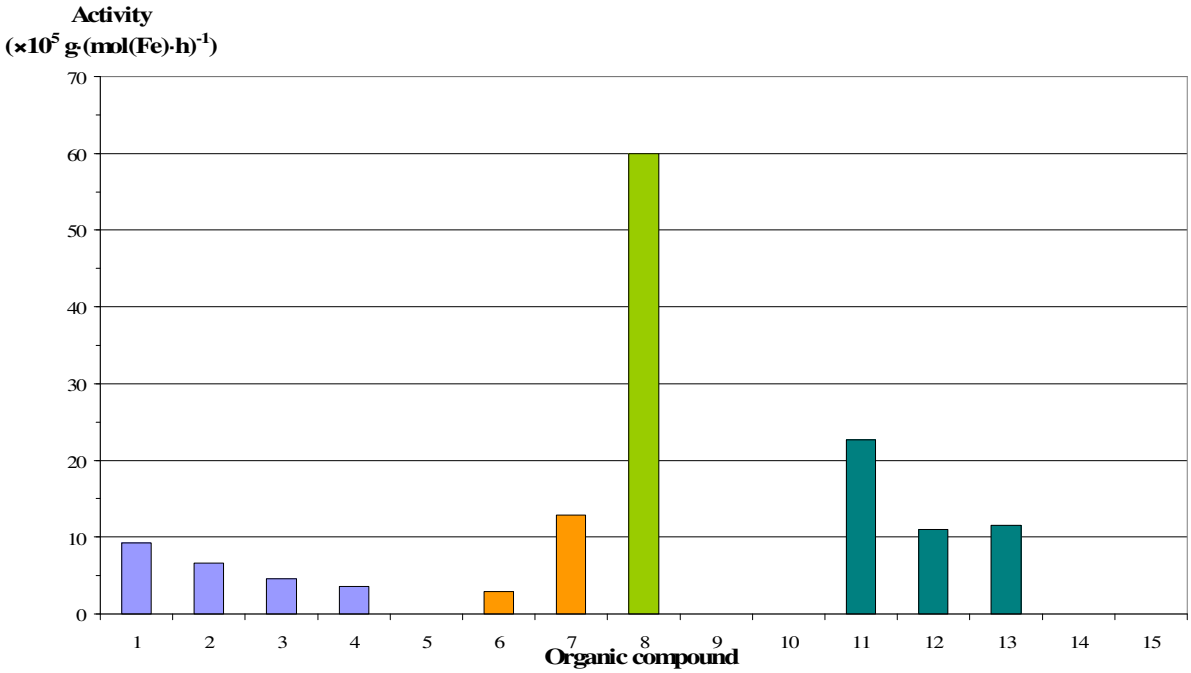

Figure 2. Results of the screening of **1**-**15**.

A monitoring of the catalytic reaction is illustrated in Figure 3 when diol **8** was engaged (which exhibits the highest activity among all tested compounds). In spite of a weak exothermic measurement of 12 °C, all parameters were correctly monitored during the test allowing the comparison between all the cocatalysts. Variations of activity were only due to the structure of cocatalysts and not to uncontrolled parameters.

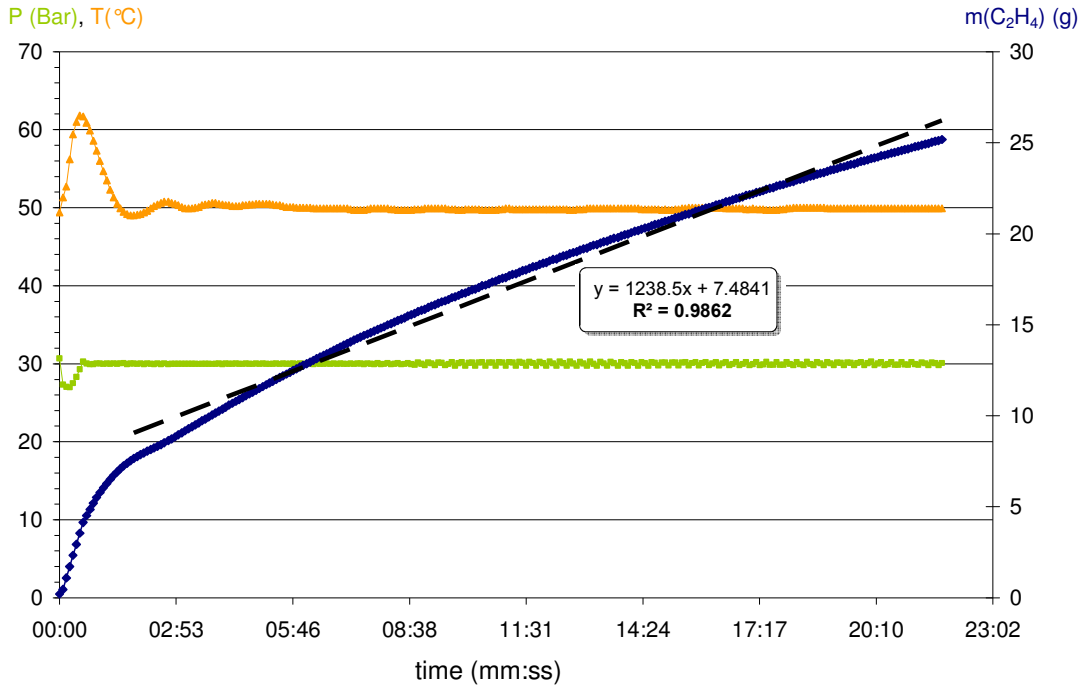

Figure 3. Monitoring of the parameters during catalysis

III. Optimization of the system

The reaction of TMA with diols leads to multinuclear cocatalysts depending on the reaction conditions (solvent and stoichiometry of the reagents). Indeed, as frequently observed in aluminum chemistry,[17,23,24] varying the solvent, the reaction time and the organic compounds/Al ratio gives a full range of multinuclear derivatives. The aim of this part of our work is to improve our system by optimizing both the diol/$AlMe_3$ and the Al/Fe ratios.

1. Optimization of the diol/$AlMe_3$ ratio

Considering the results obtained in paragraph II, the optimization was carried out with compound **8** and the results are summarized on Figure 4. The graph is divided into two parts

(Figure 4). For a **8**/$AlMe_3$ ratio< 1, the catalytic system is active for the oligomerization of ethylene. The optimum activity is obtained for the 2/3 ratio (Table 3, entries 1-4), up to 189×10^5 g·(mol(Fe)·h)$^{-1}$. While for a **8**/$AlMe_3$ ratio> 1, the catalytic system is inactive in oligomerization (Table 3, entries 5 and 6).

Table 3. Oligomerization of ethylene with various **8**/Al ratios.[a]

Entry	**8**/Al ratio	Reaction time (min)	Activity	*K*
1	1/5	60	23	0.66
2	1/2	24	59	0.69
3	2/3	8	189	0.70
4	4/5	60	16	0.67
5	1/1	60	0[c]	-
6	5/1	60	0[c]	-

[a] Iron precursor (10 µmol), $AlMe_3$ (500 equiv), toluene (25 mL), P_{C2H4} = 30 bar, T = 50 °C, selectivities >98%. [b] $\times10^5$ g·(mol(Fe)·h)$^{-1}$. [c] no ethylene uptake.

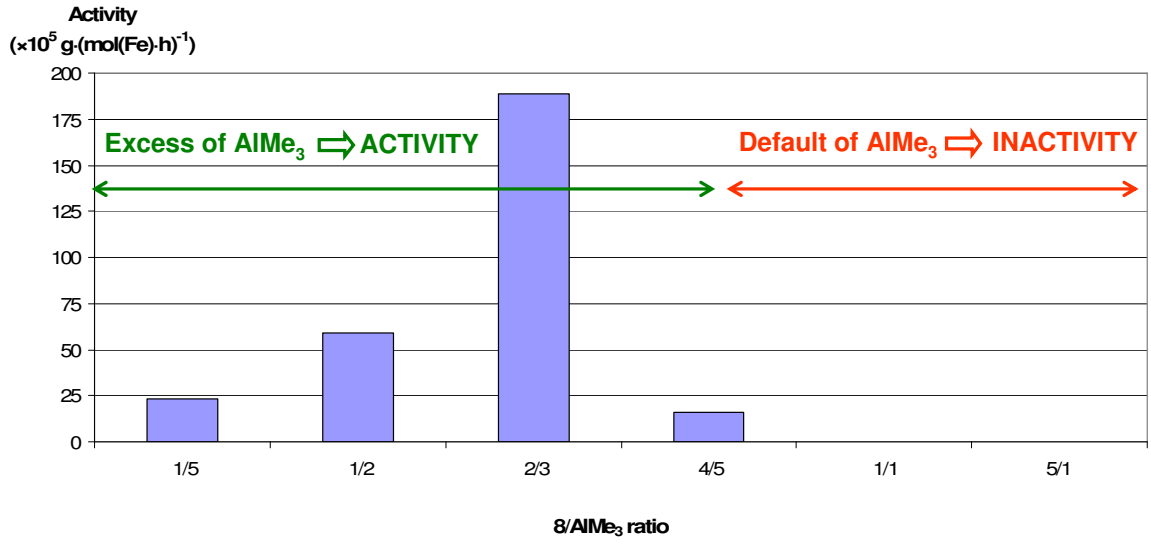

Figure 4. Screening of **8**/$AlMe_3$ ratio.

2. Optimization of the Al/Fe ratio

Increasing the Al/Fe ratio led to an improvement of the activity without changing the selectivity in α-olefins (Table 4, entries 1-4). Furthermore, the higher the ratio is, the longer the distribution is. The best activity was reached with a ratio of 500 (Table 4, entry 4, 189×10^5 g·(mol(Fe)·h)$^{-1}$). Activated by 50 equivalents of MAO, the catalytic system oligomerized ethylene with higher activity than upon activation with any ratio of cocatalysts **8**/$AlMe_3$ (Table 4, entry 5, 300×10^5 g·(mol(Fe)·h)$^{-1}$), however the selectivity in linear α-olefins is

slightly degraded (Table 4, entry 5). The increase of temperature (+40 °C) resulting from an exothermic reaction, may have degraded the catalytic species and thus its ability to produce linear α-olefins.

Table 4. Oligomerization of ethylene with various Al/Fe ratios.[a]

Entry	Al/Fe ratio	t (min)	Activity[b]	*K*	α
1	50	50	10	0.65	>99
2	100	18	84	0.66	>98
3	250	11	137	0.67	>98
4	500	8	189	0.70	>98
5[c]	50	5	300	0.71	>97

[a] Iron precursor (10 μmol), **8**/$AlMe_3$=2/3, toluene (25 mL), P_{C2H4} = 30 bar, T = 50 °C. [b] $\times 10^5 g\cdot(mol(Fe)\cdot h)^{-1}$. [c] MAO was used as cocatalyst.

IV. Study involving well-defined cocatalysts

Highly active systems for the oligomerization of ethylene by iron(II) complex **A** were obtained. All the cocatalysts reported in paragraphs II and III were tested *in situ* without further characterizations. A better way to correlate the structure of the activator and the activity is to consider well-defined cocatalysts.

1. Synthesis of cocatalysts

Many structures composed by two equivalents of diols compounds and three equivalents of trimethylaluminum have been mentioned in the literature.[25-30] Pasynkiewicz and Ziembkowska synthesized the first alkylaluminum diolate complex $[Me_5Al_3(OCH_2C_6H_4CH_2O)_2]$ by reaction of TMA with 1,2-di(hydroxymethyl)benzene.[28] Based on the procedure of Ziemkowska,[31] a cocatalyst involving 1,2-catechol **11** (Scheme 7) was synthesized.

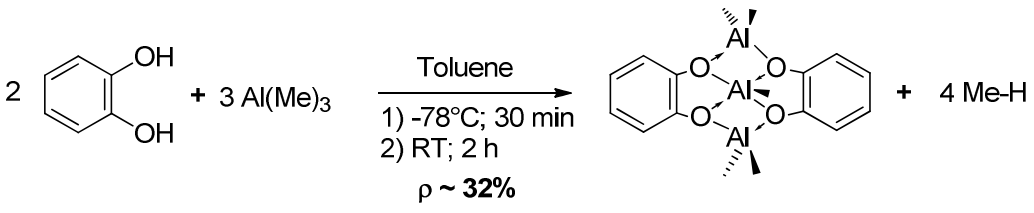

11 **16**

Scheme 7. Synthesis of complex **16**.

The ^{1}H NMR spectrum of the white solid obtained after toluene evaporation indicated a mixture of products (Figure 5). In addition to the signals of the trinuclear complex (Figure 6), broad signals were observed that could be attributed to oligomeric products also called alucones.[29] Some of these oligomeric products were insoluble in the NMR solvent and so the exact percentage of trinuclear complex among the reaction products could not be determined.

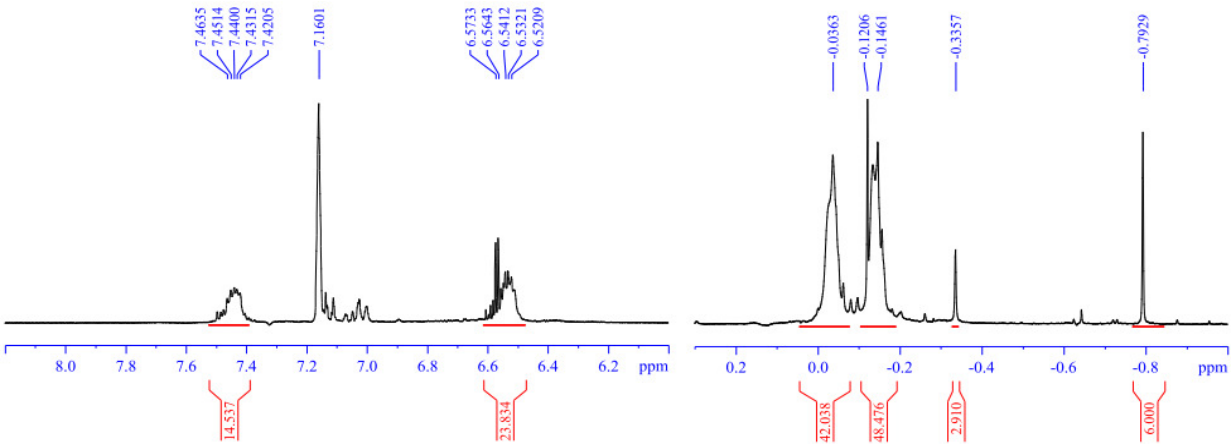

Figure 5. ^{1}H NMR spectrum of the solid obtained after reaction of **11** and TMA.

Due to the very low solubility of alucones in common organic solvents, their structures cannot be easily determined. However, the use of Al^{t}Bu$_3$ allowed the determination of the structures of some alucones.[26] Indeed, the reaction of ethane-1,2-diol with Al^{t}Bu$_3$ in *n*-hexane solution resulted in oligomeric compounds with general formula $[Al(^{t}Bu)_{2x}(OCH_2CH_2O)_{1.5-x}]_n$ ($0.3 \leq 2x \leq 0.8$). In this study, the authors pointed out the importance of the diol/Al ratio. Using a 1/1 molar ratio yielded predominantly a trinuclear aluminum complex with general formula $[Al_3(^{t}Bu)_5(OCH_2CH_2O)_2]$ and no alucones were formed. On the contrary, an excess of aluminum (diol/Al = 1/2) produced a large quantity of insoluble materials (alucones). In this case, a low yield of $[Al_2(^{t}Bu)_3(OCH_2CH_2O)(OCH_2CH_2OH)]$ was obtained and a proposed synthesis of *tert*-butyl alucones was established. Based on this study, a possible route to complex **16** and alucones is described in Scheme 8. The first step of the reaction produces the binuclear complex with pentacoordinated metal atoms chelated and bridged by mono-deprotonated catechol ligands. The complex is stabilized by the presence of intramolecular hydrogen bonds.[26] The reaction of one methyl group with a hydroxyl entity results in the formation of an intermediate which isomerizes to give either the trinuclear complex **16** or alucones. The reaction of this isomer with AlMe$_3$ would result in the formation of the final

trinuclear complex **16**. Self condensation of this isomer may lead to lightly cross-linked alucones.

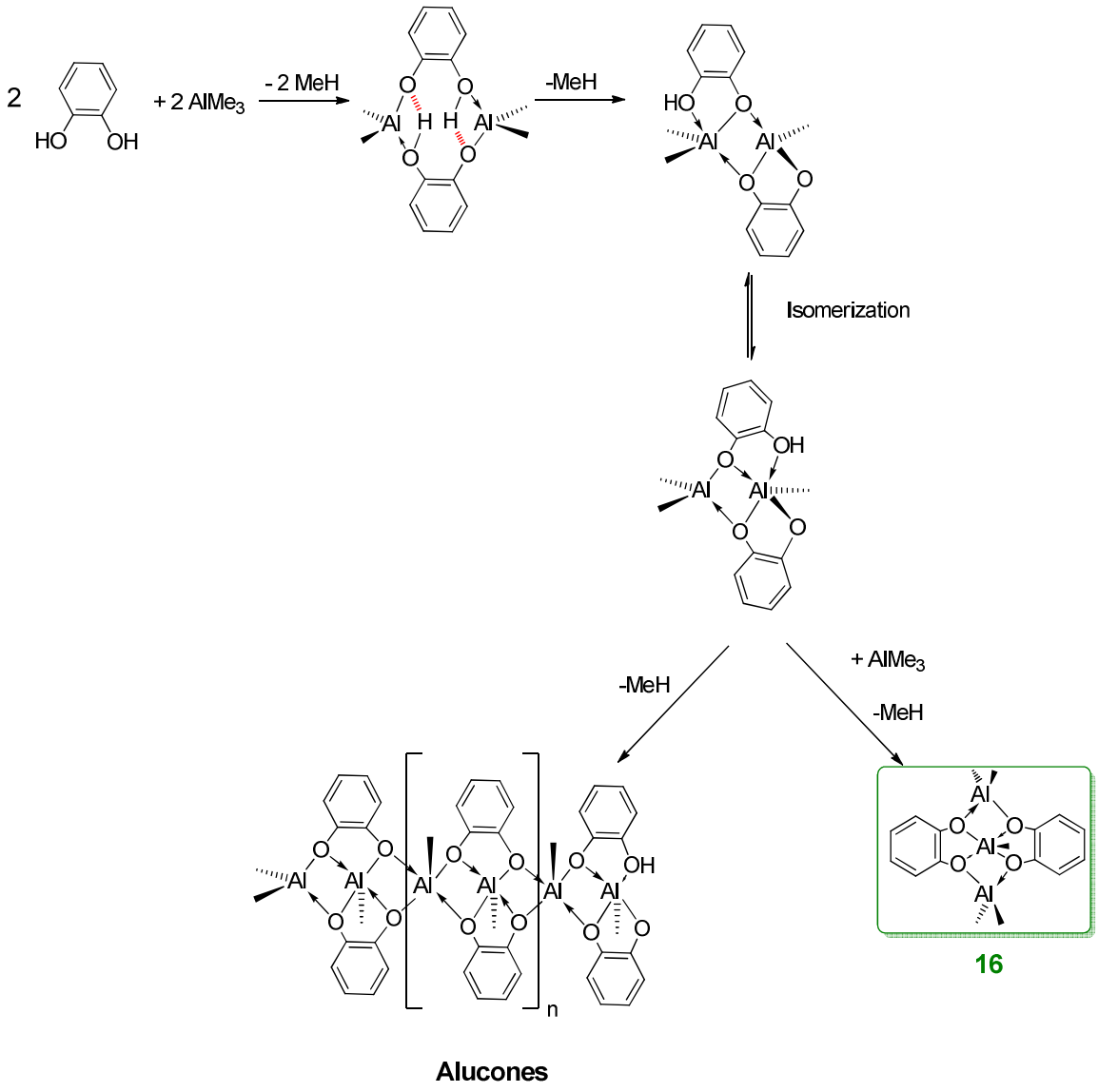

Scheme 8. Proposed mechanism for the formation of **16** and alucones.

The yield of the synthesis of **16** was quite low (32%) because of the formation of undesired products (alucones) and because of the sublimation made to obtain the highly pure product (>99%). The white amorphous solid remaining after sublimation was insoluble in any solvent and was not characterized. The symmetrical trinuclear complex was characterized by ^{1}H and $^{13}C\{^{1}H\}$ NMR spectroscopy in C_6D_6. The protons of the two methyl groups bound to

the tetracoordinated aluminum are inequivalent due to the methyl ligand on the central aluminum atom (Figure 6).

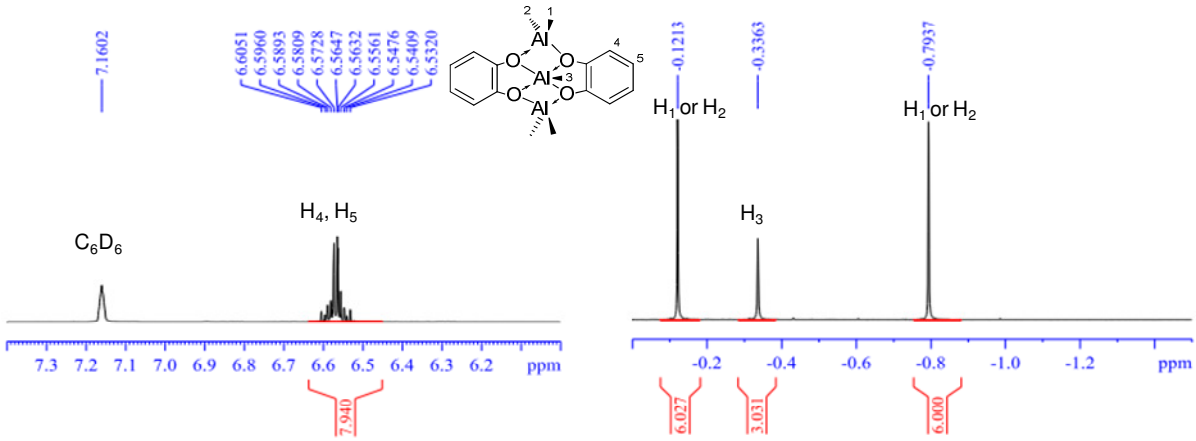

Figure 6. ^{1}H NMR spectrum of **16** in C_6D_6.

Although the signals of the methyl groups were well defined on the ^{1}H NMR spectrum, the chemical shift expected at -0.34 ppm corresponding to the methyl bound to the pentacoordinated aluminum atom was probably too weak to be detected by ^{13}C{^{1}H} NMR spectroscopy (Figure 7). The shifts of the various resonances are consistent with the literature values.[31] The two signals at -9.75 and -13.02 ppm correspond to the methyl groups bound to the tetracoordinated aluminum atoms.

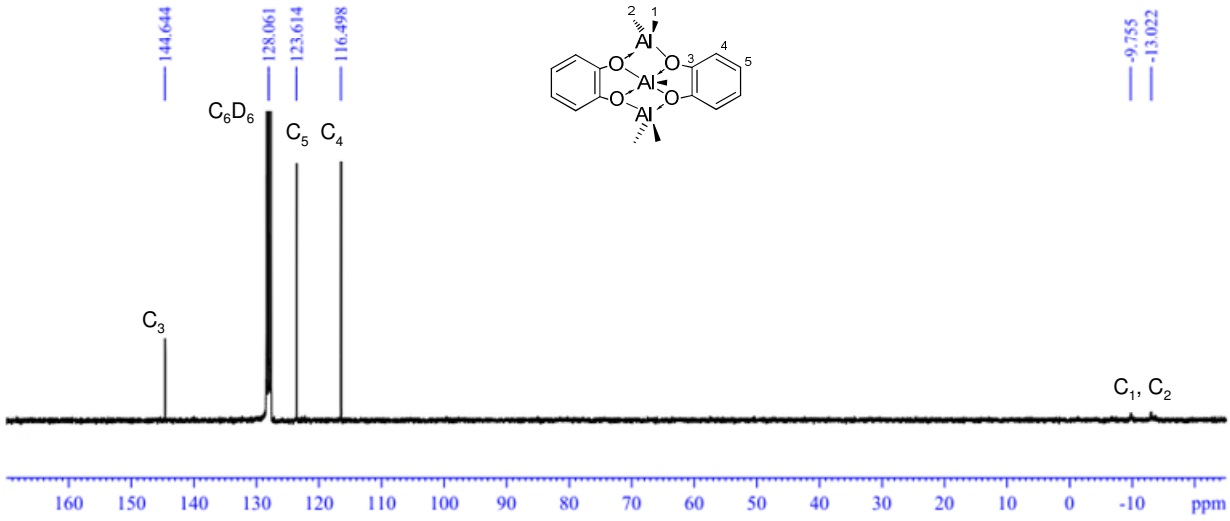

Figure 7. ^{13}C{^{1}H} NMR spectrum of **16** in C_6D_6.

The product of the reaction of 2,2'-dihydroxybiphenyl **8** with $AlMe_3$ in toluene was a mixture of trinuclear complex **17** and alucones. Sublimation of this mixture provided the desired cocatalyst in low yield (40%) (Scheme 9). The trinuclear structure was characterized by ^1H NMR spectroscopy in C_6D_6 and in C_7D_8. Comparison of the spectra pointed out the solvent effect on the signals of the methyl groups (Figure 8). Signals of methyl groups were shifted to lower values in C_7D_8, the main difference being observed for the methyl bound to the central aluminum atom (Figure 8, -0.59 in C_6D_6 *vs* -0.70 in C_7D_8).

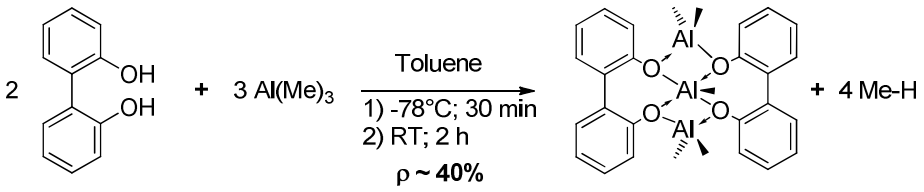

8 **17**

Scheme 9. Synthesis of complex **17**.

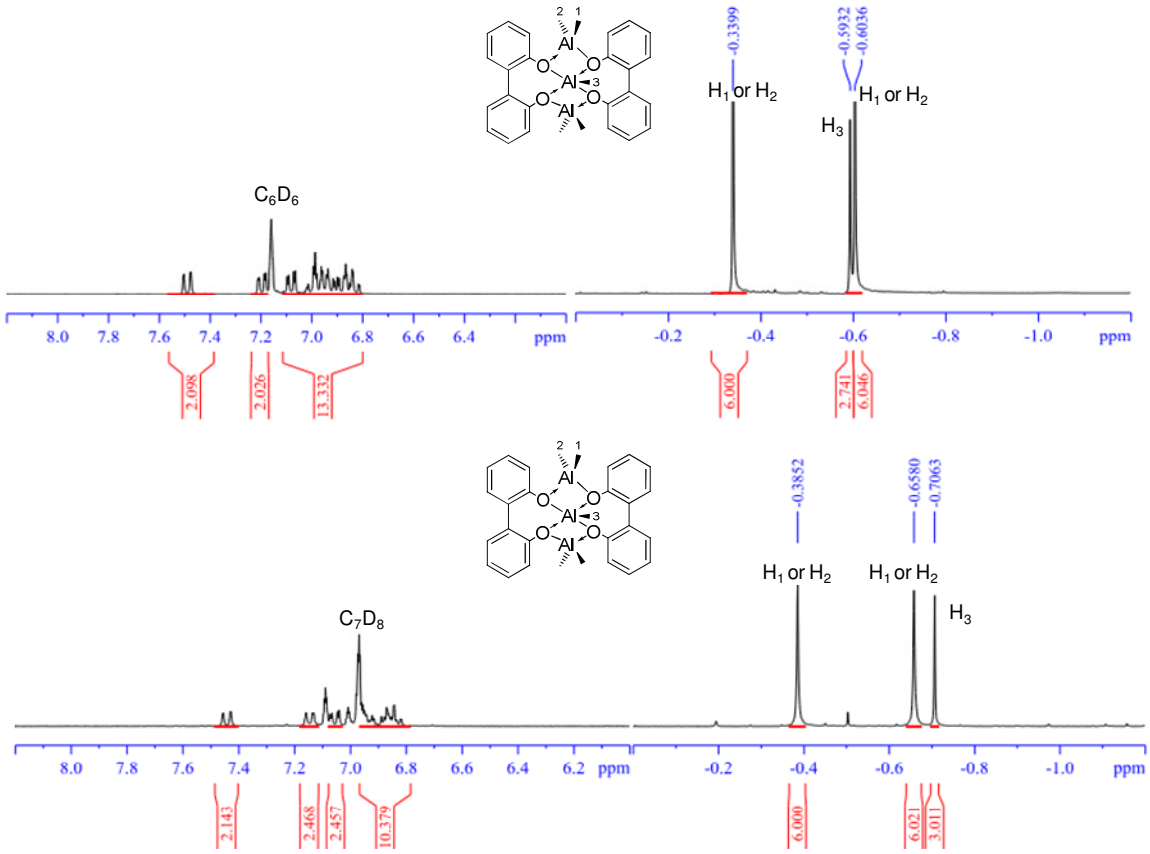

Figure 8. ^1H NMR spectrum of **17** in C_6D_6 (top) and in C_7D_8 (down).

Compound **18** was obtained after 10 days of reaction according to literature procedures (Scheme 10).[32] Although the authors reported on high yield synthesis, the trinuclear compound was isolated by filtration as a white solid in low yield (28%). Compound **18** was characterized by ^{1}H NMR spectroscopy in C_6D_6 (Figure 9).

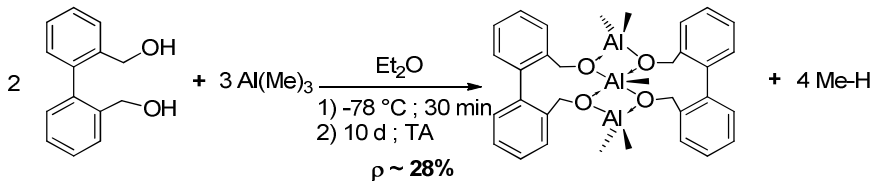

10 **18**

Scheme 10. Synthesis of complex **18**.

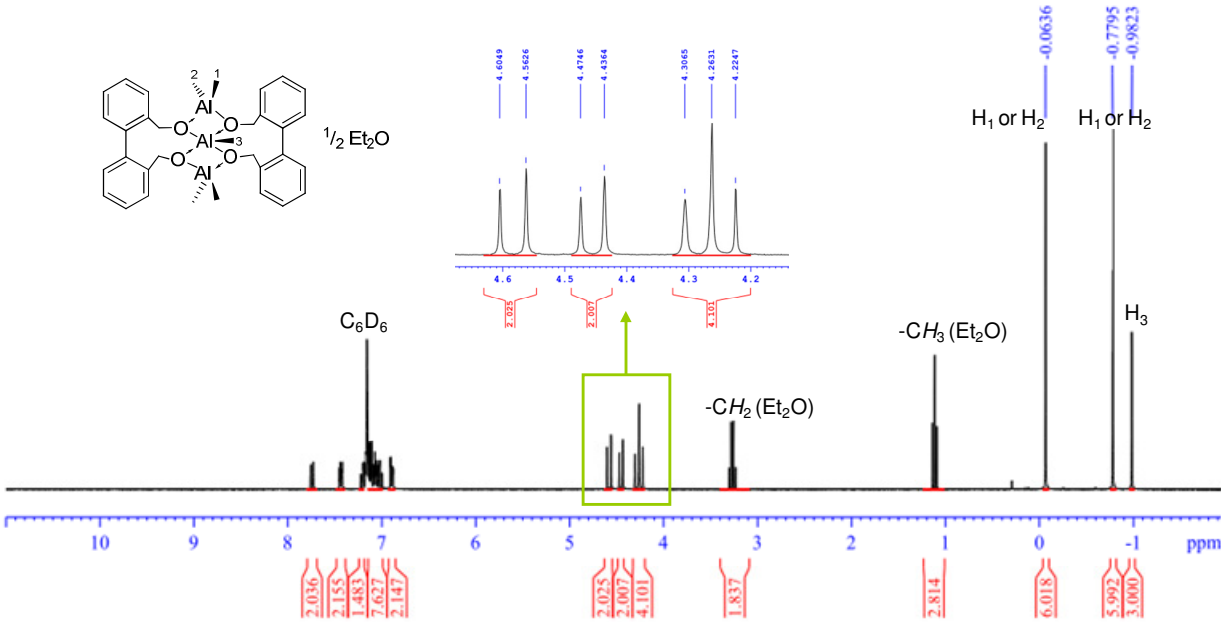

Figure 9. ^{1}H NMR of compound **18**·1/2 Et_2O in C_6D_6.

Ziemkowska succeeded in crystallizing compound **18** from toluene (Figure 10). The geometry around the central pentacoordinated aluminum atom is distorted trigonal bipyramidal with O2 and O4 occupying the axial positions and O1, O3 and C29 defining the equatorial sites. In comparison with compound **17**, the presence of the CH_2 groups increases the flexibility around the aluminum atoms. Consequently, it decreases their accessibility and

consecutively the reactivity. The CH_2 protons are inequivalent and appear as four doublets in the ^1H NMR spectrum (Figure 9).

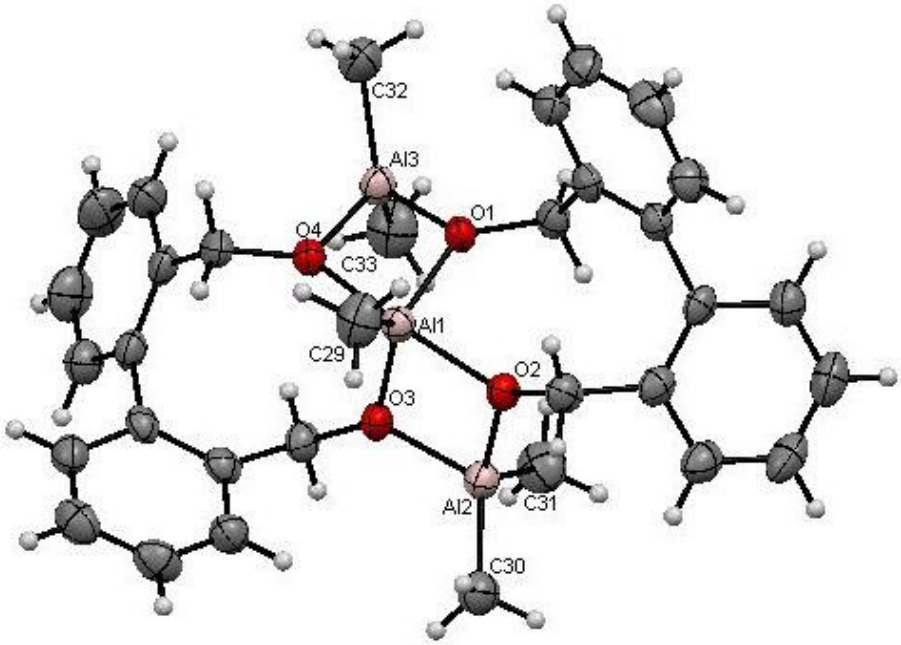

Figure 10. ORTEP and atom numbering of **18**. Thermal ellipsoids include 50% of the electron density.

The nature of the diol considerably affects the shifts of the methyl groups bound either to the tetracoordinated aluminum centers or to the pentacoordinated one. Indeed, the resonance for the methyl group bound to the pentacoordinated aluminum atom center is shifted to low values for **18** in comparison with **16** and **17** (Figure 11,-0.33 ppm for **16**, -0.59 ppm for **17** and -0.98 ppm for **18**).

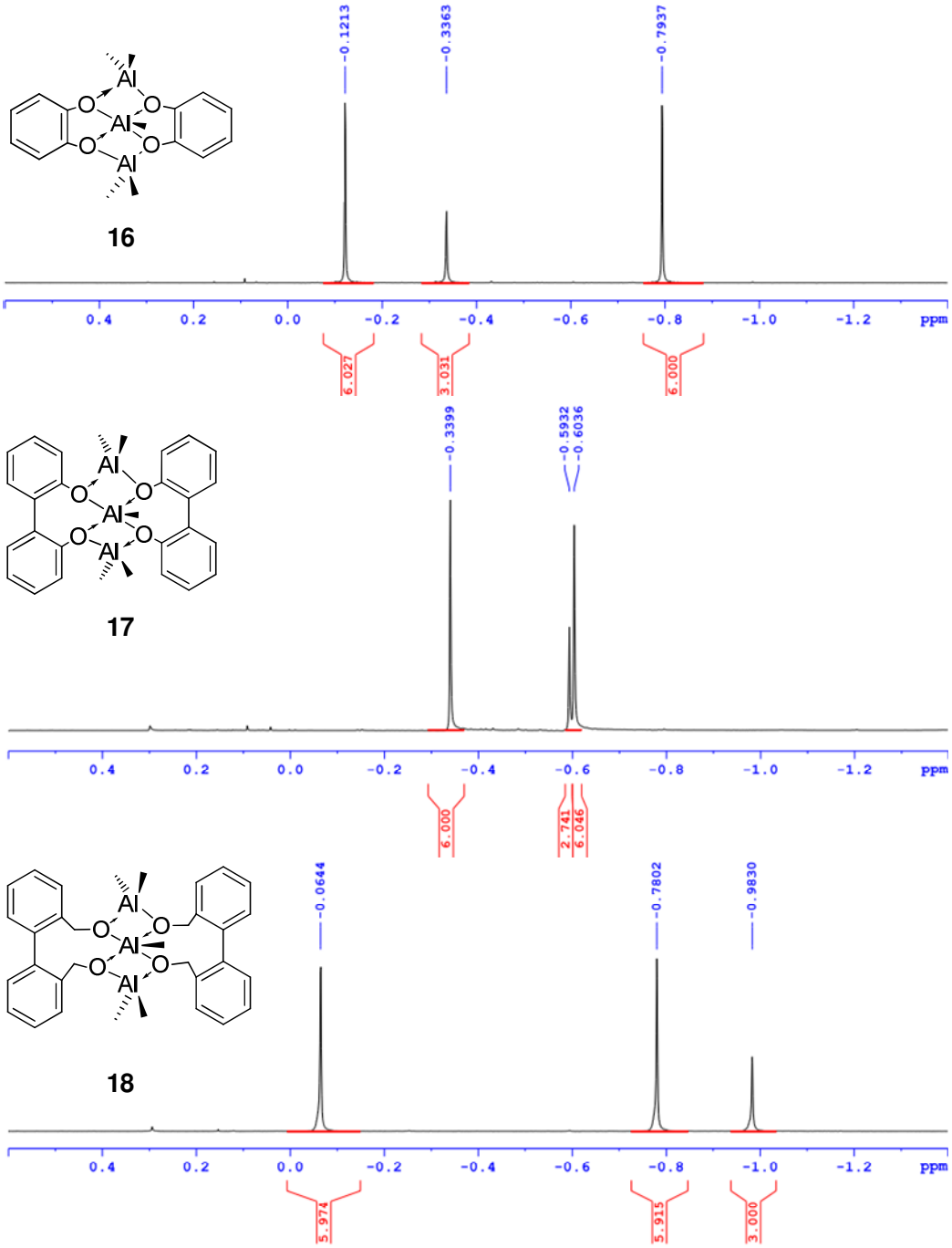

Figure 11. Comparison of ^{1}H NMR spectra of **16** (top), **17** (middle) and **18** (down) in the range of [0.6, -1.4 ppm] in C_6D_6.

The series of isolated cocatalysts was completed by the synthesis of complexes **19** and **20** which were obtained in high yield (Scheme 11).[33] In comparison with compound **16**, the increase of space between the two hydroxyl functions on a phenyl ring led to variations in the structure of product. Formation of the trinuclear complex for 1,3- and 1,4-benzenediols is not

feasible due to the large distance between two hydroxyl functions. The reaction of either resorcinol **14** or hydroquinone **15** with $AlMe_3$ produced tetranuclear structures.[33] Besides the two central tetracoordinated aluminum atoms, the terminal aluminum sites are more accessible than for other cocatalyst (**16**-**18**) and potentially better mimic the structure on the surface of MAO.[1]

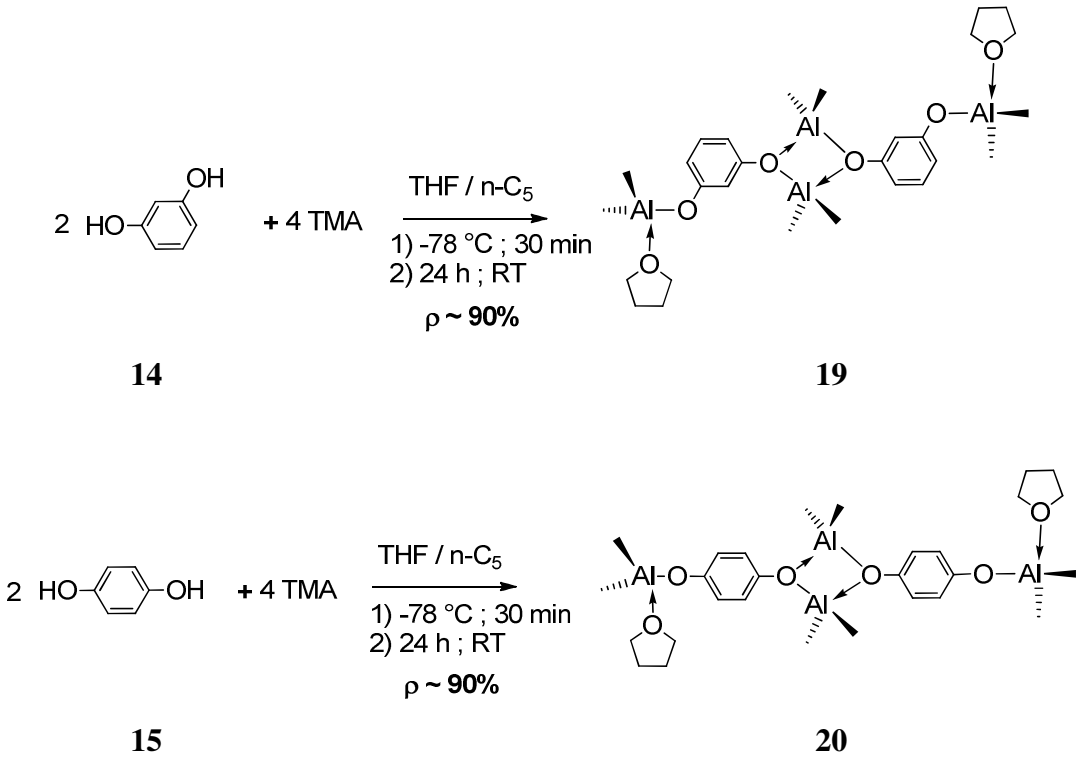

Scheme 11. Synthesis of complexes **19** and **20**.

The relatively low solubility of the desired products in common organic solvents restrained NMR spectrum to be recorded in DMSO-d_6 (Figure 12). The solubilization of **19** in DMSO-d_6 led to the symmetric product **19'**. As a Lewis base, DMSO induces the cleavage of the dative oxygen-aluminum bonds involved in the bridging interaction in the binuclear moiety (Scheme 12).[34]A similar reaction was also observed when **19** was reacted with pyridine.[33] Chemical shifts of tetrahydrofuran were consistent with the signals of the non-coordinated solvent.

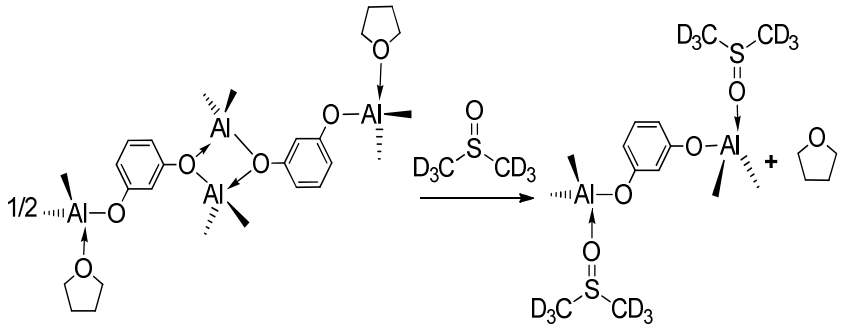

19 **19'**

Scheme 12. Reaction of **19** with DMSO.

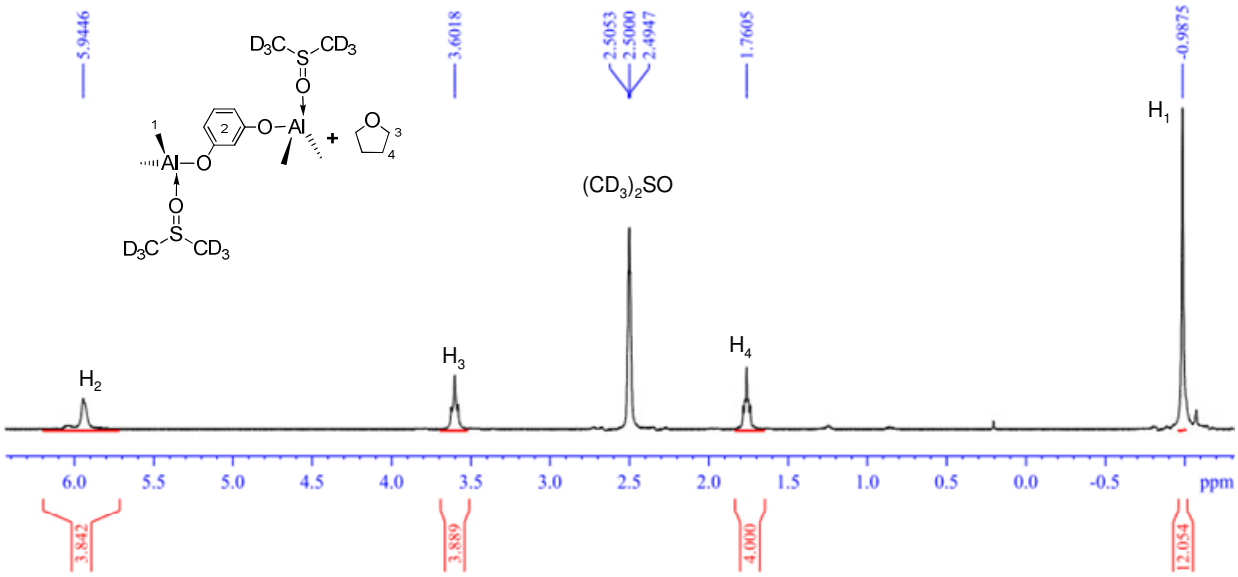

Figure 12. ^{1}H NMR of compound **19'** in $(CD_3)_2SO$.

2. Iron precursors activated by isolated structures

Activated by isolated cocatalyst **16**, iron(II) bis(imino)pyridine **A** oligomerized ethylene with an activity up to 8.7×10^5 g·(mol(Fe)·h)$^{-1}$ (Table 5, entry 1). Oligomers were obtained in a full range of C_4-C_{24} (K = 0.68) with high selectivity in linear α-olefins (>98%). Reduction of the Al/Fe ratio from 250 to 10 could be reached by increasing the amount of iron complex used for the catalytic test (100 µmol). No beneficial effect was observed but the activity obtained was comparable (4.7×10^5 g·(mol(Fe)·h)$^{-1}$, Table 5, entry 2).

Cocatalyst **16** and **17** activate the iron complex with lower activities than their mixtures [**11**/$AlMe_3$] and [**8**/$AlMe_3$] (Table 5, entry 1 *vs* entry 3 for **16** and entry 5 *vs* entry 6 for **17**). We have previously established that reaction of TMA with 1,2-dihydroxybenzene **11** results in the trinuclear aluminum complex **16** and probably oligomeric aluminum compounds. The difference in reactivity could be explained by the nature of the counter ion if ion pairs are supposed as active species. The two counterions would be [Alucones-Cl]$^-$ and [**16**-Cl]$^-$, respectively. Because of its oligomeric structure, the charge on [Alucones-Cl]$^-$ is possibly delocalized over the whole structure and consequently is more diffuse, making the anion less coordinating than [**16**-Cl]$^-$. The cationic iron center is thus expected to be more active. Alucones can mimic the cage structure of the MAO. The activity obtained with a **11**/ratio of 2/3 remained lower than for a ratio of 1/2 (Table 5, entry 3 *vs* entry 4). A ^{1}H NMR comparison between the two reaction mixtures was inconclusive. In fact, despite the slight decrease of integrations of signals corresponding to oligomeric products for the ratio diol/$AlMe_3$ of 1/2, the general spectral appearance was quite similar. The same explanations were proposed for the behavior of complex **17**.

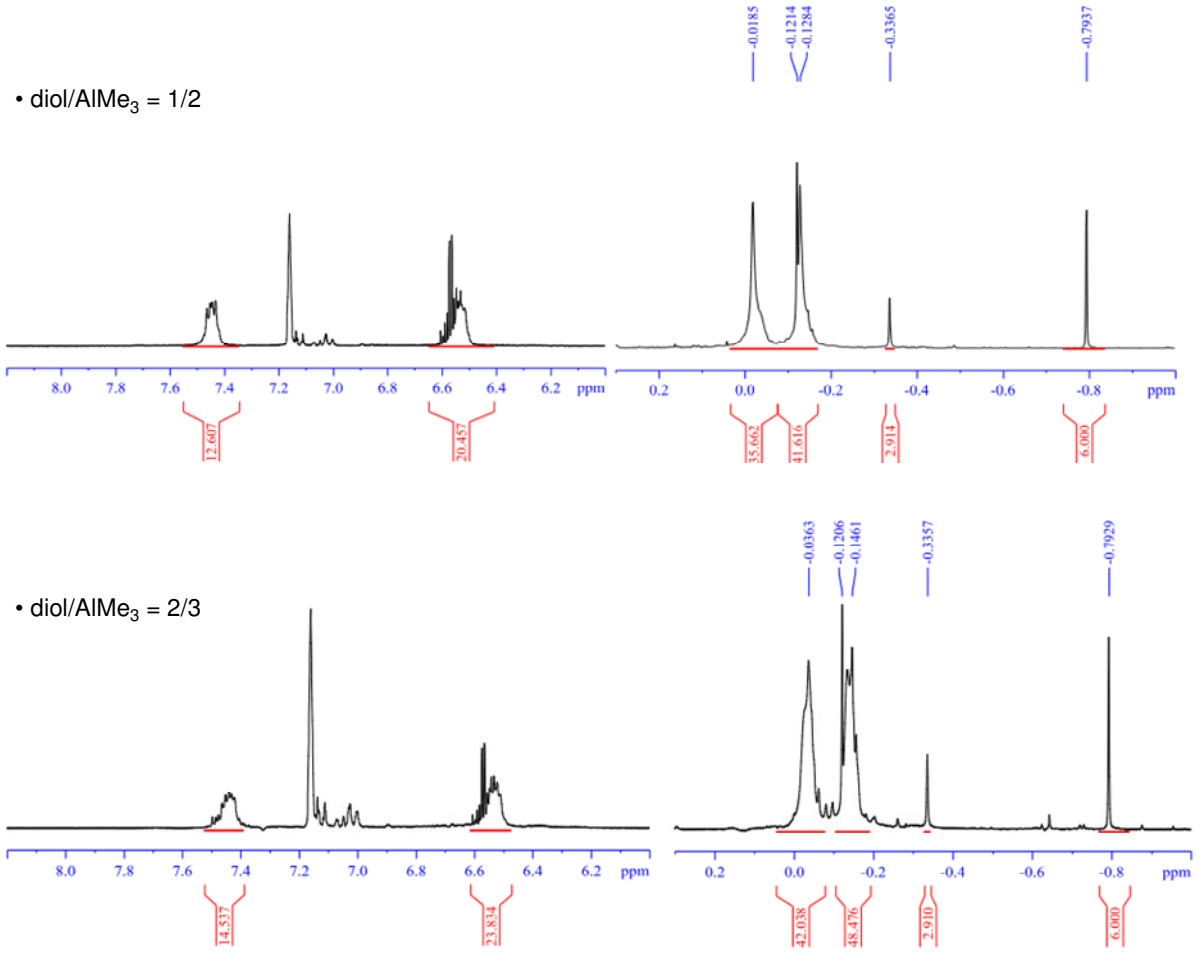

Figure 13. Comparison of ^{1}H NMR spectra of various ratios of **11**/$AlMe_3$ (in C_6D_6).

The trinuclear aluminum complex **17** showed better results than **16** (8.7×10^5 g·(mol(Fe)·h)$^{-1}$ for **16** *vs* 12.2×10^5 g·(mol(Fe)·h)$^{-1}$ for **17**) (Table 5, entries 1 and 5, respectively). Here we could consider two parameters: the size of the counterion that helps to stabilize the active species and to form the ion pairs and the Lewis acidity of the pentacoordinated aluminum. ^{1}H NMR study revealed strong variations of the signals for the methyl groups on both tetracoordinated and pentacoordinated aluminum (Figure 11). The chemical shift of the methyl bound to the central aluminum in complex **17** (-0.59 ppm) is low-field shifted in comparison with complex **16**. The hypothesis of a higher Lewis acidity for the central aluminum of complex **17** was made to explain this result. This difference could be the reason of an easier alkylation of the iron complex (first step of the activation process) and as a result, a better activity.

For complex **18**, chemical shifts corresponding to the methyl groups bound to tetracoordinated aluminum were in the same range as for complex **16** whereas the signal of the methyl group bound to the pentacoordinated aluminum was shifted to the lowest value (-0.98 ppm) among the different trinuclear compounds **16**, **17** and **18**. According to our previous argument on the correlation between chemical properties of cocatalysts and activity, cocatalyst **18** should give the best activity. Unfortunately no activity was obtained (Table 5, entry 7). The reason of this inactivity could be due to the geometry of the cocatalyst. Indeed, the CH_2 groups on complex **18** would allow rotations and so prevent the accessibility of the methyl groups. Complexes **19** and **20** provided inactive systems (Table 5, entries 8 and 9).

Table 5. Activation of iron precursors by well-defined cocatalyst.[a]

Entry	Cocatalyst	Activity[b]	*K*	α
1	**16**	8.7	0.68	>99
2[c]	**16**	4.7	0.67	>99
3[d]	**11**/$AlMe_3$	12.0	0.68	>99
4[e]	**11**/$AlMe_3$	16.8	0.67	>98
5	**17**	12.2	0.68	>98
6[d,f]	**8**/$AlMe_3$	76.0	0.68	>98
7	**18**	0[g]	-	-
8	**19**	0[g]	-	-
9	**20**	0[g]	-	-

[a] Iron precursor (10 µmol), Al/Fe = 250, toluene (25 mL), P_{C2H4} = 30 bar, T = 50 °C, 60 min. [b] $\times10^5$ g·(mol(Fe)·h)$^{-1}$. [c] Iron precursor (100 µm), Al/Fe = 10, toluene (25 mL), P_{C2H4} = 30 bar, T = 50 °C, 60 min. [d] Cocatalysts were used in mixture (diol/$AlMe_3$ = 2/3). [e] cocatalyst was used in mixture (diol/$AlMe_3$=1/2). [f] Reaction time = 30 min. [g] no ethylene uptake.

3. Addition of free alkylaluminum

In order to get more information about the activation process and to minimize the quantity of cocatalyst, several experiments involving various amounts of cocatalyst and the addition of different alkylaluminum compounds were investigated. Without any additional alkylaluminum and under the same conditions, cocatalyst **17** exhibited an activity of 12.2×10^5 $g\cdot(mol(Fe)\cdot h)^{-1}$ (Table 6, entry 1). Addition of more trimethylaluminum led to a decrease of activity from 9.5 to 5.8×10^5 $g\cdot(mol(Fe)\cdot h)^{-1}$ (Table 6, entries 2 and 3). Attempts to reduce the amount of cocatalysts and to tune the ratio cocatalyst/TMA led to inactive catalytic systems (Table 6, entries 4 to 7). Regardless of the nature of additional alkylaluminum compounds used with **17**, no activity was obtained in ethylene oligomerization (Table 6, entries 8 to 10). Surprisingly, by mixing 250 equivalents of the tetranuclear aluminum compound with **19** and 50 equivalents of TMA, the activation of iron precursor occurred (Table 6, entry 11 *vs* entry 12). However, increasing further the quantity of TMA decreased the activity (Table 6, entry 12 *vs* entry 13). The use of different alkylaluminum and chloroalkylaluminum such as $AlEt_3$, Al^iBu_3 or $AlEt_2Cl$ did not induce active catalysts (Table 6, entries 14-16).

Table 6. Effect of alkylaluminum on oligomerization reaction.[a]

Entry	Cocatalyst	Alkylaluminum	(Cocata./AlR_3/Fe) Ratio	Activity[b]	*K*
1	**17**	-	250/-/1	12.2	0.68
2	**17**	$AlMe_3$	250/1/1	9.5	0.68
3	**17**	$AlMe_3$	250/10/1	5.8	0.67
4	**17**	$AlMe_3$	2/1/1	0[c]	-
5	**17**	$AlMe_3$	2/2/1	0[c]	-
6	**17**	$AlMe_3$	10/1/1	0[c]	-
7	**17**	$AlMe_3$	10/5/1	0[c]	-
8	**17**	$AlEt_3$	250/50/1	0[c]	
9	**17**	Al^iBu_3	250/50/1	0[c]	
10	**17**	$AlEt_2Cl$	250/50/1	0[c]	
11	**19**	-	250/-/1	0[c]	
12	**19**	$AlMe_3$	250/50/1	6.1	0.69
13	**19**	$AlMe_3$	250/125/1	2.1	0.68
14	**19**	$AlEt_3$	250/50/1	0[c]	
15	**19**	Al^iBu_3	250/50/1	0[c]	
16	**19**	$AlEt_2Cl$	250/50/1		

[a] Iron precursor (10 µmol), toluene (25 mL), P_{C2H4} = 30 bar, T = 50 °C, t = 60 min. [b] $\times10^5$ $g\cdot(mol(Fe)\cdot h)^{-1}$, selectivities>98%. [c] no ethylene uptake.

4. Evaluation of other catalytic systems

We finally checked that the new optimized cocatalysts were not specific to the ferrous bis(imino)pyridine complex. We thus engaged the ferric **C** and ferrous **D** complexes chelated by 1,2-dihydro-1,10-phenanthroline ligand under its anionic form and its neutral one described in Chapter II. The ability of the new well-defined cocatalyst **17** to activate the iron bis(imino)pyridine complex for the transformation of higher olefin (pentene) was also studied.

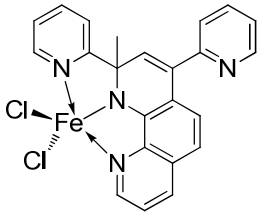

C

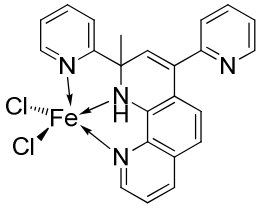

D

Scheme 13. 1,2-dihydro-1,10-phenanthroline ferrous **C** and ferric **D** complexes.

The precatalyst **C** showed good and stable activity in the presence of cocatalyst **17** at a ratio Al/Fe = 250 (Table 7, entry 1). Ethylene consumption was steady over 1 h with an activity of 1.43×10^5 g·(mol(Fe)·h)$^{-1}$ that is slightly lower than when MAO was used as activator (2.16×10^5 g·(mol(Fe)·h)$^{-1}$, Table 7, entry 2) under the same conditions. Short chain oligomers were obtained with up to 76 wt% of butenes with a selectivity in 1-butene >97 wt%. The iron(II) complex **D** was inactive toward ethylene transformation when activated by either cocatalyst **17** or MAO (Table 7, entries 3 and 4).

Table 7. Activation of iron precursors by cocatalyst **17** and MAO.[a]

Entry	Iron precursor	Cocatalyst	Activity[b]	Oligomer distribution[c,d]			PE
				C_4 (1-C_4)[e]	C_6 (1-C_6)[e]	$C_{\geq 8}$	
1	**C**	**17** (250)	1.43	76 (97)	13 (90)	13	2
2	**C**	MAO (200)	2.16	63 (97)	18 (90)	7	12
3	**D**	**17** (500)	0[f]	-			-
4	**D**	MAO (500)	0[f]	-			-

[a] Iron precursor (20 µmol), toluene (25 mL), P_{C2H4} = 30 bar, T = 80 °C, 60 min. [b] $\times10^5$ g·(mol(Fe)·h)$^{-1}$. [c] Determined by GC. [d] wt% among all the products formed. [e] wt% in the C_n fraction. [f] no ethylene uptake.

The comparison of the reactivity of the catalytic system towards higher LAOs was studied and revealed that **17** did not allow the conversion of 1-pentene (Table 8, entry 1). Oligomerization of higher olefins by iron complex resulted in lower activities in comparison with ethylene, probably due to the slower insertion process. Indeed, the oligomerization even if slow (total conversion of 1-pentene in 120 min), was possible upon activation with MAO and resulted mainly in dimers and trimers: 90% of decenes and 10% of pentadecenes. After hydrogenation (150 °C, 50 bar of hydrogen with small amount of palladium, 5% on activated carbon) of the crude medium, linear and branched products were detected among the C10 fraction: 54% of linear olefins and 46% of mono-branched olefins while only branched olefins were produced in the C_{15} fraction (Table 8, entry 2).

Upon treatment with MAO, iron(II) bis(imino)pyridine precursor was observed to transform only 1-pentene when an equimolar mixture of 1-C_5/2-C_5 was engaged (Table 8, entry 3). The distribution of oligomers remained unchanged when compared to the test with 1-pentene. Indeed if we only consider 1-C_5 transformation, 93% of C_{10} (with 57% of linear olefins and 43% of branched product) and 7% of C_{15} was produced. 2-C_5 insertion in the Fe-H^+ bond is unfavorable compared to 1-C_5. This process could allow the separation of internal linear olefin. After hydrogenation, three main products were observed on the GC spectrum. Among the C_{10} fraction, 4-methyl-nonane and decane were obtained while only 4-methyl-tetradecane was observed for the C_{15} fraction.

Table 8. Dimerization and trimerization of pentenes by iron complex (**A**).

Entry	Olefin	C_5	Oligomer distribution [c,d]	
			C_{10} (linear/branched)[e]	C_{15}
1[b]	1-C_5	100	-	-
2	1-C_5	0	90 (54/46)	10
3	1-C_5/2-C_5 (1/1)	40	56 (57/43)	4

[a] Iron precursor (0.10 mmol), (MAO) Al/Fe = 250, toluene (25 mL), T = 40 °C, 120 min[b]Cocatalyst **17** was used (Al/Fe = 250). [c] Determined by GC. [d] wt% among all the products formed. [e] wt% in the C_n fraction.

Analysis of the various dimers formed allowed us to propose a mechanism for the dimerization of 1-pentene (Scheme 14). It involves an iron hydride species that is the result of β-H elimination. From this species, there are two possibilities for 1-pentene insertion: 1,2-insertion process (Scheme 14, black arrow) or 2,1-insertion (Scheme 14, green arrow). From each of these two species, there are again two possibilities for another 1-pentene insertion.

The linear decenes are only formed by the 2,1-insertion of 1-pentene into the Fe-C_5^+, while branched decenes are either produced by the 2,1-insertion into the Fe-(1-Me)-C_4^+ or by 1,2-insertion into the Fe-C_5^+ moiety. As no quantitative amount of di-branched alkanes was detected after hydrogenation, the 1,2-insertion of 1-pentene into the Fe-(1-Me)-C_4^+bond is probably not favorable. Fink and coworkers studied the mechanism of propylene dimerization by iron complexes.[35] They reported that for all studied iron complexes, the second 2,1-insertion into the Fe-^{i}Pr$^+$ bond is widely promoted in comparison with the 1,2-insertion. Finally, the mono-branched pentadecene was obtained by 2,1-insertion of 1-decene (produced by isomerization of internal decene) into the Fe-(1-Me)-C_4^+.

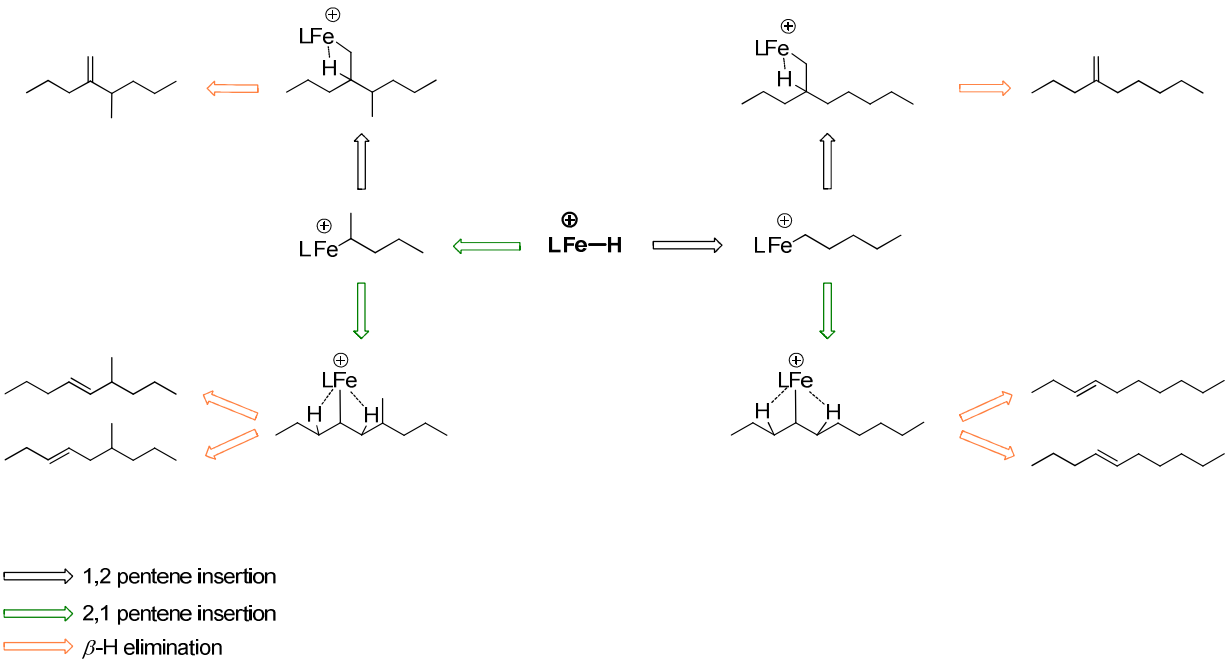

Scheme 14. Mechanism of 1-pentene dimerization with the iron catalyst (**A**).

Conclusion

We have established that reactions of phenol, alcohol and diol derivatives with TMA lead to cocatalysts promoting the iron-catalyzed oligomerization of ethylene. The primary screening involving aryloxide and alkoxide ligands showed activity up to 5×10^5 $g\cdot(mol(Fe)\cdot h)^{-1}$ with a Al/Fe ratio of 500. Oligomers in the range C_4-C_{24}were obtained with good selectivity for α-olefins (>98%). A library of diols was then been tested by forming the cocatalysts *in situ*. The aromatic diol ligands showed the highest activities with an optimum obtained with 2,2'-dihydroxybiphenyl. The 2,2'-dihydroxybiphenyl/$AlMe_3$ ratio has a crucial impact on the catalysis, the optimum being obtained for a 2/3 ratio. From this ratio, trinuclear aluminum complexes were formed and characterized by ^1H and ^{13}C NMR. Activated by 250 equivalents of these well-defined aluminum complexes, the iron(II) bis(imino)pyridine precursor oligomerizes ethylene with high activities (up to 10^6 $g\cdot(mol(Fe)\cdot h)^{-1}$). The oligomer distribution in all cases is of the Schulz-Flory type, and the *K* value characteristic of this distribution is around 0.70. Oligomers were obtained with high selectivity for linear α-olefins (>98%). The isolated cocatalyst was also successfully used to activate our iron(III) complex showing the potential of our system.

Experimental section

General considerations

All operations were carried out using standard Schlenk techniques under inert atmosphere. Toluene, THF, pentane and dichloromethane were dried by a solvent purification system (SPS-M-Braun) and heptane was distilled over sodium. Starting materials were purchased from Aldrich and used without further purification. Alkylaluminum and methylaluminoxane (MAO) were purchased for Chemtura and used without further purification. Deuterated solvents (C_6D_6 and $(CD_3)_2SO$) were purchased from Sigma-Aldrich or Eurisotop. The solvents were freeze-pumped and stored over 4 Å molecular sieves under argon.The ^{1}H and $^{13}C\{^{1}H\}$ NMR spectra were recorded on a Bruker AC 300 MHz at 293 K unless otherwise stated. All chemical shifts are reported in ppm *vs* $SiMe_4$ and were determined with reference to residual solvent peaks.[36] All coupling constants are given in Hertz. Chemical shifts values (δ) are given in ppm. Gas chromatographic analysis were performed on a Agilent 6850 series II equipped with a flame ionization detector and using an Agilent Pona column (50 m, 0.2 mm diameter, 0.5 μm film thickness).

Synthesis of aluminum complexes

- **Synthesis of complex A**

To a solution of $FeCl_2 \cdot 4H_2O$ (0.878 g, 4.45 mmol) in dried THF (20 mL) was added a solution of bis(imino)pyridine ligand (1.583 g, 4.64 mmol) in 20 mL of dried THF. The blue solution was added overnight under inter atmosphere. The blue precipitate was collected by filtration, washed once with dried THF (30 mL) to remove excess of ligand and three times with dried diethyl ether (3×25 mL). The blue powder was dried for 3 h under vacuum (10^{-2} Torr) to yield the pure complex (1.92 g, 91% yield).

FT-IR (cm^{-1}): 3081w, 2978w, 2859w, 1623m ($\upsilon_{C=N}$), 1586m, 1484s, 1370m, 1263s, 1230s, 1112w, 1063s, 906w, 827w, 809s, 787m, 751s, 738m, 720s, 548m, 489w, 469w.

The syntheses of complexes **C** and **D** were described in Chapter II.

- **Synthesis of complex $[AlMe_2(OPh)]_2$**

A solution of phenol (0.390 g, 4.14 mmol) in 10 mL of dried *n*-heptane (4.7 ppm of water) was added dropwise to a dried *n*-heptane solution (10 mL) of $AlMe_3$ (0.40 mL, 4.14 mmol) at -78 °C. The reaction was exothermic and some gas evolved. The solution was stirred for 30 min. The colorless solution was allowed to warm to room temperature and stirred for 30 min. The solvent volume was reduced under vacuum to ca. 5 mL. The resulting colorless solution was stored at -35 °C overnight after which some solid formed and was identified as the desired complex (0.497 g, 80% yield).

^{1}H NMR (300 MHz, C_6D_6): δ 7.16 – 6.93 (m, 8H), 6.82 – 6.78 (m, 2H),-0.29 (s, 12H).

- **Synthesis of complex 16**

To a suspension of 1,2-catechol (1.10 g, 10 mmol) in 30 mL of dried toluene (4.1 ppm of water) at -78 °C was added drop wise a solution of $AlMe_3$(1.47 mL, 15 mmol) over 30 minutes in 20 mL of dried toluene. The reaction was exothermic and some gas evolved. The solution was stirred for 30 min. The colorless solution was allowed to warm to room temperature and stirred for 2 h. The solution turned cloudy during the reaction. The solvent was distilled off under vacuum. The complex was sublimed off (T = 150 °C, p = 10^{-3} Torr) as a white solid from the post reaction mixture (0.620 g, 32% yield).

^{1}H NMR (300 MHz, C_6D_6): δ 6.73 – 6.40 (m, 8H), -0.12 (s, 6H), -0.34 (s, 3H), -0.79 (s, 6H).

^{13}C NMR (300 MHz, C_6D_6): δ 114.6, 123.6, 116.5, -9.7, -13.0.

- **Synthesis of complex 17**

To a suspension of 2,2'-dihydroxybiphenyl (3.74 g, 20.1 mmol) in 50 mL of dried toluene (3.9 ppm of water) at -78 °C was added dropwise within 30 min a solution of $AlMe_3$ (2.17 mL, 30.2mmol) in 60 mL of dried toluene. The reaction was exothermic and some gas evolved. The solution was further stirred for 30 min. The colorless solution was allowed to warm to room temperature and stirred for 2 h. The solution turned cloudy during the reaction. The solvent was distilled off under vacuum. The complex was sublimed (T = 190 °C, p = 10^{-5}Torr) as a white solid from the post reaction mixture (2.10 g, 40% yield).

^{1}H NMR (300 MHz, C_6D_6): δ 7.40 (dd, *J* = 8.2, 0.9 Hz, 2H), 7.10 (dd, *J* = 7.6, 1.5 Hz, 2H), 6.99 (dd, *J* = 7.6, 1.9 Hz, 2H), 6.93 – 6.71 (m, 10H), -0.43 (s, 6H), -0.69 (s, 3H), -0.70 (s, 6H).

- **Synthesis of complex 18·1/2Et_2O**

To a solution of trimethylaluminum (1.2 mL, 12.0 mmol) in 20 mL of dried diethyl ether (8.2 ppm of water) at -78 °C was added dropwise a solution of 2,2'-di(hydroxymethyl)biphenyl (1.71 g, 8 mmol) in 200 mL of dried diethyl ether. The reaction was exothermic and some gas evolved. The solution was stirred for 30 min. The colorless solution was allowed to warm to room temperature and stirred for 10days. A white solid precipitated, which was collected by filtration, washed with dried diethyl ether (3×30 mL) and dried under vacuum overnight to yield the pure compound **18** (0.600 g, 28% yield).

^{1}H NMR (300 MHz, C_6D_6): δ 7.83 – 7.68 (m, 2H), 7.48 – 7.39 (m, 2H), 7.21 (dd, *J* = 7.4, 1.4 Hz, 2H), 7.15 – 6.99 (m, 8H), 6.90 (dd, *J* = 7.7, 1.4 Hz, 2H), 4.58 (d, *J* = 12.7 Hz, 2H), 4.45 (d, *J* = 11.5 Hz, 2H), 4.26 (t, *J* = 12.3 Hz, 4H), 3.27 (q, J = 7.0 Hz, 2H), 1.12 (t, J = 7.0 Hz, 3H) -0.06 (s, 6H), -0.78 (s, 6H), -0.98 (s, 3H).

- **Synthesis of complex 19·THF**

To a solution of trimethylaluminum (2.13 mL, 20.2 mmol) in 10 mL of dried *n*-pentane (2.1 ppm of water) at room temperature was added dropwise to a solution of resorcinol (1.09 g, 9.9 mmol) in 20 mL of dried tetrahydrofuran. Some gas evolved during the addition. Immediately after the addition of the diol, a white solid precipitated. The suspension was stirred overnight at room temperature. No evolution was observed. The solid was filtered, washed with diethyl ether (3×30 mL)and dried under vacuum to afford compound **19** (2.6 g, 90% yield).

^{1}H NMR (300 MHz, DMSO): δ 5.94 (s, 4H), 3.60 (t, *J* = 6.5 Hz, 4H), 1.76 (m, 4H), -0.98 (s, 12H).

- **Synthesis of complex 20**

To a solution of trimethylaluminum (2.13 mL, 20.2 mmol) in 10 mL of dried *n*-pentane (2.1 ppm of water) at room temperature was added dropwise a solution of hydroquinone (1.09 g, 9.9 mmol) in 20 mL of dried tetrahydrofuran. Some gas evolved during the addition. Immediately after the addition of the diol compound a white solid precipitated. The suspension was stirred overnight at room temperature. No evolution was observed. The solid was filtered, washed with three 30 mL portions of diethyl ether and dried in vacuum to afford an 88% (2.4 g, 4.95 mmol) yield of compound **20**.

Pentene dimerization and trimerization

The olefins were distilled and filtered over Al_2O_3 under inert atmosphere to remove poisoning peroxide compounds. Tests were run in a 250 mL Fischer-Porter reactor. Hydrogenation of the catalytic mixture was performed to get the exact value of the proportion of linear versus branched olefins.. Hydrogenations were run for 3 h in a 25 mL stainless steel reactor equipped with hydrogen consumption monitoring and mechanical stirring at 150 °C under 50 bar of hydrogen pressure. Reduced palladium (5%) on activated carbon was used for this reaction.

Ethylene oligomerization

Studies were performed either in a 6-parallel semi-batch autoclaves (T464) or semi-batch mono autoclave (T95).

- T464 :

The reactors were placed under an inert nitrogen atmosphere before the toluene, the iron complex and the activator were added. The total volume of solutions introduced was 25 mL. The ethylene pressure immediately increased to 30 bar and the temperature to 50 °C. The mechanical agitation was then set to 1000 rpm and the ethylene uptake was measured. The test was stopped after 1 h or after 25 g of ethylene was consumed. The autoclave was then cooled to room temperature and depressurized. The liquid effluents were weighed. The catalyst and the cocatalyst were quenched by addition of 2 mL of a 10% H_2SO_4 solution in water. Aliquots of gaseous and liquid effluents were then analyzed by GC. The reactors were then washed three times with xylene at 140 °C and dried under vaccum (10^{-2}Torr) at 140 °C overnight. Finally, the reactor was cooled down to room temperature and fed up with ethylene (30 bar).

- T95 :

The catalytic reactions were carried out in a magnetically stirred 250 mL stainless steel autoclave. The reactor was placed under an atmosphere of ethylene before the toluene, the iron precursor and the cocatalyst were introduced. The reactor was sealed and fed with ethylene of the desired pressure (30 bar in our case). The reactor was heated to 50 °C and magnetic stirring was set to 1000 rpm. During catalysis, the pressure was maintained through a continuous feed of ethylene from a bottle placed on a balance used to monitor the ethylene uptake. At the end of the test, stirring was stopped and the reactor was cooled down to 25 °C. The gaseous effluents were collected in a 15 L polyethylene bottle filled with water. The reactor was then cooled to -5 °C and liquid effluents were collected from the bottom of the reactor. The liquid effluents were weighed. The catalyst and the cocatalyst were quenched by addition of 2 mL of a 10% H_2SO_4 solution in water. Aliquots of gaseous and liquid effluents were then analyzed by GC. The reactor was then washed three times with xylene at 140 °C and dried under vaccum (10^{-2} Torr) at 140 °C overnight. Finally, the reactor was cooled down to room temperature and fed up with ethylene (30 bar).

Bibliography

1. Chen, E. Y. X.; Marks, T. J. *Chem. Rev.* **2000**, *100*, 1391.
2. Gibson, V. C.; Redshaw, C.; Solan, G. A. *Chem. Rev.* **2007**, *107*, 1745.
3. Radhakrishnan, K.; Cramail, H.; Deffieux, A.; Francois, P.; Momtaz, A. *Macromol. Rapid Commun.* **2003**, *24*, 251.
4. Bianchini, C.; Giambastiani, G.; Luconi, L.; Meli, A. *Coord. Chem. Rev.* **2010**, *254*, 431.
5. Bianchini, C.; Giambastiani, G.; Rios, I. G.; Mantovani, G.; Meli, A.; Segarra, A. M. *Coord. Chem. Rev.* **2006**, *250*, 1391.
6. Kaminsky, W.; Kulper, K.; Brintzinger, H. H.; Wild, F. R. W. P. *Angew. Chem. Int. Ed. Engl.* **1985**, *24*, 507.
7. Reddy, S. S.; Sivaram, S. *Prog. Polym. Sci.* **1995**, *20*, 309.
8. Mason, M. R.; Smith, J. M.; Bott, S. G.; Barron, A. R. *J. Am. Chem. Soc.* **1993**, *115*, 4971.
9. Sugano, T.; Matsubara, K.; Fujita, T.; Takahashi, T. *J. of Mol. Catal.* **1993**, *82*, 93.
10. Siedle, A. R.; Lamanna, W. M.; Newmark, R. A.; Stevens, J.; Richardson, D. E.; Ryan, M. *Macromol. Symp.* **1993**, *66*, 215.
11. Semikolenova, N. V.; Zakharov, V. A.; Talsi, E. P.; Babushkin, D. E.; Sobolev, A. P.; Echevskaya, L. G.; Khysniyarov, M. M. *J. Mol. Catal. A: Chem.* **2002**, *182–183*, 283.
12. Hao, P.; Chen, Y. J.; Xiao, T. P. F.; Sun, W. H. *J. Organomet. Chem.* **2010**, *695*, 90.
13. Zhang, M.; Hao, P.; Zuo, W. W.; Jie, S. Y.; Sun, W. H. *J. Organomet. Chem.* **2008,***693*, 483.
14. Liu, H.; Zhang, L.; Chen, L.; Redshaw, C.; Li, Y.; Sun, W. H. *Dalton Trans.* **2011**, *40*, 2614.
15. Speiser, F.; Braunstein, P.; Saussine, L.; Welter, R. *Inorg. Chem.* **2004**, *43*, 1649.
16. Cazaux, J. B.; Braunstein, P.; Magna, L.; Saussine, L.; Olivier-Bourbigou, H. *Eur. J. Inorg. Chem.* **2009**, *2009*, 2942.
17. Martinez, G.; Pedrosa, S.; Tabernero, V.; Mosquera, M. E. G.; Cuenca, T. *Organometallics* **2008**, *27*, 2300.
18. Hair, G. S.; Cowley, A. H.; Jones, R. A.; McBurnett, B. G.; Voigt, A. *J. Am. Chem. Soc.* **1999**, *121*, 4922.
19. Britovsek, G. J. P.; Clentsmith, G. K. B.; Gibson, V. C.; Goodgame, D. M. L.; McTavish, S. J.; Pankhurst, Q. A. *Catal. Commun.* **2002**, *3*, 207.

20. Bryliakov, K. P.; Semikolenova, N. V.; Zudin, V. N.; Zakharov, V. A.; Talsi, E. P. *Catal. Commun.* **2004**, *5*, 45.

21. Martinez, J.; Cruz, V.; Ramos, J.; Gutierrez-Oliva, S.; Martinez-Salazar, J.; Toro-Labbe, A. *J. Phys. Chem. C* **2008**, *112*, 5023.

22. Talsi, E. P.; Babushkin, D. E.; Semikolenova, N. V.; Zudin, V. N.; Panchenko, V. N.; Zakharov, V. A. *Macromol. Chem. Phys.* **2001**, *202*, 2046.

23. Lin, C. H.; Ko, B. T.; Wang, F. C.; Lin, C. C.; Kuo, C. Y. *J. Organomet. Chem.* **1999**, *575*, 67.

24. Krempner, C.; Reinke, H.; Weichert, K. *Organometallics* **2007**, *26*, 1386.

25. Jiang, Z.; Interrante, L. V.; Kwon, D.; Tham, F. S.; Kullnig, R. *Inorg. Chem.* **1991**, *30*, 995.

26. McMahon, C. N.; Alemany, L.; Callender, R. L.; Bott, S. G.; Barron, A. R. *Chem. Mat.* **1999**, *11*, 3181.

27. McMahon, C. N.; Obrey, S. J.; Keys, A.; Bott, S. G.; Barron, A. R. *J. Chem. Soc. , Dalton Trans.* **2000**, 2151.

28. Pasynkiewicz, S.; Ziemkowska, W. *J. Organomet. Chem.* **1992**, *423*, 1.

29. Ziemkowska, W. *Coord. Chem. Rev.* **2005**, *249*, 2176.

30. Ziemkowska, W. *Inorg. Chem. Commun.* **2001**, *4*, 757.

31. Ziemkowska, W. *Main Group Metal Chem.* **2001**, *24*, 111.

32. Ziemkowska, W. *Polyhedron* **2002**, *21*, 281.

33. Kaul, F. A. R.; Tschinkl, M.; Gabbai, F. P. *J. Organomet. Chem.* **1997**, *539*, 187.

34. Cottone; Morales, D.; Lecuivre, J. L.; Scott, M. J. *Organometallics* **2001**, *21*, 418.

35. Babik, S. T.; Fink, G. *J. Organomet. Chem.* **2003**, *683*, 209.

36. Fulmer, G. R.; Miller, A. J. M.; Sherden, N. H.; Gottlieb, H. E.; Nudelman, A.; Stoltz, B. M.; Bercaw, J. E.; Goldberg, K. I. *Organometallics* **2010**, *29*, 2176.

CHAPTER V

Nickel(II) and Iron(II) Complexes with Imino-Imidazole chelating Ligands bearing Pendant Donor Groups (SR, OR, NR_2, PR_2) as Precatalysts in Ethylene Oligomerization

Abstract: New imino-imidazole ligands bearing a pendant donor function L were synthesized in excellent yields. The corresponding nickel(II) complexes $[NiCl_2(\text{imino-imidazole-L})]_n$ (L = $(CH_2)_2SMe$ (**S1**), $(CH_2)_2OMe$ (**O1**), $(CH_2)_2NEt_2$ (**N1**), $(CH_2)_2PPh_2$ (**P1**), (C_6H_4)-*p*-OMe (**O2**), $(CH_2)_3OMe$ (**O3**), $(CH_2)_3CH_3$ (**C1**); n = 1, 2) were prepared and characterized by FT-IR spectroscopy and elemental analysis. Furthermore, the coordination geometry around the metal center in the binuclear complex $\mathbf{Ni_{S1}}$ and the mononuclear complexes $\mathbf{Ni_{N1}}$ and $\mathbf{Ni_{O2}}$ was unambiguously established by single crystal X-ray diffraction. All complexes have been evaluated for the oligomerization of ethylene in the presence of $AlEtCl_2$ or MAO (methylaluminoxane) as cocatalyst, and mostly dimers and trimers were produced. Better activities were observed with $AlEtCl_2$ as cocatalyst than with MAO. This concept was applied to iron complexes. Unfortunately, these systems remained inactive toward ethylene transformation.

Résumé : Une nouvelle famille de ligands imidazole-imines possédant une fonction hémilabile L a été synthétisée. Les complexes de nickel correspondants de formule générale $[NiCl_2(\text{imidazole-imine-L})]_n$ avec L = $(CH_2)_2SMe$ (**S1**), $(CH_2)_2OMe$ (**O1**), $(CH_2)_2NEt_2$ (**N1**), $(CH_2)_2PPh_2$ (**P1**), (C_6H_4)-*p*-OMe (**O2**), $(CH_2)_3OMe$ (**O3**), $(CH_2)_3CH_3$ (**C1**) et n = 1, 2 ont été obtenus avec de très bons rendements et caractérisés par spectrométrie infrarouge, analyses élémentaires et diffractions des rayons X. Une structure binucléaire a été déterminée pour le complexe $\mathbf{Ni_{S1}}$ tandis que les complexes $\mathbf{Ni_{N1}}$ et $\mathbf{Ni_{O2}}$ ont donné lieu à des systèmes mononucléaires. Activés par le MAO et l'EADC, tous les précurseurs de nickel ont oligomérisé l'éthylène pour donner essentiellement des dimères et des trimères. Les activités obtenues avec l'EADC se sont révélés meilleures qu'avec le MAO. La généralisation de ce concept à des précurseurs de fer a donné des systèmes inactifs en catalyse.

Introduction

The transition-metal catalyzed oligomerization of ethylene to short chain α-olefins has triggered considerable attention over decades. Long after the discovery of the "nickel effect" by Wilke *et al*.,[1] renewed interest was generated by the work of Brookhart and co-workers on the development of nickel-based complexes chelated by α-diimine ligands.[2,3] This resulted in the development of a wide range of nickel precatalysts bearing P,P-,[4-6] P,N-,[7-12] P,O-,[13-19] N,N-[20-25] or N,O-[26-31] type bidentate ligands. Understandably, tridentate ligands tend to be developed with the advantage of offering an even wider diversity.[32-34] One strategy consists in introducing an additional donor group on bidentate ligands and this was successfully implemented for iron-catalyzed[35-37] and titanium-catalyzed[38-42] oligomerization. Herein, we report the straightforward synthesis of imino-imidazole ligands bearing a pendant donor group. The corresponding nickel(II) complexes were prepared, characterized and evaluated for ethylene oligomerization using $AlEtCl_2$ or MAO as cocatalysts. This strategy was also extended to iron complexes.

I. Synthesis and characterization of the ligands and Ni(II) complexes

Ligands **S1-C1** were obtained in excellent yield (>95%) by condensation reaction between 1-methyl-1*H*-imidazole-2-carboxaldehyde and the corresponding amines. The volatility of the different amino precursors, except the phosphino derivative, allows easy purification. The ligands were characterized by ^{1}H NMR, ^{13}C NMR and FT-IR spectroscopy. The nickel(II) complexes (**Ni$_{S1}$-Ni$_{C1}$**) were then prepared by reaction of [$NiCl_2$(DME)] (DME = dimethoxyethane) with a slight excess of the corresponding ligand in CH_2Cl_2 (Scheme 1).

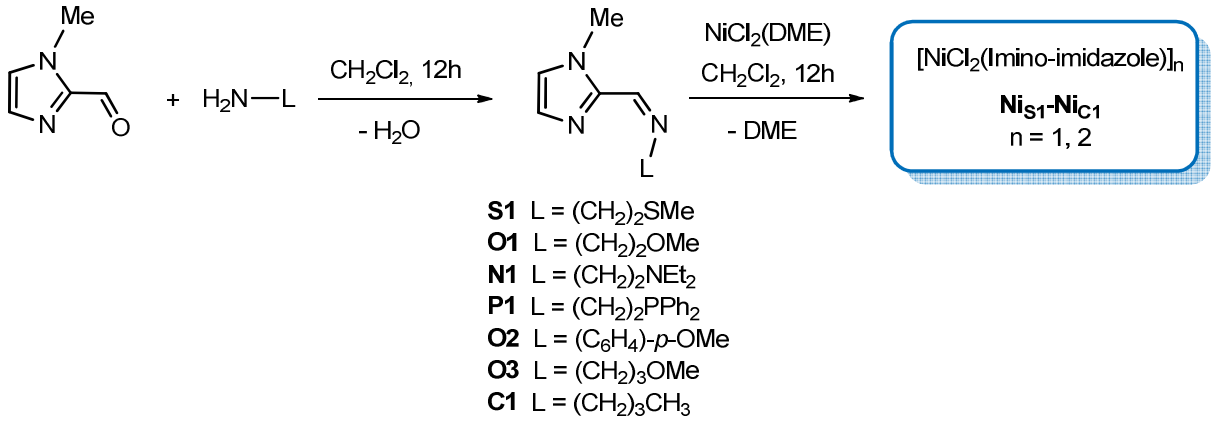

Scheme 1. Synthesis of ligands (**S1-C1**) and the corresponding nickel(II) precatalysts (**Ni$_{S1}$-Ni$_{C1}$**).

All complexes were obtained in high yields (~90%) and characterized by FT-IR spectroscopy and elemental analysis. The coordination of the ligand was confirmed by the shift of the absorption band of the imino group ($\nu_{C=N}$) to lower wavenumbers and its weaker intensity in comparison to that for the free ligand (1650 to 1641 cm^{-1} for **S1** and **Ni$_{S1}$**, respectively; see Experimental Section). Elemental analyses confirmed the presence of one ligand per metal center in each complex. X-ray diffraction studies on **Ni$_{S1}$**, **Ni$_{N1}$** and **Ni$_{O2}$'** unambiguously established the coordination geometry around the metal center (Scheme 2).

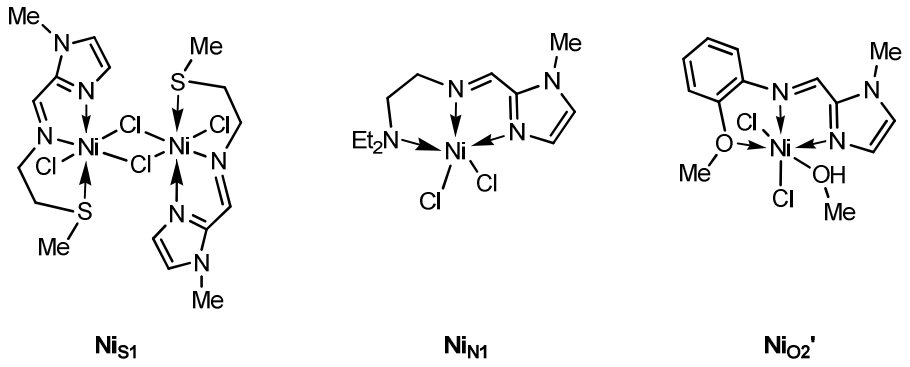

Scheme 2. Crystallographically characterized complexes **Ni$_{S1}$**, **Ni$_{N1}$** and **Ni$_{O2}$'**.

Single crystals of $\mathbf{Ni_{S1}}$ suitable for X-ray diffraction analysis were grown by slow diffusion of diethyl ether into a methanol solution of the complex. The molecular structure of complex $\mathbf{Ni_{S1}}$ is shown in Scheme 3 and selected bond distances and angles are listed in Table 1. In the solid state, the complex adopts a dinuclear structure and the N,N,S tridentate coordination mode of the ligand is established (Ni(1)-S(4) = 2.524(10) Å). A terminal chloride ligand and two bridging chlorides complete the metal coordination spheres. The existence of a C_2 axis passing through Cl(3) atoms results in the planarity of the central Ni_2Cl_2 moiety. The Ni-Ni separation of 3.586 Å is too long to represent any significant direct interaction and this is consistent with their d^8 electronic configuration. The six-coordinated metal centers adopt a distorted octahedral coordination geometry, as indicated by the values of the Cl(3)-Ni(1)-N(10) and S(4)-Ni(1)-N(7) angles (97.53(8)° and 80.98(8)°) and by the values of the Cl(3)-Ni(1)-N(7) and Cl(3)(2)-Ni(1)-Cl(2) angles (173.41(7)° and 174.79(3)°, respectively).

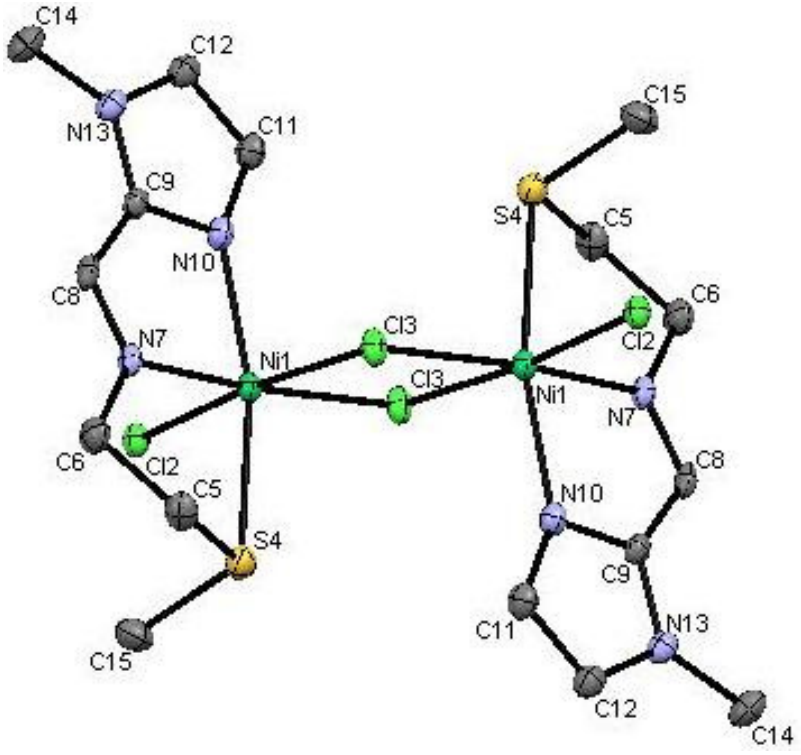

Scheme 3. ORTEP view of the nickel(II) complex $\mathbf{Ni_{S1}}$. H atoms are omitted for clarity. Ellipsoids are drawn at a 50% probability level.

Single crystals of $\mathbf{Ni_{N1}}$ were obtained by slow diffusion of diethyl ether into an acetonitrile solution of the complex. The complex adopts an overall distorted trigonal-bipyramidal geometry in which the imino nitrogen atom N(7) and the chlorine atoms Cl(2)

and Cl(3) form the equatorial plane (Scheme 4). The nitrogen donor atoms of the N,N,N tridentate ligand and the Ni center are almost coplanar. Selected bond distances and angles are given in Table 1. The Ni-N bond distance of the chelating pendant donor function is longer (2.178(4) Å) than Ni-N distances of either the imidazole ring (2.105(4) Å) or the imino group (2.038(4) Å).

Crystals of **Ni_{O2}'**, obtained by slow diffusion of diethyl ether into a methanol solution of complex **Ni_{O2},** revealed that one molecule of MeOH is bonded to the metal. This leads to a distorted octahedral coordination geometry for the Ni center (Scheme 5), as evidenced by a Cl(3)-Ni(1)-N(7) angle of 89.56(11)°. The molecule of MeOH is coordinated to the metal via a dative bond as established by the presence of a H atom on the oxygen and by the Ni(1)-O(20) distance (2.154(4) Å).[23] The pendant donor group occupies an equatorial coordination site with a Ni(1)-O(18) bond length of 2.211(4) Å. The Ni-N distances are 2.030(4) Å (Ni(1)-N(7)) and 2.068(4) Å (Ni(1)-N(10)), respectively. Although the metal center in complexes **Ni_{S1}** and **Ni_{O2}'** adopts an octahedral coordination geometry, there are slight differences in the interligand angles between these structures. For example, the Cl(2)-Ni(1)-Cl(3) angle is wider in complex **Ni_{O2}'** (95.78(6)°) than in **Ni_{S1}** (93.01(3)°) and the Cl(3)-Ni(1)-O(20) angle of 169.58(10)° in **Ni_{O2}'** is smaller than the Cl(3)(2)-Ni(1)-Cl(2) angle of 174.79(3)° in **Ni_{S1}**.

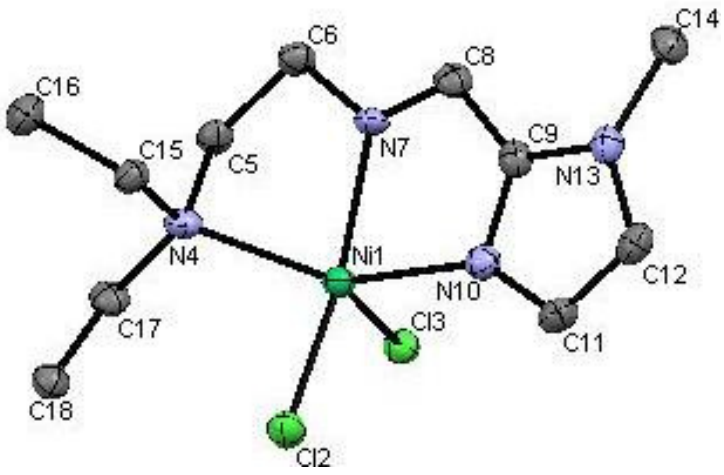

Scheme 4. ORTEP view of the nickel(II) complex **Ni_{N1}**. H atoms are omitted for clarity. Ellipsoids are drawn at a 50% probability level.

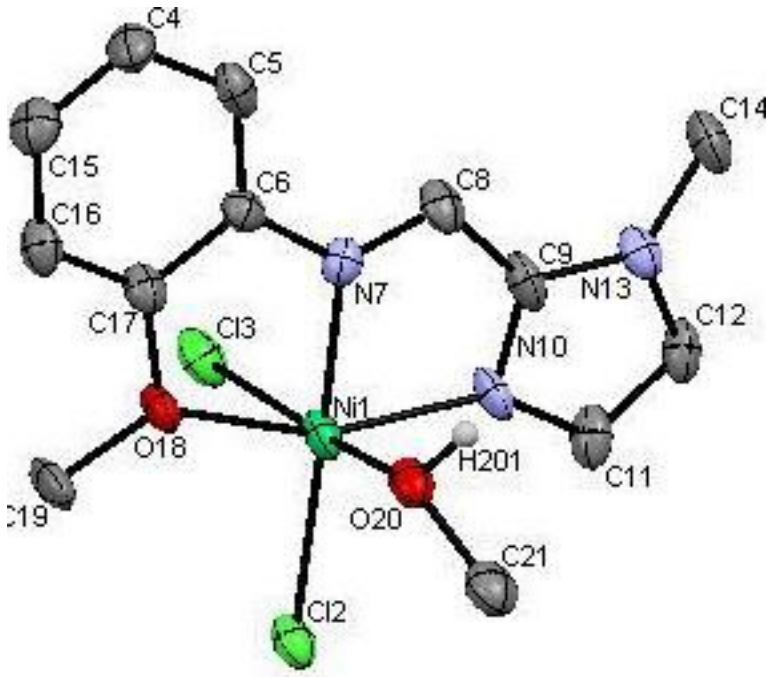

Scheme 5. ORTEP view of the nickel(II) complex **Ni_{O2}'**. H atoms are omitted for clarity (except for MeOH). Ellipsoids are drawn at a 50% probability level.

Table 1. Selected bond distances (Å) and angles (°) for complexes **Ni_{S1}**, **Ni_{N1}** and **Ni_{O2}'**.

	Ni_{S1}	**Ni_{N1}**	**Ni_{O2}'**
Ni(1)-X[a]	2.524(10)	2.178(4)	2.211(4)
Ni(1)-N(7)	2.056(2)	2.038(4)	2.030(4)
Ni(1)-N(10)	2.070(3)	2.105(4)	2.068(4)
C(6)-N(7)	1.454(4)	1.446(5)	1.419(6)
N(7)-C(8)	1.273(4)	1.282(6)	1.281(6)
Ni(1)-Cl(3)	2.382(8)	2.312(12)	2.373(15)
Ni(1)-Cl(2)	2.387(9)	2.276(12)	2.343(15)
Ni(1)-O(20)	-	-	2.154(4)
N(7)-Ni(1)-N(10)	79.84(10)	77.99(14)	80.78(17)
X-Ni(1)-N(7)[a]	80.98(8)	78.97(14)	75.88(15)
X-Ni(1)-N(10)[a]	160.69(8)	151.76(14)	156.05(15)
Cl(3)-Ni(1)-N(7)	173.41(7)	98.62(11)	89.56(11)
Cl(3)-Ni(1)-N(10)	97.53(8)	102.49(11)	97.51(13)
Cl(2)-Ni(1)-Cl(3)	93.01(3)	106.30(5)	95.78(6)
Y-Ni(1)-Cl(2)[b]	174.79(3)	-	90.74(10)
Cl(3)(2)-Ni(1)-Cl(3)	83.56(3)	-	-

[a] X = S(4) for **Ni_{S1}**, X = N(4) for **Ni_{N1}** and X = O(18) for **Ni_{O2}'**. [b] Y = Cl(3)(2) for **Ni_{S1}**, Y = O(20) for **Ni_{O2}'**.

II. Ethylene oligomerization with the Ni-complexes Ni_{S1}-Ni_{C1}.

Nickel complexes **Ni_{S1}-Ni_{C1}** were used as precatalysts for the oligomerization of ethylene. Experiments were carried out at 5 or 10 bar and 45 °C in *n*-heptane or in toluene. When activated by 15 equivalents of ethylaluminum dichloride ($AlEtCl_2$) at 5 bar and 45 °C, complex **Ni_{S1}** presents an interesting activity (1.63×10^6 g·(mol(Ni)·h)$^{-1}$) and compares favorably with [$NiCl_2$(DME)] used as reference (Table 2, entries 1 and 2). Due to the lack of solubility of complexes **Ni_{S1}-Ni_{C1}**, toluene was preferred to *n*-heptane. This led to an increase of the activity (3.14×10^6 g·(mol(Ni)·h)$^{-1}$) for **Ni_{S1}** with no significant effect on the reaction selectivity (Table 2, entry 3). A good stability of the precatalyst **Ni_{S1}** was observed over more than half an hour after activation in these solvents. As expected, adjusting the pressure to 10 bar of ethylene resulted in an increase of activity without affecting the distribution of oligomers (Table 2, entry 4). Substitution of the thioether group in **Ni_{S1}** by an ether as in **Ni_{O1}** led to a slight improvement of the activity (Table 2, entries 4 and 5) while marginal effects on both activity and selectivity were observed when an amino or a phosphino group was introduced, as in complexes **Ni_{N1}** and **Ni_{P1}**, respectively (Table 2, entries 6 and 7). This suggests that the functionalization introduced on the imino-imidazole backbone has only a limited role, which was confirmed to a certain degree by the use of complex **Ni_{C1}**, which also presents comparable performances (Table 2, entry 10). Interestingly, the presence of an oxygen donor atom improved slightly the activity (Table 2, entry 5). The best activity (12.03×10^6 g·(mol(Ni)·h)$^{-1}$) was obtained when a non flexible linker was introduced between the imine and the functional group, as in complex **Ni_{O2}** (Table 2, entry 8), which emphasizes the interest for a tridentate behavior of the ligand. Lengthening the linker to three carbon atoms as in complex **Ni_{O3}** has however a detrimental effect on the activity (Table 2, entry 9). For all the complexes, the selectivity for 1-butene was relatively low (in a range 8-18%), probably due to the known isomerization ability of nickel(II)/$AlEtCl_2$ catalytic systems.[20,43]

Table 2. Ethylene oligomerization with precatalysts $\mathbf{Ni_{S1}}$-$\mathbf{Ni_{C1}}$ using $AlEtCl_2$ as cocatalyst.[a]

Entry	Precatalyst	Time (min)	P_{C2H4} (bar)	Activity[b]	Selectivity (wt%)[c]		
					C_4 (1-C_4)[d]	C_6 (1-C_6)[d]	C_{6+}
1[e]	$[NiCl_2(DME)]$	85	5	0[f]	-	-	-
2[e]	$\mathbf{Ni_{S1}}$	75	5	1.63	79 (6)	21 (2)	-
3	$\mathbf{Ni_{S1}}$	40	5	3.14	83 (14)	16 (2)	1
4	$\mathbf{Ni_{S1}}$	15	10	9.56	84 (18)	14 (2)	2
5	$\mathbf{Ni_{O1}}$	15	10	11.08	86 (13)	13 (3)	1
6	$\mathbf{Ni_{N1}}$	15	10	9.79	86 (12)	13 (2)	1
7	$\mathbf{Ni_{P1}}$	15	10	9.87	87 (8)	11 (1)	2
8	$\mathbf{Ni_{O2}}$	15	10	12.03	83 (18)	16 (3)	1
9	$\mathbf{Ni_{O3}}$	15	10	8.98	86 (10)	13 (2)	1
10	$\mathbf{Ni_{C1}}$	15	10	9.90	83(18)	17(3)	-

[a] Ni (20 μmol), Al/Ni = 15, toluene (100 mL), 45 °C. [b] $\times 10^6$ $g_{C2H4\ converted}\cdot(mol(Ni)\cdot h)^{-1}$. [c] Determined by GC. [d] C_n, wt% of hydrocarbons with n carbon atoms in oligomers, 1-C_n, wt% of terminal alkene in the C_n fraction. [e] heptane was used instead of toluene. [f] no ethylene uptake

Precatalysts $\mathbf{Ni_{S1}}$-$\mathbf{Ni_{C1}}$ were then evaluated using methylaluminoxane (MAO) as cocatalyst (Table 3). At 30 bar and 45 °C, the activities of complexes $\mathbf{Ni_{S1}}$-$\mathbf{Ni_{C1}}$ were approximately one order of magnitude lower than with $AlEtCl_2$ as activator. It should be noted that under more dilute conditions than in Table 2 ([Ni] = 0.2 mM *vs.* [Ni] = 1 mM in Table 3), no significant production of oligomers was observed, which led us to carry out the catalytic tests under more concentrated conditions. Variations of selectivities were more significant than with $AlEtCl_2$ as cocatalyst. The selectivity for dimers was improved to 94% when complex $\mathbf{Ni_{N1}}$ was used in combination with 500 equivalents of MAO (Table 3, entry 4) and the selectivities for α-olefins was higher than with $AlEtCl_2$, up to 56% for 1-butene in the C_4 fraction (Table 3, entry 1). Similar or slightly higher activities (from 0.93×10^6 to 1.15×10^6 $g\cdot(mol(Ni)\cdot h)^{-1}$) were observed when the ligand bears an ether, an amino or a phosphino moiety, as in $\mathbf{Ni_{O1}}$, $\mathbf{Ni_{N1}}$, and $\mathbf{Ni_{P1}}$, respectively, instead of a thioether group (0.84×10^6 $g\cdot(mol(Ni)\cdot h)^{-1}$), as in $\mathbf{Ni_{S1}}$ (Table 3, entries 1, 2, 4 and 6). Increasing the molar ratio of MAO to nickel complexes $\mathbf{Ni_{O1}}$ or $\mathbf{Ni_{N1}}$ from 500 to 1000 led to higher activities but to a decrease of the selectivity in butenes (from 93% to 88% for $\mathbf{Ni_{O1}}$ and from 94% to 88% for $\mathbf{Ni_{N1}}$) and in 1-butene (from 40% to 32% for $\mathbf{Ni_{O1}}$ and from 32% to 31% for $\mathbf{Ni_{N1}}$) in the C_4 fraction (Table 3, entries 2-5). No significant ethylene uptake was noticed when the molar ratio of activator to Ni was under 500. Similarly to the observations made with $AlEtCl_2$ as cocatalyst, introduction of a rigid linker as in $\mathbf{Ni_{O2}}$ resulted in a slight improvement of the activity (Table 3, entries 2 and 7) while increasing the length of the alkyl linker, as in complex $\mathbf{Ni_{O3}}$, led to a slight decrease of activity (Table 3, entries 2 and 8). Surprisingly, a significantly amount of higher

olefins was produced with catalyst **Ni_{O3}** (Table 3, entry 8). As observed with EADC activation, complex **Ni_{C1}** afforded a comparable activity (Table 3, entry 9).

Table 3. Ethylene oligomerization with precatalysts **Ni_{S1}-Ni_{C1}** using MAO as cocatalyst.[a]

Entry	Precatalyst	Al/Ni	Activity[b]	Selectivity (wt%)[c]		
				C_4 (1-C_4)[d]	C_6 (1-C_6)[d]	C_{6+}
1	**Ni_{S1}**	500	0.84	91 (56)	5 (19)	4
2	**Ni_{O1}**	500	0.93	93 (40)	4 (12)	3
3[e]	**Ni_{O1}**	1000	2.44	88 (32)	9 (11)	3
4	**Ni_{N1}**	500	1.15	94 (32)	4 (8)	2
5[e]	**Ni_{N1}**	1000	2.21	88 (31)	9 (10)	3
6	**Ni_{P1}**	500	1.01	89 (38)	7 (13)	4
7	**Ni_{O2}**	500	1.04	88 (30)	8 (9)	4
8	**Ni_{O3}**	500	0.90	80 (51)	7 (33)	13
9	**Ni_{C1}**	500	0.93	86 (40)	10(11)	4

[a] Ni (20 µmol), toluene (20 mL), ethylene pressure 30 bar, 45 °C, 50 min. [b] $\times 10^6$ $g_{C2H4\ converted} \cdot (mol_{Ni} \cdot h)^{-1}$. [c] Determined by GC. [d] wt% in the C_n fraction. [e] reaction time: 30 min.

III. Extension to corresponding iron(II) complexes

The same strategy was applied to iron precursors. New ligands were involved in this campaign (Scheme 6, **S2**-**S6** and **N2**). Amines used for the synthesis of ligands **S3**-**S6** were obtained by reaction of 2-chloroethylamine hydrochloride with the corresponding benzenethiol derivatives in the presence of potassium carbonate in dichloromethane. Complexes were synthesized by reaction of metal precursor ($FeCl_2$, $FeCl_2 \cdot 1.5THF$ or $FeCl_2 \cdot 4H_2O$) with the corresponding ligand in the appropriated solvent (*n*-BuOH, THF or cyclohexane). All complexes were obtained in moderate to high yields (60-90%) and characterized by FT-IR spectroscopy. The coordination of the ligand was confirmed by the shift of the absorption band of the imino group ($\nu_{C=N}$) to lower wavenumbers and its weaker intensity in comparison to that for the free ligand (1650 to 1628 cm^{-1} for **S6** and **Fe_{S6}**, respectively; see Experimental Section).

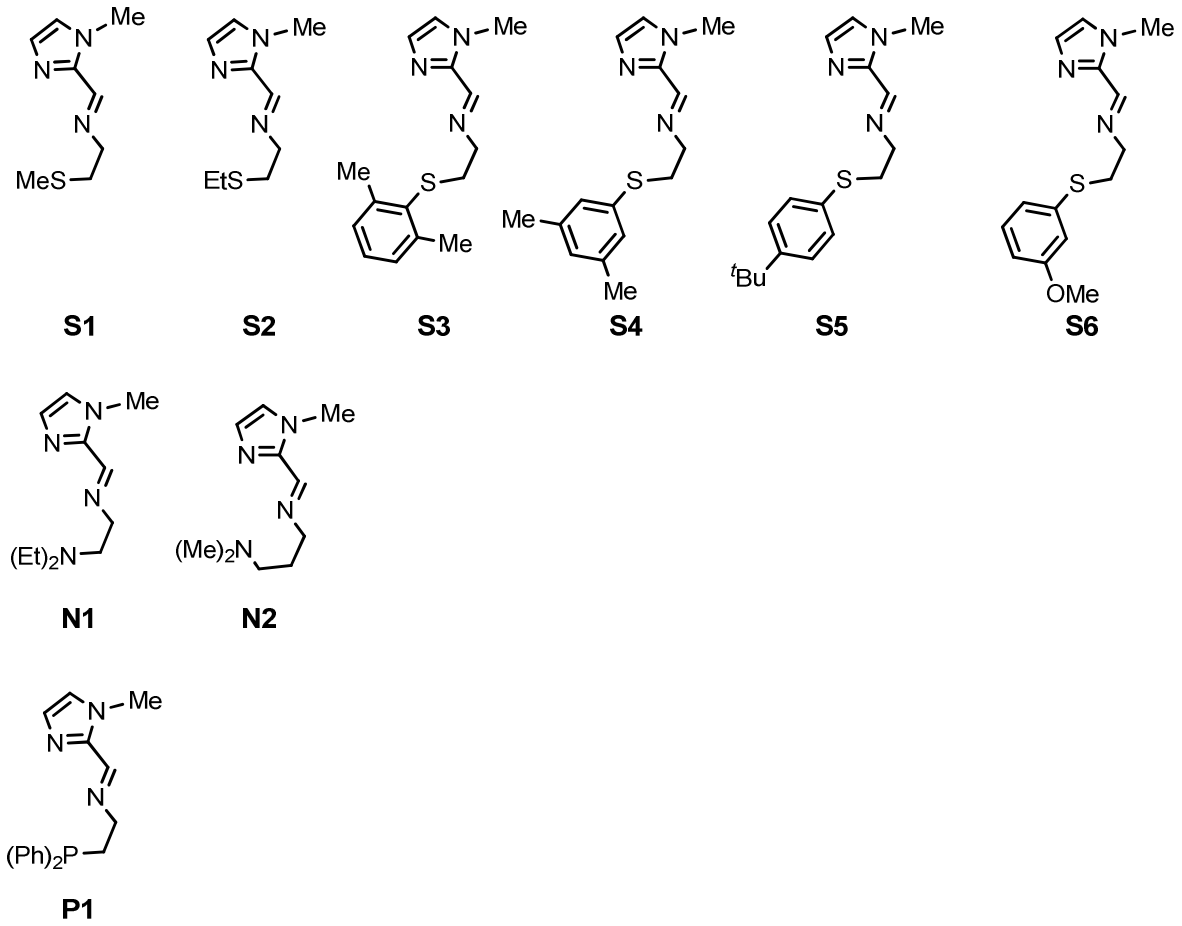

Scheme 6. Ligands involved in the synthesis of iron complexes.

Precatalysts $\mathbf{Fe_{S1}}$-$\mathbf{Fe_{P1}}$ were then evaluated using methylaluminoxane (MAO) as cocatalyst (Al/Fe = 500). However, at 30 bar and 50 °C, none of the tested complexes were active for the oligomerization of ethylene.

Conclusion

A series of nickel(II) complexes containing imino-imidazole ligands with a pendant donor group have been synthesized and fully characterized. Single crystal X-ray diffraction studies confirmed the tridentate coordination mode of the ligand, whether the complex crystallizes in a binuclear form, as for $\mathbf{Ni_{S1}}$, or in a mononuclear form, as for $\mathbf{Ni_{N1}}$ and $\mathbf{Ni_{O2}}$'. Upon activation by $AlEtCl_2$, the precatalysts $\mathbf{Ni_{S1}}$-$\mathbf{Ni_{C1}}$ exhibit very high productivities toward ethylene oligomerization leading to short chain olefins (C_4-C_6), however with a low selectivity for α-olefins. Higher selectivities in butenes and 1-butene are observed when the precatalysts were activated with MAO. However in this case, the turnover frequencies were generally lower by one order of magnitude. Regarding the ether derivatives and irrespective of the cocatalyst used, the rigid linker 1,2-phenylene was preferred over the flexible alkyl chains containing two or three carbon atoms. Upon activation of MAO, no activity was observed with iron complexes.

Acknowledgement

We thank IFP Energies nouvelles for the permission to publish these results and for their support. We are grateful to Erwann Jeanneau (Université Claude Bernard - Lyon 1) for the crystal structure determinations.

Experimental section

General considerations

All manipulations were carried out using standard Schlenk techniques under inert atmosphere. Toluene, THF, pentane and dichloromethane were dried by a solvent purification system (SPS-M-Braun). Dimethoxyethane (DME) and cyclohexane were distilled over sodium/benzophenone. Methanol, acetonitrile and *n*-butanol were degassed and dried over molecular sieves (4 Å). Commercial starting materials were purchased from Sigma-Aldrich and Alfa Aesar and used without further purification. Deuterated solvents (CD_2Cl_2 and $(CD_3)_2CO$) were purchased from Sigma-Aldrich or Eurisotop, freeze-pumped and stored over 4 Å molecular sieves under argon. The ^{1}H, $^{31}P\{^{1}H\}$, and $^{13}C\{^{1}H\}$ NMR spectra were recorded on a Bruker AC 300 MHz instrument at 293 K unless otherwise stated. All chemical shifts are reported in ppm *vs* $SiMe_4$ and were determined with reference to residual solvent peaks.[44] ^{31}P NMR chemical shifts are reported in ppm relative to a 85% H_3PO_4 solution in water. All coupling constants are given in Hertz. Chemical shifts values (δ) are given in ppm. Gas chromatographic analysis were performed on a Agilent 6850 series II equipped with a flame ionization detector and using an Agilent Pona column (50 m, 0.2 mm diameter, 0.5 µm film thickness). FT-IR spectra were recorded in the region 4000-450 cm^{-1} on a Perkin-Elmer Spectrum one FT-IR spectrometer (ATR mode, ZnSe diamond). Elemental analyses were performed by the Service Central d'Analyses of the CNRS (Vernaison, France).

Synthesis of the ligands (S1-C1)

- **Synthesis of N-((1-methyl-1H-imidazol-2-yl)methylene)-2-(methylthio)ethanamine (S1)**

2-(methylthio)ethanamine (0.46 mL, 4.89 mmol) was added to a solution of 1-methyl-1*H*-imidazole-2-carbaldehyde (0.490 g, 4.45 mmol) in dichloromethane (15 mL) and the mixture was stirred for 1 h at room temperature. Small amount of $MgSO_4$ was added to the yellow reaction mixture. The solution was then filtered via canula. The solvent and the small excess of 2-(methylthio)ethanamine were evaporated to afford the desired product as a pale yellow oil in 95% yield.

^{1}H NMR (300 MHz, CD_2Cl_2): δ 8.28 (m, 1H), 7.05 (d, 1H, *J* = 1.0 Hz), 6.95 (s, 1H), 3.95 (s, 3H), 3.77 (td, 2H, *J* = 6.8, *J* =1.3 Hz), 2.79 (t, 2H, *J* = 6.8 Hz), 2.12 (s, 3H).

^{13}C{^{1}H} NMR (75 MHz, CD_2Cl_2): δ 154.60, 143.50, 129.39, 125.24, 61.36, 35.52, 15.86.

FT-IR (cm^{-1}): 2967m, 1650s ($\nu_{C=N}$), 1518w, 1475m, 1437m, 1369w, 1287m, 1203w, 1174w, 1149w, 1067s, 919w, 748m, 707m, 691m, 500w, 468w.

- **Synthesis of N-((1-methyl-1H-imidazol-2-yl)methylene)-2-(ethylthio)ethanamine (S2)**

Ligand **S2** was prepared according to the method described for **S1** using 2-(ethylthio)ethylamine (0.39 mL, 3.41 mmol) and 1-methyl-1*H*-imidazole-2-carbaldehyde (0.342 g, 4.13 mmol) and isolated as a pale yellow oil in 90% yield.

^{1}H NMR (300 MHz, CD_2Cl_2): δ 8.28 (m, 1H), 7.05 (d, 1H, *J* = 1.0 Hz), 6.95 (s, 1H), 3.95 (s, 3H), 3.76 (td, 2H, *J* = 6.8, *J* =1.3 Hz), 2.82 (t, 2H, *J* = 6.8 Hz) 2.56 (q, 2H, *J* = 7.4 Hz), 1.24 (t, 3H, *J* = 7.4 Hz).

^{13}C{^{1}H} NMR (75 MHz, CD_2Cl_2): δ 154.51, 143.47, 129.36, 125.22, 61.92, 35.51, 32.89, 26.37, 15.06.

FT-IR (cm^{-1}): 2965w, 2922w, 1649s ($\nu_{C=N}$), 1516w, 1476m, 1436s, 1367w, 1286m, 1263w, 1225w, 1191w, 1148s, 1018w, 919m, 797w, 754s, 707m, 690m, 611w, 497w.

- **Synthesis of 2-((2,6-dimethylphenyl)thio)ethanamine**

2,6-dimethylbenzenethiol (0.38 mL, 2.89 mmol) was added to a solution of 2-chloroethylamine hydrochloride (0.439 g, 3.78 mmol) and potassium carbonate (1.19 g, 8.67 mmol) in dichloromethane (15 mL). The mixture was stirred overnight at room temperature.

Small amount of $MgSO_4$ was added to the reaction mixture. The solution was then filtered via canula and the solvent was evaporated. The product was purified by distillation (10^{-2} mbar, 130°C) and obtained as colorless oil in 70% yield.

^{1}H NMR (300 MHz, CD_2Cl_2): δ 7.10 (m, 3H), 2.74 (m, 2H), 2.72 (m, 2H), 2.54 (s, 6H), 1.54 (s, 2H).

- **Synthesis of 2-((2,6-dimethylphenyl)thio)-N-((1-methyl-1H-imidazol-2-yl)methylene)ethanamine (S3)**

Ligand **S3** was prepared according to the method described for **S1** using 2-((2,6-dimethylphenyl)thio)ethanamine (0.223 g, 1.23 mmol) and 1-methyl-1*H*-imidazole-2-carbaldehyde (0.123 g, 1.12 mmol) and isolated as a pale yellow oil in 90% yield.

^{1}H NMR (300 MHz, CD_2Cl_2): δ 8.23 (m, 1H), 7.10 (m, 3H), 7.04 (m, 1H), 6.94 (s, 1H), 3.89 (s, 3H), 3.69 (t, 2H, *J* = 6.8 Hz), 2.96 (t, 2H, J = 6.8 Hz), 2.53 (s, 6H).

FT-IR (cm^{-1}): 2921w, 1650s ($\nu_{C=N}$), 1478m, 1460m, 1436s, 1410m, 1375w, 1287w, 1149w, 1085m, 1049m, 919w, 771s, 707w, 690w, 487w.

- **Synthesis of 2-((3,5-dimethylphenyl)thio)ethanamine**

2-((3,5-dimethylphenyl)thio)ethanamine was synthesized according to the method described for 2-((2,6-dimethylphenyl)thio)ethanamine using 3,5-dimethylbenzenethiol (1.97 mL, 14.47 mmol), potassium carbonate (5.99 g, 43.41 mmol) and 2-chloroethylamine hydrochloride (2.18 g, 18.81 mmol). The product was obtained as a colorless oil in 60% yield.

^{1}H NMR (300 MHz, CD_2Cl_2): δ 6.97 (m, 2H), 6.83 (m, 1H), 2.96 (t, 2H, *J* = 6.2 Hz), 2.85 (t, 2H, *J* = 6.2 Hz), 2.27 (s, 3H) 1.43 (s, 2H).

- **Synthesis of 2-((3,5-dimethylphenyl)thio)-N-((1-methyl-1H-imidazol-2-yl)methylene)ethanamine (S4)**

Ligand **S4** was prepared according to the method described for **S1** using 2-((3,5-dimethylphenyl)thio)ethanamine (0.538 g, 2.97 mmol) and 1-methyl-1*H*-imidazole-2-carbaldehyde (0.327 g, 2.97 mmol) and isolated as a pale yellow oil in 87% yield.

^{1}H NMR (300 MHz, CD_2Cl_2): δ 8.25 (s, 1H), 7.06 (m, 1H), 6.98 (m, 2H), 6.97 (s, 1H), 6.82 (s, 1H), 3.83 (s, 3H), 3.80 (t, 2H, *J* = 6.7 Hz), 2.96 (t, 2H, *J* = 6.7 Hz), 2.56 (s, 6H).

FT-IR (cm^{-1}): 2919w, 1650s ($\nu_{C=N}$), 1599m, 1581m, 1477m, 1437s, 1411m, 1368w, 1287m, 1228w, 1149w, 1085m, 1032s, 919w, 834m, 797m, 759s, 770s, 487w.

- **Synthesis of 2-((4-(tert-butyl)phenyl)thio)ethanamine**

2-((4-(*tert*-butyl)phenyl)thio)ethanamine was synthesized according to the method described for 2-((2,6-dimethylphenyl)thio)ethanamine using 4-(*tert*-butyl)benzenethiol (2.02 mL, 12.03 mmol), potassium carbonate (4.99 g, 36.09 mmol) and 2-chloroethylamine hydrochloride (1.81 g, 15.64 mmol). The product was obtained as a colorless oil in 55% yield.

^{1}H NMR (300 MHz, CD_2Cl_2): δ 7.31 (m, 4H), 2.96 (t, 2H, *J* = 6.0 Hz) 2.83 (t, 2H, *J* = 6.0 Hz), 1.42 (s, 2H), 1.33 (s, 9H).

- **Synthesis of 2-((4-(tert-butyl)phenyl)thio)-N-((1-methyl-1H-imidazol-2-yl)methylene)ethanamine (S5)**

Ligand **S5** was prepared according to the method described for **S1** using 2-((4-(*tert*-butyl)phenyl)thio)ethanamine (0.578 g, 2.21 mmol) and 1-methyl-1*H*-imidazole-2-carbaldehyde (0.243 g, 2.21 mmol) and isolated as a pale yellow oil in 88% yield.

^{1}H NMR (300 MHz, CD_2Cl_2): δ 8.25 (s, 1H), 7.30 (m, 4H), 7.05 (d, 1H, *J* = 1.1 Hz), 6.94 (m, 1H), 3.88 (s, 3H), 3.79 (t, 2H, *J* = 6.7 Hz), 3.21 (t, 2H, *J* = 6.7 Hz), 1.29 (s, 9H).

FT-IR (cm^{-1}): 2961w, 1650s ($\nu_{C=N}$), 1478s, 1437s, 1362m, 1286m, 1148m, 1120s, 1083m, 1030m, 1012m, 919m, 820s, 754m, 707w, 690w, 548m.

- **Synthesis of 2-((3-methoxyphenyl)thio)ethanamine**

2-((3-methoxyphenyl)thio)ethanamine was synthesized according to the method described for 2-((2,6-dimethylphenyl)thio)ethanamine using 3-methoxybenzenethiol (1.76 mL, 14.26 mmol), potassium carbonate (5.91 g, 42.78 mmol) and 2-chloroethylamine hydrochloride (2.15 g, 18.54 mmol). The product was obtained as a colorless oil in 70% yield.

^{1}H NMR (300 MHz, CD_2Cl_2): δ 7.19 (m, 1H), 6.90 (m, 2H), 6.71 (m, 1H), 3.78 (s, 3H), 2.99 (t, 2H, *J* = 6.2 Hz) 2.96 (t, 2H, *J* = 6.1 Hz), 1.30 (s, 2H).

- **Synthesis of 2-((3-methoxyphenyl)thio)-N-((1-methyl-1H-imidazol-2-yl)methylene)ethanamine (S6)**

Ligand **S6** was prepared according to the method described for **S1** using 2-((3-methoxyphenyl)thio)ethanamine (0.544 g, 2.97 mmol) and 1-methyl-1H-imidazole-2-carbaldehyde (0.327 g, 2.97 mmol) and isolated as a pale yellow oil in 91% yield.

^{1}H NMR (300 MHz, CD_2Cl_2): δ 8.24 (s, 1H), 7.19 (m, 1H), 7.05 (s, 1H), 6.92 (m, 3H), 6.70 (m, 1H), 3.90 (s, 3H), 3.83 (t, 2H, *J* = 6.7 Hz), 3.76 (s, 3H), 3.22 (t, 2H, *J* = 6.7 Hz). FT-IR

(cm^{-1}): 2966w, 1650s ($\nu_{C=N}$), 1588s, 1574s, 1477s, 1437m, 1368w, 1283s, 1247m, 1230s, 1149w, 1078m, 1022s, 919w, 861m, 764w, 707w, 686s, 566w.

- **Synthesis of N,N-diethyl-N'-((1-methyl-1H-imidazol-2-yl)methylene)ethane-1,2-diamine (N1)**

Ligand **N1** was obtained according to the method described for **S1** using *N,N*-(diethyl)ethylenediamine (0.73 mL, 5.21 mmol) and 1-methyl-1*H*-imidazole-2-carbaldehyde (0.521 g, 4.73 mmol) and isolated as a yellow oil in 94% yield.

^{1}H NMR (300 MHz, CD_2Cl_2): δ 8.25 (td, 1H, *J* = 1.3, *J* = 0.5 Hz), 7.04 (d, 1H, *J* = 1.1 Hz), 6.94 (s, 1H), 3.95 (s, 3H), 3.64 (td, 2H, *J* = 6.8, *J* = 1.3 Hz), 2.72 (t, 2H, *J* = 6.8 Hz), 2.56 (q, 4H, *J* = 7.1 Hz), 1.00 (t, 6H, *J* = 7.1 Hz).

^{13}C{^{1}H} NMR (75 MHz, CD_2Cl_2): δ 154.16, 143.83, 129.23, 124.99, 60.70, 47.84, 35.44, 12.36.

FT-IR (cm^{-1}): 2967m, 1650s ($\nu_{C=N}$), 1518w, 1475m, 1437m, 1369w, 1287m, 1203w, 1174w, 1149w, 1067s, 919w, 748m, 707m, 691m, 500w, 468w.

- **Synthesis of N,N-dimethyl-N3-((1-methyl-1H-imidazol-2-yl)methylene)propane-1,3-diamine (N2)**

Ligand **N2** was obtained according to the method described for **S1** using *N,N*-diethyl-1,3-propanediamine (0.31 mL, 2.45 mmol) and 1-methyl-1*H*-imidazole-2-carbaldehyde (0.270 g, 2.45 mmol) and isolated as a yellow oil in 91% yield.

^{1}H NMR (300 MHz, CD_2Cl_2): δ 8.26 (td, 1H, *J* = 1.4, *J* = 0.6 Hz), 7.03 (d, 1H, *J* = 1.0 Hz), 6.93 (s, 1H), 3.95 (s, 3H), 3.58 (td, 2H, *J* = 6.9, *J* = 1.3 Hz), 2.31 (t, 2H, *J* = 6.8 Hz), 2.17 (s, 6H), 1.79 (m, 2H).

^{13}C{^{1}H} NMR (75 MHz, CD_2Cl_2): δ 15.64, 143.78, 129.19, 125.02, 60.18, 57.81, 45.66, 35.51, 29.51.

FT-IR (cm^{-1}): 2943m, 1649s ($\nu_{C=N}$), 1462m, 1438s, 1368w, 1287m, 1149m, 1041w, 920w, 843w, 803m, 751s, 708m, 690m, 546w, 482w.

- **Synthesis of 2-(diphenylphosphino)-N-((1-methyl-1H-imidazol-2-yl)methylene)ethanamine (P1)**

2-(Diphenylphosphino)ethanamine (0.707 g, 3.08 mmol) was added to a solution of 1-methyl-1*H*-imidazole-2-carbaldehyde (0.339 g, 3.08 mmol) in dichloromethane (15 mL) and the reaction mixture was stirred overnight at room temperature under inert atmosphere. The solvent was evaporated under reduced pressure to afford the desired product as yellow oil in 95% yield.

^{1}H NMR (300 MHz, CD_2Cl_2): δ 8.27 – 8.19 (m, 1H), 7.51 – 7.29 (m, 10H), 7.04 (d, 1H, *J* = 1.0 Hz), 6.92 (s, 1H), 3.85 (s, 3H), 3.78 – 3.66 (m, 2H), 2.60 – 2.35 (m, 2H).

^{13}C{^{1}H} NMR (75 MHz, CD_2Cl_2): δ 153.95, 143.55, 139.14 (d, *J* = 13.4 Hz), 133.11 (d, *J* = 18.9 Hz), 129.35, 128.90 (d, *J* = 6.6 Hz), 128.77, 125.18, 59.08 (d, *J* = 19.5 Hz), 35.47, 30.31 (d, *J* = 13.1 Hz).

^{31}P{^{1}H} NMR (121 MHz, CD_2Cl_2): δ -21.67.

FT-IR (cm^{-1}): 3051w, 1650s ($\nu_{C=N}$), 1518w, 1478m, 1434s, 1412w, 1345w, 1287m, 1147w, 1025w, 919w, 739m, 697m, 631m, 534s.

- **Synthesis of 2-methoxy-N-((1-methyl-1H-imidazol-2-yl)methylene)ethanamine (O1)**

Ligand **O1** was prepared according to the method described for **S1** using 2-(methoxy)ethylamine (0.39 mL, 4.54 mmol) and 1-methyl-1*H*-imidazole-2-carbaldehyde (0.455 g, 4.13 mmol) and isolated as a pale yellow oil in 92% yield.

^{1}H NMR (300 MHz, CD_2Cl_2): δ 8.26 (s, 1H), 7.04 (s, 1H), 6.94 (s, 1H), 3.95 (s, 3H), 3.75 – 3.68 (m, 2H), 3.67 – 3.60 (m, 2H), 3.33 (s, 3H).

^{13}C{^{1}H} NMR (75 MHz, CD_2Cl_2): δ 154.96, 143.59, 129.32, 125.12, 72.53, 61.64, 58.86, 35.46.

FT-IR (cm^{-1}): 2875m, 1650s ($\nu_{C=N}$), 1518w, 1475m, 1437m, 1366w, 1287m, 1236w, 1191w, 1118s, 1026w, 955w, 919m, 802m, 757m, 708m, 690m, 558w, 473w.

- **Synthesis of 2-methoxy-N-((1-methyl-1H-imidazol-2-yl)methylene)aniline (O2)**

Ligand **O2** was obtained according to the method described for **S1** using 2-(methoxy)aniline (0.39 mL, 3.49 mmol) and 1-methyl-1*H*-imidazole-2-carbaldehyde (0.350 g, 3.18 mmol) and isolated as an orange oil in 95% yield.

^{1}H NMR (300 MHz, $(CD_3)_2CO$): δ 8.47 (d, 1H, *J* = 0.5 Hz), 7.28 (s, 1H), 7.24 – 7.16 (m, 1H), 7.12 (d, 1H, *J* = 1.0 Hz), 7.08 (td, 2H, *J* = 8.0, *J* = 1.5 Hz), 7.02 – 6.94 (m, 1H), 4.14 (s, 3H), 3.85 (s, 3H).

$^{13}C\{^{1}H\}$ NMR (75 MHz, $(CD_3)_2CO$): δ 153.36, 153.22, 144.39, 142.02, 130.52, 127.64, 126.78, 121.86, 121.37, 113.07, 56.23, 35.84.

FT-IR (cm^{-1}): 3102w, 2951w, 2835w, 1685w, 1626s ($\nu_{C=N}$), 1585m, 1514m, 1439m, 1464m, 1430s, 1366w, 1288m, 1234s, 1178w, 1149w, 1115m, 1048w, 1025m, 965w, 919w, 869m, 816m, 745m, 687w, 631m, 536s.

- **Synthesis of 3-methoxy-N-((1-methyl-1H-imidazol-2-yl)methylene)propan-1-amine (O3)**

Ligand **O3** was obtained according to the method described for **S1** using 2-(methoxy)propylamine (0.80 mL, 9.23 mmol) and 1-methyl-1*H*-imidazole-2-carbaldehyde (0.924 g, 8.39 mmol). Compound **O3** was obtained as a yellow oil in 91% yield.

^{1}H NMR (300 MHz, CD_2Cl_2): δ 8.27 (dd, 1H, *J* = 1.4, *J* = 0.5 Hz), 7.03 (d, 1H, *J* = 1.1 Hz), 6.94 (s, 1H), 3.95 (s, 3H), 3.61 (td, 2H, *J* = 6.8, *J* = 1.3 Hz), 3.44 (t, 2H, *J* = 6.4 Hz), 3.30 (s, 3H), 1.90 (q, 2H, *J* = 6.6 Hz).

$^{13}C\{^{1}H\}$ NMR (75 MHz, CD_2Cl_2): δ 153.85, 143.70, 129.21, 125.05, 70.64, 58.80, 58.66, 35.48, 31.37.

FT-IR (cm^{-1}): 2925m, 2869m, 1649s ($\nu_{C=N}$), 1517w, 1476m, 1437m, 1287m, 1184w, 1148w, 1118s, 1088m, 1020w, 962w, 809m, 755m, 707m, 508w, 481m.

- **Synthesis of N-((1-methyl-1H-imidazol-2-yl)methylene)butan-1-amine (C1)**

Using the same procedure as for the synthesis of **S1**, **C1** was obtained as a yellow oil in 95% yield using *n*-butylamine (0.48 mL, 4.89 mmol) and 1-methyl-1*H*-imidazole-2-carbaldehyde (0.490 g, 4.45 mmol).

^{1}H NMR (300 MHz, CD_2Cl_2): δ 8.27 (d, *J* = 6.2 Hz, 1H), 7.03 (s, 1H), 6.93 (s, 1H), 3.95 (s, 3H), 3.56 (td, *J* = 6.8, 1.2 Hz, 2H), 1.64 (dq, *J* = 12.2, 6.9 Hz, 2H), 1.50 – 1.32 (m, 2H), 0.94 (t, *J* = 7.3 Hz, 3H).

$^{13}C\{^{1}H\}$ NMR (75 MHz, CD_2Cl_2): δ 153.31, 143.77, 129.11, 124.92, 61.93, 35.41, 33.52, 20.76, 14.00.

FT-IR (cm^{-1}): 2930m, 1650s ($\nu_{C=N}$), 1517w, 1476m, 1437s, 1413w, 1366w, 1287m, 1149w, 1026w, 972w, 919w, 859w, 748m, 708m, 628s, 528s, 468m.

Synthesis of the iron and nickel complexes

- **Synthesis of [$NiCl_2$(DME)]**

In a 250 mL round bottom flask, $NiCl_2 \cdot 6H_2O$ (20.1 g, 84.5 mmol) was heated to 130 °C under vacuum for 1.5 h. The green solid turned yellow. Triethyl orthoformate (27.7 g, 186.9 mmol) and 40 mL of freshly distilled dimethoxyethane (DME) were added. The mixture was refluxed for 2.5 h. The resulting solid was filtered, washed with DME (2×30 mL) and anhydrous pentane (3×40 mL) and dried under vacuum. The desired product was obtained as a yellow solid in 74% yield.

Anal. Calc. for $C_4H_{10}Cl_2NiO_2$: C, 21.87; H, 4.59; Ni, 26.71. Found: C, 21.47; H, 4.73; Ni, 26.12.

- **Synthesis of $NiCl_2${N-((1-methyl-1H-imidazol-2-yl)methylene)-2-(methylthio)ethanamine} (Ni_{S1})**

To a suspension of [$NiCl_2$(DME)] (0.463 g, 1.48 mmol) in dichloromethane (15 mL) was added 1.05 equiv of ligand **S1** (0.284 g, 1.55 mmol) in dichloromethane (10 mL). The reaction mixture was stirred overnight at room temperature after which the solvent volume was reduced to 10 mL. Diethyl ether (20 mL) was added to precipitate a green solid which was washed with diethyl ether (3×20 mL) and dried under vacuum. The complex was obtained as a green powder in 92% yield.

FT-IR (cm^{-1}): 3133w, 2919m, 1641m ($\nu_{C=N}$), 1542w, 1494s, 1425s, 1362m, 1290m, 1217w, 1179m, 1090m, 1029s, 952m, 847s, 817m, 735s, 710s, 665w, 569w, 477s, 470w.

Anal. Calc. for $C_8H_{13}Cl_2N_3NiS$: C, 30.71; H, 4.19; N, 13.43. Found: C, 30.46; H, 3.91; N, 13.40.

- **Synthesis of $NiCl_2${2-methoxy-N-((1-methyl-1H-imidazol-2-yl)methylene)ethanamine} (Ni_{O1})**

Complex Ni_{O1} was prepared according to the method described for Ni_{S1} using [$NiCl_2$(DME)] (0.304 g, 1.06 mmol) and ligand **O1** (0.186 g, 1.12 mmol) and obtained as a pale blue solid in 94% yield.

FT-IR (cm^{-1}): 3128w, 2928w, 1625m ($\nu_{C=N}$), 1542w, 1494s, 1450s, 1418s, 1354w, 1291m, 1243w, 1184m, 1115s, 1058m, 966s, 925w, 859w, 831w, 790s, 725s, 707m, 663m, 564w, 482s, 468m.

Anal. Calc. for $C_8H_{13}Cl_2N_3NiO$: C, 32.37; H, 4.41; N, 14.16. Found: C, 32.25; H, 4.51; N, 13.53.

- **Synthesis of $NiCl_2${N,N-diethyl-N'-((1-methyl-1H-imidazol-2-yl)methylene)ethane-1,2-diamine} (Ni_{N1})**

Complex $\mathbf{Ni_{N1}}$ was obtained according to the method described for $\mathbf{Ni_{S1}}$ using [$NiCl_2$(DME)] (0.459 g, 1.36 mmol) and ligand **N1** (0.279 g, 1.43 mmol) and isolated as an orange powder in 89% yield.

FT-IR (cm^{-1}): 2924w, 160m ($\nu_{C=N}$), 1546w, 1486w, 1450m, 1424s, 1385w, 1346s, 1290w, 1229w, 1148w, 1087m, 1036w, 955m, 881w, 827s, 763s, 734m, 703m, 664m, 615w, 615w, 548m, 474w.

Anal. Calc. for $C_{11}H_{20}Cl_2N_4Ni$: C, 39.10; H, 5.97; N, 16.58. Found: C, 38.96; H, 5.87; N, 16.28.

- **Synthesis of $NiCl_2${2-(diphenylphosphino)-N-((1-methyl-1H-imidazol-2-yl)methylene)ethanamine} (Ni_{P1})**

Complex $\mathbf{Ni_{P1}}$ was obtained according to the method described for $\mathbf{Ni_{S1}}$ using [$NiCl_2$(DME)] (0.180 g, 0.40 mmol) and ligand **P1** (0.136 g, 0.42 mmol) as a brown powder in **91%** yield.

FT-IR (cm^{-1}): 3051w, 1619w ($\nu_{C=N}$), 1538w, 1487m, 1434s, 1347w, 1290w, 1174w, 1101m, 998w, 849w, 741s, 692s, 666s, 512m, 484m.

Anal. Calc. for $C_{19}H_{20}Cl_2N_3NiP$: C, 50.60; H, 4.47; N, 9.32. Found: C, 49.53; H, 4.71; N, 9.40.

- **Synthesis of $NiCl_2${2-methoxy-N-((1-methyl-1H-imidazol-2-yl)methylene)aniline} (Ni_{O2})**

Complex $\mathbf{Ni_{O2}}$ was prepared according to the method described for $\mathbf{Ni_{S1}}$ using [$NiCl_2$(DME)] (0.530 g, 1.54 mmol) and ligand **O2** (0.347 g, 1.61 mmol) and isolated as a yellow powder in 95% yield.

FT-IR (cm^{-1}): 3084w, 2959w, 1602m ($\nu_{C=N}$), 1540w, 1488s, 1439s, 1421s, 1370w, 1323m, 1297w, 1278w, 1248s, 1190m, 1169m, 1120m, 1089w, 1047w, 1017m, 968m, 938m, 823w, 806m, 755s, 728s, 698m, 667w, 607m, 587w, 479w.

Anal. Calc. for $C_{12}H_{13}Cl_2N_3NiO$: C, 41.79; H, 3.80; N, 12.19. Found: C, 41.22; H, 3.80; N, 11.85.

- **Synthesis of $NiCl_2${3-methoxy-N-((1-methyl-1H-imidazol-2-yl)methylene)propan-1-amine} (Ni_{O3})**

Complex $\mathbf{Ni_{O3}}$ was obtained according to the method described for $\mathbf{Ni_{S1}}$ using [$NiCl_2$(DME)] (0.494 g, 1.59 mmol) and ligand **O3** (0.302 g, 1.67 mmol) and isolated as a green powder in 95% yield.

FT-IR (cm^{-1}): 2949w, 2834w, 1629m ($\nu_{C=N}$), 1542w, 1495m, 1448w, 1424m, 1374w, 1289m, 1213w, 1180w, 1118m, 1081s, 1044s, 976m, 960m, 931w, 848s, 766w, 746s, 710s, 665w, 623w, 492m, 481m, 463w.

Anal. Calc. for $C_9H_{15}Cl_2N_3NiO$: C, 34.78; H, 4.86; N, 13.52;. Found: C, 34.76; H, 4.99; N, 13.35.

- **Synthesis of $NiCl_2${N-((1-methyl-1H-imidazol-2-yl)methylene)butan-1-amine} (Ni_{C1})**

Complex $\mathbf{Ni_{C1}}$ was prepared according to the method described for $\mathbf{Ni_{S1}}$ using [$NiCl_2$(DME)] (0.277 g, 0.94 mmol) and ligand **C1** (0.172 g, 1.04 mmol) and isolated as a pale blue powder in 95% yield.

FT-IR (cm^{-1}): 3111m, 2957m, 2866m, 1619m ($\nu_{C=N}$), 1539w, 1372w, 1290 m, 1184m, 1086w, 1043w, 960m, 849m, 793s, 707m, 666m, 559w, 465w.

Anal. Calc. for $C_9H_{15}Cl_2N_3Ni$: C, 36.66; H, 5.13; N, 14.25. Found: C, 37.10; H, 5.41; N, 14.36.

- **Synthesis of $FeCl_2${N-((1-methyl-1H-imidazol-2-yl)methylene)-2-(methylthio)ethanamine} (Fe_{S1})**

To a solution of [$FeCl_2 \cdot 4H_2O$] (0.272 g, 1.37 mmol) in dried cyclohexane (5 mL) was added 1.05 equiv of ligand **S1** (0.263 g, 1.44 mmol) in cyclohexane (5 mL). The reaction mixture was stirred and heated (55 °C) overnight after which a red solid precipitated. The solid was washed with dried diethyl ether (3×10 mL) and dried under vacuum. The complex was obtained as a red powder in 95% yield.

FT-IR (cm^{-1}): 3090w, 2921m, 1623m ($\nu_{C=N}$), 1590m, 1539w, 1487s, 1456s, 1411s, 1348m, 1292s, 1166m, 1077w, 1023w, 959m, 846w, 781s, 708w, 667m, 623w, 491m, 458m.

- **Synthesis of $FeCl_2${N-((1-methyl-1H-imidazol-2-yl)methylene)-2-(ethylthio)ethanamine} (Fe_{S2})**

Complex $\mathbf{Fe_{S2}}$ was prepared according to the method described for $\mathbf{Fe_{S1}}$ using [$FeCl_2 \cdot 4H_2O$] (0.259 g, 1.31 mmol) and ligand **S2** (0.271 g, 1.05 mmol) and isolated as a red powder in 85% yield.

FT-IR (cm^{-1}): 2926m, 1632m ($\nu_{C=N}$), 1597m, 1487m, 1451s, 1418m, 1169w, 1049w, 956w, 850m, 772s, 707w, 664m, 478w.

- **Synthesis of $FeCl_2${2-((2,6-dimethylphenyl)thio)-N-((1-methyl-1H-imidazol-2-yl)methylene)ethanamine} (Fe_{S3})**

To a suspension of $FeCl_2$ (0.121 g, 0.95 mmol) in dried *n*-BuOH (10 mL) was added 1.05 equiv of ligand **S3** (0.287 g, 1.05 mmol) in *n*-BuOH (10 mL). The reaction mixture was stirred and heated (55 °C) overnight after which a yellow solid precipitated. The solid was washed with dried diethyl ether (3×20 mL) and dried under vacuum. The complex was obtained as a yellow powder in 85% yield.

FT-IR (cm^{-1}): 2932w, 1620m ($\nu_{C=N}$), 1543m, 1491w, 1453s, 1421m, 1377w, 1349w, 1288m, 1239w, 1168m, 1034m, 1008w, 963m, 847m, 771s, 745m, 705m, 665m, 542w.

- **Synthesis of $FeCl_2${2-((3,5-dimethylphenyl)thio)-N-((1-methyl-1H-imidazol-2-yl)methylene)ethanamine} (Fe_{S4})**

Complex $\mathbf{Fe_{S4}}$ was prepared according to the method described for $\mathbf{Fe_{S3}}$ using $FeCl_2$ (0.133 g, 1.05 mmol) and ligand **S4** (0.316 g, 1.15 mmol) and isolated as a red powder in 85% yield.

FT-IR (cm^{-1}): 3010w, 2926m, 1622m ($\nu_{C=N}$), 1597m, 1582m, 1522w, 1489m, 1462s, 1432m, 1420m, 1324w, 1256m, 1169w, 1051w, 1022s, 956w, 860m, 775s, 707w, 664m, 520w, 483w, 478w.

- **Synthesis of $FeCl_2${2-((4-(tert-butyl)phenyl)thio)-N-((1-methyl-1H-imidazol-2-yl)methylene)ethanamine} (Fe_{S5})**

Complex $\mathbf{Fe_{S5}}$ was prepared according to the method described for $\mathbf{Fe_{S3}}$ using $FeCl_2$ (0.136 g, 1.07 mmol) and ligand **S5** (0.356 g, 1.18 mmol) and isolated as a pink powder in 84% yield.

FT-IR (cm^{-1}): 2961m, 2871w, 1610m ($\nu_{C=N}$), 1490m, 14551s, 1432s, 1361w, 1326w, 1286m, 1191m, 1172m, 1120m, 1085w, 1048w, 1011m, 958w, 929w, 854m, 836w, 823s, 785s, 776s, 703m, 667w, 551s, 501w, 464w.

- **Synthesis of $FeCl_2${2-methoxy-N-((1-methyl-1H-imidazol-2-yl)methylene)ethanamine} (Fe_{S6})**

Complex $\mathbf{Fe_{S6}}$ was prepared according to the method described for $\mathbf{Fe_{S3}}$ using $FeCl_2$ (0.141 g, 1.10 mmol) and ligand **S6** (0.337 g, 1.22 mmol) and isolated as an orange powder in 95% yield.

FT-IR (cm^{-1}): 3010w, 2949w, 1628m ($\nu_{C=N}$), 1578w, 1545m, 1493m, 1481m, 1453s, 1416m, 1347w, 1248s, 1181w, 1169m, 1101w, 1076w, 1043m, 1024s, 964m, 854s, 782s, 768s, 743m, 705w, 691m, 667m, 589w, 542m, 460w.

Anal. Calc. for $C_{14}H_{17}Cl_2FeN_3OS$: C, 41.82; H, 4.26; N, 10.45;. Found: C, 41.70; H, 4.18; N, 10.04.

- **Synthesis of $FeCl_2${N,N-diethyl-N'-((1-methyl-1H-imidazol-2-yl)methylene)ethane-1,2-diamine} (Fe_{N1})**

To a solution of ligand **N1** (0.106 g, 0.51 mmol) in dried THF (15 mL) was added 1 equiv of [$FeCl_2 \cdot 1.5THF$] (0.119 g, 0.51 mmol) in THF (10 mL). The reaction was stirred and overnight at room temperature after which a purple solid precipitated. The solid was washed with diethyl ether (3×20 mL) and dried under vacuum. The complex was obtained as a purple powder in 90% yield.

FT-IR (cm^{-1}): 2970w, 1615m ($\nu_{C=N}$), 1542w, 1452s, 1423s, 1386w, 1347m, 1287m, 1232w, 1147w, 1084m, 1036w, 954m, 827s, 764s, 734m, 701w, 663m, 545m, 506w, 469w.

- **Synthesis of $FeCl_2${N,N-dimethyl-N3-((1-methyl-1H-imidazol-2-yl)methylene)propane-1,3-diamine} (Fe_{N2})**

Complex $\mathbf{Fe_{N2}}$ was prepared according to the method described for $\mathbf{Fe_{N1}}$ using [$FeCl_2 \cdot 1.5THF$] (0.235 g, 1.0 mmol) and ligand **N2** (0.194 g, 1.0 mmol) and isolated as a red powder in 92% yield.

FT-IR (cm^{-1}): 2951w, 1614m ($\nu_{C=N}$), 1542m, 1451s, 1423s, 1360w, 1284m, 1186w, 1154m, 1105w, 1055s, 1015m, 970w, 958m, 875w, 827s, 802s, 706m, 666m, 476w.

- **Synthesis of $FeCl_2${2-(diphenylphosphino)-N-((1-methyl-1H-imidazol-2-yl)methylene)ethanamine } (Fe_{P1})**

Complex **Fe_{P1}** was prepared according to the method described for **Fe_{S3}** using $FeCl_2$ (0.150 g, 1.18 mmol) and ligand **P1** (0.400 g, 1.24 mmol) and isolated as an orange powder in 95% yield.

FT-IR (cm^{-1}): 2924m, 1573m ($\nu_{C=N}$), 1538w, 1483m, 1454m, 1434s, 1418m, 1351w, 1290m, 1261w, 1175w, 1092s, 1061s, 1000m, 952m, 795s, 777m, 742s, 693s, 667m, 619w, 601w, 519s, 502m, 468m.

X-ray crystal structure determination of Ni_{S1}, Ni_{N1} and Ni_{O2}'.

Diffraction data were collected on a Nonius KappaCCD diffractometer with graphite monochromated Mo-Kα radiation (λ = 0.71073 Å). Data were collected using Ψ scans; the structure was solved by direct methods using the SIR97 software and the refinement was by full-matrix least squares on F^2. No absorption correction was used.

Crystal data and structure refinement for compounds **Ni_{S1}**, **Ni_{N1}** and **Ni_{O2}'**.

	Ni_{S1}	**Ni_{N1}**	**Ni_{O2}'**
Formula	$C_{16}H_{26}C_{l4}N_6Ni_2S_2$	$C_{11}H_{20}Cl_2N_4Ni$	$C_{13}H_{17}Cl_2N_3NiO$
Molecular weight	625.79	337.92	376.91
Crystal system	monoclinic	monoclinic	orthorhombic
Space group	*C*2/c	$P2_1/n$	*P*bca
a (Å)	20.270(2)	7.065(1)	14.005(4)
b (Å)	6.9459(6)	11.305(2)	12.137(3)
c (Å)	19.414(3)	18.417(3)	17.913(4)
α (°)	90	90	90
β (°)	116.69(2)	99.170(10)	90
γ (°)	90	90	90
Cell volume (Å³)	2442.1(7)	1452.2(4)	3044.8(13)
Density	1.702	1.546	1.644
Z	4	4	8
F(000)	1280	704	1552
T (K)	100	100	150
θ Range (°)	3.5, 29.4	3.4, 29.5	3.3, 29.2
h	-27/27	-9/9	-11/17
k	-9/9	-15/14	-16/16
l	0/26	-25/25	-24/24
μ (mm^{-1})	2.17	1.69	1.63
Measd. reflexions	17288	18853	8163
Indep. reflexions	3120	3683	2738
R_{int}	0.044	0.067	0.110
$R[F^2 > 2\sigma(F^2)]$	0.040	0.059	0.076
$wR(F^2)$ (all data)	0.102	0.204	0.240
S	1.00	1.04	0.84
$\Delta\rho_{min}$, $\Delta\rho_{max}$ (e.Å^{-3})	-1.14, 0.73	-1.15, 1.24	-2.12, 2.03

Procedures for ethylene oligomerization

Catalytic reactions were performed either in a semi-batch mono autoclave (when $AlEtCl_2$ was used as cocatalyst) or in six parallelized semi-batch autoclaves (when MAO was used as cocatalyst).

- **Procedure for ethylene oligomerization using $AlEtCl_2$ as cocatalyst.**

Catalytic reactions were carried out in a magnetically stirred 250 mL stainless steel autoclave. The reactor was placed under an atmosphere of ethylene before the toluene, the nickel precursor and the cocatalyst were introduced. The total volume of solutions introduced was 100 mL. The reactor was sealed and fed with ethylene to the desired pressure. The reactor was heated at 45 °C and the magnetic stirring was set to 1000 rpm. During catalysis, the pressure was maintained through a continuous feed of ethylene from a bottle placed on a balance used to monitor the ethylene uptake. At the end of the test, instantly after turning off the feed of ethylene, aliquots of gaseous and liquid effluents were collected and analyzed by GC. Stirring was then stopped and the reactor was cooled down to 25 °C. The gaseous effluents were quantified using a flowmeter and collected in a 15 L polyethylene bottle filled with water. The liquid effluents were weighed. The catalyst and the cocatalyst were quenched by addition of 2 mL of a 10% H_2SO_4 solution in water. Aliquots of gaseous and liquid effluents were analyzed by GC. The reactor was then washed three times with xylene at 140 °C and dried under vacuum (10^{-2} Torr) at 140 °C overnight. Finally, the reactor was cooled down to room temperature and filled with ethylene (30 bar).

- **Procedure for ethylene oligomerization using MAO as cocatalyst.**

Tests were run in six parallelized 100 mL reactors with ethylene consumption monitoring and mechanical stirring. The reactors were placed under an inert atmosphere of nitrogen before the toluene, the nickel complex and the activator were added. The total volume of solutions introduced was 25 mL. The ethylene pressure was immediately increased to 30 bar and the temperature to 45 °C (or 50 °C for iron complexes). The mechanical agitation was then set to 1000 rpm and the ethylene uptake was measured. The test was stopped after 1 h or after 25 g of ethylene was consumed. The autoclave was then cooled to

room temperature and depressurized. The liquid effluents were weighed. The catalyst and the cocatalyst were quenched by addition of 2 mL of a 10% H_2SO_4 solution in water. Aliquots of liquid effluents were then analyzed by GC. The reactors were then washed three times with xylene at 140 °C and dried overnight in vacuum (10^{-2} Torr) at 140 °C. Finally, the reactor was cooled down to room temperature and filled with ethylene (30 bar).

Bibliography

1. K.Ziegler; H.G.Gellert; E.Holzkamp; G.Wilke *Brennst. Chem.* **1954,** *35*, 321.
2. Johnson, L. K.; Killian, C. M.; Brookhart, M. *J. Am. Chem. Soc.* **1995,** *117*, 6414.
3. Johnson, L. K.; Mecking, S.; Brookhart, M. *J. Am. Chem. Soc.* **1996,** *118*, 267.
4. Dennett, J. N. L.; Gillon, A. L.; Heslop, K.; Hyett, D. J.; Fleming, J. S.; Lloyd-Jones, C. E.; Orpen, A. G.; Pringle, P. G.; Wass, D. F.; Scutt, J. N.; Weatherhead, R. H. *Organometallics* **2004,** *23*, 6077.
5. Bianchini, C.; Gonsalvi, L.; Oberhauser, W.; Semeril, D.; Bruggeller, P.; Gutmann, R. *Dalton Trans.* **2003,** 3869.
6. Anselment, T. M. J.; Vagin, S. I.; Rieger, B. *Dalton Trans.* **2008,** 4537.
7. Braunstein, P. *Chem. Rev.* **2005,** *106*, 134.
8. Flapper, J.; Kooijman, H.; Lutz, M.; Spek, A. L.; van Leeuwen, P. W. N. M.; Elsevier, C. J.; Kamer, P. C. J. *Organometallics* **2009,** *28*, 1180.
9. Guan, Z.; Marshall, W. J. *Organometallics* **2002,** *21*, 3580.
10. Speiser, F.; Braunstein, P.; Saussine, W. *Acc. Chem. Res.* **2005,** *38*, 784.
11. Sun, W. H.; Zhang, W.; Gao, T.; Tang, X.; Chen, L.; Li, Y.; Jin, X. *J. Organomet. Chem.* **2004,** *689*, 917.
12. Weng, Z.; Teo, S.; Hor, T. S. A. *Organometallics* **2006,** *25*, 4878.
13. Pietsch, J.; Braunstein, P.; Chauvin, Y. *New J. Chem.* **1998,** *22*, 467.
14. Heinicke, J.; He, M.; Dal, A.; Klein, H. F.; Hetche, O.; Keim, W.; Flörke, U.; Haupt, H. J. *Eur. J. Inorg. Chem.* **2000,** *2000*, 431.
15. Malinoski, J. M.; Brookhart, M. *Organometallics* **2003,** *22*, 5324.
16. Liu, W.; Malinoski, J. M.; Brookhart, M. *Organometallics* **2002,** *21*, 2836.
17. Heinicke, J.; Köhler, M.; Peulecke, N.; Keim, W. *J. Catal.* **2004,** *225*, 16.
18. Kuhn, P.; Semeril, D.; Matt, D.; Chetcuti, M. J.; Lutz, P. *Dalton Trans.* **2007,** 515.
19. Kermagoret, A.; Braunstein, P. *Dalton Trans.* **2008,** 822.
20. Gibson, V. C.; Spitzmesser, S. K. *Chem. Rev.* **2002,** *103*, 283.
21. Killian, C. M.; Johnson, L. K.; Brookhart, M. *Organometallics* **1997,** *16*, 2005.

22. Svejda, S. A.; Brookhart, M. *Organometallics* **1998,** *18*, 65.

23. Hou, X.; Liang, T.; Sun, W. H.; Redshaw, C.; Chen, X. *J. Organomet. Chem.* **2012,** *708-709*, 98.

24. Song, S.; Li, Y.; Redshaw, C.; Wang, F.; Sun, W. H. *J. Organomet. Chem.* **2011,** *696*, 3772.

25. Chai, W.; Yu, J.; Wang, L.; Hu, X.; Redshaw, C.; Sun, W. H. *Inorg. Chim. Acta* **2012,** *385*, 21.

26. Chen, Y.; Wu, G.; Bazan, G. C. *Angew. Chem. Int. Ed.* **2005,** *44*, 1108.

27. Kermagoret, A.; Braunstein, P. *Dalton Trans.* **2008,** 1564.

28. Speiser, F.; Braunstein, P.; Saussine, L. *Inorg. Chem.* **2004,** *43*, 4234.

29. Yang, Q. Z.; Kermagoret, A.; Agostinho, M.; Siri, O.; Braunstein, P. *Organometallics* **2006,** *25*, 5518.

30. Younkin, T. R.; Connor, E. F.; Henderson, J. I.; Friedrich, S. K.; Grubbs, R. H.; Bansleben, D. A. *Science* **2000,** *287*, 460.

31. Zhou, Z.; Hao, X.; Redshaw, C.; Chen, L.; Sun, W. H. *Catal. Sci. Technol.* **2012,** *2*, 1340.

32. Adewuyi, S.; Li, G.; Zhang, S.; Wang, W.; Hao, P.; Sun, W. H.; Tang, N.; Yi, J. *J. Organomet. Chem.* **2007,** *692*, 3532.

33. Adewuyi, S.; Li, G.; Zhang, S.; Wang, W.; Hao, P.; Sun, W. H.; Tang, N.; Yi, J. *J. Organomet. Chem.* **2007,** *692*, 3532.

34. Ajellal, N.; Kuhn, M. C. A.; Boff, A. D. G.; Hoerner, M.; Thomas, C. M.; Carpentier, J. F.; Casagrande, O. L., Jr. *Organometallics* **2006,** *25*, 1213.

35. Carney, M.; Small, B. L. Chevron Phillips Chemical. Diimine metal complexes, methods of synthesis, and methods of using in oligomerization and polymerization. WO2007013931, **2007**.

36. Small, B. L.; Rios, R.; Fernandez, E. R.; Carney, M. J. *Organometallics* **2007,** *26*, 1744.

37. Small, B. L.; Rios, R.; Fernandez, E. R.; Gerlach, D. L.; Halfen, J. A.; Carney, M. J. *Organometallics* **2010,** *29*, 6723.

38. Hara, R.; Kinoshita, S.; Suzuki, Y. Mitsui Chemical Inc. Catalyst for olefin polymerization, and manufacturing method of ethylene polymer. JP2009072665, **2007**.

39. Kinoshita, S.; Suzuki, Y. Mitsui Chemical Inc. Catalyst for olefin polymerization, and manufacturing method of ethylene polymer. JP2009072666, **2007**.

40. Isao, H.; Ishii, S.; Kawamura, K. Mitsui Chemical Inc. Transition metal complex compounds, olefin oligomerization catalysts including the compounds, and processes for producing olefin oligomers using the catalysts. WO2009005003, **2009**.

41. Isao, H.; Ishii, S.; Kawamura, K.; Kazumori, K. Mitsui Chemical Inc. Transition metal complex compounds, olefin oligomerization catalysts including the compounds, and processes for producing olefin oligomers using the catalysts. EP2174928, **Jun 27, 2008**.

42. Suzuki, Y.; Kinoshita, S.; Shibahara, A.; Ishii, S.; Kawamura, K.; Inoue, Y.; Fujita, T. *Organometallics* **2010,** *29*, 2394.

43. Chavez, P.; Rios, I. G.; Kermagoret, A.; Pattacini, R.; Meli, A.; Bianchini, C.; Giambastiani, G.; Braunstein, P. *Organometallics* **2009,** *28*, 1776.

44. Fulmer, G. R.; Miller, A. J. M.; Sherden, N. H.; Gottlieb, H. E.; Nudelman, A.; Stoltz, B. M.; Bercaw, J. E.; Goldberg, K. I. *Organometallics* **2010,** *29*, 2176.

CONCLUSION GÉNÉRALE & PERSPECTIVES

Conclusion générale

L'objectif de cette thèse était d'étudier de nouveaux systèmes catalytiques à base de fer pour l'oligomérisation de l'éthylène. Nous nous sommes intéressés à des complexes de fer(III) possédant des ligands monoanioniques tridentes. Deux voies d'accès à ces systèmes ont été abordées : la réaction entre un ligand anionique de type L,X,L et un précurseur de fer(III) ainsi que l'oxydation de précurseurs de fer(II). L'intérêt a également été porté sur le développement de nouvelles familles de ligands tridentes N,N,L (L = N, O, S, P) ainsi que sur la recherche de nouveaux activateurs, le MAO et le MMAO restants les seuls cocatalyseurs efficaces dans le domaine de l'oligomérisation de l'éthylène par les complexes du fer.

Les résultats obtenus sur les complexes de fer(III) chélatés par le ligand anionique 1,2-dihydro-1,10-phénantroline ont permis d'éclaircir certains points. Les efforts effectués sur l'optimisation de la synthèse du complexe ainsi que les caractérisations par FT-IR, SM, DRX, EXAFS et XANES ont conduit à une détermination de la structure du pré-catalyseur de fer(III) (Figure 1). Ainsi, nous avons conçu le premier système catalytique de fer(III) chélaté par un ligand anionique actif en oligomérisation de l'éthylène. L'étude comparée avec différents complexes de fer 1,2-dihydro-1,10-phénatroline nous a permis d'établir la synergie entre le degré d'oxydation +III du centre métallique, le mode de chélation du ligand anionique et la géométrie du complexe obtenu.

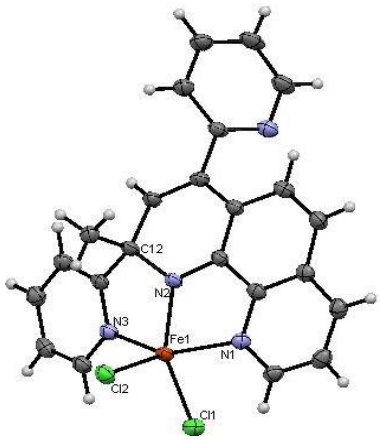

Figure 1. Structure du complexe fer(III) 1,2-dihydro-1,10-phénantroline déterminée par DRX.

Les oligomères formés sont des oléfines linéaires paires légères (63% en C_4 ; 18% en C_6) avec une très bonne sélectivité en oléfines linéaires alpha (>97% pour le butène-1 et >90% pour l'hexène-1). Le même mode opératoire de synthèse appliqué aux ligands bis(pyridylimino)isoindoline et bis(2-picolyl)amine a conduit à la formation de complexes de fer(III) qui se sont avérés inactifs vis-à-vis de l'éthylène. Ce travail a donné lieu à une publication parue dans Organometallics en 2011.

L'oxydation par l'oxygène des complexes de fer(II) chélatés par des ligands tridentes N,NH,N potentiellement anioniques, s'est révélée être une voie intéressante dans la synthèse des précurseurs de fer(III). Ces complexes ont démontré des caractéristiques structurales et catalytiques innovantes. Concernant la synthèse, nous avons mis en évidence (via une étude DRX sur les ligands bis(pyridylimino)isoindoline) que lors de l'étape d'oxydation l'amine centrale se déprotonait pour se lier au fer de manière covalente et que dans le même temps le pont Fe-O-Fe entre deux entités monomériques se formait (Figure 2). Le caractère binucléaire des complexes oxydés ainsi que le mode de chélation du ligand (anionique) ont été confirmés par l'analyse par spectrométrie infrarouge. Seul le système de fer(III) 1,2-dihydro-1,10-phénantroline s'est avéré actif en oligomérisation de l'éthylène (13.5×10^5 g·(mol(Fe)·h)$^{-1}$). L'hypothèse d'une espèce active binucléaire a été confortée par les différences d'activité, de sélectivité et de distribution des produits entre le complexe binucléaire et le précurseur mononucléaire de fer(III) développé dans le chapitre II (Figure 1). Nous avons synthétisé le premier complexe de fer binucléaire présentant une liaison Fe-O-Fe actif en oligomérisation de l'éthylène, en présence de MAO.

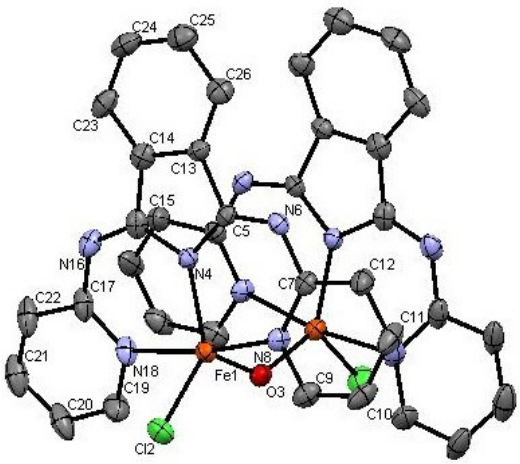

Figure 2. Structure du complexe binucléaire de fer(III) obtenu par oxydation.

Le développement de nouveaux activateurs pour l'activation des complexes de fer en oligomérisation de l'éthylène fut une part importante de mon travail de recherche. Cette démarche avait pour but de trouver des substituts aux aluminoxanes qui possèdent certaines contraintes majeures dans leur mise en oeuvre : stabilité thermique très limitée, durée de vie courte, solubilité dans les hydrocarbures très limitée, nécessité d'utiliser des rapports molaires très élevés par rapport au fer. Par ailleurs, nous souhaitions mieux comprendre le mode d'activation des précurseurs de fer par les aluminoxanes qui restent les seules espèces permettant d'accéder à des systèmes réellement actifs.

Nous avons synthétisés de nouveaux activateurs par réaction entre un composé organique protique et le triméthylaluminium. Dans un premier temps, nous avons mis en œuvre des composés phénoliques que nous avons fait réagir sur le triméthylaluminium. Nous avons étudié l'impact de l'encombrement stérique en positions *ortho* ou *para* du phénol. Ainsi, la réaction du phénol avec le triméthylaluminium a conduit à la formation d'une espèce binucléaire symétrique (Schéma 1). Activé par cette espèce (Al/Fe = 500), le complexe de fer(II) bis(imino)pyridine catalyse l'oligomérisation de l'éthylène avec une activité de 9.3×10^5 $g\cdot(mol(Fe)\cdot h)^{-1}$ produisant des oligomères de C_4 à C_{24} (constante de Schulz-Flory K = 0.70) avec une excellente sélectivité en α-oléfines linéaires similaire à celle obtenue avec le MAO (>98%). Ce résultat montre que le MAO n'est pas le seul activateur permettant d'accéder à des systèmes catalytiques à base de fer efficaces en oligomérisation de l'éthylène. Nous avons pu mettre en évidence la forte influence de l'encombrement stérique en *ortho* et *ortho'* du phénol sur l'activation du dérivé de l'aluminium formé vis-à-vis du fer (pour des rapports Al/Fe = 500). Une augmentation de cet encombrement induit une diminution notable de l'activité du système catalytique [dérivé de l'aluminium/fer bis(imino)pyridine] avec très peu d'effet sur la sélectivité en α-oléfines linéaires. L'impact de la substitution du phénol en position *para* est beaucoup moins marqué.

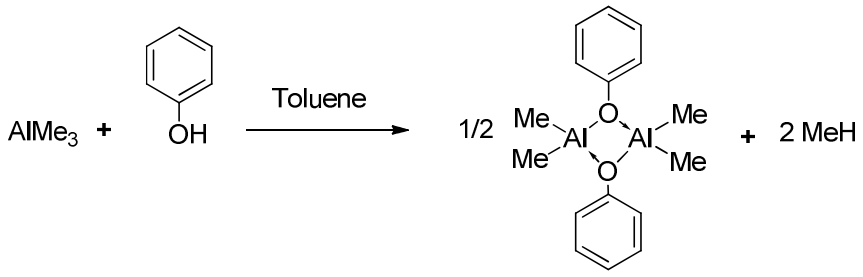

Schéma 1. Réaction entre le phénol et le TMA.

Un second screening focalisé autour des composés de types diols et aminophenols non substitués a conduit à des systèmes donnant de meilleures activités par rapport à leurs homologues phénoliques. La première partie de cette étude a été faite sur des activateurs formés *in situ*. Nous avons pu démontrer que l'espacement entre les deux fonctions hydroxy ainsi que la nature de la chaîne alkyle séparant ces deux fonctions impactaient les performances catalytiques. L'évaluation d'une bibliothèque de composés a permis de définir le 2,2'-dihydroxybiphényle comme étant le meilleur candidat. Nous avons également démontré l'importance du rapport molaire 2,2'-dihydroxybiphényle/$AlMe_3$ sur la performance du système Al/Fe en catalyse avec un optimum pour le rapport 2,2'-dihydroxybiphenyle/$AlMe_3$ de 2/3. Fort de ce résultat, nous avons synthétisé et isolé les espèces trinucléaires correspondantes de l'aluminium que nous avons parfaitement caractérisées par RMN (Schéma 2). La synthèse de ces composés a conduit à de faibles rendements du à la formation d'oligomères d'aluminium appelés alucones difficilement caractérisables. Ces espèces isolées ont permis l'activation des précurseurs de fer(II) et de fer(III) (10^6 g·(mol(Fe)·h)$^{-1}$) pour des ratios Al/Fe élevés (Al/Fe = 250).

S'il n'a pas été possible d'établir une corrélation entre les caractéristiques de ces dérivés de l'aluminium et les performances du système catalytique correspondant, nous avons cependant réussi à activer les complexes de fer avec des espèces isolées et parfaitement caractérisées ce qui constitue en soit une réelle innovation dans le domaine (bien que les activités restent inférieures à celles obtenues avec le MAO). Une demande de brevet français a été déposée sur cette partie du travail. Une publication est en cours de rédaction.

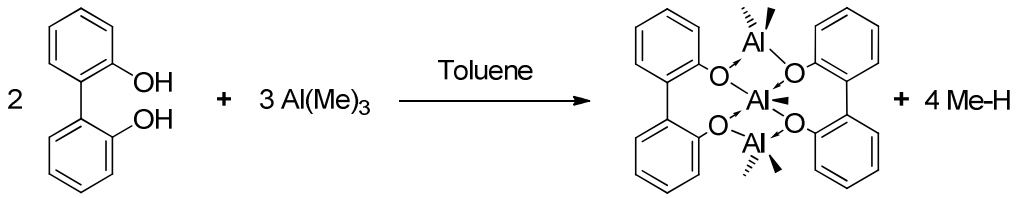

Schéma 2. Synthèse des complexes trinucléaires d'aluminium.

En parallèle de ces travaux, une bibliothèque de ligands tridentes imidazoles-imine fonctionnalisés par un bras hémilabile a été élaborée en faisant varier le type d'hétéroatome de la fonctionnalisation mais aussi la taille et la nature du bras espaceur. La présence d'un bras hémilabile confère une certaine diversité électronique (nature de l'hétéroatome) et stérique (substituants liés à l'hétéroatome) au complexe. Ceci permet de mieux appréhender

l'impact des variations structurales du complexe sur la catalyse. En association avec le nickel, nous avons pu vérifier le mode de chélation tridente de ces ligands par analyse DRX. Les complexes adoptent soit une géométrie octaédrique (Figure 3, cas du ligand N,N,S(Me)) soit une géométrie trigonale bipyramidale déformée (Figure 3, cas du ligand N,N,N(Et)$_2$).

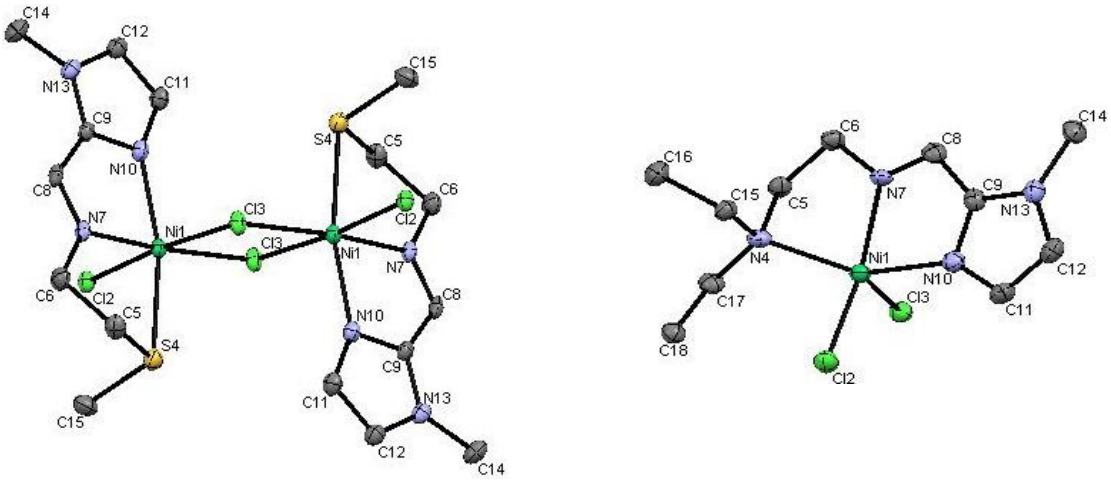

Figure 3. Complexes de nickel binucléaire (à gauche) et mononucléaire (à droite).

Activés par l'$AlEtCl_2$, tous les précurseurs de nickel se sont révélés très actifs en oligomérisation de l'éthylène (~10^7 $g\cdot(mol(Ni)\cdot h)^{-1}$)) conduisant essentiellement à des dimères et trimères présentant de faibles sélectivités en α-oléfines. L'utilisation de MAO comme activateur a conduit à des activités plus faibles mais à des sélectivités en α-oléfines améliorées. Quelque soit l'activateur utilisé, les complexes de nickel comportant une fonctionnalisation éther (-OMe) ont donné les meilleures performances avec un optimum pour le ligand possédant un bras espaceur phénylène. Les écarts d'activités obtenus n'ont cependant pas été suffisamment significatifs pour élaborer une corrélation entre la nature du ligand et l'activité catalytique. Activés par le MAO, les complexes analogues du fer chélatés par ces ligands se sont révélés inactifs en catalyse. Ce travail a donné lieu au dépôt d'une demande de brevet français et à une publication acceptée dans J. Organomet. Chem.

Perspectives

Ce travail a mis en évidence le potentiel des précurseurs de fer au degré d'oxydation trois portant un ligand azoté anionique tridente pour l'oligomérisation de l'éthylène. Cela ouvre de larges perspectives pour la conception de nouveaux ligands de type L,NH,L ou L,OH,L conduisant à de nouveaux systèmes catalytiques à base de fer. Les ligands recherchés devront être innovants tout en pouvant présenter des similitudes structurales aux ligands déjà décrits. L'innovation pourra venir de l'utilisation de différents précurseurs de fer. L'ensemble de cette étude permettra une compréhension accrue de l'impact du ligand, de son mode de chélation, du degré d'oxydation du fer et du précurseur sur la catalyse.

Les activités élevées obtenues avec les complexes binucléaires de fer(III), possédant une liaison Fe-O-Fe, issus d'une oxydation des complexes de fer(II) permettent d'envisager la conception "on purpose" de complexes binucléaires possédant une géométrie analogue. Il s'agira d'étudier différents protocole d'oxydation afin de pouvoir envisager une compréhension du mécanisme de formation de ces espèces. La généralisation à de ce concept à d'autres familles de ligands L,NH,L ou L,OH,L devra être envisagée. Une étude sur la réaction entre le complexe binucléaire de fer et un cocatalyseur de structure connue pourrait permettre de vérifier que le caractère binucléaire du catalyseur est conservé après activation.

Enfin, l'utilisation de dérivés de l'aluminium de structures parfaitement définies a ouvert une piste innovante dans le domaine de l'oligomérisation de l'éthylène par les complexes de fer. Une étude plus approfondie de ces espèces devrait permettre une compréhension accrue de l'étape d'activation. Cela permettrait, entre autres, de pouvoir isoler la paire d'ions formée *in situ*. Une perspective à envisager serait d'étudier différents designs d'activateurs d'aluminium (via un choix judicieux du composé organique) en fonction de la réactivité ciblée. D'un point de vue économique, il s'agirait de se détacher du TMA (coût élevé) via l'utilisation d'autres alkylaluminiums (triéthylaluminium, triisobutylaluminium…). Il serait également intéressant d'étudier la réactivité d'autres métaux de transition tels que le titane, le chrome ou en encore le nickel (tous pouvant être activés par le MAO) vis-à-vis des nouveaux activateurs trinucléaires d'aluminium.

LISTE DES BREVETS, ARTICLES ET COMMUNICATIONS

Brevets :

- P.-A. Breuil, A. Boudier, L. Magna, H. Olivier-Bourbigou : « *Nouvelle composition catalytique à base de nickel et procédé d'oligomérisation des oléfines utilisant ladite composition*» - N° dépôt 11/02.731

- P.-A. Breuil, A. Boudier, H. Olivier-Bourbigou : « *Procédé de séparation du pentène-2 d'une coupe C_5 contenant du pentène-2 et du pentène-1 par oligomérisation sélective du pentène-1*» - N° dépôt 11/02.847

- P.-A. Breuil, A. Boudier : « *Composition catalytique et procédé d'oligomérisation des oléfines utilisant ladite composition*» - N° dépôt 12/00.398

Articles :

- Boudier A. *et al.* Novel Catalytic System for Ethylene Oligomerization: An Iron(III) Complex with an Anionic N,N,N Ligand. *Organometallics*, **2011**, *30*, 2640-2642.

- Boudier A. *et al.* Nickel(II) Complexes with Imino-Imidazole chelating Ligands bearing Pendant Donor Groups (SR, OR, NR_2, PR_2) as Precatalysts in Ethylene Oligomerization. *J. Organomet. Chem.*, **2012**, Accepted.

Communications :

- Communication orale : GECOM-CONCOORD 2011, Merlimont (France), 15 mai au 20 mai 2011. *« Développement de nouveaux systèmes catalytiques de fer(III) chélatés par des ligands anioniques : Application à l'oligomérisation de l'éthylène. »*
  (Adrien Boudier, Pierre-Alain Breuil, Lionel Magna, Hélène Olivier-Bourbigou et Pierre Braunstein)

- Poster : ISHC 2012, Toulouse (France), 9 juillet au 13 juillet 2012. « *Oxidation of iron(II) complexes: A New Route to active Catalysts for Ethylene Oligomerization.* »
  (Adrien Boudier, Pierre-Alain Breuil, Lionel Magna, Hélène Olivier-Bourbigou et Pierre Braunstein)

Adrien BOUDIER

Design, synthèse et caractérisation de nouveaux ligands et activateurs pour l'oligomérisation de l'éthylène par les complexes de fer.

Résumé :

Cette thèse décrit le développement de nouveaux systèmes catalytiques à base de fer ainsi que l'étude de leur réactivité vis-à-vis de l'éthylène. Dans un premier temps, nous nous sommes intéressés au développement de précurseurs de fer(III) associés à des ligands monoanioniques tridentes. Deux voies de synthèse ont été envisagées. La première décrit la complexation d'un ligand anionique sur le précurseur $FeCl_3$ et la seconde passe par l'oxydation d'un complexe de fer(II) associé à un ligand neutre conduisant à une espèce binucléaire. Activés par le MAO, ces catalyseurs de fer(III) constituent les premiers complexes du genre permettant l'oligomérisation de l'éthylène. L'accent a également été porté sur la recherche de nouveaux activateurs. Des complexes d'aluminium répondant à nos attentes ont été obtenus par réaction entre un alcool et le triméthylaluminium. Selon la nature de l'alcool, la structure des activateurs peut être soit binucléaire ou trinucléaire. Enfin, des complexes de fer et de nickel associés à des ligands imino-imidazoles possédant un bras hémilabile ont été synthétisés. Une fois activés, les systèmes à base de nickel ont montré de bonnes activités en catalyse.

Mots-clés : oligomérisation, éthylène, fer, nickel, activateur, ligand monoanionique, ligands imidazoles imines.

Abstract:

This thesis describes the development of new catalytic systems based upon iron complexes and their reactivity toward ethylene. First, we focused our interest on the synthesis of iron(III) precursors chelated by monoanionic ligand. These complexes were obtained either by reaction of the monoanionic ligand with $FeCl_3$ or through oxidation of the iron(II) complex. The second reaction led to binuclear complexes. When activated by MAO, both iron(III) complexes led to active systems for the oligomerization of ethylene. Then, another aim of the thesis was to design new well-defined cocatalysts for the activation of iron complexes. The study of the reaction between an alcohol and the trimethylaluminum allowed us to reach this aim. Aluminum complexes adopted either a binuclear framework or a trinuclear one, depending on the nature of alcohol reagent. Besides this work, new iron and nickel complexes chelated by imino-imidazole ligands bearing a pendant donor function L were synthesized. All complexes have been evaluated for the oligomerization of ethylene in the presence of $EtAlCl_2$ or MAO as cocatalyst. Nickel complexes were active toward ethylene transformation.

Keywords: oligomerization, ethylene, iron, nickel, activators, monoanionic ligand, imino-imidazole ligands.